Identification of molecular targets in the treatment of stroke

De Bilbao, Fabienne

Identification of molecular targets in the treatment of stroke

Fabienne de Bilbao

Service de Psychiatrie Gériatrique
Département de Psychiatrie
HUG, Belle Idée
1225 Chêne-Bourg

Thèse d'habilitation au Titre de Privat-Docent à la Faculté de Médecine de Genève

2010

Acknowledgements

I would like to express my sincere gratitude to Professor P. Giannakopoulos for his continued support in my scientific and academic career at the University of Geneva. Many thanks to Dr. D. Arsenijevic, joint main co-author, for the work of all these years. My thanks also go to Dr. P. Vallet for collaboration in many experiences. The excellent technical assistance of P. Lovero, M. Surini, N. Flores and M. Muhlematter is gratefully acknowledged. Finally, I would like to thank Professor D. Ricquier and Professor W. Wahli who kindly provided the UCP2 and PPARβ mouse models respectively.

Article I: F. de Bilbao, E. Guarin, P. Nef, P. Vallet, P. Giannakopoulos and M. Dubois-Dauphin (2000) Cell death is prevented in thalamic fields but not in injured neocortical areas after permanent focal ischaemia in mice overexpressing the anti-apoptotic protein Bcl-2. *Eur J Neurosci* 12:921-934.

Article IV: D. Arsenijevic, F. de Bilbao, P. Vallet, A. Hemphill, B. Gottstein, D. Richard, P. Giannakopoulos and W. Langhans (2007) Decreased infarct size after focal cerebral ischemia in mice chronically infected with Toxoplasma gondii. *Neuroscience* 150:537-546.

Summary

Ischemic stroke is a heterogeneous disorder with a complex pathophysiology. Experimental models of cerebral ischemia may contribute to our understanding of the mechanisms occurring during ischemic brain injury, and therefore be of relevance to detect anti-ischemic molecules against stroke. Although currently thrombolytic agents are the only approved therapy for this disorder, neuroprotection offers a viable strategy to treat acute ischemic stroke patients. The acute neuronal degeneration in the ischemic core upon stroke is followed by a second wave of cell death in the ischemic penumbra and neuroanatomically connected sites. This temporally delayed deleterious event of programmed cell death (also called apoptotic cell death) often exceeds the initial damage of stroke and, thus, contributes to significant losses of neurological functions. Because these events are delayed and potentially reversible, the injured neurons in these regions around the ischemic core zone are salvable and constitute the target of neuroprotective strategies. Therefore, using genetically modified mice, we discuss here novel alternative strategies to abrogate the death cascade *in vivo* in a model of permanent focal ischemia induced by permanent middle cerebral artery occlusion. Evaluations of these new strategies include two mitochondrial effectors, namely the anti-apoptotic protein Bcl-2, and the uncoupling protein-2 (UCP2), known to attenuate some deleterious effects of ischemia such as oxidative stress and calcium homeostasis alterations. In addition, a nuclear transcription factor, the peroxisome proliferator-activated receptor β (PPARβ), which may regulate the expression of UCP2 and is abundantly expressed in the brain, has recently emerged as a potential tool to limit ischemic injury. Indeed, among the main biologic phenomena thought to be influenced by PPAR activation, cytokine-mediated inflammatory processes and activation of anti-oxidant mechanisms are of key importance for cell damage after acute cerebral ischemia. Finally, it is well described that the so-called “ischemic tolerance” phenomenon could constitute an additional strategy to limit brain damage. Among the potential inducers of ischemic tolerance are the infectious agents. However, results from the literature are conflicting and findings supporting that chronic infection may confer protection against subsequent ischemia warrant further

investigations. As chronic murine toxoplasmosis may be of particular interest in the study of infection-related effects on brain ischemia, because of its association with the regulation of the oxidative state as well as activation of pro-inflammatory/anti-inflammatory mechanisms, we have also explored the impact of chronic *Toxoplasma gondii* infection on brain ischemic injury outcomes. On the basis of these experimental data, the present work supports the idea that exploiting the ability of each of these new molecular strategies to reduce cell death induced by stroke injury might be a valuable perspective in the context of the ongoing efforts to identify therapeutic alternatives for this devastating pathology.

Abbreviations: ADP, adinosine diphosphate; ATP, adenosine triphosphate; BBB, blood–brain barrier; CBF, cerebral blood flow; CNS, central nervous system; CuZnSOD, Copper/zinc superoxide dismutase; GSH, glutathione; GPx, glutathione peroxidase; GR, GSH reductase; H_2O_2, hydrogen peroxide; IFNγ, interferon-γ; IL1β, interleukin-1β; IL6, interleukin-6; IL10 interleukin-10; KO, knockout; LPS, lipopolysaccharide; MCAO, middle cerebral artery occlusion; MDA, malondialdehyde; MnSOD, manganese superoxide dismutase; NGF,nerve growth factor; $O_2^{-\bullet}$, superoxide anion; PCD, programmed cell death; PPARβ, peroxisome proliferator-activated receptor β; ROS, reactive oxygen species; SOCS, suppressor of cytokine signaling proteins; SOD, superoxide dismutase; TGFβ, transforming growth factor-β; TNFα, tumor necrosis factor-α; TUNEL, Terminal deoxynucleotidyl Transferase Biotin-dUTP Nick End Labeling; UCP2, uncoupling protein-2; WT, wild-type.

Introduction

In an ever-aging society, brain ischemia is one of the major causes of death and chronic disability worldwide, and has significant clinical and socioeconomic impact. Approximately 1/6 of all human beings will suffer at least one stroke in their lives (Seshadri *et al*., 2006). Twenty percent of stroke patients die the first month and those who survive for more than 6 months will be dependent on others (Bonita, 1992). Countermeasures to lower the post-ischemic consequences for a society in need to diminish health costs make an understanding of this deleterious process strongly required. In the past 20 years, substantial efforts have been made to understand the biochemical and molecular mechanisms involved in ischemia-induced cerebral damage and to develop drugs that protect the brain. With regard to ischemic stroke, two major approaches have been developed. One approach is to try to establish reperfusion to the compromised region by dissolution of the clot using thrombolytic drugs (vascular approach). At present, recombinant tissue-plasminogen activator (rt-PA) is the only thrombolytic drug approved for the treatment of acute ischemic stroke. The use of rt-PA is restricted to administration within 3 h of the stroke, which is a challenging admission target. Furthermore, its use increases the risk of hemorrhagic transformation (Wardlaw *et al*., 1997), which limits its acceptability. The second approach is to develop compounds, so-called neuroprotective agents that could interfere with the ischemic cascade of events (cellular approach). The term “neuroprotection” encompasses a diverse range of potential therapies, including modulators of the excitatory amino acid system, modulators of calcium influx, metabolic activators, anti-edema agents, inhibitors of leukocyte adhesion, free radical scavengers, and other agents. There objectives are to limit the size of the infarct by interfering with the multiple pathways and cascades of biochemical, molecular, and electrophysiological events that interact to cause the death of brain cells following ischemia (Figure 1). The assumption here is that the core area of damage (infarction) will not be salvaged but that the area that surrounds the core, the penumbra (see section 2.1.), despite being compromised with low blood flow, can be saved by either reflow or administration of a neuroprotectant. If left untreated, the penumbral region will become part of the core region (Ginsberg, 2003). Thus,

protection should attenuate many of the clinical problems of stroke, including motor disability and spatial hemi-neglect. Various strategies directed towards greater protection against the consequences of cerebral ischemia have been experimentally tested. However, although there are several therapeutic agents (antagonists of NMDA receptors, calcium channel blockers, anti-oxidants) that have demonstrated efficacy in experimental studies, clinical trials have so far been more than disappointing. The greater part of the agents studied until now have failed to induce neuroprotection (Ovbiagele *et al*., 2003). Hence, we need to look for new therapeutic strategies. A clear understanding of signalling/new endogenous protective pathways is therefore needed to provide new therapeutic agents.

1. Models of cerebral ischemia

Ischemic stroke accounts for approximately 80% of all strokes and results from a thrombotic or embolic occlusion of a major cerebral artery (most often middle cerebral artery, MCA) or its branches. The use of reproducible and physiologically controlled animal models of acute stroke is an indispensable tool first to investigate the pathophysiology of cerebral ischemia, and secondly to develop novel anti-ischemic therapies *in vivo*. Large animals, such as dogs (Behringer *et al*., 2001), rabbits (Lapchak *et al*., 2002), cats (Krep *et al*., 2003), pigs (Conroy *et al*., 1998), and primates (Plautz *et al*., 2003) have been used for investigating experimentally the consequences of cerebral ischemia. These may be mostly valuable in the final stage of research on therapeutic interventions as they offer a better representation of the human cerebral organization, but a great variability in infarct size exists and the mortality in acute and chronic survival models is high. Consequently, and given the variety of their vantage points, the most widely used animals are rats and mice: animal cost is low, inbred rodents are genetically homogeneous, their cerebral circulation shows good homology to that of the humans, and at least in mice genetic modifications can be made relatively easily. Importantly, transgenic mice that overexpressed a specific gene or knockouts (KO) that lacked a specific gene provide unique avenues for basic research into

the molecular mechanisms that contribute to ischemic cell damage and development of novel therapeutic interventions (Liang *et al.,* 2004).

For the study of stroke physiopathological mechanisms, several animal models have been established in rodents. In these paradigms, neuronal damage occurs by different mechanisms and time windows. Surgical occlusion of major arteries is widely used. Rodent cerebral ischemic models can be divided into two groups: the global forebrain ischemia which is typically transient and the focal cerebral ischemia with and without reperfusion (Traystman, 2003; Rami *et al.*, 2008). In the global ischemia models, which consist of the so-called four-vessel occlusion or two-vessel occlusion of extracranial arteries in rats and gerbils, circulation is interrupted throughout the entire brain for variable periods and is followed by the reperfusion of carotid arteries; in these models, injury is delayed and develops selectively in cells most vulnerable to ischemic damage, such as in the hippocampus (CA1 region), medium-sized neurons in the striatum, and Purkinje cells in cerebellum. However these models are now used much less because they are considered to generate the cerebral consequences of cardiac arrest, rather than that of ischemic stroke.

Most experimental models of focal ischemia were developed to induce cerebral ischemia within the MCA territory in order to be relevant to clinical situation (Del Zoppo *et al*., 1992). They are divided into techniques including reperfusion of the ischemic tissue (transient focal cerebral ischemia) and those without reperfusion (permanent focal cerebral ischemia) and are commonly studied during occlusion of a middle cerebral artery (MCAO) in rats and mice. Permanent MCAO by microsurgical coagulation permit to study cerebral ischemia without the effect of reperfusion. It has been first introduced in the rat by Tamura *et al*. (1981). Proximal MCA occlusion induces severe ischemia in the striatum with milder cortical ischemia while a distal MCAO results in a neocortical infarct exclusively. In the transient MCAO model, reperfusion of the MCA territory is reconstituted and leads to a variable infarct size depending on the duration of ischemia. In these transient models, the caudatoputamen is primarily affected and the neocortex is involved to a variable extent. Despite the possible problems of reperfusion injury, the damage is less than when the occlusion is permanent.

Although human stroke is a complex and heterogeneous phenomenon, it is difficult to develop a unitary animal model system. However, these models allow

the investigation of dynamics in cellular responses to an ischemic insult, and offer an opportunity to develop treatment strategies against the ischemic brain injury.

2. Pathophysiology of acute ischemic stroke

2.1. The core region and the ischemic penumbra

Ischemia is defined as a reduction in cerebral blood flow (CBF), sufficient to cause metabolic or functional deficits and is typically caused by the occlusion of an artery supplying a specific territory of the brain. The characteristics of the brain injury depend on the severity and duration of the CBF reduction. In the animal model of permanent MCAO, blood flow is crucially absent in the central region of the brain (infarct core), and tissue damage evolved rapidly. But in the peripheral cortex adjacent to the core, the ischemic penumbra is a region where blood flow deficits are less severe and energy loss is modest, due to residual perfusion from collateral blood vessels. The concept of 'penumbra' during focal cerebral ischemia was introduced by Astrup in 1981, and refers to the regions of brain tissue where blood flow is sufficiently reduced to cause hypoxia, severe enough to arrest physiological function, but not so complete as to cause irreversible failure of energy metabolism and cellular necrosis (Ginsberg, 2003). If the blood flow is not restored within hours, the penumbral region will become part of the core region (Green *et al*., 2003) (Figure 1). A time window for therapeutic opportunity therefore exists in this potentially salvageable region.

2.2. Progression of the ischemic injury

2.2.1. *Infarct progression*

Infarct progression can be divided into three phases (Dirnagl *et al*., 1999). During the acute phase, tissue injury is established within a few minutes after the onset of ischemia and results directly from the ischemia-induced energy failure and the resulting terminal depolarization of cell membranes. The largest increment of infarct volume occurs during the subsequent subacute phase in which the infarct

core expands into the penumbra. During this phase, the infarct core expands into the peri-infarct penumbra until it becomes congruent with it after 4–6 hours. The main mechanisms of this infarct expansion are peri-infarct depolarization and cell biological disturbances referred to as molecular cell injury (Figure 2). Finally, in the delayed phase of injury, secondary phenomena such as inflammation and programmed cell death (PCD) occur and may contribute to a further progression of injury. This phase may last for several days or even weeks.

2.2.2. *Infarct size measurement*

Enlargement of the infarcted tissue by edema results in overestimation of infarct volume, that is why the calculation of corrected infarct volume is used to compensate for the effect of brain edema (Lin *et al.*, 1993; Takano *et al*., 1997). Generally, the corrected infarct volume is calculated by substracting the volume of the unaffected ipsilateral from the volume of the contralateral hemisphere. In the various papers presented below, infarct volumes were calculated by multiplying the area of the lesion with the slice thickness. This corrected infarct volume was used to compensate for brain edema which is essential to exclude the possibility that therapeutic intervention might reduce edema but not salvage brain tissue at risk of infarction (Guegan *et al.,* 1998).

2.3. Secondary degeneration through neural connections with the primary infarcted area

There are few detailed studies on neuropathologic changes in remote, non-ischemic areas following focal cerebral infarction. However, neuropathologic changes have also been shown to occur in distant non-ischemic area after focal cerebral ischemia and this ischemic damage develops more slowly than the observed acute changes of the infarcted area. Because of its extensive synaptic connections with the cerebral cortex (Jacobson and Trojanowski, 1975), the thalamus undergoes this type of secondary neuronal degeneration induced by cortical infarct in rats and humans (Fujie *et al*., 1990; Tamura *et al*., 1991).

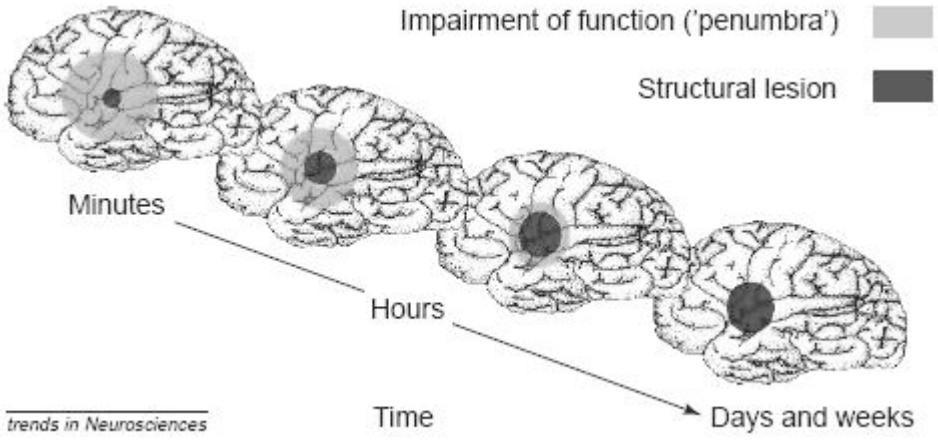

Figure 1: Regression of the functional neurological deficit while the structural lesion grows. Early in the course of stroke, clinical symptoms mostly reflect an impairment of function (grey) but not necessarily a structural lesion (black, core region). If the blood flow is not restored within hours, the penumbral region will become part of the core region (from Dirnagl *et al*., 1999).

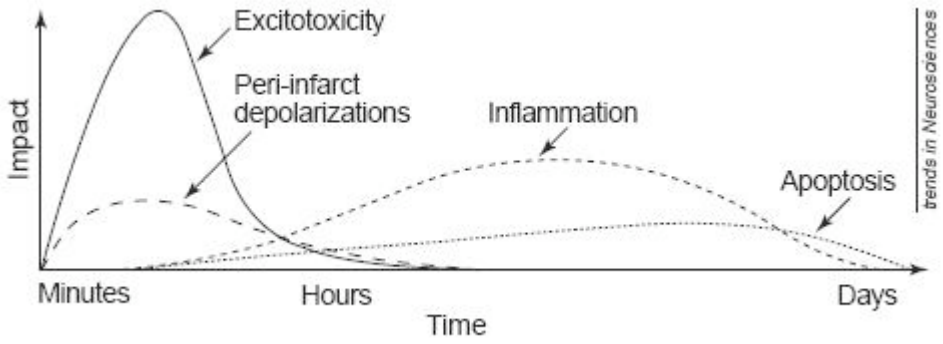

Figure 2: Graph representing the temporal profile of the main pathophysiological mechanisms underlying acute focal cerebral ischemia. Very early after the onset of the occlusion, excitotoxic mechanisms can damage neurones. Excitotoxicity triggers a number of events that can further contribute to the demise of the tissue. These include peri-infarct depolarizations and the more-delayed mechanisms of inflammation and programmed cell death. The x-axis reflects the evolution of the cascade over time, while the y-axis aims to illustrate the impact of each element of the cascade on final outcome (from Dirnagl *et al*., 1999).

Since this region lies outside the ischemic area, shrinkage of the ipsilateral thalamus after MCAO seems to be a secondary ischemic neuronal damage that takes a long time to develop (several months) (Fujie *et al*., 1990). This process is of considerable clinical interest, as the critical period during which this neurodegeneration may be blocked offers a large window for therapeutic intervention. Moreover, this retrograde neurodegeneration is clinically well identified (Tamura *et al*., 1991) and thalamic damage is frequently associated with aphasia and severe memory impairment in humans (Bogousslavsky *et al*., 1988).

The process of cellular injury and death are very different in these regions. Indeed, there appear two major modes of cell death that participate in ischemic cell death: necrosis and apoptosis (MacManus and Buchan, 2000; Unal-Cevik *et al*., 2004). While necrosis is mostly dominant in the core tissue, penumbral cells die by means of either mode, with apoptosis being more common for cells further away from the core (Smith, 2004). Thalamic secondary ischemic neuronal damage seems to be apoptotic as judged by morphological features (Soriano *et al*., 1996). However, unlike the infarct area, very little attention has been paid to the molecular mechanisms that underlie the vulnerability of thalamic neurons to ischemia. In particular, it is unclear whether apoptotic-related cell death genes are involved in these secondary changes induced by permanent focal ischemia.

2.4. Modes of neuronal cell death following ischemic stroke

Until the 1980s, it was believed that neuronal death following acute brain ischemia occurred only via the mechanism of necrosis. However, later studies elucidated the role of apoptosis which is a programmed cell death. The term apoptosis was proposed in 1972 by English scientists Kerr, Wyllie and Currie. They coined this term from the Greek word meaning “falling off”, as leaves do in autumn, to describe this natural, timely death of cells that is realized via cell fragmentation to apoptotic bodies, which are then consumed by the adjacent phagocytosing cells. Following brain ischemia dying cells may be subdivided into two categories. In the severely affected tissue, the necrotic process predominated and is characterized to be passive, very rapid, and followed by the uncontrolled release of inflammatory cellular contents. However, there is an increasing

morphological and biochemical evidence indicating that in the ischemic brain, apoptosis occurs next to necrosis.

2.4.1 *Necrosis and apoptosis: Morphological features*

In the necrotic mode of cell-death, an energy-independent mode of death, the cells suffer a major insult, resulting in cell swelling, formation of cytoplasmic vacuoles, distended endoplasmic reticulum, condensed, swollen or ruptured mitochondria, disrupted organelle membranes, swollen and ruptured lysosomes, and eventually disruption of the cell membrane (Trump *et al*., 1997). This loss of cell membrane integrity results in the release of the cytoplasmic contents into the surrounding tissue, sending chemotatic signals with eventual recruitment of inflammatory cells.

Apoptosis is an energy-dependent physiological process that leads to cellular self-destruction (Kroemer *et al.*, 2009). In contrast to the necrotic mode of cell-death, membrane integrity is preserved during apoptosis. Apoptotic cells can be recognized by stereotypical morphological changes: the cell shrinks, shows deformation and looses contact to its neighbouring cells. Its chromatin condenses and marginates at the nuclear membrane, the plasma membrane is blebbing or budding, and finally the cell is fragmented into compact membrane-enclosed structures, called 'apoptotic bodies' which contain cytosol, the condensed chromatin, and organelles (Figure 3). The apoptotic bodies are engulfed by macrophages and thus, unlike necrosis, are removed from the tissue without causing an inflammatory response. Those morphological changes are a consequence of characteristic molecular and biochemical events occurring in an apoptotic cell, most notably the activation of proteolytic enzymes, named caspases (see section 3.8.4.), which mediate the cleavage of DNA into oligonucleosomal fragments as well as the cleavage of a multitude of specific protein substrates which usually determine the integrity and shape of the cytoplasm or organelles (Saraste and Pulkki, 2000).

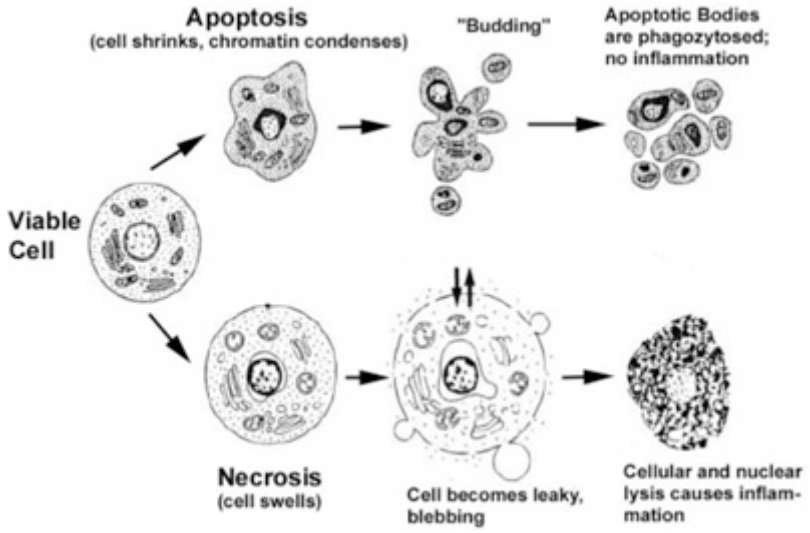

Figure 3: Hallmarks of the apoptotic and necrotic cell death process. Apoptosis includes cellular shrinking, chromatin condensation and margination at the nuclear periphery with the eventual formation of membrane-bound apoptotic bodies that contain organelles, cytosol and nuclear fragments and are phagocytosed without triggering inflammatory processes. The necrotic cell swells, becomes leaky and finally is disrupted and releases its contents into the surrounding tissue resulting in inflammation. Modified from Van Cruchten and Van Den Broeck (2002).

2.4.2 *Methodology for detecting apoptosis in situ: DNA Fragmentation*

There are many ways of detecting apoptosis at different stages on histological sections (Galluzzi *et al.*, 2009a). One commonly used method is called TUNEL (Terminal deoxynucleotidyl Transferase Biotin-dUTP Nick End Labeling). One of the major characteristics of apoptosis is the degradation of DNA after the activation of endonucleases. This DNA cleavage leads to strand breaks within the DNA. The TUNEL method identifies cells with DNA strand breaks *in situ* by using terminal deoxynucleotidyl transferase to transfer biotin-dUTP to the cleaved ends of the DNA. The dUTP can then be labeled with a variety of probes to allow detection by light microscopy. However, necrosis can also result in similar DNA cleavage and cell death may display mixed features, with signs of both apoptosis and necrosis, a fact that lead to the introduction of new terms like “aponecrosis” (Kroemer *et al.*, 2009). Therefore, it is currently highly recommended to

demonstrate cell death with additional methods or complementary techniques recently reviews by Galluzzi *et al.* (2009a).

3. Ischemic cascade of events

Within minutes of vascular occlusion a complex sequence of pathophysiological spatial and temporal events (ischemic cascade) occurs. These series of biochemical reactions constitute the ischemic cascade. These events are interconnected in complex ways. Major pathogenic events occurring after permanent MCAO include energy failure, elevation of intracellular Ca^{2+} level, excitotoxicity, spreading depression, production of free radicals, blood–brain barrier (BBB) disruption, inflammation and apoptosis. Each step in this complex, interdependent series of events offers a potential point to intervene and prevent neuronal death (Figure 4).

3.1. Energy failure

The first consequence of CBF reduction is the depletion of substrates, particularly oxygen and glucose, which are necessary for energy production. Because energy is depleted, the cell cannot maintain ion gradients and membrane depolarization occurs (Phan *et al*., 2002). Membrane depolarization allows opening of voltage-operated calcium channels resulting in a disruption of normal regulation of neuronal calcium homeostasis. Calcium enters the cells causing the release of neurotransmitters from the presynaptic neuron, notably glutamate.

3.2. Excitotoxicity

After depolarization, excitotoxic amino acids, especially glutamate, are released into the extracellular compartment from presynaptic neurons in large amounts, already in the very early phase of ischemia. Excitotoxicity is based on an overstimulation of glutamate receptor subtypes (Bano and Nicotera, 2007) that act as ligand-gated Ca^{2+}-channels. Their prolonged activation results in a non-physiological increase of the intracellular Ca^{2+} levels and constitutes a death-

signaling event leading necrosis but that can also initiate molecular events that lead to apoptosis (Dirnagl *et al.*, 1999).

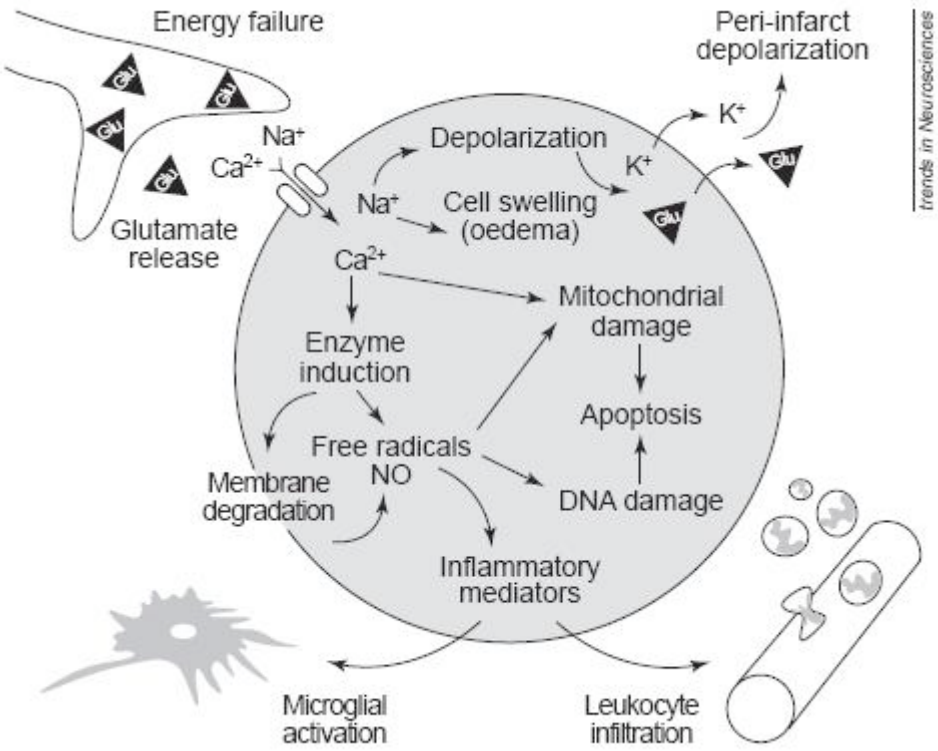

Figure 4: Simplified overview of molecular injury pathways leading to ischemic cell death. Energy failure leads to the depolarization of neurones. Diffusion of glutamate in the extracellular space can propagate a series of spreading waves of depolarization (peri-infarct depolarizations). Water shifts to the intracellular space via osmotic gradients and cells swell (edema). The intracellular messenger Ca^{2+} overactivates numerous enzyme systems (proteases, lipases, endonucleases, etc.). Free radicals are generated, which damage membranes, mitochondria and DNA, in turn triggering caspase-mediated cell death (apoptosis). Free radicals also induce the formation of inflammatory mediators, which activate microglia and lead to the invasion of inflammatory cells (leukocyte infiltration) via up-regulation of endothelial adhesion molecules. Injury pathways can be blocked at numerous sites, providing multiple approaches for the amelioration of both necrotic and apoptotic tissue injury (from Dirnagl *et al.*, 1999)

3.3. Spreading depression

It is recognized that cellular injury within the penumbral region may also occur from recurrent waves of spreading depression starting from within the ischemic core and extending outwards to surrounding normal tissue (Hartings *et al*., 2003; Dreier *et al*., 2006). Spreading depression is of pathological importance as it consumes energy and increases infarct volume (Mies *et al*., 1993). The most likely source for these depolarizations is the elevated extracellular K^+ level and increase in the glutamate release at the boundaries between the ischemic core and the penumbra (Dijkhuizen *et al*., 1999). This is probably, at least partly, why glutamate antagonists reduce the volume of brain infarcts because these drugs are potent inhibitors of spreading depression (Iijima *et al*., 1992).

3.4. Calcium toxicity

The excitotoxic elevation of intraneuronal Ca^{2+} is one of the major events during glutamate excitotoxicity and cerebral ischemia in mediating brain injury. Pathological increased flux of Ca^{2+} into the cytoplasm leads to the activation of numerous lipases and phosphatases. In an apparent attempt to prevent these potentially lethal events and to ensure that homeostasis is maintained, Ca^{2+} is sequestered by mitochondria leading mitochondrial disturbances (Siesjö *et al*., 1999). Vast mitochondria Ca^{2+} sequestration contributes to the activation of the permeability transition pore. Permeability transition pore opening (Siesjo *et al*., 1999) results in cell death because it causes an arrest of aerobic adenosine triphosphate (ATP) synthesis, loss of the mitochondrial transmembrane potential, rupture of the outer mitochondrial membrane, release of calcium from mitochondrial matrix and release of pro-apoptotic factors (see section 3.8.). As a result of formation of cytotoxic products such as free radicals, irreversible mitochondrial damage, and inflammation, both necrotic and apoptotic cell death are triggered by excess of intracellular Ca^{2+} (for a review see Lipton, 1999) (Figure 5).

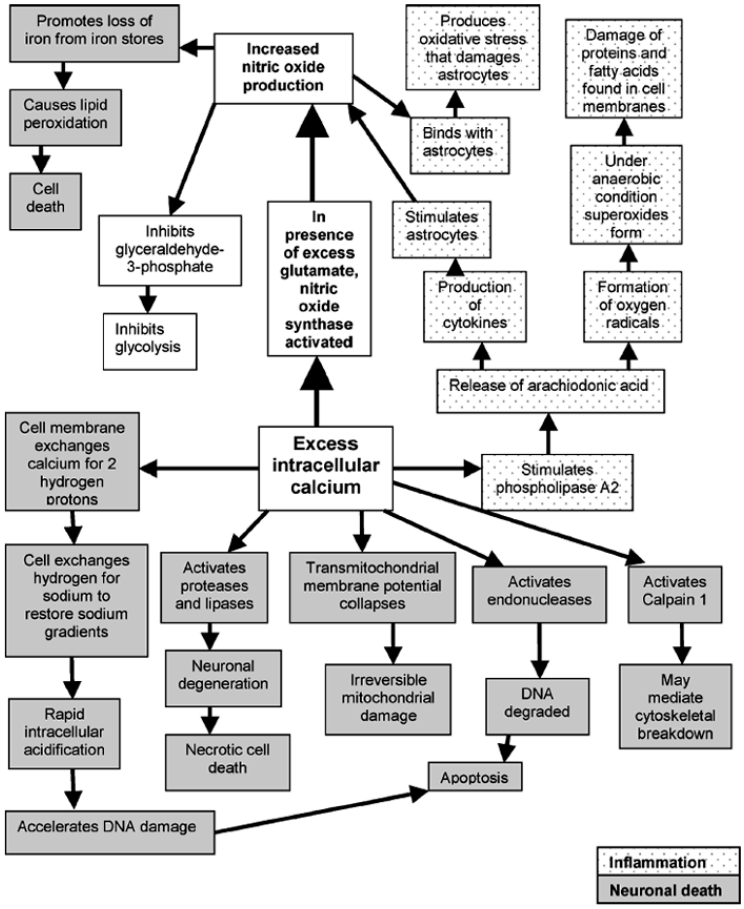

Figure 5: Destructive phenomena precipitated by excess intracellular calcium (from McIlvoy, 2005).

3.5. Generation of reactive oxygen species and anti-oxidant defense mechanisms

3.5.1. *Reactive oxygen species production following ischemia*

ROS (reactive oxygen species) is an acronym used to describe a variety of molecules and free radicals (chemical species with one unpaired electron) derived from molecular oxygen. Following cerebral ischemia, whereas oxygen levels are depleted, there is a paradoxical rise in ROS species. Numerous reports suggest that mitochondria are the major source of ROS (Kudin *et al*., 2008) during transient/permanent focal and global cerebral ischemia (Dirnagl *et al*., 1995; Murakami *et al*., 1998; Peters *et al*., 1998). Among the many features accompanying mitochondrial permeability transition induced by ischemia, loss of GSH, cytochrome c, substrates and pyridine nucleotides are characteristic and

lead to a paradoxical increase in ROS production from the impaired mitochondria. This occurs by multiple means: (a) loss of GSH from the matrix decreases the antioxidant capacity resulting in an increase in the amount of ROS (Anderson and Sims, 2002); (b) loss of cytochrome c impairs the flow of electrons in the respiratory chain inducing overreduction of the complexes, favouring the generation of ROS (Andreyev *et al.*, 2005); (c) reduction in the matrix concentration of electron acceptors, i.e. NAD+, results in ROS emission from the α-ketoglutarate dehydrogenase complex (Starkov *et al.*, 2004). ROS are also a byproduct of ATP generation in mitochondria via the electron transport chain. Electrons escape from the chain and reduce O_2 to the superoxide anion $O_2^{-\bullet}$ (Maier and Chan, 2002). Under mitochondrial stress induced by ischemia, when electron transport chain slows down, this production of $O_2^{-\bullet}$ is greatly increased (Chan, 2001). Because $O_2^{-\bullet}$ formation overrides the anti-oxidant defense of the cell (see below), $O_2^{-\bullet}$ is not detoxified but it may generate free radicals directly involved in oxidative damage in ischemic conditions (for a review see Lipton, 1999). Superoxide anions may react with nitric oxide ($NO^{\cdot}$) to form highly reactive peroxynitrite ($ONOO^{-}$) and with hydrogen peroxide (H_2O_2) in the presence of Fe^{2+} to form hydroxyl radicals ($O_2^{-\bullet} + H_2O_2 \rightarrow OH^{\bullet} + OH^{-}$). Hydroxyl radicals are extremely reactive, and rapidly attack unsaturated fatty acids in membranes causing lipid peroxidation as well as membrane proteins, impairing their functions. Peroxynitrite is a mediator of neurodegeneration that may damage and kill cells by induction of lipid peroxidation and protein tyrosin nitration. Peroxidation of lipids can disrupt the organization of the membrane, causing changes in fluidity and permeability, inhibition of metabolic processes, and alterations of ion transport (Nigam and Schewe, 2000). Damage to mitochondria induced by lipid peroxidation can lead to further ROS generation (Green and Reed, 1998). In addition, lipid peroxides degrade to reactive aldehyde products, including malondialdehyde (MDA) which may serve as indicators of oxidative stress *in vivo* (Arsenijevic *et al.*, 2001).

Monoamine oxidases, located in the mitochondrial outer membrane, are also generators of ROS. Their potential for H_2O_2 generation may exceed that of other mitochondrial sources and they may be a major source of H_2O_2 in tissues following ischemia (Andreyev *et al.*, 2005).

ROS can also be generated intracellularly from the NADPH oxidase system, a complex enzyme system that is present in phagocytes. Another consequence of focal cerebral ischemia is a drop in ATP levels due to ATP increased utilization to maintain normal cell functions. As ATP levels drop, its metabolites including hypoxanthine increase. Superoxide anion is generated following the degradation of hypoxanthine by the xanthine oxidase enzyme (Lo *et al.,* 2003). Free radicals are also generated during the inflammatory response after ischemia (Lo *et al*., 2003).

The ROS are involved in mitochondrial disturbances by causing damage to mitochondrial DNA (Salazar and Van Houten, 1997) and facilitating the mitochondrial transition pore formation that lead to the passage of high molecular solutes, including apoptosis-related protein, from the matrix to the cytosol (Chan, 2001; Kroemer and Reed, 2000). ROS may cause oxidative stress with changes in genes and gene expression, alterations in protein structure and membrane phospholipid degradation (Lipton, 1999).

3.5.2. *Cellular anti-oxidant defense mechanisms*

Cells have several anti-oxidant defense mechanisms to counterbalance the potential deleterious effects of ROS (for review see Chan *et al.*, 2001). The accumulation of ROS can initially be counteracted by anti-oxidative factors including superoxide dismutase (SOD), glutathione peroxidase (GPx), and catalase. Other small molecular anti-oxidants, including glutathione (GSH) and ascorbic acid are also involved in the detoxification of free radicals. It is of importance to note that only when ROS are overproduced, the endogenous anti-oxidative mechanisms become exhausted and cell damage takes place (Nicotera, 2002). Based on their cellular distribution and anatomical localization, three types of SODs exist in brain cells. Copper/zinc SOD (CuZnSOD) is a major cytosolic enzyme, manganese SOD (MnSOD) is a mitochondrial enzyme, whereas extracellular SOD is an isoform that is localized in extracellular space, cerebrospinal fluid, and cerebral vessels. All three SOD isoforms detoxify $O_2^{-\bullet}$ to H_2O_2, which is scavenged by peroxisomal catalase or GPx, at the expense of GSH (Figure 6). The tripeptide GSH is a major cellular thiol participating in cellular redox regulations and exhibits several functions in the brain chiefly acting as a

major anti-oxidant. The synthesis of GSH is mostly located in glial cells in the brain providing precursors that neurons require to make their own GSH (Bharath *et al.*, 2002). Synthesized in the cytosol of cells, a fraction of cytosolic GSH is transported into the mitochondrial matrix where it plays a critical role in defending mitochondria against oxidants through control of mitochondrial electron transport chain-generated oxidants. Hence its regulation may be a key target to influence cell death following ischemia (Chan, 2001). Glutathione is regenerated from oxidized GSH by GSH reductase (GR) in the presence of NADPH (Figure 6). Glutathione peroxidase is also primarily located in glial cells in the brain. There is evidence indicating low efficiency of the GSH system in detoxifying H_2O_2 in neurons compared with its efficiency in astroglial cells (Iwata-Ichikawa *et al.*, 1999). Although neurons have MnSOD, the fact that GPx has been described mainly in glia suggests an interaction between neurons and glia in order to defend the brain against free radical toxicity. The role of ROS in the pathophysiology of cerebral ischemia is further confirmed with the use of genetically modified mice with altered levels of anti-oxidant enzymes (for review see Chan, 2001). As an example, MnSOD-deficient mice have increased mitochondrial infarct size and neurologic deficit, whereas MnSOD overexpression increased mitochondrial tolerance (Silva *et al*., 2005).

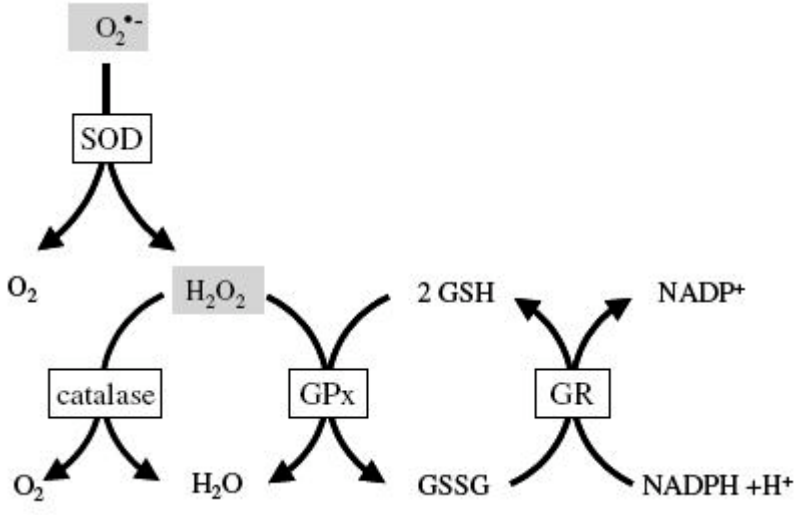

Figure 6: anti-oxidant mechanisms are present in the cell that removes ROS. Superoxide ($O_2^{\bullet-}$), a by-product of the mitochondrial respiratory chain, is dismutated by SODs to oxygen and H_2O_2. This peroxide is further reduced to water by glutathione peroxidase (GPX) and/or catalase to avoid possible build up of oxidative stress. GSH serves as electron donor for the reactions catalyzed by GPx and is oxidized to GSSG. The GSH consumed in the GPx reaction is regenerated by GR in a reaction that requires NADPH as cosubstrate (from Dringen, 2005).

3.6. Blood-brain barrier disruption

Besides cerebral cellular damage, oxidative stress is an early stimulus of BBB disruption through activation of matrix metalloproteinases and through endothelial cell damage (Brouns and De Deyn, 2009). BBB disruption leads to vasogenic edema, influx of toxic substances, inflammation, and presumably hemorrhagic complications after stroke. Brain edema aggravates the ischemic process by its volumetric effect causing to local compression of microcirculation, rise of intracranial pressure, and dislocation of parts of the brain. Finally, the BBB disruption facilitates transmigration of inflammatory cells, promoting the inflammatory response.

3.7. Inflammation

Inflammation is generally a beneficial response of an organism to infection but, when prolonged or inappropriate, it can be detrimental. Neuronal loss in acute brain ischemic injury has been associated with inflammatory processes (Brouns and De Deyn, 2009). Brain inflammation is characterized by activation of microglia and astrocytes, expression of key inflammatory mediators, but limited invasion of circulating immune cells. Inflammation induces rapid expression of key inflammatory mediators – cytokines, chemokines – which in turn up-regulate adhesion molecules, increase permeability of the BBB, facilitating invasion of peripheral immune cells, induce release of potentially toxic molecules and compromise brain cells. All these events may further amplify tissue damage by many mechanisms. In addition, the inflammatory reaction might also be linked to apoptosis because of production of toxic mediators by activated inflammatory cells and because blockade of these mediators attenuate post-ischemic inflammation and reduce apoptotic cell death in the ischemic brain (Dirnagl *et al*., 1999). Post-ischemic inflammation is, therefore, a promising target for therapeutic intervention in ischemic stroke.

3.7.1. *Cellular types and inflammation*

Several cell types contribute to post-ischemic inflammation. First of all, microglia and astrocytes are activated by ROS. Astrocytes may protect neurons by multiple mechanisms, including nerve growth factor synthesis but also contribute to cell death (Stoll *et al*., 1998). They are capable of secreting inflammatory factors such as cytokines and chemokines (Brouns and De Deyn, 2009). Twenty-four hours after focal ischemia, an intense microglial reaction develops in the ischemic tissue, particularly in the penumbra, and within days most microglial cells transform into phagocytes (Morioka *et al*., 1993). Macrophages and microglial cells contribute to tissue recovery by scavenging necrotic debris. They can also release a variety of substances many of which are cytotoxic and/or cytoprotective. Resident microglial activation precedes macrophage infiltration and the vast majority of macrophages in the infarcted area are derived from local microglia (Schilling *et al*., 2003). Few hours after ischemia onset, circulating leukocytes (neutrophils, lymphocytes and monocytes) migrate into the brain, release more pro-inflammatory mediators leading to secondary injury of the penumbra (Brouns and De Deyn, 2009). Adhesion molecules play a pivotal role in the infiltration of leukocytes into the brain parenchyma (Stoll *et al*., 1998). Whereas neutrophils are the first leukocyte subtype cells to arrive to the ischemic tissue, infiltration of monocytes starts only after a delay of several days (Brouns and De Deyn, 2009). Infiltrating leukocytes, as well as resident brain cells, including neurons and glia, may release pro-inflammatory mediators, such as cytokines, chemokines and oxygen/ nitrogen free radicals that contribute to the evolution of tissue damage.

3.7.2. *Pro-inflammatory and anti-inflammatory cytokines*

Cytokines are important inflammatory mediators that are produced by immune cells and resident brain cells after ischemia. They are primary mediators of the inflammatory response. The most studied cytokines related to inflammation in stroke are interleukin-1β (IL1β), tumor necrosis factor-α (TNFα), interleukin-6 (IL6), interleukin-10 (IL10), nerve growth factor (NGF), interferon-γ (IFNγ) and transforming growth factor-β (TGFβ). Among those cytokines, IL1, IFNγ and IL6

appear to exacerbate cerebral injury whereas IL10, TGFβ and NGF may be neuroprotective. Pleiotropic functions are described for TNFα.

3.7.2.1. *Pro-inflammatory cytokines*

The pro-inflammatory cytokine IL1β is the main pro-inflammatory cytokine and represents a crucial mediator of neurodegeneration induced by cerebral ischemia in rodents. IL1β is synthesized as a precursor molecule, pro-IL1β, which is cleaved and converted into the biologically active form of the cytokine by caspase-1, formerly referred to as interleukin-1β-converting enzyme (Thornberry *et al.*, 1992). Consistent with a potential damaging effect, increased IL1β mRNA in blood mononuclear cells was associated with worse neurological outcome in ischemic stroke patients (Kostulas *et al.,* 1999), and acute stroke patients showed a positive correlation of plasma IL1β levels with poor clinical outcome at 3 months (Mazzotta *et al.*, 2004). In rodents, IL1β protein levels increase very early following permanent MCAO (Davies *et al.*, 1999) and both systemic administration of IL1 receptor antagonist and intracerebral injection of IL1β neutralizing antibody to rats markedly reduces brain damage induced by focal stroke (Yamasaki *et al.*, 1995; Relton *et al.,* 1996). Inhibition of caspase-1 by Ac-YVAD.cmk triggers neuroprotection in rodent models of permanent ischemia (Rabuffetti *et al.,* 2000) further implicating IL1β in ischemic pathophysiology. IL1β expression is closely associated with an up-regulation of endothelial leucocyte adhesion molecule, reaching a peak between 6 and 12 h after the onset of ischemia (Wang and Feuerstein, 1995). The main source of the cytokine are endothelial cells, microglia and macrophages, although it may also be expressed by neurons and astrocytes (Mabuchi *et al.*, 2000).

IFNγ is considered as a key regulator of immune and inflammatory responses. While absent from normal brain parenchyma, it may play a role in T-cell recruitment in stroke. IFNγ induces microgliosis and astrogliosis, synthesis of TNFα, IL1β, chemokines and oxygen free radicals all of which can potentiate ischemic brain damage (Lambertsen *et al.*, 2004). The role of IFNγ in permanent MCAO is controversial, with one group demonstrating an elevated IFNγ mRNA

and another study unable to corroborate this response. IFNγ mRNA is increased in rat brain tissue after permanent MCAO and correlated with the size of the brain lesion at 1 h to 6 days after the lesion, supporting a role for this cytokine in stroke (Li *et al.,* 2001) whereas no relevant induction of IFNγ has been detected in the study of Lambertsen *et al*. (2004), arguing against a major role of endogenous IFNγ in the development of tissue injury following focal ischemia. Invading T-cells are the major source of cerebral IFNγ (Baird, 2006). IFNγ from a non-T-cell source may promote T-cell interactions with the vascular wall and enhance migration of inflammatory cells across the BBB to sites of inflammation in the human central nervous system (Omari and Dorovini-Zis, 2003).

IL6 is largely thought of as a pro-inflammatory cytokine, but its role in ischemic stroke is more obscure. In patients with acute brain ischemia, plasma concentrations of IL6 are strongly associated with stroke severity and long-term clinical outcome (Smith *et al.*, 2004). This is in contrast to the results from animal studies suggesting that IL6 may exert a neuroprotective role during stroke (Loddick *et al.*, 1998).

3.7.2.2. *Anti-inflammatory cytokines*

To restrain inflammation, pro-inflammatory reactions are closely interconnected with counter-regulatory anti-inflammatory pathways. Amongst these, IL10 and TGFβ have been demonstrated to have anti-inflammatory effects, providing significant protection against ischemic brain damage. IL10 is synthesized in the central nervous system (CNS) and is up-regulated in experimental stroke (Strle *et al.*, 2001). Patients with acute ischemic stroke have high IL10 concentrations in cerebrospinal fluid (Tarkowski *et al*., 1997) and an elevated numbers of peripheral blood mononuclear cells secreting IL10 (Pelidou *et al*., 1999). Furthermore, subjects with low IL10 levels have an increased risk of stroke (van Exel *et al.,* 2002). IL10 acts by suppressing the expression of cytokine receptors as well as the production of the pro-inflammatory molecules IL1β and TNFα (Sawada *et al.,* 1999). Both gene transfer (Ooboshi *et al*., 2005) and exogenous administration of IL10 (Spera *et al*., 1998) in cerebral ischemia models have beneficial effects. However, these studies were undertaken on post-ischemic exogenous

administration of this cytokine (Spera *et al.*, 1998; Ooboshi *et al.*, 2005). To investigate the impact of chronic IL10 up-regulation on the outcome of ischemia, we recently produced transgenic mice over-expressing murine IL10. Our data indicate that constitutive IL10 over-expression is associated with a striking resistance to cerebral ischemia that may be attributed to changes in the basal redox properties of glial/endothelial cells (see Annexe).

Expression of TGFβ has been reported to increase in microglia and astrocytes in animal models of cerebral ischemia, with low levels in neurons (Flanders *et al.*, 1998). Overexpression of TGFβ using an adenoviral vector protected mouse brains from focal ischemia and this neuroprotective effect may result from the inhibition of chemokines (Pang *et al.*, 2001). More recent investigations showed that cultured neurons may be protected from ischemia-like insults by microglia-secreted TGFβ (Lu *et al.*, 2005). Because the increase in TGFβ message generally occurs several days after the ischemic insult, it is proposed that TGFβ may contribute to the recovery of ischemic stroke (Flanders *et al.*, 1998).

Neuroprotective effects of NGF have been demonstrated *in vivo* following permanent cerebral ischemia (Guegan *et al.*, 1998). The neuroprotective effect of NGF involved the impairment of apoptotic cell death as well as the enhancement of anti-oxidant enzyme activities (Guegan *et al.*, 1999). In addition, NGF mRNA levels are enhanced following MCAO (Lindvall *et al.,* 1992). Although NGF is expressed in neurons, *in vitro* study evidenced for NGF production and NGF-like activity in astrocytes (Furukawa *et al.*, 1986) and *in vivo studies* confirmed NGF expression in astrocyte-like cells after brain injury (Lee *et al.*, 1998).

3.7.2.3. *The dual functions of TNFα*

TNFα has pleiotropic functions and may influence apoptosis or survival through different pathways (Hallenbeck, 2002). During the first hours after the ischemic insult, expression of TNFα is increased in neurons; at later stages expression is observed in microglia / macrophages and in cells of the peripheral immune system (Stoll *et al.*, 1998). To date, the role of TNFα has not been fully clarified.

Inhibition of TNFα reduces brain infarction in rats subjected to permanent MCAO (Barone et al., 1997; Yang *et al.,* 1998). However, neuronal damage caused by focal brain ischemia is exacerbated in mice genetically deficient in p55 TNF receptors (Bruce *et al.*, 1996). The pleiotropic activities of TNFα might be due to different pathways through which TNFα signals. There are at least two TNFα receptors, namely p55 and p75TNF. Deletion of the p55 gene results in increased brain damage, as compared with wild-type (WT) and p75-deficient mice following transient focal ischemia (Gary *et al.,* 1998). Moreover, ischemic preconditioning caused up-regulation of neuronal p55 receptor up-regulation (Pradillo *et al.*, 2005). However, as both receptors may activate intracellular mechanisms contributing either to the induction of cell death mechanisms or to anti-inflammatory and anti-apoptotic functions, the roles of p55 and p75 in modulating cell death／survival remain unclear (Hallenbeck, 2002).

3.7.3. *Chemokines*

Chemoattractant cytokines, chemokines, are regulatory polypeptides that mediate cellular communication and leukocyte recruitment in inflammatory and immune responses. Expression of chemokines such as monocyte chemoattractant protein-1, macrophage inflammatory protein-1α and fractalkine following focal ischemia is thought to have a deleterious effect by increasing leukocyte infiltration (Stamatovic *et al.,* 2003). In addition to chemotactic properties, chemokines were found to also participate BBB 'opening' during the transmigration of monocytes (Dimitrijevic *et al.,* 2006). Astrocytes, as well as neurons possess cell surface receptors specific for various chemokines (Hesselgesser and Horuk, 1999; Stumm *et al*., 2002).

3.8. Apoptosis

Triggered by a number of processes, including excitotoxicity, ROS formation, inflammation, mitochondrial and DNA damage, and cytochrome c release from mitochondria, apoptosis occurs after ischemic injury, particularly within the ischemic penumbra (MacManus and Buchan, 2000).

3.8.1. *Mechanisms of apoptosis*

The mechanisms of apoptosis are highly complex and sophisticated, involving an energy-dependent cascade of molecular events.

To date, research indicates that there are two main apoptotic pathways: the extrinsic or death receptor pathway (Valmiki and Ramos, 2009) and the intrinsic or mitochondrial pathway (Galluzzi *et al.*, 2009b). However, there is now evidence that the two pathways are linked and that molecules in one pathway can influence the other. The extrinsic and intrinsic pathways converge on the same terminal, or execution pathway. This pathway is initiated by the cleavage of caspase-3 whose active fragment induces DNA fragmentation, degradation of cytoskeletal and nuclear proteins, cross-linking of proteins, formation of apoptotic bodies, expression of ligands for phagocytic cell receptors and finally uptake by phagocytic cells.

3.8.2. *Signaling pathways to apoptosis*

The extrinsic pathway of apoptosis (Figure 7) begins outside the cell and is mediated by the activation of so-called “death receptors” which are cell surface receptors that transmit apoptotic signals after ligation with specific ligands like TNF or FAS. Death receptors belong to the tumor necrosis factor receptor (TNFR) gene superfamily, including Fas/CD95, and the TRAIL receptors DR-4 and DR-5 (Ashkenazi, 2002). Ligand-mediated activation of these receptors promotes activation of pro-caspase-8 (Benchoua *et al.*, 2001). Activated caspase-8 functions as an initiator caspase, leading to the subsequent cleavage and activation of effector caspases, such as caspase-3, -6 and -7. This results in the cellular destruction of proteins and thus, to cell death (Slee *et al.*, 1999). Hybrid mice that are deficient in both Fas and TNF expression are strongly resistant to ischemic injury compared with the WT strain (Martin-Villalba *et al.,* 1999). Extensive signaling crosstalk exists between the extrinsic and intrinsic cell death pathways, as in certain situations, the intrinsic pathway is required for the full induction of the receptor-mediated extrinsic induction of apoptosis (Yin *et al.*, 2002).

The intrinsic pathway of apoptosis (Galluzzi *et al.*, 2009b) (Figure 7), referred to as the mitochondrial pathway, is triggered by intracellular stimuli such as Ca^{2+} overload and overgeneration of ROS. Mitochondria are pivotal regulators of cell death through their role in energy production, cellular calcium homeostasis, production of reactive oxygen species and capacity to release apoptogenic proteins. Consequently, mitochondria are emerging as the target of choice for therapeutic intervention. The stimuli that initiate the intrinsic pathway produce intracellular signals that may act in either a positive or negative fashion. Negative signals involve the absence of certain growth factors, hormones and cytokines that can lead to failure of suppression of death programs, thereby triggering apoptosis. Other stimuli that act in a positive fashion include radiation, toxins, hypoxia, hyperthermia, viral infections, free radicals or other types of severe cell stress. All of these stimuli cause changes in the inner mitochondrial membrane, increased levels of intracellular calcium as well as oxidative stress. These may result to the opening of the mitochondrial permeability transition pore, loss of the mitochondrial transmembrane potential which lead to mitochondrial swelling and release of apoptogenic factors such as cytochrome c and SMAC/DIABLO from the intermembrane space into the cytosol (Henry-Mowatt *et al*., 2004; Galluzzi *et al.*, 2009b) that activate cell death cascades (mitochondria-mediated cell death).
Cytochrome *c* binds and activates Apaf-1 (apoptotic protease-activating factor 1) as well as pro-caspase-9, forming an “apoptosome” (Hill *et al*., 2004). The apoptosome then recruits and activates caspase-9, which, in turn, activates the downstream effector caspases, including caspase-3, thereby converging on the extrinsic pathway and leading to apoptosis (Henry-Mowatt *et al*., 2004; Galluzzi *et al.*, 2009b). The loss of cytochrome *c* from the intermembrane space also favours apoptosis through the mitochondrial formation of $O_2^{-\bullet}$ as a consequence of electron flow slow down (Cai and Jones, 1998). Under normal conditions, caspase activity is held in check by a protein family known as inhibitor of apoptosis proteins (IAPs), of which at least 10 have been identified (Lavrik *et al.*, 2005). As part of the intrinsic apoptosis pathway, the SMAC/DIABLO protein released from the mitochondria promotes apoptosis by directly interacting with IAPs and disrupting their ability to inactivate the caspase enzymes (Henry-Mowatt *et al*., 2004; Galluzzi *et al.*, 2009b). Since the release of mitochondrial proteins is

of central importance in mediating and enhancing apoptotic pathways, those mitochondrial events must be kept under strict control of regulatory mechanisms which are in many ways dependent on members of the Bcl-2 family which will be discussed in the next section.

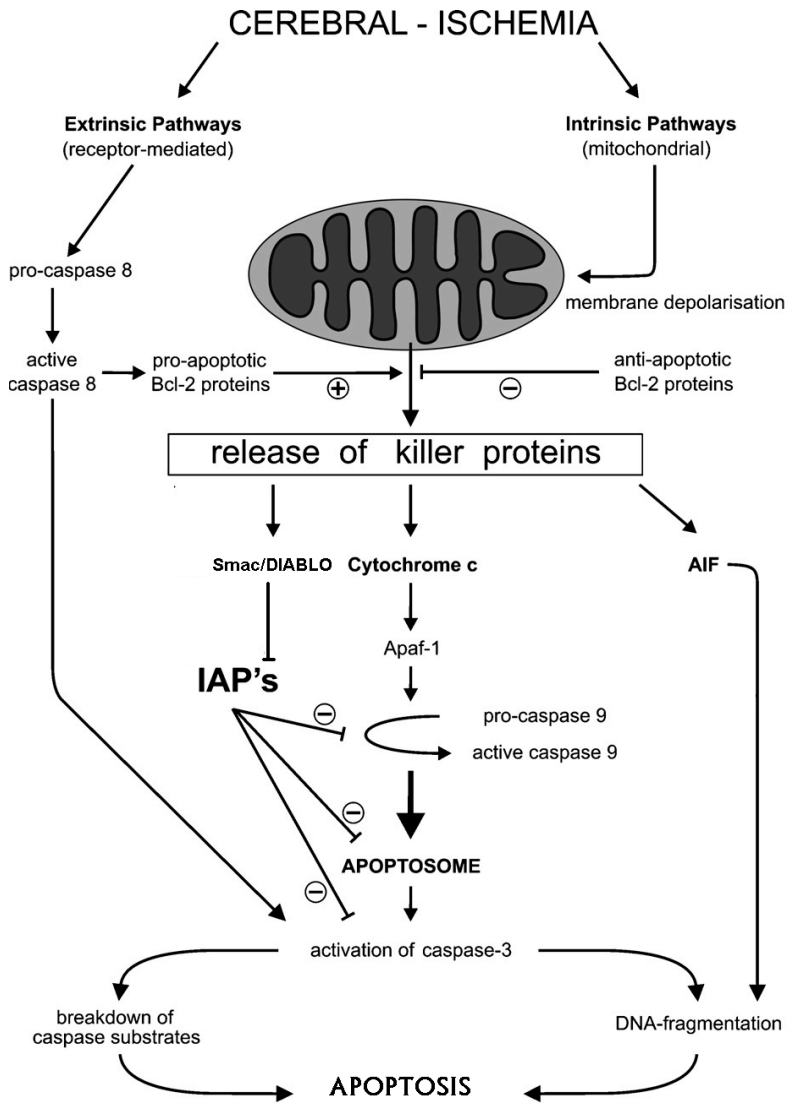

Figure 7: Following cerebral ischemia, neuronal cell death may proceed via the intrinsic (mitochondrial) pathway. In this pathway, intracellular stress signals are mediated through the Bcl-2 family of proteins. Upon activation, proapoptotic members of the Bcl-2 family trigger the release of killer proteins (cytochrome c, Smac/DIABLO) from the mitochondrial intermembranous space by outer membrane permeabilisation. Cytochrome c is released from the mitochondria and associates with Apaf-1 and then caspase-9 to form the apoptosome. This pathway then converges to the extrinsic pathway at the level of caspase-3 activation. The endogenous protective functions of IAPs which restrain caspase-9 and caspase-3 activity under normal condition, are abolished by Smac/DIABLO which is released from damaged mitochondria. The extrinsic and intrinsic pathways are largely independent, but in certain conditions, the extrinsic pathway engages the mitochondrial one via the activation of Bid, a pro-apoptotic member of the Bcl-2 family (from Rami *et al.*, 2008). Apaf1, apoptotic protease-activating factor 1; AIF, apoptosis-inducing ligand; IAPs, inhibitor of apoptosis proteins.

3.8.3. *The Bcl-2 family of proteins*

The central players of these apoptotic mitochondrial events are members of the Bcl-2 (B-cell lymphoma 2) family of proteins (Cory and Adams, 2002). Some of these proteins (such as Bcl-2 and Bcl-XL) are anti-apoptotic, while others (such as Bad, Bak, Bax or Bid) are pro-apoptotic (for exhaustive review see Danial and Korsmeyer, 2004). It is thought that the main mechanism of action of the Bcl-2 family of proteins is the regulation of cytochrome c release from the mitochondria via alteration of mitochondrial membrane permeability.

Bcl-2 itself, the founding member, is a proto-oncogene first identified at the chromosomal breakpoint of t(14;18) bearing human follicular B cell lymphoma (Bakhshi *et al*., 1985). Located primarily in the outer mitochondrial membrane, it inhibits apoptosis giving birth to the notion that its inhibition could constitute a crucial step in ischemic cell death (see section 4, Article I). Indeed, the anti-apoptotic Bcl-2 proteins act to prevent permeabilization of the mitochondrial outer membrane by inhibiting the action of the pro-apoptotic multi-domain Bcl-2 proteins Bax and Bak (Reed, 1998). Following cellular stress, the pro-apoptotic Bcl-2 proteins which are often found in the cytosol, relocate to the surface of the mitochondria where the anti-apoptotic proteins are located. This interaction between pro- and anti-apoptotic proteins disrupts the normal function of the anti-apoptotic Bcl-2 proteins and can lead to the formation of pores in the mitochondria and the release of cytochrome c. This in turn leads to the formation of the apoptosome and the activation of the caspase cascade. The intrinsic pathway is characterized by the activation of the multi-domain pro-apoptotic proteins Bax or Bak which move to the mitochondrial membrane and disrupt the function of the anti-apoptotic Bcl-2 proteins thereby allowing permeabilization of the mitochondrial membrane. A current model of how Bcl-2 family members regulate apoptosis is described Figure 8.

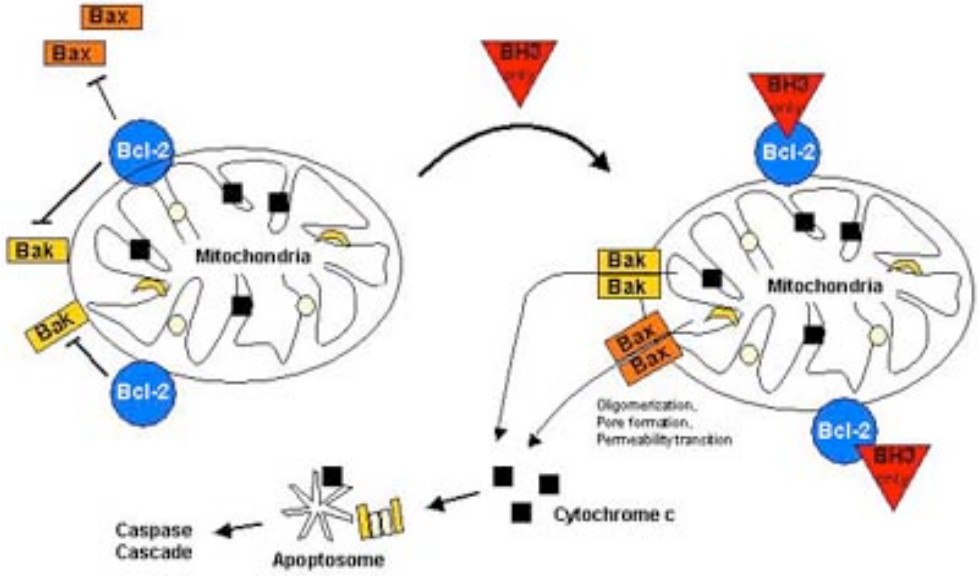

Figure 8: Regulation of apoptosis by the Bcl-2 family.
In a viable cell, the pro-apoptotic Bcl-2 family members Bax, Bak, and BH3-only proteins are antagonized by anti-apoptotic members such as Bcl-2. Specific apoptotic stress signals trigger the activation of particular BH3-only proteins (the sentinels that detect intracellular damage) which then interact with anti-apoptotic Bcl-2 members on the outer mitochondrial membrane, resulting in the release of Bax-like pro-apoptotic factors. Bax-like factors undergo a conformational change, insert into the outer mitochondrial membrane where they provoke permeabilization of the outer mitochondrial membrane, the release of pro-apoptotic factors from the inner mitochondrial membrane into the cytosol, such as cytochrome c, and subsequently activation of the caspase cascade (from Borner, 2003).

3.8.4. *Execution Pathway: Caspases are central initiators and executioners of apoptosis*

The caspases are cysteine proteases (their catalytical activity depends on a critical cysteine-residue) of central importance in the apoptotic signaling network (Galluzzi *et al.*, 2009b). In the cell, caspases are widely expressed in an inactive pro-enzyme form and once activated can often activate other pro-caspases, allowing initiation of a protease cascade. This proteolytic cascade amplifies the apoptotic signaling pathway and thus leads to rapid cell death. Once caspases are initially activated, there seems to be an irreversible commitment towards cell death. To date, the pro-apoptotic caspases can be divided into the group of initiator caspases (caspases-2, -8, -9 and –10), the group of executioner

caspases (caspases-3, -6, and –7) and into the group of inflammatory caspases (caspase-1,-4,-5) (Cohen, 1997; Rai *et al*., 2005). Caspases-1, -8 and -9 are involved in cerebral ischemia (Mergenthaler *et al*., 2004).

The initiator caspases are recruited to and activated at death inducing signaling complexes either in response to the ligation of cell surface death receptors (extrinsic pathways) or in response to signals originating from inside the cell (intrinsic pathways). The extrinsic and intrinsic pathways both end at the point of the execution phase, considered the final pathway of apoptosis. It is the activation of the execution caspases that begins this phase of apoptosis. Execution caspases activate cytoplasmic endonuclease, which degrades nuclear material, and proteases that degrade the nuclear and cytoskeletal proteins. Caspase-3 (also called Cpp32), caspase-6, and caspase-7 function as effector or "executioner" caspases, cleaving various substrates that ultimately cause the morphological and biochemical changes seen in apoptotic cells (Slee *et al*., 2001). Caspase-3 is considered to be the most important of the executioner caspases and is activated by any of the initiator caspases (caspase-8, caspase-9, or caspase-10). Caspase-3 specifically activates the endonuclease CAD (caspase-activated DNAse) (Sakahira *et al*., 1998). CAD then degrades chromosomal DNA within the nuclei and causes chromatin condensation. Caspase-3 also induces cytoskeletal reorganization and disintegration of the cell into apoptotic bodies. Caspase-3 activation may be a downstream event in the apoptotic cascade induced by cerebral ischemia (Phan *et al*., 2002). The importance of caspase-3 activation in ischemic death is underscored by the finding that its inhibition with the highly selective antagonist z-DEVD-fmk significantly protect neurons against ischemic death (Hara *et al*., 1997).

4. Cerebral ischemia and the Bcl-2 protein

Article I: F. de Bilbao, E. Guarin, P. Nef, P. Vallet, P. Giannakopoulos and M. Dubois-Dauphin (2000) Cell death is prevented in thalamic fields but not in injured neocortical areas after permanent focal ischaemia in mice overexpressing the anti-apoptotic protein Bcl-2. *Eur J Neurosc* 12:921-934.

4.1. Bcl-2 mechanism of protection against damage

As described in section 3.8.3., Bcl-2 strongly protects against apoptosis. One way it does this is to prevent cytochrome c release and thus prevent activation of the caspase proteases (Monney *et al.*, 1996; Yang *et al*., 1997). It also protects downstream from the mitochondrial release of cytochrome c (Reed, 1997). *In vitro*, Bcl-2 has been shown to prevent cell death by decreasing the cellular generation of ROS induced by GSH depletion (Kane *et al.*, 1993). Overexpression of Bcl-2 may prevent lipid peroxidation, protect cells from H_2O_2-induced oxidative deaths (Hockenbery *et al*., 1993) and shifts the cellular redox state to a more reduced state by promoting anti-oxidant defenses (SOD and catalase activities) (Ellerby *et al.*, 1996). Enhanced oxidative stress and higher susceptibility to pro-oxidants are evident in the brains of Bcl-2 KO mice (Hochman *et al.*, 1998). In addition, it may block necrotic cell death in conditionally immortalized nigral neurons resulting from exposure to calcium ionophores, glucose withdrawal, membrane peroxidation, free radical formation, and glutamate excitotoxicity (Behl *et al*., 1993; Zhong *et al*., 1993). It has also profound protective effects on mitochondrial function, greatly enhancing maximal Ca^{2+} uptake and reducing the ability of increased mitochondrial Ca^{2+} to impair respiration, presumably by preventing opening of the mitochondrial permeability transition pore (Murphy *et al.*, 1996). These effects are likely to protect against necrotic cell death. As the consequent alteration of calcium homeostasis, lipid peroxidation, and membrane

damage is an important component of glutamate excitotoxicity and ischemic cell death, these data provide evidence that Bcl-2 could constitute a potential therapeutic application in the treatment of stroke.

4.2. Bcl-2 and cerebral ischemia

Permanent MCAO in rats led to a decrease in expression of Bcl-2 and Bcl-X in neurons of the penumbra, the great majority of which go on to die (Gillardon *et al.*, 1996). The author's findings suggest that a shift in the ratio of cell death repressor Bcl-2 to cell death effector Bax may contribute to neuronal apoptosis in the infarcted thalamus and cortex. There is every reason to believe that elevated Bax/Bcl-2 will be damaging and that the elevation of Bcl-2 in nonvulnerable regions may well be protective. In transgenic mice overexpressing Bcl-2, the volume of the brain infarction following permanent MCAO was reduced by 50% (Martinou *et al.*, 1994) whereas Bcl-2 KO mice showed an increased infarct after transient MCAO (Hata *et al.*, 1999). Neuroprotection following permanent/transient MCAO was also reported in rats transfected with viral vectors carrying the bcl-2 gene in cerebral cortex or striatum (Linnik *et al.,* 1995; Lawrence *et al.,* 1996). Using gene therapy, Zhao *et al.* (2003) showed that overexpression of Bcl-2 protects against damage to the infarct margin induced by focal ischemia with and without reperfusion, by inhibiting cytosolic accumulation of cytochrome c and caspase-3 activation. This suggests a potential therapeutic strategy for stroke. Permanent focal ischemia induces Bcl-2 protein synthesis in cortical neurons localized at the margin of infarction (Guegan *et al.*, 1998) suggesting that these neurons may survive ischemic injury. Overexpression of Bcl-2 strongly protects against global ischemia (Antonawich *et al.*, 1998), can protect neural cells from delayed death resulting from chemical hypoxia and may do so by an anti-oxidant mechanism (Myers *et al.*, 1995). However, the role of Bcl-2 in promoting cell survival after ischemia is controversial as Wiessner *et al.* (1999) showed that Bcl-2 transgenic mice did not reveal any reduction of infarct volume after permanent MCAO as assessed by MRI. Therefore the role, as well as the cellular and molecular basis of the anti-apoptotic action of Bcl-2 following ischemia remains to be clarified.

As ischemia is a pathological condition that features excessive apoptosis, it thus may benefit from inhibiting apoptosis with specific agents. Therefore, identification and exploitation of new targets remains a considerable focus of attention. As a potential method of anti-apoptotic therapy to evaluate the potential therapeutic modality of the anti-apoptotic protein Bcl-2 include the use transgenic models of focal cerebral ischemia. Although several reports demonstrated that overexpression of Bcl-2 prevents ischemic neuron damage, the mechanisms underlying neuroprotection by Bcl-2 are not well understood. In Article I, we clarified several issues. First, in order to assess the effects of focal ischemia on the expression of molecules which have been implicated in the regulation of apoptosis, we studied in detail the expression levels of members of the Bcl-2 family*, bax* and *bcl-xl*, as well as *cpp32* (caspase-3) transcripts, in WT mice 1, 3, 7 and 14 days following permanent MCAO. Second, using mice that overexpressed the human Bcl-2 proto-oncogene, we examined whether *in vivo* endogenous Bcl-2 overexpression may prevent neuronal damage by altering the course of these molecular events in the infarcted area. Third, it is well known that neuropathologic changes also occur in distant non-ischemic area (i.e. remote thalamic areas) after focal cerebral ischemia (see section 2.3.); however the mechanisms of cell death involved in these secondary changes remain unclear. Thus, we tested whether 1) the apoptotic-related transcripts *cpp32*, *bax* and *bcl-xl* are induced and 2) Bcl-2 could protect against cell death in these areas.

European Journal of Neuroscience, Vol. 12, pp. 921–934, 2000

Cell death is prevented in thalamic fields but not in injured neocortical areas after permanent focal ischaemia in mice overexpressing the anti-apoptotic protein Bcl-2

Fabienne de Bilbao, Ernesto Guarin,[1] Patrick Nef,[1] Philippe Vallet, Panteleimon Giannakopoulos and Michel Dubois-Dauphin
University Hospital Geneva, Department of Psychiatry, 2, Chemin du Petit Bel-Air, 1225 Geneva, Switzerland
[1]Hoffmann-La Roche, CH-4002 Basel, Switzerland

Keywords: apoptosis, caspase, MCAO, penumbra, thalamus

Abstract

Previous studies have suggested that various apoptotic-related proteins could be involved in the death process induced by cerebral ischaemia. In order to further clarify their role and examine how the anti-apoptotic protein Bcl-2 could influence this process, the time-course of mRNA expression of various cell death genes was studied from 1 to 14 days following permanent occlusion of the middle cerebral artery in wild-type (WT) and Bcl-2 transgenic mice, within and outside the area of infarction. No differences of the infarct sizes were observed between the two groups of mice, showing that the extent of neuronal injury could not have been lowered by the Bcl-2 transgene. Seven days after the ischaemic insult, the mRNA expression of the cell death gene effector *cpp32* was dramatically upregulated in the penumbra of WT and Bcl-2 transgenic mice. Interestingly, the *cpp32* transcript was markedly induced from 3 days in the ipsilateral thalamus of the two groups of mice. However, apoptotic bodies were observed in the thalamic field of WT but not transgenic mice. This suggests that *cpp32* mRNA may be induced in an attempt to kill the injured cells and, in contrast to the penumbra, cell death in the thalamus may be prevented in Bcl-2 transgenic mice. Based on these results, the pathophysiological mechanisms that underly neuronal damage following ischaemia need consideration in order to evaluate the extent of neuroprotection that may be afforded by the Bcl-2 anti-apoptotic protein. Although the present study does not confirm previous data showing a protective role of Bcl-2 in neocortical infarcted areas, it suggests that anti-apoptotic therapies may constitute a possible treatment for areas of the brain remote from those directly affected by ischaemia.

Introduction

In humans, ischaemia is caused by reduced blood supply and most frequently occurs after thrombosis or embolus of the medial cerebral artery (Yates, 1976). Brain tissue directly affected by a stroke can be divided into a necrotic core region and a surrounding penumbral region. The ischaemic penumbra corresponds to those areas which initially have flow rates adequate for survival but which subsequently may become recruited in the infarction process. Although cells of the ischaemic core are destined to die by necrosis, those of the penumbra undergo at least partially a delayed death by apoptosis (Barinaga, 1998) which could be reverted with appropriate pharmacological agents. Besides the penumbral area, subcortical areas which undergo neuropathological changes following cortical ischaemia are also potentially salvageable. Because of its extensive synaptic connections with the cerebral cortex (Jacobson & Trojanowski, 1975), the thalamus undergoes a secondary neuronal degeneration induced by cortical infarct in rats and humans (Fujie *et al*., 1990; Tamura *et al*., 1991). These neurodegenerative changes have been shown to be progressive after occlusion of the middle cerebral artery (MCAO) in the rat (Fujie *et al*., 1990; Hara *et al*., 1993) and seem to be apoptotic as judged by DNA fragmentation (Gillardon *et al*., 1996; Soriano *et al*., 1996). This process is of considerable clinical interest, as the critical period during which this neurodegeneration may be blocked offers a large window for therapeutic intervention. Moreover, this retrograde neurodegeneration is clinically well identified (Tamura *et al*., 1991), and thalamic damage is frequently associated with aphasia and severe memory impairment in humans (Bogousslavsky *et al*., 1988). However, little attention has been paid to the molecular mechanisms that underly the vulnerability of thalamic neurons to ischaemia. In particular, it is unclear whether apoptotic-related cell death genes are involved in these secondary changes induced by permanent focal ischaemia.

Apoptosis is an active process of cell death with organized biochemical events that regulates normal development of the central nervous system (CNS). In the adult brain, apoptotic cell death appears to be a feature of chronic or acute pathological states. The Bcl-2 family of proteins, a major class of apoptotic intracellular regulators, has been identified in mammals (Merry & Korsmeyer, 1997). Some of these proteins, e.g. Bcl-2 and Bcl-xl, prevent apoptosis, whereas others, e.g. Bax, promote it. Bax and Bcl-xl play major roles in regulating cell death during the development of the nervous system (Motoyama *et al*., 1995; Deckwerth *et al*., 1996) and in the adult *in vivo* (Deckwerth *et al*., 1996; Parsadanian *et al*., 1998; White *et al*., 1998). Although Bcl-2 does not play a critical function during development, the Bcl-2 protein has been shown to be a potent inhibitor of cell death following injury and in pathological states

Correspondence: Dr F. de Bilbao, as above.
E-mail: fabienne.debilbao@medecine.unige.ch

Received 10 November 1999, revised 10 November 1999, accepted 29 November 1999

(Dubois-Dauphin *et al.*, 1994; Martinou *et al.*, 1994; Kostic *et al.*, 1997). Caspases or cysteine proteases are important executors of apoptotic cell death as they ensure the proleolytic cleavage of a number of key proteins (Salvesen & Dixit, 1997). Among these proteases, Cpp32 (caspase 3) is an important neuronal death effector in the brain during development (Kuida *et al.*, 1996). In particular, it appears that Cpp32 plays a critical role for developmental cortical cell death, as supernumerary cells were consistently located in the cortex of newborn Cpp32-deficient mice. Several studies have analysed the expression of *bcl-2* and caspase family genes following ischaemia. Following permanent MCAO, the overexpression of *bcl-2* has been thought to partly protect neuronal cells against ischaemia (Martinou *et al.*, 1994). Asahi *et al.* (1997) did not detect any change in the expression of *bcl-2* and *bcl-x* mRNAs, whereas Gillardon *et al.* (1996) showed a decrease of Bcl-2 and Bcl-xl immunostaining in the infarcted cortex and thalamus. *Bax* (Gillardon *et al.*, 1996) and *cpp32* (Asahi *et al.*, 1997) mRNAs are increased in the ischaemic cerebral hemisphere. The Cpp32 activated protease has also been shown to mediate apoptosis in the CNS following transient injury (Chen *et al.*, 1998; Namura *et al.*, 1998).

In order to clarify the molecular events underlying neuronal cell death induced by permanent ischaemia in the cerebral cortex and remote thalamic areas and see whether Bcl-2 overexpression may alter the course of these degenerative events, we studied in detail the expression of *cpp32*, *bax* and *bcl-xl* transcripts in both wild-type (WT) and Bcl-2 transgenic mice 1, 3, 7 and 14 days following permanent MCAO. Unlike previously described (Martinou *et al.*, 1994), our data report that the overexpression of Bcl-2 does not efficiently protect cortical neurons from death. In contrast, we report for the first time that the overexpression of Bcl-2 may favour neuronal survival in remote thalamic areas.

Materials and methods

Surgical preparation

Two-month-old WT male mice (CMU 200-zootechnie; C57BL/6 strain) and transgenic male mice overexpressing the human Bcl-2 proto-oncogene (line 57, Dubois-Dauphin *et al.*, 1994; Martinou *et al.*, 1994) were used in this study. The transgenic mice were backcrossed with the WT ones, which can exclude that the effects of the transgene observed in the present study are a result of a different vascular phenotype of the two strains of mice. Animals were anaesthetized intraperitoneally with chloral hydrate (400 mg/kg), the right temporoparietal region of the head was shaved and a 2-mm incision was made vertically between the orbit and the ear. Under an operating microscope, an incision was made dividing the temporal muscle, and the left lateral aspect of the skull was exposed by reflecting the temporal muscle surrounding soft tissue. A small burr hole (1 mm^2) was made with a high-speed microdrill through the outer surface of the semitranslucent skull just over the visibly identified medial cerebral artery at the level of the parietal cerebral artery. Saline was applied to the area throughout the procedure to prevent heat injury. The inner layer of the skull was removed with fine forceps, the dura and arachnoid were opened, and right MCAO was performed by electrocoagulation (by means of a small-vessel cauterizer) without damaging the brain surface. If the brain surface was visibly damaged or if the middle cerebral artery bled owing to incomplete artery occlusion/coagulation, the animal was killed and not used for the study. The duration of surgery did not exceed 15 min in any case. WT and transgenic mice were allowed to recover postsurgery for 1 day ($n = 3$ for each group), 3 days ($n_{WT} = 2$ and $n_{Bcl-2} = 3$), 7 days ($n_{WT} = 7$ and $n_{Bcl-2} = 4$) and 14 days ($n = 3$ for each group), and processed for *in situ* hybridization. Three animals were not subjected to ischaemia and served as controls. All animal procedures were approved by local animal usage committees (University of Geneva and Canton Veterinary Office).

Probe synthesis

The probe synthesis has been described in a previous study (de Bilbao *et al.*, 1999). Briefly, sense and antisense 35S-labelled riboprobes were synthesized for *in situ* hybridization by incubation of 2 mg of linearized full-length *bax* α, *bcl-xl* or *cpp32*β mouse cDNA clones in pBSK vector, with 200 mCi ^{35}S-CTP (1250 Ci/mmol; NEN Life Science Products, Boston, USA), 10 mM unlabelled ATP, GTP and UTP, 40 units Rnasin (Promega, Madison, USA), 0.1 M DTT, 4 mL 5 × transcription buffer and 10 units of T3 or T7 RNA polymerase (Promega) for 90 min at 37 °C. The probe was treated with RNase-free DNase I (Promega) to remove template DNA. Alkaline hydrolysis was performed with 0.1 M carbonate buffer (45, 48 or 50 min) to reduce the size of probes to an average length of 150 bp (facilitate the probe penetration in the tissue sections). Riboprobes were purified on Quick Spin G-50 Sephadex columns.

In situ *hybridization*

WT and transgenic animals were re-anaesthetized with fluothane and their brains were carefully removed and frozen in cold isopentane (–25 °C). Serial coronal sections (14 µm thick) were cut in a cryostat, air-dried and kept at –80 °C for *in situ* hybridization processing according to the method previously described (Nef *et al.*, 1996). Before hybridization, sections were fixed for 15 min in 4% paraformaldehyde in phosphate-buffered saline (PBS). Sections were then rinsed in PBS and an acetylation step for 10 min in 0.1 M triethanolamine (pH 8) and 0.25% (v/v) acetic anhydride was performed. The sections were dehydrated through graded alcohols and air-dried. Denatured probe was added to the hybridization mix (0.3 M NaCl, 0.02 M Tris–HCl pH 8.0, 5 mM EDTA, 10% dextran sulphate, 1 × Denhardt's, 0.5 mg/mL tRNA, 0.1 M DTT, 50% deionized formamide) to obtain a final concentration of ~ 30 000 c.p.m./mL of hybridization solution, and the sections were hybridized for 16 h at 60 °C in humid conditions (50% formamide, 20% 4 × SSC and 30% H_2O). After hybridization, slides were washed in 4 × SSC, incubated for 30 min at 65 °C in a stringent wash solution (0.15 M NaCl, 0.02 M Tris–HCl pH 7.5, 5 mM EDTA, 0.1 M DTT) and treated with 20 µg/mL RNase A (Type II-A, Sigma) for 15 min at 37 °C. Final washes were performed in 2 × SSC and 0.1 × SSC, 15 min at 60 °C each, and the sections were dehydrated through graded alcohols and air-dried. The slides were exposed overnight against an X-ray film to determine the time of development. Sections were then dipped in Kodak NTB-2 nuclear emulsion (Eastman Kodak), air-dried for one night and processed for emulsion development 2 weeks later, or 8 weeks for low signal detection (*cpp32* mRNA in adult mice). Slides were developed with Kodak D-19, fixed with Kodak Fix and air-dried. Using additional sections, the specificity of the riboprobes was confirmed by Northern blot analysis (de Bilbao *et al.*, 1999) and was checked by hybridization experiments using sense cRNA m*bax*, m*cpp32* or m*bcl-xl* probes. In these conditions, no autoradiographic labelling was detected confirming the specificity of the hybridization signals (data not shown).

In situ *detection of DNA fragmentation*

Because the TUNEL method is difficult to perform on fresh frozen sections, additional mice were operated as previously described and allowed to recover from surgery for 7 days ($n_{WT} = 3$ and $n_{Bcl-2} = 3$).

They were then perfused through the ascending aorta with a solution of 4% paraformaldehyde in PBS (pH 7.35). Brains were removed and processed for paraffin embedding. Sections (7 μm) of the whole infarct area were cut with a microtome and collected on slides pretreated with 3-aminopropyltriethoxy-silane (Sigma). Each 10 sections were postfixed in a solution of 4% paraformaldehyde (10 min) and processed with the terminal deoxytransferase-mediated deoxyuridine triphosphate nick end-labelling (TUNEL) method according to our previous studies (de Bilbao & Dubois-Dauphin, 1996) in order to assess neuronal DNA fragmentation. Controls for TUNEL staining were investigated by omitting TdT.

Double-immunofluorescent labelling

With the aim of determining if the DNA fragmented features could be of neuronal origin, double-staining for colocalization of immunoreactivity of a mouse neuronal specific marker (NeuN) with DNA damage was performed on brain sections throughout the rostro-caudal extent of the ischaemic insult for WT and Bcl-2 animals. After rapid removal of paraffin, sections were heated in a microwave oven for 3×5 min in citrate buffer 0.01 M, pH 6 and cooled for 20 min. They were then processed for the NeuN immunostaining.

NeuN immunofluorescence

Sections were incubated in 10% normal horse serum (Dako, Switzerland) for 20 min and in the mouse anti-neuronal nuclei monoclonal antibody (1 : 1000, Chemicon, Temecula, CA, USA) for 1 h. After washing, they were incubated for 30 min in a R-phycoerythrin (RPE)-labelled secondary antibody (goat antimouse immunoglobulins 1%, Dako). Finally, after the washing procedure, sections were coverslipped using a mounting medium (glycerol/PBS, 3 volumes : 1 volume) and examined under a fluorescent microscope. No staining was observed when the first antibody was omitted.

In situ *detection of DNA fragmentation*

Sections were rinsed again and directly incubated in terminal deoxynucleotidyl transferase (TdT) tampon (30 mM Tris pH 7.2; 140 mM sodium cacodylate, 1 mM cobalt chloride). TdT (0.3 U/μL) and fluorescein-12-dUTP (0.2 nM per 10 U TdT; Boehringer Mannheim) in TdT buffer were then added to cover the sections in a humid atmosphere at 37 °C for 60 min. The reaction was stopped with $2 \times$ SCC (300 mM NaCl, 30 mM sodium citrate). Sections were washed with PBS for 10 min. Omission of either fluorescein-labelled nucleotides or the reaction enzyme TdT produced negative results.

Photomicrographs of double-immunofluorescent staining were constructed using the Metafluor Imaging System (Visitron, Germany).

Bcl-2 immunohistochemistry

Some alternate sections were processed for Bcl-2 immunostaining to confirm that the protein was expressed in vulnerable regions after MCAO. Briefly, sections were submitted to an immersion fixation (PAF, 30 min at 4 °C), rinsed in 0.1 M PBS, permeabilized in PBS/0.1% Triton X-100 + 10% normal horse serum and incubated overnight at 4 °C in a mouse monoclonal antibody specific to the human Bcl-2 (Dako) diluted 1 : 60 in PBS/Triton X-100. Sections were then rinsed and incubated for 90 min at room temperature in a biotinylated horse-antimouse antibody (1:100). After several washings in PBS, sections were incubated with the ABC complex solution (Vectastain ABC kit, Vector Laboratories). Tissue-bound peroxidase was visualized using diaminobenzidine (DAB, 0.05%, 0.6% H_2O_2 in 30% PBS 0.1 M, pH 7.4). Negative controls included deletion of the primary or secondary antibody.

Data analysis

Sections were counter-stained with cresyl violet for the histological identification of the nuclear boundaries and penumbral areas and mounted in Eukitt. Brain sections were visualized at the microscopic level under bright- and dark-field illumination.

Infarcted area

For each animal, quantification of the infarcted area was performed on cresyl violet-stained sequential sections (every five sections) throughout the rostro-caudal extent of the lesion. The rostro-caudal extent of the infarct was the same in both groups of mice. For each brain slice, the area of infarction and the area of the whole section (total cortex area in the right and left hemisphere) were calculated using a computer-assisted image analysing system (Software 'Morphometry', Samba 2005 TITN, Alcatel). For each animal, infarcted and whole section areas were summed and the percentage of infarcted tissue was calculated. A mean number of percentage infarcted area was calculated for each group of mice at all post-ischaemic time points.

Penumbral area

To further determine the effect of Bcl-2 on the penumbral area, quantification of the penumbral area was performed in WT ($n = 5$) and transgenic mice ($n = 3$) 7 days post-occlusion. The microscopic field for measurement was the infarct border localized at the medial part of the necrotic core. Penumbral area measurements were performed at $\times 10$ magnification using the computer-assisted image analysing system. For each mouse, the penumbral area was calculated every 140 μm throughout the rostro-caudal extent of the infarct ($n = 10$ sections for each animal). Areas were summed for each animal and a mean surface area was calculated for each group of mice. Values are expressed in pixels.

In order to quantify the *in situ* results, the number of silver grains per cell was calculated for each mouse in 20 cells of the penumbral area and the contralateral cortex using a Software 'Autoradiography' (Samba 2005 TITN, Alcatel). A mean number of silver grains per cell per area was calculated for each group of mice. This study was performed for *cpp32*, *bax* and *bcl-xl* transcripts 7 days post-MCAO.

Thalamus

In both WT ($n = 3$) and Bcl-2 transgenic mice ($n = 3$), the number of TUNEL-labelled cells was assessed in the thalamic fields where high levels of *cpp32* transcripts were observed. For each animal, apoptotic nuclei were counted under low-power microscopic fields ($\times 20$) on eight sections at the thalamic coordinates that showed the highest concentration of *cpp32* mRNA-labelled cells (–1.22 mm relative to Bregma) 7 days post-ischaemia. A mean number of TUNEL-labelled cells was calculated for each group of mice. As described above for the penumbral area, the number of silver grains per cell was calculated for each mouse in 20 cells of the ventral posteromedial and posterolateral thalamic nuclei. The same analysis was performed in the contralateral thalamus. A mean number of grains per cell per area was calculated for each group of mice. This study was performed for *cpp32*, *bax* and *bcl-xl* transcripts 7 days post-MCAO.

Statistical analysis

Data are presented as mean ± standard deviation. Differences in infarct areas were assessed using an analysis of variance (ANOVA) followed by the Fisher's test. For the penumbral area and the number

of thalamic TUNEL-labelled cells, the Mann–Whitney *U*-test was applied. $P < 0.05$ was considered statistically significant.

Results

Infarcted areas following MCAO in WT and Bcl-2 transgenic mice

No neurological deficits (forelimb, circling) were observed after surgical intervention. In all animals, microscopic observation revealed that the infarction was localized in areas that were supplied by the occluded medial cerebral artery. Infarction was confined primarily to the neocortex (frontal association, motor, somatosensory cortices) and was generally limited medially by a small subcortical infarct in the dorsolateral caudate putamen. Generally, cortical infarction extended rostro-caudally from the coronal level of olfactory nuclei to the first coronal levels of substantia nigra. In all animals, the topography of the lesions was similar whatever the post-ischaemic day, but infarcted regions were clearly smaller 7 days post-ischaemia than those observed after 3 days post-ischaemia.

The mean percentages of the section area that was infarcted in WT and Bcl-2 transgenic mice 1, 3, 7 and 14 days after permanent focal ischaemia are presented in Table 1. There was no significant difference between WT and Bcl-2 transgenic mice at any time point tested after ischaemia ($P > 0.05$, Figs 1 and 2). However, in each group of mice, the percentage of the area infarcted 7 days after ischaemia was significantly smaller than that at 3 days post-ischaemia ($P < 0.05$). This result mostly reflects the effect of brain oedema on infarct volume as described previously (Lin *et al.*, 1993). By 7 days post-occlusion, the margin between infarcted and non-infarcted area became obvious as the extent of the peri-infarct area was clearly delineated by a penumbral area consisting of a layer of cells probably of microglial origin. The same observations were made 14 days post-ischaemia. In order to determine if the presence of the Bcl-2 protein could alter the size of the penumbra, the thickness of the penumbra was measured in WT and transgenic mice 7 days after MCAO (Fig. 3). Our results demonstrate that the penumbral areas were similar in WT and Bcl-2 transgenic mice ($P > 0.05$).

Expression of cpp32, bax *and* bcl-xl *mRNAs after MCAO in WT and Bcl-2 transgenic mice infarcted and peri-infarcted areas*

Two kinds of nuclei were observed in cresyl violet-counterstained sections. Some nuclei displayed a clear cresyl violet staining, others were more deeply stained, round in shapes and smaller. Although caution must be taken for data based on morphologic criteria, we considered that the former mostly corresponded to neurons, whereas the latter seemed to correspond to glial cells. The *bax* and *bcl-xl* autoradiographic labellings were observed in these two kinds of nuclei, whereas *cpp32* mRNA was mostly localized in neuronal cells. No modification of the radiolabelling was observed in the hemisphere contralateral to MCAO at each postoperative time examined. Consistent with previous results (de Bilbao *et al.*, 1999), *bcl-xl* and *bax* mRNAs were widely expressed in brain structures of non-operated animals, whereas a low expression of *cpp32* mRNA was observed except in the piriform and entorhinal cortices.

TABLE 1. Percentage of section area with cerebral infarction 1, 3, 7 and 14 days following permanent MCAO in WT and Bcl-2 transgenic mice

Survival time (days)	WT mice (*n*)	Infarcted area (%)	Bcl-2 transgenic mice (*n*)	Infarcted area (%)
1	3	9.77 ± 0.74	3	12.23 ± 2.25
3	2	10.58 ± 4.78	3	11.01 ± 1.49
7	7	7.78 ± 0.95*	4	6.78 ± 0.78*
14	3	6.42 ± 0.80	3	6.01 ± 1.49

Values are mean ± SD. In each group of mice, the percentage of infarcted area 7 days after ischaemia was significantly smaller compared with 3 days post-ischaemia (*$P < 0.05$, Fisher's test), reflecting resorption of brain oedema. There were no significant differences between WT and Bcl-2 transgenic mice at any time point studied.

At each time point studied, the same results were observed in WT and Bcl-2 transgenic mice.

One and 3 days after MCAO, the distribution and density of *bcl-xl* and *bax* mRNAs were not changed. In the ischaemic core, few *bcl-xl* mRNA-labelled cells were observed located in neocortical layers II and III, while numerous *bax* mRNA-labelled cells were found scattered throughout the core. The effect of MCAO on *cpp32* mRNA expression is shown in Fig. 4. One day after MCAO, the pattern of mRNA labelling was unchanged (Fig. 4A), but *cpp32* mRNA became activated from 3 days post-MCAO as a few labelled cells were observed in the penumbra at the level of the neocortex and caudate putamen infarct borders (Fig. 4B; compare Fig. 4E and F). The observation of hybridized cells strongly suggests that *cpp32* mRNA upregulation was of neuronal origin (Fig. 4F). In the core, a few scattered *cpp32* mRNA-labelled cells were found.

From 7 days post-MCAO, *bax* mRNA radiolabelling was almost confluent and markedly augmented in the penumbra in the neighbouring neocortex and caudate putamen areas (compare Fig. 5A and B). As assessed by microscopic observation, these cells were of glial and neuronal origin and were uniformly distributed throughout the penumbra area (Fig. 5E and F). However, as assessed by our quantitative study (Table 2), the number of silver grains per cell was only slightly increased and does not reach a statistical level ($P > 0.05$). Cells located in the penumbra displayed a moderate *bcl-xl* mRNA labelling which was not significantly different from transcript levels in the control side ($P > 0.05$; Table 2, Fig. 5C). From 7 days, numerous cells had invaded the necrotic core and presumably corresponded to activated macrophages. In agreement with previous results (Okada *et al.*, 1998), these cells displayed high levels of *bcl-xl* mRNA but low levels of *bax* mRNA. A few labelled *bax* mRNA cells that mostly corresponded to neurons were also found scattered in the core. *Cpp32* mRNA transcript levels significantly increased in the penumbral zones almost in the neocortical area of the infarct border ($P < 0.05$; Table 2, Figs 4C and D, and 5D). Moreover, a few radiolabelled cells were observed scattered in the overall ipsilateral hemisphere. In the ischaemic core, occasional *cpp32* mRNA radiolabelling was observed.

From 14 days, a strong glial proliferation was observed in the penumbral area. It displayed an intense *bax* mRNA signal. A thin layer of *bcl-xl* mRNA-radiolabelled cells was observed in the external border of the penumbra that mostly corresponded to glial elements. Cells displaying *cpp32* mRNA radiolabelling were still observed. *Cpp32* mRNA-labelled cells were found scattered in the whole ipsilateral ischaemic hemisphere. In the core, the radiolabelling was similar to that observed 7 days post-ischaemia.

Expression of cpp32, bax *and* bcl-xl *mRNAs after MCAO in non-infarcted areas of WT and Bcl-2 transgenic mice*

Interestingly, a consistent upregulation of *cpp32* mRNA occurred at the level of the ipsilateral thalamus 3 days after MCAO (Fig. 6B). As assessed by our quantitative study, cellular transcript levels were significantly increased in the ipsilateral thalamus 7 days post-MCAO ($P < 0.05$; Table 2). According to the mouse brain atlas of Franklin & Paxinos (1997), the structures affected were the ventral poster-

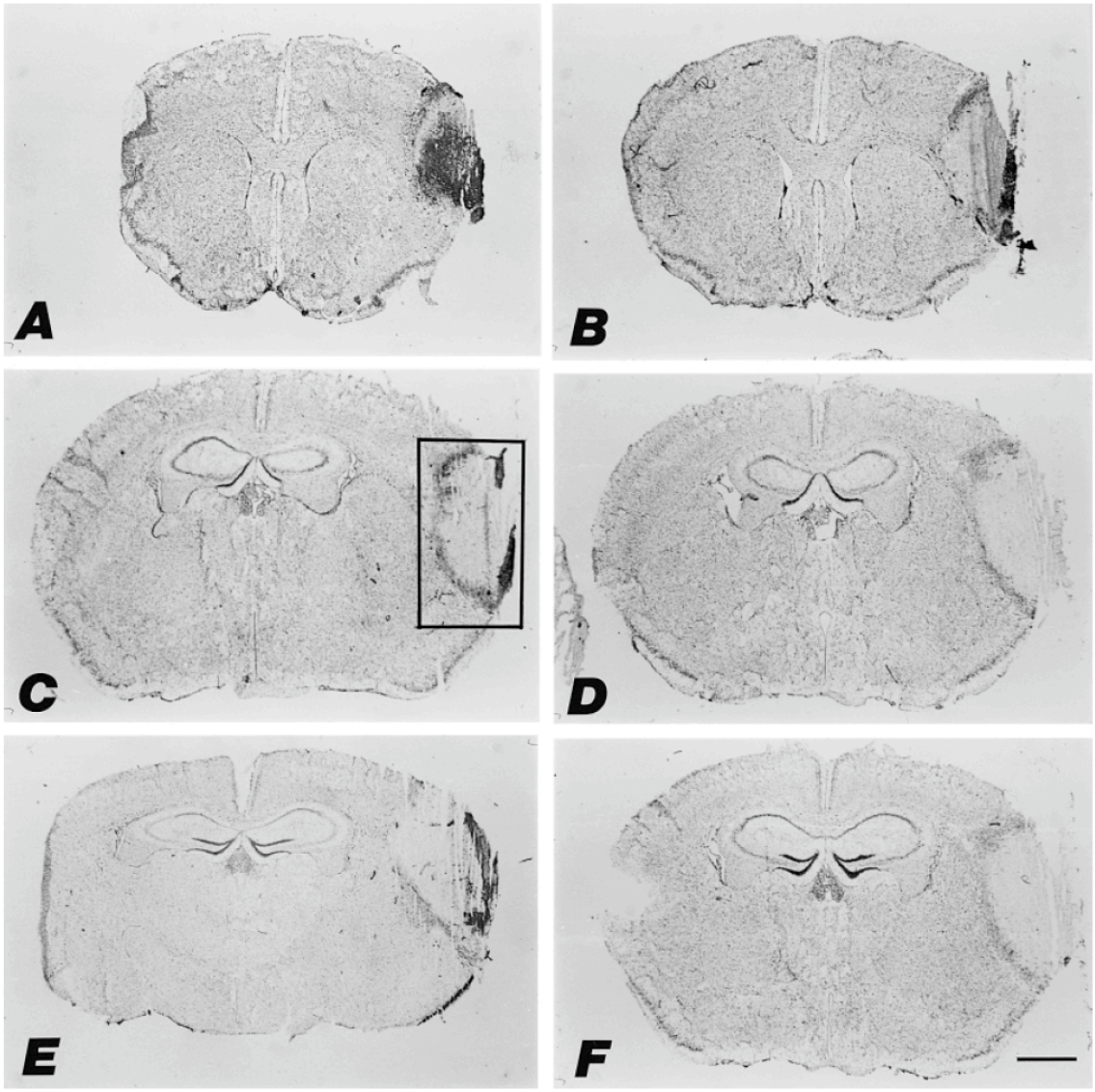

FIG. 1. Representative rostro-caudal levels of coronal brain sections showing an ischaemic infarct 7 days after permanent middle cerebral artery occlusion in WT (A, C, E) and Bcl-2 transgenic mice (B, D, F). Brain sections were stained with cresyl violet. The infarction was generally confined primarily to the neocortex. The Bcl-2 transgene did not reduce the infarct size. Scale bar, 1.22 mm.

omedial, posterolateral thalamic nuclei and the posterior thalamic nuclear group. The density of labelled cells peaked at 7 days post-ischaemia and was sustained 14 days after MCAO. In contrast, no modifications of *bax* and *bcl-xl* mRNA levels were observed ($P > 0.05$; Table 2, Fig. 6C and D). There were no differences between WT and Bcl-2 transgenic mice.

Examination of emulsion slides revealed that *cpp32* mRNA labelling emanated mainly from neuronal elements (Fig. 6E and F).

Bcl-2 immunohistochemistry

Given these results, it was essential to verify that the presence of the transgene overlaps areas of ischaemic cell damage. Whereas WT mice were devoid of Bcl-2-immunolabelled cells (Fig. 7A and E), high levels of the Bcl-2 transgene were seen in the cytoplasm of neurons in brain areas that were lesioned by MCAO, i.e. the neocortex and the caudate putamen (Fig. 7B). Labelled cells were also observed in thalamic nuclei (Fig. 7F).

DNA fragmentation

The negative control in the absence of TdT gave no labelled cells. No TUNEL labelling was observed in the contralateral non-ischaemic hemisphere. Seven days following ischaemia, two kinds of labelled cells were observed in WT and transgenic mice. Many TUNEL-labelled cells exhibited a diffuse staining throughout their cytoplasm

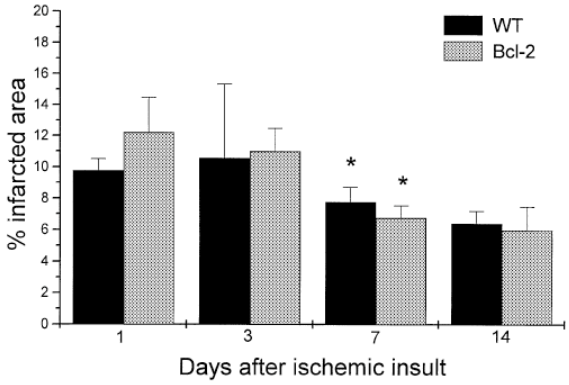

FIG. 2. Percentage of the section area that was infarcted 1, 3, 7 and 14 days following MCAO in WT and Bcl-2 transgenic mice. The number of animals used for this experiment is indicated in Table 1. The mean infarcted area is expressed as a percentage of the whole brain region examined. For each brain slice examined, the area of infarction and the area of the whole section (total area of the right and left hemispheres) were measured using a computer-assisted image analysing system. For each animal, the infarcted areas and whole section areas were summed independently and then the percentage of infarcted tissue was calculated. At all post-ischaemic time points, the mean percentage infarcted area was calculated for each group of mice. No significant differences were observed between the two groups of mice. However, the size of the infarct was reduced 7 days post-occlusion when compared with 3 days. This was observed for both groups of mice. $^*P < 0.05$. Bars and lines represent mean ± SD.

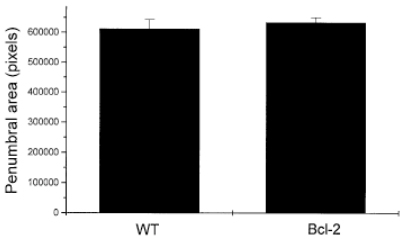

FIG. 3. Penumbral areas calculated 7 days after MCAO in WT ($n = 5$) and Bcl-2 transgenic mice ($n = 3$). The microscopic field for measurement was the infarct border localized at the medial part of the necrotic core. Measurements were performed at magnification × 10. For each mouse, the penumbral area was calculated on 10 sections spaced by 140 µm throughout the rostro-caudal extent of the infarct. Calculated areas were summed for each mouse and a mean surface was calculated for each group of mice. Values are expressed in pixels. No significant differences were observed between the two groups of mice. Bars and lines represent mean ± SD.

which had the appearance of necrosis, whereas other cells displayed the characteristic appearance of apoptosis (chromatin condensation, apoptotic bodies). Necrotic cells were mostly encountered in the core of the infarct. In the inner border zone of infarction, numerous cells displaying a necrotic profile were observed intermingled with apoptotic bodies (Fig. 7C and D). These two kinds of cells were almost encountered in the striatal border zone. In the neocortical border zone labelled cells were almost located in layers II and III and generally displayed a necrotic morphology. Few apoptotic bodies were present in the penumbra (Fig. 8A), the ipsilateral corpus callosum, the caudate putamen and the adjacent cortex that were spared from ischaemia. As assessed by double-immunofluorescent staining, TUNEL-labelled cells of neuronal origin (NeuN-positive) were observed intermingled with apoptotic bodies in the penumbra area (Fig. 8A). In the core, NeuN-positive cells were occasionally encountered (Fig. 8A). The same pattern of labelling was observed in WT and Bcl-2 transgenic mice.

In the thalamic area of WT mice, numerous TUNEL-labelled nuclei were seen in the ventrolateral, ventral posterolateral and ventral posteromedial thalamic nuclei (Franklin & Paxinos, 1997, Fig. 7G). Most of the TUNEL-labelled features corresponded to apoptotic bodies. However, combined immunofluorescence revealed that TUNEL-positive cells of neuronal origin could be observed (Fig. 8B). In contrast, only rarely labelled cells were observed in Bcl-2 transgenic mice (Fig. 7H). The mean number of apoptotic bodies was 95 ± 51 and 12 ± 7 in WT and transgenic mice, respectively ($P < 0.05$, Fig. 9). No TUNEL-labelled cells displaying a necrotic morphology, as seen in the infarcted area, were observed in thalamic nuclei (Fig. 7G).

Discussion

A main result of this study is that the overexpression of Bcl-2 does not lead to a decrease of the infarct and penumbral sizes induced *in vivo* by MCAO. Moreover, this study reveals that increased levels of *cpp32* mRNA and DNA fragmentation occur in the ipsilateral thalamus following MCAO. This suggests that *cpp32* mRNA may participate in the regulation of cellular vulnerability in this area, and, because DNA fragmentation was specifically detected in the thalamus of WT but not transgenic mice 7 days post-ischaemia, it is proposed that Bcl-2 may prevent apoptotic cell death in this area.

Despite the presence of the Bcl-2 protein in cortical areas affected by ischaemia, the infarct and penumbral sizes were not reduced in Bcl-2 transgenic mice when compared with WT ones. In addition, we did not detect any changes in the labelling pattern of TUNEL-stained cells between the two groups of mice. Taken together, these results indicate that Bcl-2 overexpression had no effect on cortical neuronal death induced by MCAO. These results are strongly supported by a recent finding showing that the infarct size was not reduced in *Thy1hbcl-2* mice following MCAO (Wiessner *et al.*, 1999). However, they do not confirm previous data showing that Bcl-2 overexpression in the mouse brain significantly reduced the volume of the infarct following MCAO (Martinou *et al.*, 1994). This could be partly due to the different methodologies used for quantification of the infarcted area. Actually, it is well known that variations of the infarct size and position might occur between animals of the same strain following MCAO (Rubino & Young, 1988; Ginsberg & Busto, 1989; Menzies *et al.*, 1992). However, in the work reported by Martinou *et al.* (1994), the areas of cerebral damage have been measured on five coronal sections at specific coordinates without considering the rostro-caudal extent and position of the infarcted area. This methodological consideration could partly explain the discrepancies observed with our results. At this point, it should also be notified that the reliability of our results can be supported by the fact that our study not only includes a greater number of animals, but was also investigated at various time-points following ischaemia. Moreover, it includes a separate quantification of the penumbral area. Although some data have reported an induction of Bcl-2 in ischaemic neuronal cells that could be indicative of a role in cell survival (Shimazaki *et al.*, 1994; Chen *et al.*, 1995, 1997), this has proved to be strongly controversial (Hara *et al.*, 1996; Asahi *et al.*, 1997). In addition, previous studies indicated that the overexpression of Bcl-2 in the brain by infection with a virus vector does not affect the infarct volume (Linnik *et al.*, 1995a; Lawrence *et al.*, 1996), but can protect infected neurons in the injured tissue. However, it should be noted that, in contrast to the present study, these experiments were performed 48 and 24 h

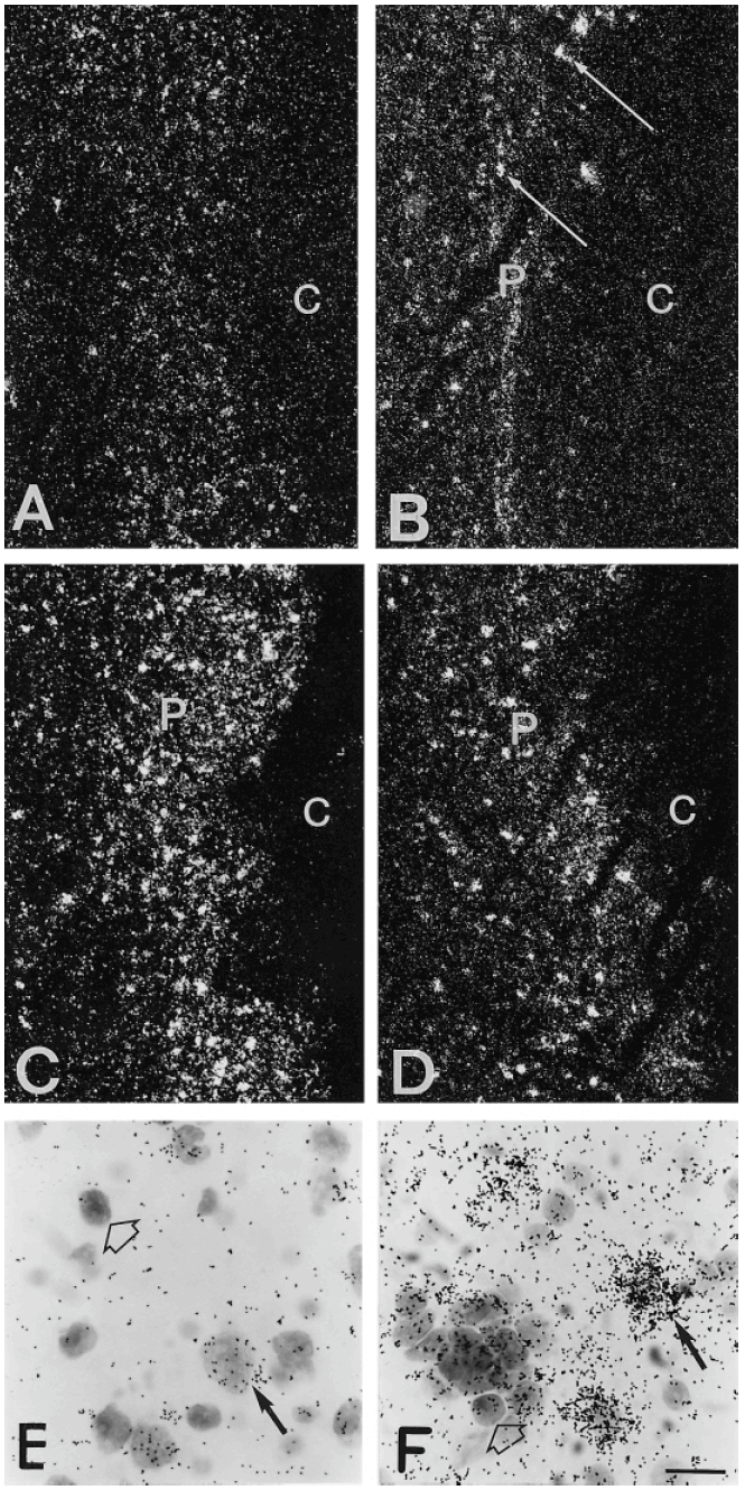

FIG. 4. Dark-field emulsion autoradiographs of coronal brain sections showing *cpp32* mRNA expression 1 (A), 3 (B) and 7 days (C and D) through the penumbral area (see the corresponding boxed region in Fig. 1C) after permanent middle cerebral artery occlusion in Bcl-2 transgenic (A–C) and WT mice (D). Whereas transcript levels were unchanged 1 day post-occlusion (A), few cells displayed a strong labelling from 3 days (B, arrows). From 7 days, numerous labelled cells were observed in the overall penumbral area (C). The same pattern of labelling was observed in WT mice (D). The cellular distribution of *cpp32* mRNA shown in A and B is demonstrated in E and F, respectively, in bright-field photomicrographs. The hybridization signal was present in neurons (black arrows) rather than glia (empty arrows) and was highly increased 3 days post-occlusion (F) when compared with 1 day post-occlusion (E). C, core; P, penumbra. Scale bar, 147 µm (A–D); 15 µm (E and F).

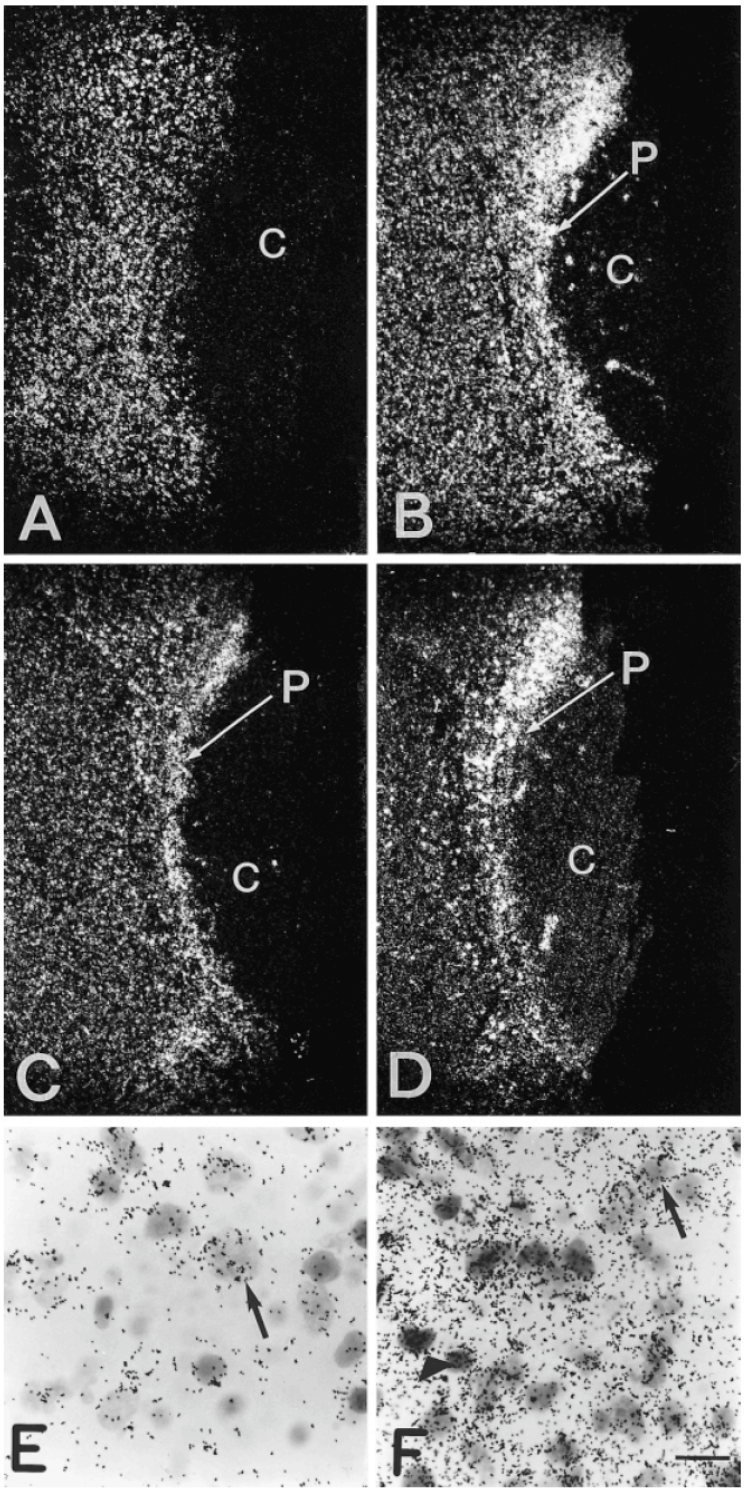

FIG. 5. Dark-field emulsion autoradiographs of adjacent brain sections showing *bax* (A and B), *bcl-xl* (C) and *cpp32* (D) mRNA radiolabellings 3 days (A) and 7 days (B–D) through the penumbral area (see the corresponding boxed region in Fig. 1C) after permanent middle cerebral artery occlusion in WT mice. Seven days post-occlusion, *bax* mRNA levels were increased (B) which was undetectable at 3 days post-occlusion (A). However, this increase did not reach statistical significance. In contrast to *bcl-xl* mRNA (C), the *cpp32* transcript levels were significantly increased in the penumbral area (D). The *bax* hybridization signal was visualized at higher magnification by bright-field microscopy 3 days (E) and 7 days (F) post-occlusion. The density of silver grains highly increased at 7 days postsurgery (F) and these were localized in neuronal (arrows) and glial (arrowheads) cells. The same observations were made in Bcl-2 transgenic mice. C, core; P, penumbra. Scale bar, 290 µm (A–D); 16 µm (E and F).

TABLE 2. Mean number of grains per cell in the cortical and thalamic fields 7 days following MCAO in WT and Bcl-2 transgenic mice

	WT mice		Bcl-2 transgenic mice	
	Ipsilateral	Contralateral	Ipsilateral	Contralateral
Penumbra-cortex				
bax	31.15 ± 7.77	26.79 ± 4.28	28.15 ± 6.7	18.73 ± 5.49
bcl-xl	20.2 ± 6.78	19.87 ± 5.15	16.79 ± 4.53	20.09 ± 7.70
cpp32	18.0 ± 6.75*	8.15 ± 4.68	17.52 ± 5.6*	10.65 ± 3.7
Thalamus				
bax	19.47 ± 6.88	19.65 ± 10.11	21.9 ± 9.32	21.2 ± 7.76
bcl-xl	15.35 ± 5.77	15.26 ± 4.44	14.71 ± 5.55	15.35 ± 5.77
cpp32	17.45 ± 5.32*	11.23 ± 3.98	24.65 ± 7.35*	11.75 ± 6.29

Values are mean ± SD. In each group of mice, the mean number of grains per cell was significantly increased for the *cpp32* transcript in the penumbral area and the ipsilateral thalamus compared with the contralateral side (*$P < 0.05$). In contrast, no difference was observed for the *bax* and *bcl-xl* transcripts. MCAO, middle cerebral artery occlusion.

following MCAO, respectively, which is clearly before the onset of cell death gene expression. A possible explanation for the absence of Bcl-2 neuroprotective effect is that the protein is synthesized in too small amounts to ensure cell survival. From this point of view, our results may indicate that higher levels of Bcl-2 could be necessary to prevent cell death following an acute stroke.

A recent report demonstrated that the resistance of cells over-expressing Bcl-2 submitted to metabolic stress similar to those observed in ischaemia might be compromised by the gap-junctions they formed with more vulnerable cells (Lin *et al*., 1998). For instance, Bcl-2 cells loose their ability to regulate cytosolic calcium concentration during ionophore exposure when they are coupled by gap junctions to less resistant glial cells *in vitro*. The authors proposed that this process could provide a basis for the propagation of injury induced in cerebral ischaemia. Because cells in the penumbral zone could be particularly subject to this kind of metabolic insult by neighbouring glial cells, this may provide a basis for the absence of Bcl-2 protective effect following MCAO. Moreover, as a substantial number of necrotic cells were detected in the penumbra in both groups of mice, it is possible that cells in the penumbra are also dying through a necrotic process which may not be prevented by Bcl-2 overexpression. In this respect, it has been previously proposed that following permanent MCAO, the necrotic process may become a prominent feature of cell death due to the persistent low blood flow (Murakami *et al*., 1997). In addition, although several *in vitro* reports have indicated that Bcl-2 can retard necrosis induced by glutathione depletion (Kane *et al*., 1993), chemical hypoxia (Shimizu *et al*., 1996) or irradiations (Fukunaga-Johnson *et al*., 1995), protection against necrosis was not as complete as in apoptosis (Shimizu *et al*., 1996). Previous reports using Bcl-2 transgenic mice have shown that Bcl-2 may play an important role in rescuing neurons from apoptotic cell death induced by a facial nerve transection (de Bilbao & Dubois-Dauphin, 1996) or in an animal model of motoneuropathy (Kostic *et al*., 1997). The fact that Bcl-2 does not efficiently protect cells against an ischaemic insult may reflect the importance of other aspects of cellular endangerment that are induced by an ischaemic insult and that could not be prevented by Bcl-2.

In respect to apoptotic-related genes expression in the penumbra, the rapid induction of *cpp32* mRNA observed in the present study points to the importance of this protease in ischaemia-induced apoptotic process and is consistent with previously published data that strongly suggests that Cpp32 activity contributes to neuronal death after transient or global ischaemia (Asahi *et al*., 1997; Chen *et al*., 1998; Namura *et al*., 1998). Previous reports have shown that *cpp32* mRNA induction is accompanied by increased protease activity and is coincidental with cell death (Chen *et al*., 1998). The spatio-temporal profile of *cpp32* mRNA induction observed in the present study further supports a role of this enzyme in ischaemic neuronal death induced by a permanent MCAO in the mouse. This early expression was not observed for *bax* and *bcl-xl* mRNAs. The fact that numerous TUNEL-positive cells are present in the infarcted areas further confirmed that the expression of *cpp32* mRNA can be associated with cell death following ischaemia. In addition, using colocalization study, our findings showed that DNA fragmented cells may be of neuronal origin. Altogether, our data agree with numerous studies showing that rodent MCAO may induce neuronal death via apoptosis outside the infarcted core (Linnik *et al*., 1995b; States *et al*., 1996; Asahi *et al*., 1997; Chen *et al*., 1997; Murakami *et al*., 1997).

Because neuronal degeneration following ischaemia is known to occur rapidly, many studies have addressed the acute changes in the ischaemic area. However, a neuronal death that takes longer to develop and that is never seen during the acute phase has been shown to occur in the thalamus following ischaemia (Fujie *et al*., 1990). To date, little is known about the expression of cell death genes in non-infarcted areas. The ipsilateral thalamus has been shown to undergo a long-term atrophy following MCAO in animal models (Fujie *et al*., 1990; Hara *et al*., 1993). This delayed neuronal death is thought to be a secondary lesion due to a retrograde degeneration of thalamocortical fibres. Within 3 days post-MCAO in the rat, Iizuka *et al*. (1990) reported a massive terminal degeneration in the ipsilateral thalamus, whereas a retrograde neuronal degeneration secondary to axonal damage in the cortical infarct was observed by 1 week post-ischaemia. One important finding of the present study is that permanent MCAO induced a selectively marked increased of *cpp32* mRNA levels 3 days after surgery. From our results, it appears that injured thalamic neurons produced mRNAs of the adverse protein Cpp32 rather than the protective protein Bcl-xl. As assessed by DNA fragmentation, double-staining experiments, and consistent with previous works (Gillardon *et al*., 1996; Soriano *et al*., 1996), our results also seem to indicate that apoptotic neuronal death occurs in thalamic nuclei following MCAO. The regional distribution of the TUNEL labelling was coincident with the regional distribution of *cpp32* mRNA-labelled cells in the thalamic subfields, suggesting a close parallel between *cpp32* mRNA expression and cell death. Altogether, these observations suggest that the induction of the *cpp32* gene might play a causative role in the cell death observed in the thalamus. In contrast with previous results (Gillardon *et al*., 1996), we did not observe increased levels of *bax* mRNA expression in thalamic neurons. However, these authors analysed total mRNA expression 6 h following ischaemia. It cannot be excluded that these *bax* mRNA changes reflected a transitory phenomenon.

As assessed by DNA fragmentation, our results also provide evidence for a protective role of Bcl-2 in the delayed neuronal death process induced by ischaemia in the thalamic area. This effect was observed despite the upregulation of *cpp32* mRNA. Therefore, the protective effect of Bcl-2 should result rather from interactions with cell death molecules at the post-transcriptional level as previously suggested (de Bilbao *et al*., 1999). Of course, it is not clear from our results whether Bcl-2 ensures a long-term neuroprotection of thalamic neurons. Such issues should be addressed by further studies of long-delayed cell injury after MCAO. Finally, it is of interest that significantly fewer TUNEL-positive cells were observed in the ipsilateral thalamus of Bcl-2 transgenic mice when compared with WT ones, despite the lack of protection provided by Bcl-2 in the infarct area. Therefore, one can argue that the mechanisms that

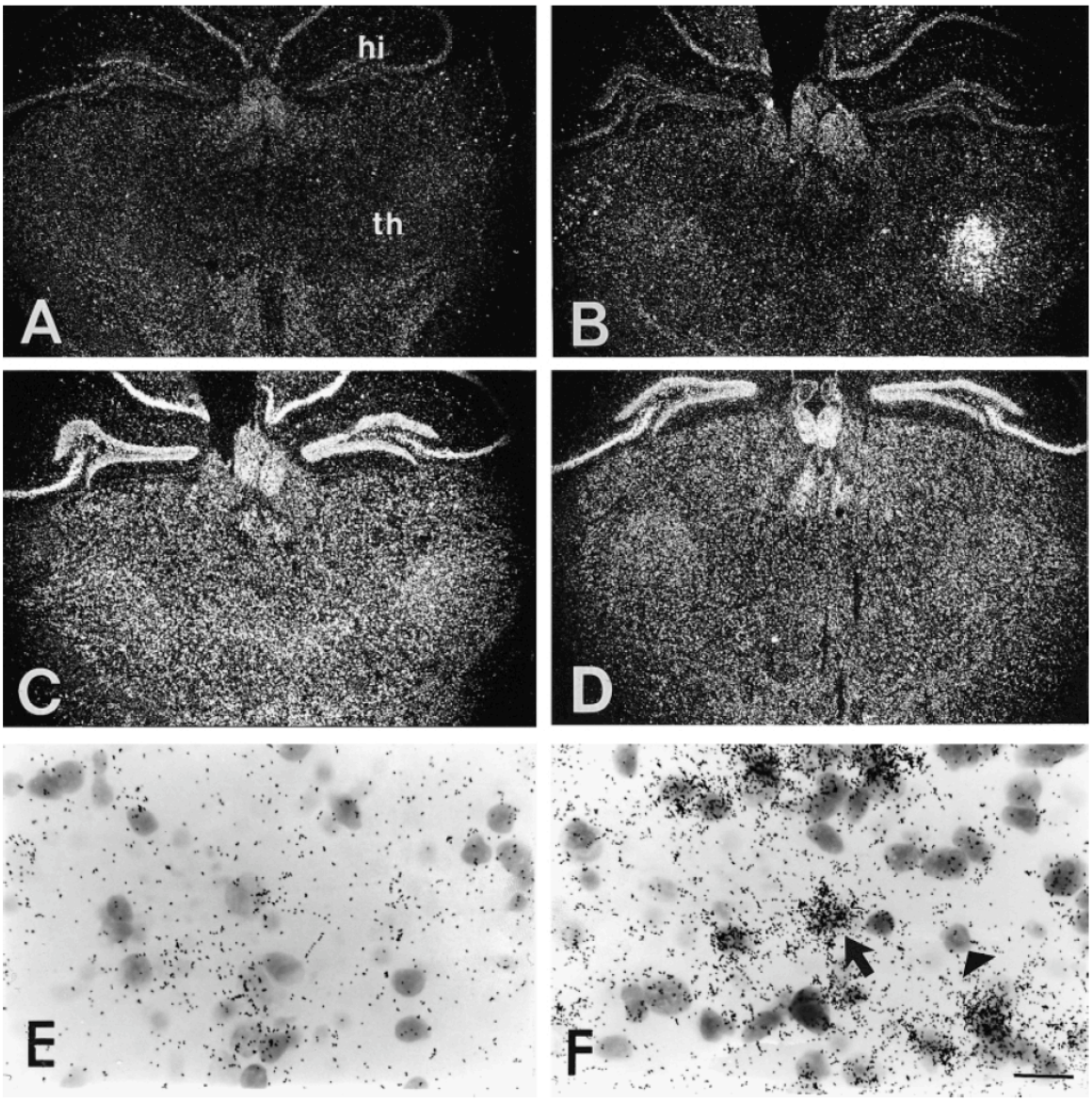

FIG. 6. Dark-field emulsion autoradiographs of coronal brain sections through the thalamic field showing *cpp32* (A and B), *bax* (C) and *bcl-xl* (D) mRNAs expression after permanent middle cerebral artery occlusion (MCAO) in Bcl-2 transgenic mice. A strong increase of *cpp32* mRNA was observed 7 days after MCAO in the ventral thalamic nuclei (B). This phenomenon was not observed 1 day post-occlusion (A). In contrast, *bax* and *bcl-xl* transcripts expressions were unchanged (C and D). The *cpp32* hybridization signal was visualized at higher magnification by bright-field microscopy 1 day (E) and 3 days post-occlusion (F). From 3 days, the transcript level was already highly increased in cells of neuronal origin (arrow). The arrowhead indicates a glial cell. The same results were obtained in WT mice. hi, hippocampus; th, thalamus. Scale bar, 640 µm (A–D) and 14 µm (E and F).

FIG. 7. Immunostaining for Bcl-2 in the neocortex (A and B) and thalamus (E and F) of WT (A and E) and Bcl-2 transgenic mice (B and F) on the occlusion side 7 days postsurgery. Note that immunolabelling was absent in WT mice (A,E). In transgenic mice, Bcl-2 positive cells were observed throughout the neocortex (B) and the thalamic nuclei (F). Note that the infarcted area (C) was devoid of immunostaining (B). TUNEL-labelled cells in the penumbral area (C and D) and the ipsilateral thalamus (G and H) of WT (C and G) as well as Bcl-2 transgenic (D and H) mice 7 days post-occlusion. In the penumbra (C and D), labelled cells that displayed a necrotic morphology (arrowheads) were found intermingled with apoptotic bodies (arrows). These were observed in WT (C) and transgenic (D) mice. In contrast, in the thalamic area, TUNEL cells were observed in WT mice (G) but not Bcl-2 transgenic mice (H). Moreover, the TUNEL staining revealed apoptotic bodies exclusively (G, arrows) as the necrotic features characteristic of the penumbral area (C and D, arrowheads) were absent in the thalamus. C, core; vpm, vpl, ventral posteromedial and posterolateral thalamic nuclei. Scale bar, 10 µm (A, B, E and F); 5 µm (C, D, G and H).

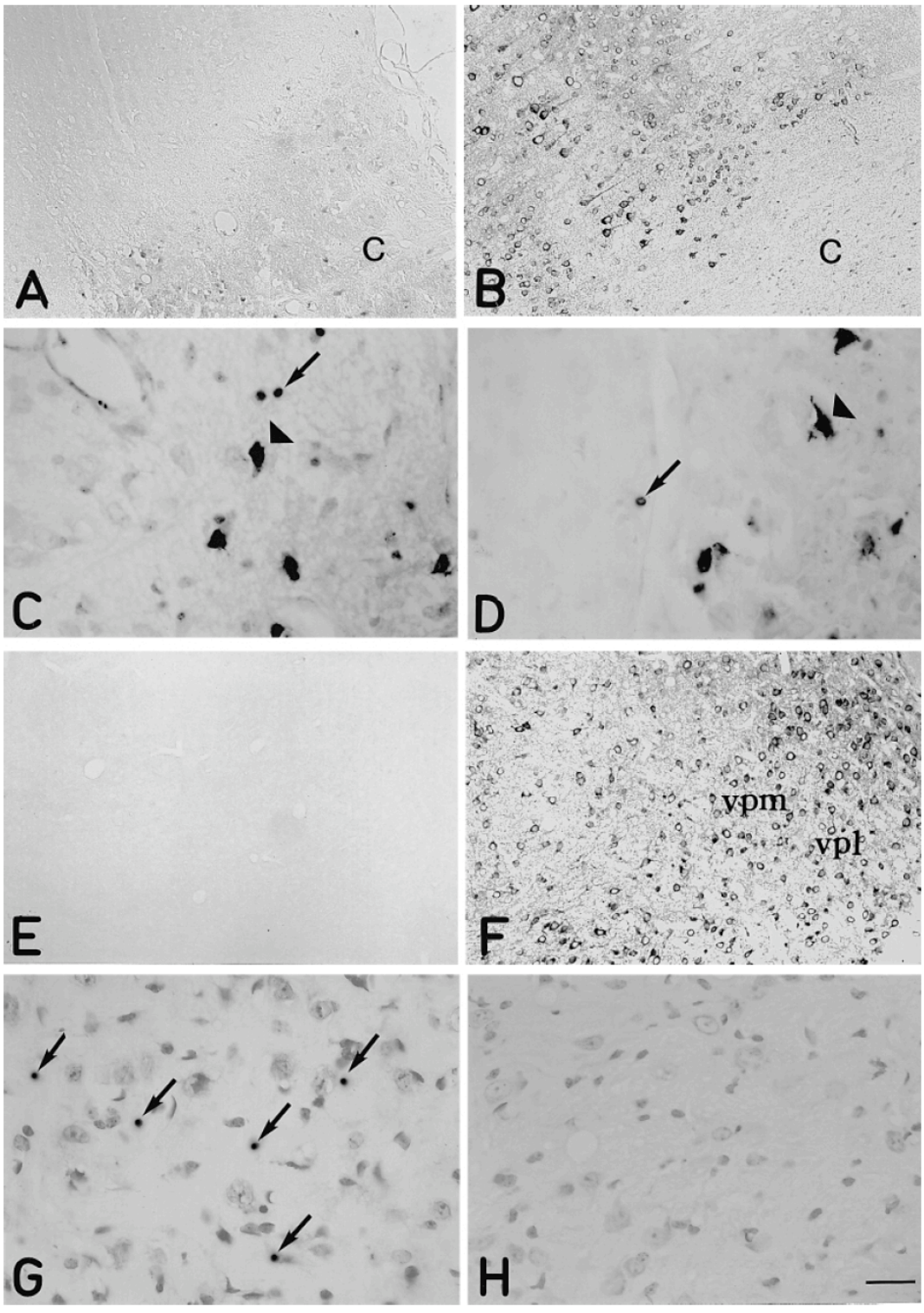
A
C
B
C
C
D
E
F
vpm
vpl
G
H

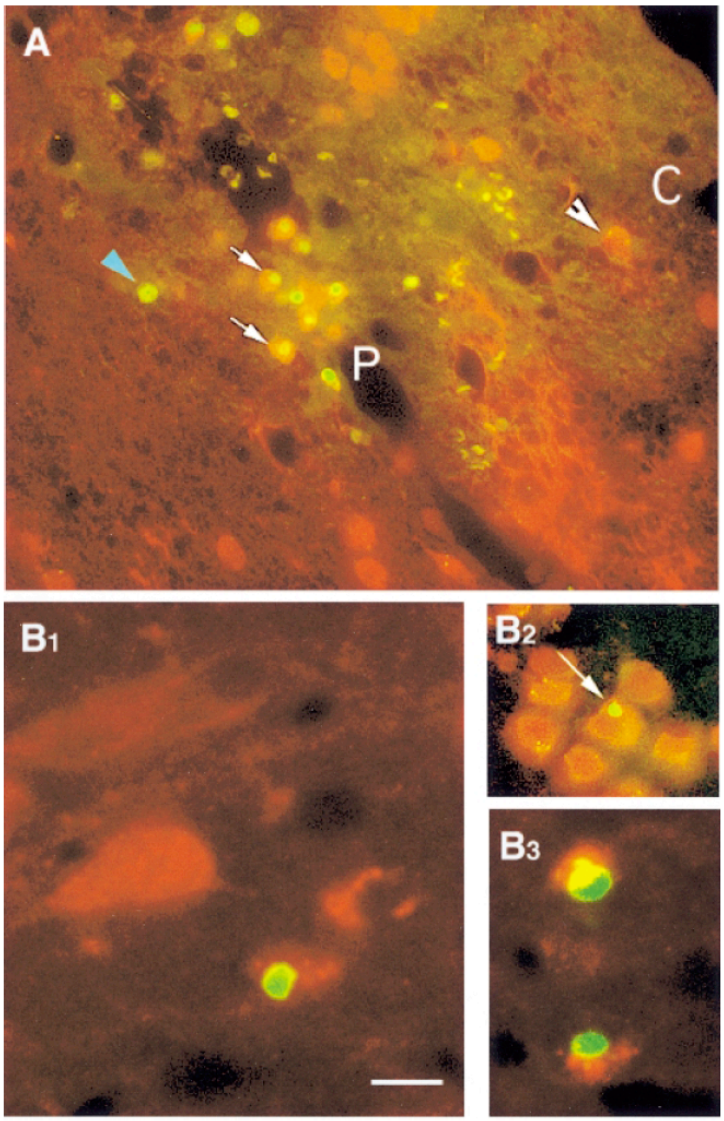

FIG. 8. Double-immunofluorescent labelling revealing the presence of the NeuN, a specific neuronal marker (red) and the TUNEL-labelled cells (yellow) in the neocortex (A) and thalamus (B_1, B_2 and B_3) of a WT mouse on the occlusion side 7 days post-ischaemia. In the neocortical infarcted area (A), neuronal cells with fragmented DNA (arrows) were found intermingled with round apoptotic bodies (blue arrowhead). In the core, neuronal cells were still occasionally observed (white arrowhead). In the thalamus (B_1, B_2 and B_3), double-stained cells could be observed (B_2, arrow), assessing that DNA fragmented features of neuronal origin occurred in the remote thalamic area. C, core; P, penumbra. Scale bar, 28 µm (A), 7 µm (B_1) and 14 µm (B_2 and B_3).

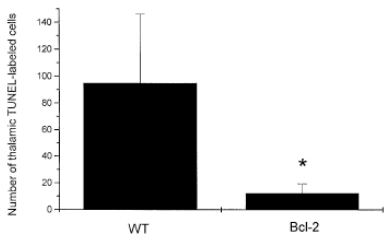

FIG. 9. Number of TUNEL-labelled cells in the thalamic nuclei in WT ($n = 3$) and Bcl-2 transgenic mice ($n = 3$) 7 days following MCAO. For each animal, cells were counted under high-power microscopic fields (× 20) on eight sections at the thalamic coordinates –1.22 mm relative to Bregma. Significant differences were seen between WT and Bcl-2 transgenic mice. $^*P < 0.05$. Bars and lines represent mean ± SD.

underly neuronal damage may be different between thalamic and cortical neurons, and that the extent of neuroprotection may depend on the injury paradigm. For instance, the thalamic neuronal death we observed is similar to that observed following target deprivation (Yamada *et al*., 1991). This hypothesis is further supported by the fact that TUNEL-labelled cells displayed different morphological characteristics in these two populations of neurons (necrotic cells were not observed in the thalamus), suggesting that multiple pathways of cell death can coexist following ischaemia (Martin *et al*., 1998). Because atrophic changes in the ipsilateral thalamus also occur in patients with cerebral infarction in the medial cerebral artery territory (Tamura *et al*., 1991), our results may have implications for functional recovery as cortical neurons that have been spared by ischaemia may not recover because they loose their thalamic afferentation. They also raise the need to explore the contribution of pathophysiological mechanisms in ischaemic neurodegeneration in an attempt to update anti-apoptotic strategies that may constitute effective approaches to limit neuronal damage in stroke.

Acknowledgements

We thank P.Y. Vallon, N. Flores, M. Muhlematter and L. Goncalves for excellent technical assistance. We also thank Drs M. Jaconi and F. Vilhardt for help with the Metafluor Imaging System photomicrographs and J.-L. Munoz for expert technical assistance in building the microcauterizer. This work was supported by the Swiss National Foundation for Scientific Research (4038-44006) and the Swiss Society for Neuroscience, IBRO (F.d.B., grant 84IB-050298).

Abbreviations

CNS, central nervous system; DAB, diaminobenzidine; MCAO, middle cerebral artery occlusion; PBS, phosphate-buffered saline; WT, wild-type.

References

Asahi, M., Hoshimaru, M., Uemura, Y., Tokime, T., Kojima, M., Ohtsuka, T., Matsuura, N., Aoki, T., Shibahara, K. & Kikuchi, H. (1997) Expression of interleukin-1β converting enzyme gene family and *bcl-2* gene family in the rat brain following permanent occlusion of the middle cerebral artery. *J. Cereb. Blood Flow Metab.*, **17**, 11–18.

Barinaga, M. (1998) Stroke-damaged neurons may commit cellular suicide. *Science*, **281**, 1302–1303.

Bogousslavsky, J., Regli, F. & Uske, A. (1988) Thalamic infarcts: clinical syndromes, etiology, and prognosis. *Neurology*, **38**, 837–848.

Chen, J., Graham, S.H., Chan, P.H., Lan, J., Zhou, R.L. & Simon, R.P. (1995) *bcl-2* is expressed in neurons that survive focal ischemia in the rat. *Neuroreport*, **6**, 394–398.

Chen, J., Jin, K., Chen, M., Pei, W., Kawaguchi, K., Greenberg, D.A. & Simon, R.P. (1997) Early detection of DNA strand breaks in the brain after transient focal ischemia: implications for the role of DNA damage in apoptosis and neuronal cell death. *J. Neurochem.*, **69**, 232–245.

Chen, J., Nagayama, T., Jin, K., Stetler, R.A., Zhu, R.L., Graham, S.H. & Simon, R.P. (1998) Induction of caspase-3-like protease may mediate delayed neuronal death in the hippocampus after transient cerebral ischemia. *J. Neurosci.*, **18**, 4914–4928.

De Bilbao, F. & Dubois-Dauphin, M. (1996) Time course of axotomy-induced apoptotic cell death in facial motoneurons of neonatal wild type and *bcl-2* transgenic mice. *Neuroscience*, **71**, 1111–1119.

De Bilbao, F., Guarin, E., Nef, P., Vallet, P., Giannakopoulos, P. & Dubois-Dauphin, M. (1999) Postnatal distribution of *cpp* 32 mRNA in the mouse central nervous system by in situ hybridization. *J. Comp. Neurol.*, **409**, 339–357.

Deckwerth, T.L., Elliott, J.L., Knudson, C.M., Johnson, E.M., Snider, W.D. & Korsmeyer, S.J. (1996) Bax is required for neuronal death after trophic factor deprivation and during development. *Neuron*, **17**, 401–411.

Dubois-Dauphin, M., Frankowski, H., Tsujimoto, Y., Huarte, J. & Martinou, J.C. (1994) Neonatal motoneurons overexpressing the Bcl-2 protooncogene in transgenic mice are protected from axotomy-induced cell death. *Proc. Natl Acad. Sci. USA*, **91**, 2459–2463.

Franklin, K.B.J. & Paxinos, G. (1997) *The Mouse Brain in Stereotaxic Coordinates*. Academic Press, San Diego, USA

Fujie, W., Kirino, T., Tomukai, N., Iwasawa, T. & Tamura, A. (1990) Progressive shrinkage of the thalamus following middle cerebral artery occlusion in rats. *Stroke*, **21**, 1485–1488.

Fukunaga-Johnson, N., Ryan, J.J., Wicha, M., Nunez, G. & Clarke, M.F. (1995) Bcl-2 protects murine erythroleukemia cells from p53-dependent and -independent radiation-induced cell death. *Carcinogenesis*, **16**, 1761–1767.

Gillardon, F., Lenz, C., Waschke, K.F., Krajewski, S., Reed, J.C., Zimmermann, M. & Kuschinsky, W. (1996) Altered expression of Bcl-2, Bcl-X, Bax, and c-Fos colocalizes with DNA fragmentation and ischemic cell damage following middle cerebral artery occlusion in rats. *Mol. Brain Res.*, **40**, 254–260.

Ginsberg, M.D. & Busto, R. (1989) Rodent models of cerebral ischemia. *Stroke*, **20**, 1627–1642.

Hara, H., Harada, K. & Sukamoto, T. (1993) Chronological atrophy after transient middle cerebral artery occlusion in rats. *Brain Res.*, **618**, 251–260.

Hara, A., Iwai, T., Niwa, M., Uematsu, T., Yoshimi, N., Tanaka, T. & Mori, H. (1996) Immunohistochemical detection of Bax and Bcl-2 proteins in gerbil hippocampus following transient forebrain ischemia. *Brain Res.*, **711**, 249–253.

Iizuka, H., Skatini, K. & Young, W. (1990) Neural damage in the rat thalamus after cortical infarcts. *Stroke*, **21**, 790–794.

Jacobson, S. & Trojanowski, J.Q. (1975) Corticothalamic neurons and thalamocortical terminal fields: an investigation in rat using horseradish peroxidase and autoradiography. *Brain Res.*, **85**, 385–401.

Kane, D.J., Sarafian, T.A., Anton, R., Hahn, H., Gralla, E.B., Valentine, J.S., Ord, T. & Bredesen, D.E. (1993) Bcl-2 inhibition of neural death: decreased generation of reactive oxygen species. *Science*, **262**, 1274–1277.

Kostic, V., Jackson-Lewis, V., de Bilbao, F., Dubois-Dauphin, M. & Przedborski, S. (1997) Bcl-2: prolonging life in a transgenic mouse model of familial amyotrophic lateral sclerosis. *Science*, **277**, 559–562.

Kuida, K., Zheng, T.S., Na, S., Kuan, C., Yang, D., Karasuyama, H., Rakic, P. & Flavell, R.A. (1996) Decreased apoptosis in the brain and premature lethality in CPP32-deficient mice. *Nature*, **384**, 368–372.

Lawrence, M.S., Ho, D.Y., Sun, G.H., Steinberg, G.K. & Sapolsky, R.M. (1996) Overexpression of Bcl-2 with herpes simplex virus vectors protects CNS neurons against neurological insults *in vitro* and *in vivo*. *J. Neurosci.*, **16**, 486–496.

Lin, T.N., He, Y.Y., Wu, G., Khan, M. & Hsu, C.Y. (1993) Effect of brain edema on infarct volume in a focal cerebral ischemia model in rats. *Stroke*, **24**, 117–121.

Lin, J.H.C., Weigel, H., Cotrina, M.L., Liu, S., Bueno, E., Hansen, A.J., Hansen, T.W., Goldman, S. & Nedergaard, M. (1998) Gap-junction-mediated propagation and amplification of cell injury. *Nature Neurosci.*, **1**, 494–500.

Linnik, M.D., Miller, J.A., Sprinkle-Cavallo, J., Mason, P.J., Thompson, F.Y., Montgomery, L.R. & Shroeder, K.K. (1995b) Apoptotic DNA fragmentation in the rat cerebral cortex induced by permanent middle cerebral artery occlusion. *Mol. Brain Res.*, **32**, 116–124.

Linnik, M.D., Zahos, P., Geschwind, M.D. & Federoff, H.J. (1995a) Expression of bcl-2 from a defective herpes simplex virus-1 vector limits neuronal death in focal cerebral ischemia. *Stroke*, **26**, 1670–1674.

Martin, L.J., Al-Abdulla, N.A., Brambrink, A.M., Kirsch, J.R., Sieber, F.E. & Portera-Cailliau, C. (1998) Neurodegeneration in excitotoxicity, global cerebral ischemia, and target deprivation: a perspective on the contributions of apoptosis and necrosis. *Brain Res. Bull.*, **46**, 281–309.

Martinou, J.C., Dubois-Dauphin, M., Staple, J.K., Rodriguez, I., Frankowski, H., Missoten, M., Albertini, P., Talabot, D., Catsicas, S., Pietra, C. & Huarte, J. (1994) Overexpression of BCL-2 in transgenic mice protects neurons from naturally occurring cell death and experimental ischemia. *Neuron*, **13**, 1017–1030.

Menzies, S.A., Hoff, J.T. & Betz, A.L. (1992) Middle cerebral artery occlusion in rats: a neurological and pathological evaluation of a reproducible model. *Neurosurgery*, **31**, 100–107.

Merry, D.E. & Korsmeyer, S.J. (1997) BCL-2 gene family in the nervous system. *Annu. Rev. Neurosci.*, **20**, 245–267.

Motoyama, N., Wang, F., Roth, K.A., Sawa, H., Nakayama, K.I., Nakayama, K., Negishi, I., Senju, S., Zhang, Q., Fujii, S. & Loh, D.Y. (1995) Massive cell death of immature hematopoietic cells and neurons in bcl-x-deficient mice. *Science*, **267**, 1506–1510.

Murakami, K., Kondo, T. & Chan, P.H. (1997) Reperfusion following focal cerebral ischemia alters distribution of neuronal cells with DNA fragmentation in mice. *Brain Res.*, **751**, 160–164.

Namura, S., Zhu, J., Fink, K., Endres, M., Srinivasan, A., Tomaselli, K.J.,

Yuan, J. & Moskowitz, M.A. (1998) Activation and cleavage of caspase-3 in apoptosis induced by experimental cerebral ischemia. *J. Neurosci.*, **18**, 3659–3668.

Nef, S., Allaman, I., Fiumelli, H., de Castro, E. & Nef, P. (1996) Olfaction in birds: differential embryonic expression of nine putative odorant receptors genes in the avian olfactory system. *Mech. Dev.*, **55**, 65–77.

Okada, S., Zhang, H., Hatano, M. & Tokuhisa, T. (1998) A physiologic role of Bcl-xl induced in activated macrophages. *J. Immunol.*, **160**, 2590–2596.

Parsadanian, A.S., Cheng, Y., Keller-Peck, C.R., Holtzman, D.M. & Snider, W.D. (1998) Bcl-xl is an apoptotic regulator for postnatal CNS neurons. *J. Neurosci.*, **18**, 1009–1020.

Rubino, G.J. & Young, W. (1988) Ischemic cortical lesions after permanent occlusion of individual middle cerebral artery branches in rats. *Stroke*, **19**, 870–877.

Salvesen, G.S. & Dixit, V.M. (1997) Caspases: intracellular signaling by proteolysis. *Cell*, **91**, 443–446.

Shimazaki, K., Ishida, A. & Kawai, N. (1994) Increase in *bcl-2* oncoprotein and the tolerance to ischemia-induced neuronal death in the gerbil hippocampus. *Neurosci. Res.*, **20**, 95–99.

Shimizu, S., Eguchi, Y., Kamiike, W., Waguri, S., Uchiyama, Y., Matsuda, H. & Tsujimoto, Y. (1996) Retardation of chemical hypoxia-induced necrotic cell death by Bcl-2 and ICE inhibitors: possible involvement of common mediators in apoptotic and necrotic signal transduction. *Oncogene*, **12**, 2045–2050.

Soriano, M.A., Ferrer, I., Rodriguez-Farré, E. & Planas, A.M. (1996) Apoptosis and c-Jun in the thalamus of the rat following cortical infarction. *Neuroreport*, **7**, 425–428.

States, B.A., Honkaniemi, J., Weinstein, P.R. & Sharp, F.R. (1996) DNA fragmentation and HSP70 protein induction in hippocampus and cortex occurs in separate neurons following permanent middle cerebral artery occlusions. *J. Cereb. Blood Flow Metab.*, **16**, 1165–1175.

Tamura, A., Tahira, Y., Nagashima, H., Kirino, T., Gotoh, O., Hojo, S. & Sano, K. (1991) Thalamic atrophy following cerebral infarction in the territory of the middle cerebral artery. *Stroke*, **22**, 615–618.

White, F.A., Keller-Peck, C.R., Knudson, C.M., Korsmeyer, S.J. & Snider, W.D. (1998) Widespread elimination of naturally occurring neuronal death in *bax*-deficient mice. *J. Neurosci.*, **18**, 1428–1439.

Wiessner, C., Allegrini, P.R., Rupalla, K., Sauer, D., Oltersdorf, T., McGregor, A.L., Bischoff, S., Böttiger, B.W. & Van Der Putten, H. (1999) Neuron-specific transgene expression of *Bcl-X$_L$* but not *Bcl-2* genes reduced lesion size after permanent middle cerebral artery occlusion in mice. *Neurosci. Lett.*, **268**, 119–122.

Yamada, K., Kinoshita, A., Kohmura, E., Sakaguchi, T., Taguchi, J., Kataoka, K. & Hayakawa, T. (1991) Basic fibroblast growth factor prevents thalamic degeneration after cortical infarction. *J. Cereb. Blood Flow Metab.*, **11**, 472–478.

Yates, P.O. (1976) Vascular disease of the central nervous system. In Blackwood, W. & Corsellis, J.A.N. (eds), *Greenfield's Neuropathology*, 3rd edn. Edward Arnold, London, UK, pp. 86–147.

4.3. Article I: Results and discussion

4.3.1. *Bcl-2 overexpression did not prevent ischemic damage in mice subjected to permanent MCAO*

Despite the presence of the Bcl-2 protein in cortical areas affected by ischemia (Figure 7B), our data shows that the overexpression of Bcl-2 does not efficiently protect cortical neurons from death, as the infarct sizes were not reduced in Bcl-2 transgenic mice. Indeed, there was no significant difference of the infarct sizes between WT and Bcl-2 transgenic mice at any time point tested (1, 3, 7 and 14 days) after ischemia ($P > 0.05$, Table 1, Figures 1 and 2). However, in each group of mice, the percentage of the area infarcted 7 days after ischemia was significantly smaller than that at 3 days post-ischemia ($P < 0.05$). This result mostly reflects the effect of brain edema on infarct volume as the development of brain edema has been shown to occur in the first 3 days after ischemia (Lin *et al*., 1993). In order to determine if the presence of the Bcl-2 protein could alter the size of the penumbra, the thickness of the penumbra was also measured in WT and transgenic mice 7 days after MCAO (Figure 3). Our results demonstrate that the penumbral areas were similar in both genotypes ($P > 0.05$). In line with these findings, no changes in the labelling pattern of TUNEL-stained cells in the penumbra were detected between WT and transgenic mice.

Although our results are strongly supported by a finding showing that the infarct size was not reduced in *Thy1hbcl-2* mice following MCAO (Wiessner *et al.*, 1999), they do not confirm numerous data showing an effect of Bcl-2 on infarct size (see section 4.2). In particular, it has been shown that Bcl-2 overexpression in the mouse brain significantly reduced the volume of the infarct following permanent MCAO (Martinou *et al*., 1994). Several possible explanations may explain this discrepancy and the present lack of effect of Bcl-2 overexpression. First, this could be partly due to the different methodologies used for quantification of the infarcted area as Martinou *et al*. (1994) measured the areas of cerebral damage on five coronal sections at specific coordinates without considering the full rostro-caudal extent of the infarcted area. In addition, it should be also notified that the reliability of our results can be supported by the fact that our study was

investigated at various time-points following ischemia. Second, it cannot be excluded that the levels of Bcl-2 were too low to prevent tissue damage due to the severity of the occlusion (permanent), with a rapid onset of energy depletion and mitochondrial membrane depolarization which could not allow apoptosis to occur. In line with this hypothesis, numerous cells displaying a necrotic profile were observed in the inner border zone of infarction (Figures 7C and 7D). Third, in this model of ischemia, apoptosis may have occurred not only through the intrinsic pathway but also through the extrinsic one (see section 3.8.2.). In these conditions, the concomitant activation of the extrinsic pathway (death-receptor-mediated) which activates caspase-3 through a pathway independent of mitochondria, could not have been prevented by Bcl-2. Consequently, acting on the intrinsic pathway could have not been sufficient to limit neuronal damage. Finally, our data are consistent with a more recent study showing that pro-caspase-3 activation, which is known to play an effector role in apoptotic cell death, was not involved in the neuronal degeneration seen after permanent MCAO in rats (Gill *et al.*, 2002). The authors concluded that rather necrotic damage instead of apoptosis may have occurred in this model.

4.3.2. *Expression of apoptotic and anti-apoptotic molecules mRNAs in the infarcted areas of ischemic WT and Bcl-2 transgenic mice*

One and 3 days after MCAO, the distribution and density of *bcl-xl* and *bax* mRNAs were unchanged. From 7 days post-MCAO, *bax* mRNA radiolabelling was almost confluent and markedly augmented in the penumbra in the neighbouring neocortex and caudate putamen areas (compare Figures 5A and 5B). As assessed by microscopic observation, these cells were of glial and neuronal origin (Figures 5E and 5F). However, as assessed by our quantitative study (Table 2), the number of silver grains per cell was only slightly increased and does not reach a statistical level ($P > 0.05$). At this time-point, cells located in the penumbra displayed a moderate *bcl-xl* mRNA labelling which was not significantly different from transcript levels in the control side ($P > 0.05$; Table 2, Figure 5C). From 7 days, numerous cells had invaded the necrotic core and presumably corresponded to activated macrophages. In agreement with previous results (Okada *et al*., 1998), these cells displayed high levels of *bcl-xl* mRNA but

low levels of *bax* mRNA. A few labelled *bax* mRNA cells that mostly corresponded to neurons were also found scattered in the core. From 14 days, a strong glial proliferation was observed in the penumbral area. It displayed an intense *bax* mRNA signal. A thin layer of *bcl-xl* mRNA-radiolabelled cells was observed in the external border of the penumbra that mostly corresponded to glial elements. Therefore, our data showed that, when compared to *bcl-xl* mRNA, *bax* mRNA levels were significantly increased following permanent MCAO. Similar results were reported by other studies (Matsushita *et al.*, 1998; Ferrer *et al.*, 2003). In addition, a decrease in immunoreactivity for Bcl-X and an increase in immunostaining for Bax were observed within the ischemic cortex of rats following permanent MCAO (Gillardon *et al.*, 1996).

Whereas the pattern of *cpp32* mRNA labelling was unchanged one day after MCAO (Figure 4A), it became activated from 3 days post-MCAO as a few labelled cells were observed in the penumbra (Figure 4B; compare Figures 4E and 4F). The observation of hybridized cells strongly suggests that *cpp32* mRNA up-regulation was of neuronal origin (Figure 4F). From 7 days, *Cpp32* mRNA transcript levels significantly increased in the penumbral zones ($P < 0.05$; Table 2, Figures 4C, 4D, and 5D). From 14 days, *cpp32* mRNA radiolabelling was still observed. In the ischemic core, occasional *cpp32* mRNA radiolabelling were observed 3, 7 and 14 days post-ischemia. In respect to these findings, the rapid induction as well as the spatio-temporal profile of *cpp32* mRNA expression could point to the importance of this protease in ischemia-induced apoptotic process. However and as already discussed, the fact that cell death process could not have been prevented in Bcl-2 transgenic mice may suggest that multiple pathways of cell death can coexist in cells of the cortical area following ischemia (Wieloch, 2001). In support with this, the transcript levels of the pro-apoptotic protein Bax were not already induced 3 days post-MCAO when cell death has already occurred. Furthermore and in accordance with the lack of effect of the transgene expression on infarct size, *bcl-xl*, *bax* and *cpp32* mRNAs levels were similar between WT and Bcl-2 transgenic mice at each time point studied.

In conclusion, it should be noted that although a variety of genes may be induced at the transcriptional level after ischemia, protein synthesis may rapidly decrease

because the translational machinery is severely affected. Therefore, the present gene up-regulations should be confirmed at the protein level.

4.3.3. *Apoptotic cell death is prevented in the thalamus of Bcl-2 transgenic mice*

An interesting finding is that, despite the lack of protection provided by Bcl-2 in the infarct area, a beneficial effect of Bcl-2 is mainly directed towards the thalamus, a brain region characterized by a delayed degeneration. Indeed, focal ischemia is known to cause secondary damage in non-ischemic remote brain areas that have synaptic contacts to the primary lesion site (see section 2.3.). The accepted hypothesis is that this secondary damage is due to retrograde degeneration of thalamocortical projections (Iizuka *et al*., 1990). Such lesions remote from the infarct may influence functional recovery in patients with stroke.

Whereas in the thalamic area of WT mice, numerous apoptotic bodies were seen in the ventrolateral, ventral posterolateral and ventral posteromedial thalamic nuclei of neuronal cells (Figures 7G and 8B), only rarely apoptotic cells were observed in Bcl-2 transgenic mice seven days post-MCAO (Figures 7H and 9). In contrast to the infarcted area, no TUNEL-labelled cells displaying a necrotic morphology were observed in thalamic nuclei (Figure 7G).

Altogether, these results indicate that the mechanisms that underly neuronal damage may be different between thalamic and cortical neurons. As assessed by DNA fragmentation, apoptotic-related cell death genes may be involved in thalamic secondary changes induced by permanent focal ischemia and, because we did not evidenced any changes in infarct size between the two genotypes, it is unlikely that sparing cortex could have prevented secondary retrograde degeneration in transgenic mice. It is rather conceivable that Bcl-2 overexpression may have limited apoptotic processes thereby limiting thalamic degeneration. The beneficial effect of Bcl-2 against thalamic neurodegeneration is of clinical interest as thalamic atrophy has been reported in patients after stroke (Tamura *et al*., 1991) and thalamic damage is frequently associated with functional deficits in humans (Bogousslavsky *et a*l., 1988).

4.3.4. *Expression of apoptotic and anti-apoptotic molecules mRNAs in the non-infarcted areas of ischemic WT and Bcl-2 transgenic mice*

Interestingly, a consistent up-regulation of *cpp32* mRNA occurred at the level of the ipsilateral thalamus in the ventral posteromedial, posterolateral thalamic nuclei and the posterior thalamic nuclear group. This up-regulation occurred from day 3 days after MCAO, peaked at 7 days post-ischemia and was sustained 14 days after MCAO (Figure 6B, Table 2). In contrast, no modifications of *bax and bcl-xl* mRNA levels were observed ($P > 0.05$; Table 2, Figures 6C and 6D). Therefore, it appears that injured thalamic neurons produced mRNAs of the adverse protein Cpp32 rather than the protective protein Bcl-xl. Consistent with the observed TUNEL staining, these results indicate that neuronal death occurs in thalamic nuclei through an apoptotic mechanism and that the induction of the *cpp32* gene might play a causative role in the cell death process. In contrast with previous results (Gillardon *et al*., 1996), we did not observe any increased levels of *bax* mRNA expression in thalamic neurons. However, these authors analyzed total mRNA expression 6 hours following ischemia. It cannot be excluded that these *bax* mRNA changes reflected a transitory phenomenon. Because we did not observe any differences in transcripts expression between WT and Bcl-2 transgenic mice, it can be concluded that the protective role of Bcl-2 in the thalamic delayed neuronal death process could have occurred despite the up-regulation of *cpp32* mRNA. However, this result is not suprising as the protective effect of Bcl-2 results from interactions with cell death molecules upstream to Cpp32/caspase-3 activation (see section 3.8.3.). Rather, future studies should determined if the active form of Cpp32 has been prevented in Bcl-2 transgenic mice.

4.4. Conclusion

Whereas the extent of cortical neuronal injury could not have been lowered by the Bcl-2 transgene, we report that cell death could have been prevented in the thalamus of Bcl-2 transgenic mice. These findings indicate that the pathophysiological mechanisms that underly neuronal damage may be different between thalamic and cortical neurons, and that the extent of neuroprotection

may depend on the injury paradigm. Because the present study does not confirm previous data showing a protective role of Bcl-2 in neocortical infarcted areas, it suggests that other death pathways of cell death may be critical following ischemia and acting on the intrinsic pathway could have not been sufficient to limit neuronal damage. Accordingly, the extrinsic pathway mediated by Fas receptor and associated proteins (FADD, DAXX, $FLIP_L$) has been recently under active investigation to assess its impact in brain ischemia (Taoufik *et al.*, 2007; Bi *et al.*, 2008). Altogether, these reports demonstrated the importance of the extrinsic pathway in neuronal death following transient and permanent MCAO. In contrast, anti-apoptotic therapies may constitute a possible treatment for areas of the brain remote from those directly affected by ischemia. Because atrophic changes in the ipsilateral thalamus also occur in patients with cerebral infarction in the medial cerebral artery territory (Tamura *et al*., 1991), our results may have therapeutic implications. However, further investigations with long-delayed cell injury after MCAO should be addressed to determine whether Bcl-2 may ensure a long-term neuroprotection of thalamic neurons.

5. Cerebral ischemia and mitochondrial Uncoupling protein-2

Article II: F. de Bilbao, D. Arsenijevic, P. Vallet, O.P. Hjelle, O.P. Ottersen, C. Bouras,* Yvette Raffin,* Karin Abou,* Wolfgang Langhans, Sheila Collins, J. Plamondon, M.C. Alves-Guerra, A. Haguenauer, I. Garcia, D. Richard, D. Ricquier and P. Giannakopoulos (2004) Resistance to cerebral ischemic injury in UCP2 knockout mice: evidence for a role of UCP2 as a regulator of mitochondrial glutathione levels. *J Neurochem* 89:1283–92.

5.1. Uncoupling proteins

Oxidative phosphorylation (Saleh *et al.*, 2002) is a mitochondrial process that uses controlled oxidation of energy substrates to generate a proton gradient across the inner mitochondrial membrane. This process involves the coupling of electron transport, through the electron transfer chain, to the active pumping of protons across the inner mitochondrial membrane. The potential energy produced by the proton gradient is used to drive phosphorylation of ADP to ATP by ATP synthase. Mitochondrial uncoupling proteins (UCPs) can dissociate oxidation from phosphorylation (ATP production) (Maragos and Korde, 2004). The term uncoupling refers to a condition in which a “leak” of protons back into the matrix bypasses ATP synthase and electron transport becomes functionally disconnected from the phosphorylation of ADP to ATP. UCPs are mitochondrial inner membrane proteins whose primary function is precisely to allow protons to re-enter the mitochondrial matrix (Figure 9). This process decreases the proton electrochemical gradient which in turn affects the synthesis of ATP. The conserved energy derived from the oxidation of substrates during this uncoupling is dissipated in the form of heat. The most studied is UCP1, found in abundance in the brown adipose tissue of rodents, neonates of other mammalian species (Nicholls and Locke, 1984).

One proposed crucial role for mild uncoupling activity is to reduce ROS production and consequent oxidative stress. The ROS may be generated when electron

transport chain slows down during “resting conditions” (wherein ATP generation is not essential) or during the inadequate supply of adinosine diphosphate (ADP) or dysfunction of ATP synthase. Excessive mitochondrial accumulation of calcium following ischemia may also cause disturbances in oxidative phosphorylation (Schinder *et al.*,, 1996), resulting in a decreased capacity for ATP production. In such conditions, the electron carrying intermediates have an increased chance to transfer single electron to molecular oxygen (O2) leading to the production of O2-• (presumably because electron flow down the electron transport chain is inhibited, thereby increasing the time of interaction between electrons and molecular oxygen) and the protons pumped out of the matrix can no longer return back (Mattiasson and Sullivan, 2006). This leads to the deregulation of the mitochondrial potential whose consequence has been proposed as the point of no return in apoptotic signaling (Iijima, 2006). The mild uncoupling due to UCPs lowers the mitochondrial membrane potential; this would be expected to reduce calcium overloading and attenuates the production of O2-• since both are dependent on the mitochondrial membrane potential (Maragos and Korde, 2004). A reduction in membrane potential decreases the generation of ROS presumably by increasing the flow of electrons through the electron transport chain, thereby decreasing the time of interaction between electrons and molecular oxygen. Lowering mitochondrial membrane potential may consequently decrease the probability of mitochondrial permeability transition pore activation, release of apoptogenic factors and activation of caspase-3 ultimately preventing cell-death activation. There are now many known examples of UCPs being up-regulated in physiological situations of oxidative stress, and thus they are widely considered to be part of the anti-oxidant defense system of eukaryotes (Krauss *et al.,* 2005).

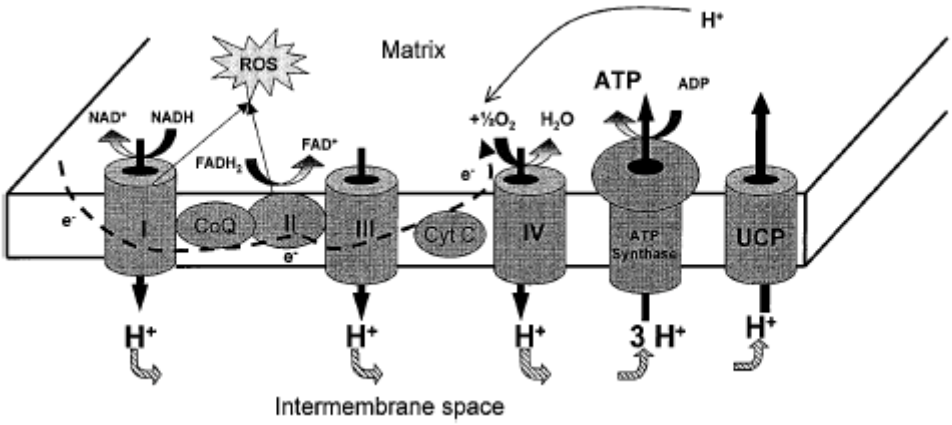

Figure 9: Coupled versus uncoupled respiration: in a tightly coupled state, protons (H^+) re-enters the mitochondrial matrix through ATP synthase to generate ATP from ADP. In less tightly, coupled states, H^+ can transit the membrane via UCPs, which result in the production of heat without concomitant production of ATP. When the proton-motive force is large, the half-life of superoxide-generating electron transport intermediates capable of reducing O2 to superoxide (ROS) is prolonged. CoQ: coenzyme Q; cyt C: cytochrome c (from Saleh *et al.*, 2002).

5.2. Uncoupling protein-2

UCP2, which is one of the members of this class of proteins, is widely expressed in various mammalian tissues (Fleury *et al.*, 1997) including brain (Richard *et al.*, 1998; Andrews *et al.,* 2005a). It has been implicated in diverse pathologic conditions such as obesity (Hidaka *et al*., 1998), diabetes (Zhang *et al*., 2001), neurodegenerative diseases (Diano *et al*., 2003; Mattiasson *et al*., 2003; Deierborg *et al*., 2008). Under normal circumstances, UCP2 is expressed predominantly in neurons in several brain regions in both rodents and primates (Horvath *et al*., 1999) although cells of the choroids plexus (Richard *et al*., 1999) as well as endothelial cells (Fink *et al*., 2005) also express this mitochondrial uncoupling protein. Following brain injury, UCP2 is induced in microglia, the residing monocytes of the brain (Clavel *et al*., 2003) as well as invading monocytes and neutrophils (Arsenijevic *et al*., 2007). In rodent, it is expressed in the hypothalamus particularly (suprachiasmatic, paraventricular, dorsomedial, ventromedial nucleus, and arcuate nuclei) (Horvath *et al*., 1999), thalamus (Horvath *et al*., 1999), hippocampus and cerebellum (Richard *et al*., 1998) suggesting that UCP2 may play a role in neuroendocrine, behavioral, autonomic functions and metabolic processes. UCP2 mRNA is also detectable in the cortex,

but levels are much lower than that seen in the hypothalamus (Richard *et al*., 1998). Species differences in brain UCP2 expression have been seen, in particular between the rat and mouse (Richard *et al*., 1999), the meaning of these differences is presently unknown.

5.3. Role of UCP2 in regulation of ROS

The hypothesis that UCP2 functions to limit ROS production received attention when it was found that macrophages from UCP2 KO mouse generate more ROS than WT mouse resulting in a striking resistance to infectious microorganisms which was reversible by quenching of ROS (Arsenijevic *et al*., 2000). *In vivo*, these animals show resistance to *Toxoplasma* infection. Mattiasson *et al.* (2003) observed that UCP2 may be induced by transient MCAO and its neuroprotective effect could occur by activating cellular redox signaling or by inducing mild mitochondrial uncoupling that prevents the induction of mitochondrial permeability transition pore and release of apoptogenic proteins (Andrews *et al*., 2005a). Furthermore, mice that overexpress human UCP2 show increased neuronal survival in hippocampal CA1 cells and decreased oxidative stress after excitotoxic cell injury induced by exposure to kainic acid (Diano *et al.*, 2003). Using an acute neurodegeneration model, the entorhinal cortex lesion paradigm, Bechmann *et al.* (2002) evidenced that up-regulation of UCP2 may protect cells against neurodegeneration and found that UCP2 expression levels are inversely correlated with caspase-3 activation. In a mouse model of Parkinson's disease, UCP2 KO mice were found to have increased *in vivo* ROS production and greater nigral dopaminergic cell loss (Andrews *et al.*, 2005b). Overexpression of human UCP2 diminishes tissue loss, oxidative damage and calcium loading after traumatic brain injury (Mattiasson *et al.*, 2003). UCP2 KO mice have a higher ROS level that delays liver regeneration (Horimoto *et al*., 2004). In rodents, UCP2 promotes survival age by reducing mitochondrial ROS production, whereas UCP2 deletion severely shortens lifespan (Andrews and Horvath, 2009).

In vitro, UCP2 may regulate mitochondrial production of H_2O_2 (Negre-Salvayre *et al.*, 1997). It has also been suggested that UCP2 act as a channel, facilitating transport of mitochondrial ROS from the mitochondrial matrix to the extramitochondrial space, where they can be more readily degraded by cytosolic

anti-oxidants such as catalase (Mattiasson *et al.*, 2003). This can be further supported by the specific increase in intracellular ROS levels observed in endothelial cells pre-treated with antisense oligonucleotides directed against UCP2 mRNA (Duval *et al*., 2002). In addition, superoxides themselves can induce the expression of UCP2 (Pecqueur *et al.*, 2001), suggesting that UCP2 could be part of an endogenous neuroprotective pathway in response to oxidative stress. ROS-suppressing property of UCP2 can inhibit apoptosis in cancer cells (Derdak *et al*., 2008), whereas inhibiting UCP2 expression increases ROS accumulation and apoptosis induced by an inflammatory damage in the hypothalamus (Degasperi *et al*., 2008).

Altogether, these results indicate that modulation of UCP2 could be imperative in limiting the mitochondrial dysfunction and subsequent cell death in cerebral ischemia. As both calcium buffering, ROS production and apoptosis are under the control of mitochondria, targeting pharmacologic intervention on mitochondria may be one solution to prevent cell death following an ischemic insult. Because UCP2 has significant effect on these mitochondrial deleterious events, targeting its expression *in vivo* may help to identify its potential therapeutic application. Whereas gain-of-function studies can provide important insights into the molecular function of UCP2, complications in interpretation can occur due to improper insertion of the transgenic protein into the mitochondrial inner membrane (Andrews *et al.,* 2005a). In addition, and as previously mentioned, UCP2 brain expression differs between mice and rats; this adds further complications to transgenic studies, particularly because UCP2 may be expressed in cells were it was previously absent. Studies involving loss-of-function mutants might be more useful. In Article II, we therefore examined the *in vivo* effects of permanent focal ischemia in mice genetically deleted for *ucp2*. First, we performed a detailed study of brain injury in WT and UCP2 KO mice, including regional and cellular distribution of UCP2 mRNA. Second, we explored the effect of *ucp2* deletion upon oxidative stress levels as well as mitochondrial anti-oxidant molecules status (namely MnSOD and GSH) in these mice before and after ischemia.

Journal of Neurochemistry, 2004, **89**, 1283–1292 doi:10.1111/j.1471-4159.2004.02432.x

Resistance to cerebral ischemic injury in UCP2 knockout mice: evidence for a role of UCP2 as a regulator of mitochondrial glutathione levels

Fabienne de Bilbao,*[,1] Denis Arsenijevic,†[,1] Philippe Vallet,* Ole Petter Hjelle,‡ Ole Petter Ottersen,‡ Constantin Bouras,* Yvette Raffin,* Karin Abou,* Wolfgang Langhans,† Sheila Collins,§ Julie Plamondon,¶ Marie-Clotilde Alves-Guerra,** Anne Haguenauer,** Irene Garcia,†† Denis Richard,¶ Daniel Ricquier** and Panteleimon Giannakopoulos*[,‡‡]

*Department of Psychiatry. University Hospitals Geneva, Geneva

†Institute of Animal Sciences, ETHZ, Zurich, Switzerland

‡Department of Anatomy, Institute of Basic Medical Sciences, University of Oslo, Norway

§Psychiatry and Behavioral Sciences and Pharmacology, Duke University Medical Center, Durham, North Carolina, USA

¶Department of Anatomy and Physiology, Faculty of Medicine, Laval University, Québec, Canada

**CNRS UPR 9078, Faculté de Médecine Necker-Enfants Malades, Paris, France

††Department of Pathology, CMU, Geneva

‡‡Old Age Psychiatry Service, University of Lausanne, Prilly, Switzerland

Abstract

Uncoupling protein 2 (UCP2) is suggested to be a regulator of reactive oxygen species production in mitochondria. We performed a detailed study of brain injury, including regional and cellular distribution of UCP2 mRNA, as well as measures of oxidative stress markers following permanent middle cerebral artery occlusion in UCP2 knockout (KO) and wild-type (WT) mice. Three days post ischemia, there was a massive induction of UCP2 mRNA confined to microglia in the peri-infarct area of WT mice. KO mice were less sensitive to ischemia as assessed by reduced brain infarct size, decreased densities of deoxyuridine triphosphate nick end-labelling (TUNEL)-labelled cells in the peri-infact area and lower levels of lipid peroxidation compared with WT mice. This resistance may be related to the substantial increase of basal manganese superoxide dismutase levels in neurons of KO mice. Importantly, we found a specific decrease of mitochondrial glutathione (GSH) levels in UCP2 expressing microglia of WT, but not in KO mice after ischemia. This specific association between UCP2 and mitochondrial GSH levels regulation was further confirmed using lipopolysaccharide models of peripheral inflammation, and in purified peritoneal macrophages. Moreover, our data imply that UCP2 is not directly involved in the regulation of ROS production but acts by regulating mitochondrial GSH levels in microglia.

Keywords: cerebral ischemic injury, glutathione, lipopolysaccharide, reactive oxygen species, superoxide dismutase, uncoupling protein 2.

J. Neurochem. (2004) **89,** 1283–1292.

Uncoupling protein 2 (UCP2) (Fleury *et al.* 1997; Boss *et al.* 2000; Ricquier and Bouillaud 2000) a homologue of the brown adipose tissue-specific proton transporter UCP1, belongs to the mitochondrial anion carrier family that are present in the inner mitochondrial membrane (el Moualij *et al.* 1997). The UCP2 gene is expressed in most tissues (Fleury *et al.* 1997; Gimeno *et al.* 1997; Pecqueur *et al.* 2001) including brain (Richard *et al.* 1998). Whereas the main function of UCP1 in rodents is to produce heat by allowing

Received October 1, 2003; revised manuscript received December 10, 2003; accepted February 5, 2004.

Address correspondence and reprint requests to Denis Arsenijevic, Institute of Animal Sciences, ETHZ, Schorenstrasse 16, Zurich, Switzerland. E-mail: denis.arsenijevic@inw.agrl.ethz.ch

[1]These authors contributed equally to this work.

Abbreviations used: GSH, glutathione; KO, knockout; MCAO, middle cerebral artery; MDA, malondialdehydes; OD, optical density; ROS, reactive oxygen species; SDH, succinate dehydrogenase; SOD, superoxide dismutase; TUNEL, deoxyuridine triphosphate nick end-labelling; UCP2, uncoupling protein 2; WT, wild type.

proton flux across the inner mitochondrial membrane to the matrix and therefore bypass ATP synthase (Ricquier *et al.* 2000), several recent lines of evidence indicate that UCP2 is a regulator of reactive oxygen species (ROS) (Arsenijevic *et al.* 2000; Ricquier *et al.* 2000). *In vivo*, we have previously shown that disruption of the UCP2 gene protects against lethal infection by *Toxoplasma gondii* (Arsenijevic *et al.* 2000) and this effect has been associated with increased ROS production by macrophages. Moreover, UCP2 has been implicated in the control of mitochondrial ROS levels (Negre-Salvayre *et al.* 1997; Lee *et al.* 1999; Arsenijevic *et al.* 2000; Yang *et al.* 2000; Li *et al.* 2001; Pecqueur *et al.* 2001) possibly by decreasing mitochondrial membrane potential (Skulachev 1998). UCP2 is induced in underfeeding (Pecqueur *et al.* 2001) and under pathological conditions (obesity, anorexia/cachexia, diabetes, cardiovascular diseases, neurodegeneration, HIV, infection, inflammation) where excessive ROS production occurs, further supporting a link between UCP2 and oxidative stress (Chavin *et al.* 1999; Cortez-Pinto *et al.* 1999; Rashid *et al.* 1999; Li *et al.* 2001; Pecqueur *et al.* 2001; Zhang *et al.* 2001). *In vitro* studies also suggest that UCP2 may lead to an increase in proton conductance through interaction with superoxide (Echtay *et al.* 2002).

ROS have been implicated in the pathogenesis of ischemic brain injury (Chan 1996). It now appears that ROS production in mammalian cells is mainly a toxic by-product of the mitochondrial electron transport chain (Raha and Robinson 2000). As ROS are highly reactive and may damage cellular components, cells have developed various strategies to dissipate free radicals and remove their oxidation products. Anti-oxidative systems involving superoxide dismutase (SOD) enzymes, glutathione (GSH) and catalase are present in the brain and are involved in ROS detoxification. In particular, previous data strongly suggest a key role of the mitochondrial manganese SOD (Mn SOD) in neuroprotection following focal ischemia (Keller *et al.* 1998; Murakami *et al.* 1998; Fujimura *et al.* 1999; Guégan *et al.* 1999). A role of intracellular GSH in protection against free radical processes induced by cerebral ischemia has also been evidenced (Love 1999). In this report, we examine the *in vivo* effects of genetic UCP2 deficiency upon oxidative stress and antioxidant levels after focal ischemia and suggest a potential mechanism by which UCP2 can alter cellular physiology in respect to its anti-oxidant function. We report a significant effect on brain infarct size, mitochondrial Mn SOD levels and provide evidence supporting a central role of UCP2 in the regulation of the mitochondrial pool of GSH.

Materials and methods

Surgical preparation, volume of the infarct

We performed permanent occlusion of the middle cerebral artery (MCAO) as previously described (De Bilbao *et al.* 2000) in 2-month-old *UCP2*$^{-/-}$ male mice (Arsenijevic *et al.* 2000) and their wild-type (WT) co-littermates ($n_{Ucp2}^{-/-} = 6$ and $n_{WT} = 5$). Three days later they were then perfused through the ascending aorta with a solution of paraformaldehyde 4% in phosphate-buffered saline (PBS, pH 7.35). Brains were removed and processed for paraffin embedding. Sections (7 μm) of the whole infarct area were cut with a microtome and collected on slides pre-treated with 3-aminopropyltriethoxy-silane (Sigma, St Louis, MO, USA). Sections were counter-stained with cresyl-violet for the histological identification of the nuclear boundaries and peri-infarct areas and mounted in Eukitt. For each animal, quantification of the infarcted area was performed on the cresyl-violet stained sections at five representative levels throughout the rostro-caudal extent of the lesion (A 0.26, −0.22, −0.40, −0.70 and −1.2 mm relative to bregma) (Franklin and Paxinos 1997). The rostro-caudal extent of the infarct was the same in both groups of mice. The infarcted area of each section was calculated by the substraction of healthy tissue areas of the contralateral to the ipsilateral side of the section (Guégan *et al.* 1998) using a computer-assisted image analyzing system (Software ≪Morphometry≫, Samba 2005 TITN, Alcatel, Grenoble, France). For each animal, volumes of infarct (mm^3) were calculated after integration of areas with the distance between each level. Results are expressed as mean ± SEM.

In situ detection of DNA fragmentation

TUNEL staining was used as an indication of DNA damage in the cell three days post ischemia. Each 10 sections were processed with the terminal deoxytransferase-mediated deoxyuridine triphosphate nick end-labelling (TUNEL) method according to our previous studies (de Bilbao *et al.* 2000) in order to assess neuronal DNA fragmentation. Controls for TUNEL staining were investigated by omitting TdT. TUNEL-labelled cells were counted in the peri-infarct area (thalamic border) under low-power microscopic fields (× 20) on three sections at the co-ordinates that showed a high concentration of TUNEL labelled cells (−1.22 mm relative to bregma) for each mice. A mean number of TUNEL-labelled cells was calculated for each group of mice.

UCP2 *in situ* hybridization temporal expression

We followed the expression of UCP2 after cerebral ischemic injury in WT animals. Six hours, 12 h and on days 1, 2, 3 and 4 post injury (four mice per groups), *in situ* hybridization was performed on brain to determine the levels of UCP2 in the tissue using a rat UCP2 probe (Richard *et al.* 1998). Mounted brains were either directly processed for immunostaining for microglia using the antibody from Dr Y. Imai (Ohsawa *et al.* 2000) or neurons using the NeuN antibody from Chemicon (Temecula, CA, USA) and/or *in situ* hybridization and then processed for hybridization (Richard *et al.* 1998).

Lipid peroxidation of brain homogenates

We investigated changes in oxidative stress 3 days following ischemia by the measurement of malondialdehydes (MDA), an indicator of endogenous lipid peroxidation on 3-day operated ($n_{ucp2}^{-/-} = 4$ and $n_{WT} = 3$) and-non-operated ($n_{ucp2}^{-/-} = 3$ and $n_{WT} = 3$) (Arsenijevic *et al.* 2001).

Western blots analysis of Mn SOD, cytochrome *c* and cytochrome oxidase

Protein extraction for both the mitochondrial and cytosolic fractions were performed as described (Fujimura *et al.* 1999). After mice

were perfused (3 days post ischemia) with ice-cold phosphate-buffered saline (PBS), brains were removed and ischemic hemisphere was separated from the contralateral hemisphere. Both hemispheres of operated and-non-operated mice ($n = 4$ per group) were homogenized in a glass tissue grinder in a solution corresponding to 600 μL per 100 mg of tissue [20 mM HEPES-KOH, pH 7.5, 250 mM sucrose, 10 mM KCl, 1.5 mM $MgCl_2$, 1 mM EDTA, 1 mM EGTA, 1 mM dithiothreitol (DTT), 0.1 mM phenylmethyulsulfonyl fluoride (PMSF), 2 μg/mL aprotinin, 10 μg/mL leupeptin, 5 μg/mL pepstatin and 12.5 μg/mL N-acetyl-leu-leu-norleucinal (ALLN)]. Homogenates were then centrifuged at 750 *g*, and the supernatant was centrifuged for a further 8000 *g* at 4°C for 20 min. Fraction of the 750-*g* supernatant was collected for Mn SOD analysis. The 8000-*g* pellet was used to obtain the mitochondrial fraction. The supernatant was further centrifuged at 100 000 *g* to obtain the protein cytosol fraction and the pellet was re-dissolved in 200 μL of the above-mentioned buffer. Succinate dehydrogenase was used as an indice of mitochondrial fraction location (Bancroft 1982) and was compared with the other fractions (see below). We then proceed for gel electrophoresis and immunodetection as previously described (Llames *et al.* 2000). Primary antibodies to Mn SOD (Calbiochem, San Diego, CA, USA, 1/200), cytochrome *c* antibody (Santa Cruz Biotechnology, Santa Cruz, CA, USA, 1/200) or cytochrome oxidase (COX) subunit IV (Molecular Probes, Eugene, OR, USA) were used. Densitometry readings of the fractions from both ischemic and non-ischemic brain of WT and *ucp2*$^{-/-}$ mice were made using ImageTool software (Scion Corporation, Frederick, MD, USA).

Glutathione levels

Brain homogenates from WT and *ucp2*$^{-/-}$ mice subjected or not to ischemia (1 and 3 days post ischemia) ($n = 4$ per group) were processed as described for western blot analysis. Total and mitochondrial fractions of GSH levels were measured using a method based on the formation of a chromophoric product resulting from the reaction of 5,5′-dithiobis-(2-nitrobenzoic acid) (DTNB, Sigma) and GSH (Calbiochem, San Diego, CA, USA) (Tietze 1969).

Immunohistochemistry

Frozen coronal sections (12 μm) from 3-day operated and non-operated mice were processed for immunostaining using the following antibodies: sheep anti-human superoxide dismutase (SOD) Mn (Calbiochem, San Diego, CA, USA, 1/100) and rabbit polyclonal anti-glutathione (GSH) 1/10, Prof. Ottersen, University of Oslo, Norway. Goat anti-rabbit immunoglobulins Alexa Fluor 568 (Molecular Probes) were used for the GSH antibody and rabbit anti-sheep immunoglobulins for the Mn SOD antibody (Dako, Carpinteria, CA, USA). We performed double staining for Mn SOD or GSH and cellular markers according to the same protocol. To label astrocytes, microglia, macrophages and neuronal cells, mouse polyclonal anti-glial fibrillary acidic protein (GFAP) clone GA5 (Sigma, 1/400), rabbit polyclonal anti-*Iba*1 (1 μg/mL, kindly provided by Prof. Y. Imai, National Center of Neurology and Psychiatry, Japan), rat anti-mouse F4/80 for macrophage (Serotec, Raleigh, NC, USA) and the mouse anti-neuronal nuclei monoclonal antibody (NeuN) 1/1000, Chemicon have been used, respectively. The GFAP, anti-*Iba*1, anti-macrophages and NeuN antibodies were detected by using Alexa Fluor 546 rabbit anti-mouse (Molecular Probes), Goat anti-rabbit immunoglobulins Alexa Fluor 568 (Molecular Probes), goat anti-rabbit FITC, goat anti-rat FITC (Nordic Immunology, Tiburg, the Netherlands), and goat anti-mouse immunoglobulins linked to AMCA (Dako), respectively. Negative controls included deletion of the primary or secondary antibody. Photomicrographs of double immnunofluorescent staining were constructed using the MetaMorph Imaging System (Visitron Systems, West Chester, PA, USA). Immunohistochemical staining of GSH and Mn SOD (for Mn SOD microglia double staining) were revealed by ABC kit peroxidase staining. Glutathione was also detected by mercury orange and phthaldialdehyde in brain sections and was similar in distribution compared with polyclonal rabbit anti-GSH immunostaining. Histological fluorescent detection of GSH was performed using phthaldialdehyde (10 mM) and mitochondria were detected using the fluorescent dye rhodamine 123.

Glutathione in mitochondria after cerebral ischemia and lipopolysaccharide injection

On days 1, 2 and 3 after ischemic injury, the ischemic hemisphere of WT mice ($n = 3$ for each group) was removed and mitochondria were isolated as follows. After mice were perfused with ice-cold PBS, brains were removed and ischemic hemisphere was separated from the contralateral hemisphere. Both hemispheres of operated and non-operated mice were homogenized in a glass tissue grinder in a solution corresponding to 600 μL (0.25 M sucrose – 1 mM EDTA) per 100 mg of tissue as described by Alexander and Griffiths (1993). This suspension was overlayed onto 0.34 M sucrose – 1 m $MgCl_2$, and 20 mM phosphate buffer, pH 7.4) and centrifuged at 700 *g* for 10 min at 4C. The resulting supernatant was centrifuged at 5000 *g* for 15 min at 4C. The resulting pellet was re-suspended in 40 mLs of 0.25 M sucrose – 1 mM EDTA and centrifuged for 10 min at 24000 *g*. This step was repeated once more. The resulting pellet was then re-suspended in 3 mLs of the following buffer (0.25 M sucrose, 2 mM EDTA, 4 mM (Bancroft 1982). Mitochondria were estimated by succinate dehydrogenase (SDH) activity assay from the mitochondria preparation. Two microlitres was used to determine the activity by the reduction of 200 μL of succinate/nitroblue tetrazolium solution. From the minimal activity of 0.14 optical density (OD)/min, all isolates were normalised. Once all mitochondrial groups were normalised for activity, isolates were divided in six subgroups – three with (G+) and three without (G–) GSH for the GSH uptake study. Mitochondria were then allowed to incubate with 1 mM GSH (Calbiochem, La Jolla, CA, USA) for 5 min at 37°C, they were then centrifuged for 15 min 8000 *g* at 4°C and washed with buffer and centrifuged again. The pellets were re-dissolved in buffer and GSH was measured (as above). The uptake is the ratio of (G+)/(G–). We also tested GSH content and uptake in lung ($n = 3$) of WT mice 1 day after 200-μg LPS injection (a time at which UCP2 is up-regulated in these tissues). The same method was used as for brain mitochondria isolation following ischemia. At the end of the experiment for brain and lung, SDH activity was determined and there were no major differences between the groups, indicating that GSH uptake differences were not related to changes in mitochondria numbers.

Peritoneal macrophage GSH levels

Peritoneal macrophages were induced by an intraperitoneal injection of thioglycolate medium (Arsenijevic *et al.* 2000). For

slide culture, cells were re-suspended in PBS glucose 0.1% and 10^5 were aliquoted to each well in a 4-well chamber and left to adhere for 30 min. LPS (1 ng/mL) was added for 10 min to induce depletion of GSH. Cells were washed with PBS and incubated for 5 min in 7 mM GSH. After washing, cells were then fixed with PAF 4% for 1 min. Cells were washed, incubated with phthaldialdehyde (10 mM) for 1 min to visualize GSH. Controls included non-treated cells. Fluorescent microscopy quantification of the intensity of cytoplasmic staining was performed by using NIH Image 1.62 program. Photomicrographs of fluorescent staining were constructed using Axiovision 3.0 (Carl Zeiss Vision GmbH).

Statistical analysis

Differences were assessed using an analysis of variance (ANOVA) followed by the Fisher's test.

Results

Ucp2 mRNA expression in focal cerebral ischemia

We determined the temporal expression and the regional distribution of *UCP2* mRNA in response to ischemic brain injury induced by permanent MCAO. *In situ* hybridization revealed a delayed induction of *UCP2* mRNA in the peri-infarct area with a strong increase by day 3 and 4 post MCAO. At this stage, labelled cells were observed in the peri-infarct area in the neocortex and caudate putamen (Fig. 1a). No labelling was observed in the neocortex of the ipsilateral hemisphere from 6 to 24 h following ischemia and the contralateral hemisphere was devoid of labelled cells throughout the post-operative period. Induced *ucp2* mRNA labelling occurred in microglial elements (Fig. 1b). Other *UCP* mRNAs expression as brain mitochondrial carrier protein 1 (Bmcp1) or BMCP1/UCP5 were unaltered following ischemia, suggesting a specific role for UCP2 in this oxidative stress paradigm (data not shown).

Ischemic brain injury is reduced in *UCP2*$^{-/-}$ mice

UCP2-deleted (*UCP2*$^{-/-}$) mice (Arsenijevic *et al.* 2000) were used to investigate the role of UCP2 in cellular damage induced by ischemia. The infarct volume was quantified 3 days after permanent MCAO in WT and *UCP2*$^{-/-}$ mice when *UCP2* mRNA was highly expressed in the peri-infarct area of WT mice. Infarct volume was significantly reduced in *UCP2*$^{-/-}$ mice (6.3 ± 0.08 mm^3, $n = 6$) when compared with WT mice (7.74 ± 0.27 mm^3, $n = 5$) ($p < 0.001$) (Fig. 1c), suggesting that the *in vivo* deletion of *UCP2* may protect neocortical areas from ischemic damage. To evaluate if differences in vascular anatomy may contribute in the lower susceptibility to injury in *UCP2*$^{-/-}$ mice, the cerebral vasculature was examined by carbon black injection in *UCP2*$^{-/-}$ and WT mice. Close inspection of the vasculature revealed no differences in the Circle of Willis or MCA between the two groups of mice (data not shown).

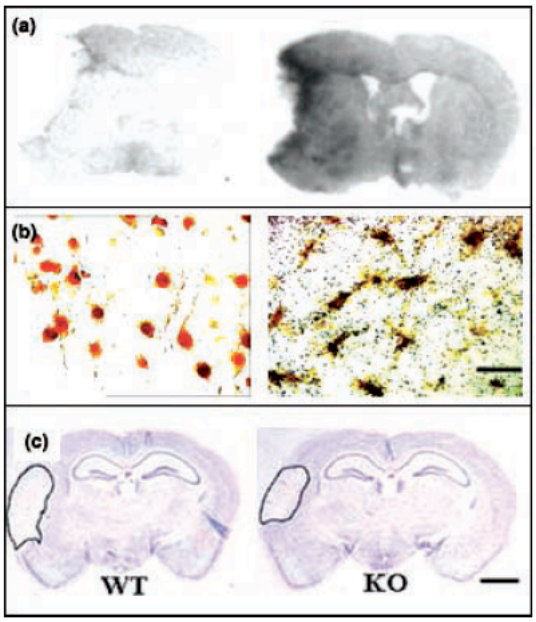

Fig. 1 UCP2 transcript expression induced by focal ischemia in wild-type (WT) mice and effect of *UCP2* deletion on infarct volumes, representative of $n = 6$ mice. (a) Film autoradiograms of coronal brain sections from WT mice illustrating the distribution of UCP2 mRNA 48 h (left) and 72 h (right) following permanent MCAO. Results showed that, from day 3 post ischemia, *UCP2* mRNA was substantially increased in the peri-infarct area. (b) Photomicrographs showing *UCP2* mRNA riboprobe hybridization (left) and immunolabelling revealing microglial cells (right) in the peri-infarct area of a WT mice 3 days post ischemia. *UCP2* mRNA expression was observed in brown microglial cells, but not in cortical neurons (red cells on the left) (scale bar, 7 μm). (c) Representative coronal brain sections showing the ischemic infarct 3 days after focal ischemia in WT and *UCP2*$^{-/-}$ (KO) mice. The surrounded areas denote the ischemic area. Brain sections were stained with cresyl violet. The infarct size was significantly reduced in *UCP2*$^{-/-}$ mice (scale bar, 120 μm).

The number of TUNEL cells is decreased in *ucp2*$^{-/-}$ mice

Neuronal damage was also assessed by a quantitative analysis of TUNEL-labelled cells. The negative control in the absence of TdT gave no labelled cells. No TUNEL labelling was observed in the contralateral non-ischemic hemisphere. The histological examination of brain sections showed that, 3 days post MCAO, many TUNEL-labelled cells were encountered in the striatal border and the neocortical border zones of the peri-infarct area as previously described (de Bilbao *et al.* 2000). Occasional labelling was observed scattered in the ipsilateral hemisphere. The same pattern of distribution was observed between the two groups of mice (not shown). The number of TUNEL-positive cells was markedly reduced in *UCP2*$^{-/-}$ mice ($n = 14 \pm 6.6$) when compared with WT mice ($n = 34 \pm 6$) ($p < 0.05$).

Translocation of cytochrome *c* to the cytosol is prevented in *UCP2*$^{-/-}$ mice

The cytosolic release of cytochrome *c* from the mitochondrial fraction represents a critical step of the cell death induced by ischemia (Guégan *et al*. 1999; Touzani *et al*. 2001). A significant amount of cytochrome *c* ($n = 3$, OD = 83.17 ± 2.63) was detected in the cytosolic fraction of WT mice 3 days after ischemia (Fig. 2a). In contrast, we did not detect any labelling in the cytosolic fraction of ischemic *UCP2*$^{-/-}$ mice ($n = 3$, OD = 0). Non-ischemic control brains did not display any cytochrome *c* in the cytosolic fraction (data not shown). This finding provides evidence that the protective effect of UCP2 depletion may be mediated partly through a decrease in cytochrome *c* release.

Levels of lipid peroxidation are decreased in *UCP2*$^{-/-}$ mice after ischemia

In order to examine whether the redox status could be altered in *UCP2*$^{-/-}$ mice, we investigated changes in the levels of MDA, an early marker of lipid peroxidation, in *UCP2*$^{-/-}$ and WT mice. In both groups of mice, a significant increase in MDA levels was observed in the ischemic brains when compared with the-non-operated controls ($p < 0.0001$). This increase was reduced by 30% in *UCP2*$^{-/-}$ mice in comparison with WT ($p < 0.0001$) (Table 1), indicating a lower oxidative injury in *UCP2*$^{-/-}$ mice. There was no difference in MDA levels between WT and *UCP2*$^{-/-}$ non-operated mice.

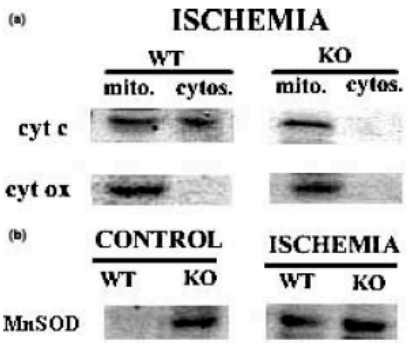

Fig. 2 Effect of *UCP2* deletion on cytochrome *c* release and Mn SOD levels before and 3 days after permanent focal cerebral ischemia. (a) Western blot analysis of brain mitochondrial (mito.) and cytosolic (cytos.) cytochrome *c* (cyt c) after ischemia in wild-type (WT) and *UCP2*$^{-/-}$ (KO) mice. Following MCAO, increased cytosolic cytochrome *c* was detected in WT mice ($n = 3$, OD = 83.17 ± 2.63) but not in *UCP2*$^{-/-}$ mice ($n = 3$, OD = 0). Cytochrome oxidase (cyt ox) analyses are shown as an internal control of mitochondrial fraction. (b) Western blot analysis of Mn SOD from control and ischemic brains of WT and KO mice. The optical density of the Mn SOD characteristic bands was significantly higher in KO mice ($n = 3$, OD = 76.2 ± 0.9) when compared with WT mice ($n = 3$, OD = 0, $p < 0.001$). Following ischemia, we report that Mn SOD levels were induced in WT ($n = 3$, OD = 78.8 ± 5.2, $p < 0.001$) and *UCP2*$^{-/-}$ ($n = 3$, OD = 85.6 ± 1.4, $p < 0.05$) mice when compared with control brains. The results are representative of three independent studies.

Mn SOD levels are increased in *UCP2*$^{-/-}$ mice

As Mn SOD is considered as the first line of defence against oxygen toxicity, we also examined its expression in both groups of mice. Western blot analysis revealed that basal levels of Mn SOD protein were high in brain tissue from the *UCP2*$^{-/-}$ mice compared with undectable levels in WT mice (Fig. 2b), indicating an up-regulation of Mn SOD. Following ischemia, Mn SOD levels were induced in WT ($p < 0.001$) and *UCP2*$^{-/-}$ ($p < 0.05$, Fig. 2b) mice (Durmaz *et al*. 1999). These results were also confirmed by immohistochemistry (Figs 3a and b). For further characterization of the cell types which overexpressed Mn SOD in *UCP2*$^{-/-}$ mice, we used neuronal (NeuN), astrocytic (GFAP) and microglial (*Iba*1) markers. Double staining experiments indicated that Mn SOD immunoreactivity was mainly located in neuronal and astrocytic cells in most brain structures, including the neocortex (Figs 3c–f). Mn SOD protein was not detected in those areas that displayed enhanced *UCP2* mRNA expression in microglia (data not shown). We did not find any changes in catalase activity in *UCP2*$^{-/-}$ mice (data not shown).

The post-ischemic decrease in mitochondrial GSH is observed in WT but not in UCP2$^{-/-}$ mice

The role of GSH against ROS and lipid peroxidation is well documented (Wendel and Feuerstein 1981). Endogenous GSH levels have been shown to correlate with the severity of the ischemic insult (Mizui *et al*. 1992). In particular, depletion of mitochondrial rather than cytosolic GSH is crucial to elicit cell damage (Reed 1993; Shan *et al*. 1993; Armstrong *et al*. 2001). We observed consistent double labelling between UCP2 and GSH prior to and after ischemia in WT mice (Figs 4a–c). Following permanent MCAO, we report a drop in total GSH levels in the ischemic hemisphere in both groups of mice ($p < 0.05$ for WT and *UCP2*$^{-/-}$ mice) (Table 1). Mitochondrial GSH levels were significantly decreased in the ischemic hemispheres of WT mice ($p < 0.05$). In contrast, mitochondrial GSH levels were not reduced in ischemic *UCP2*$^{-/-}$ mice ($p > 0.05$) (Table 1). This result was confirmed by fluorescent microscopy, as GSH immunolabelling was stronger in microglial mitochondria of *UCP2*$^{-/-}$ compared with WT mice (Fig. 4d–k). Therefore, it appears that *UCP2*$^{-/-}$ mice have a dysregulated mitochondrial GSH flux response compared with WT mice following cerebral ischemia.

Temporal association between the decreased mitochondrial GSH levels following central or peripheral inflammation and induction of UCP2 in WT mice

One day post ischemia, when *UCP2* mRNA is not yet increased, we report a dramatic decrease of total brain GSH

Table 1 Anti-oxidative status of WT and *UCP2*$^{-/-}$ mice subjected or not to ischemia

	WT mice		UCP2$^{-/-}$ mice	
Brain tissue	Non-operated	Ischemic	Non-operated	Ischemic
MDA	30.97 ± 3.69	70 ± 2.48***	34.5 ± 4	48.4 ± 1.3**††††
Total GSH	1.36 ± 0.1	0.908 ± 0.06*	1.38 ± 0.09	0.844 ± 0.25*
Mitochondrial GSH	0.097 ± 0.02	0.061 ± 0.008*	0.085 ± 0.019	0.09 ± 0.042†

Malondialdehydes (MDA), an indicator of endogenous lipid peroxidation, total and mitochondrial GSH levels, were measured in the brain of WT and *UCP2*$^{-/-}$ mice 3 days post MCAO and compared with non-operated mice. *Indicates statistical significance between operated and non-operated mice of the same group (*$p < 0.05$, **$p < 0.001$, ***$p < 0.0001$). † Indicates statistical significance between *UCP2*$^{-/-}$ and WT mice with the same treatment (†$p < 0.05$, ††$p < 0.01$, †††$p < 0.001$, ††††$p < 0.0001$) (ANOVA test). MDA and GSH values are given as nmol/g and nmol/mg of tissue, respectively. Each value is expressed as mean ± SEM. Although we cannot exclude a possible effect of operation to MDA and GSH levels, this is an unlikely scenario as several previous reports have demonstrated that most biochemical and morphological markers used in the present study are only marginally affected in sham-operated animals compared with animals with cerebral ischemia (Mizui *et al.* 1992; Suzuki *et al.* 1999; Candelario-Jalil *et al.* 2001; Pratico *et al.* 2002).

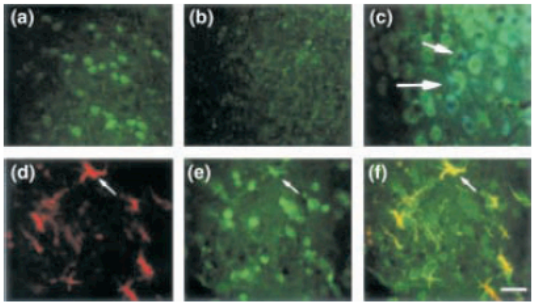

Fig. 3 Mn SOD immunolabelling in wild-type and *UCP2*$^{-/-}$ mice. (a, b) As assessed by immunohistochemistry, basal Mn SOD expression was increased in the cortical area of control *UCP2*$^{-/-}$ mice (a) compared with WT (b). (c) Mn SOD immunoreactivity (green) was detected in neuronal perikarya (blue cells, arrows) of non-operated *UCP2*$^{-/-}$ mice. Three days post ischemia, Mn SOD immunolabelling was induced in both group of mice (not shown). (d, e, f) Three days post ischemia, Mn SOD immunoreactivity (green cells, arrow) was also detected in astrocytic cells (red cells, GFAP-positive, arrow) of WT and *UCP2*$^{-/-}$ mice (arrow), but not in the microglial cells which normally expressed *UCP2* mRNA. (f) is the overlay of (d) and (e) (scale bar, 20 μm).

(0.65 ± 0.02 nmol/mg of tissue) in ischemic WT mice as compared with controls (1.6 ± 0.1 nmol/mg of tissue, $p < 0.001$). In contrast, mitochondrial GSH levels were not altered at this time (0.3 ± 0.02 nmol/mg of tissue vs. 0.26 ± 0.01 nmol/mg of tissue, $p > 0.05$). A substantial decrease of mitochondrial GSH levels occurs 3 days post ischemia (0.017 ± 0.003 nmol/mg of tissue, $p < 0.0001$), indicating an association between mitochondrial GSH decrease and *UCP2* mRNA induction. Importantly, LPS has been shown to induce UCP2 in the lung of mice (Pecqueur *et al.* 2001). In this other experimental paradigm, a significant decrease in mitochondrial GSH (0.014 ± 0.006 vs. 0.085 ± 0.010 nmol/mg of tissue, $p < 0.0001$) was also observed 1 day after LPS treatment when UCP2 is increased.

Induction of UCP2 following central or peripheral inflammation in WT mice is also associated with an increased capacity of mitochondrial GSH uptake *in vitro*

We next investigated whether UCP2 induction could alter mitochondrial GSH uptake. The increase in GSH uptake was temporally correlated with *UCP2* mRNA induction following ischemia. Three days after ischemia, when mitochondrial GSH levels are dramatically decreased, the mitochondrial GSH uptake capacity was 6-fold increased (0.683 ± 0.212 nmol/mg of tissue) compared with non-operated mice (0.111 ± 0.006 nmol/mg of tissue, $p < 0.005$). This increase was not observed 1 day post ischemia ($p > 0.05$). In the lung from LPS-treated mice, a 2.3-fold increase in mitochondrial GSH uptake was observed (0.220 ± 0.026 nmol/mg of tissue) when compared with non-treated tissues (0.093 ± 0.007 nmol/mg of tissue, $p < 0.001$). UCP2 induction thus appears to be temporally associated with an increased capacity for mitochondrial GSH uptake.

GSH depletion and uptake are decreased in peritoneal macrophages of *ucp2*$^{-/-}$ mice

In order to determine if the relationship between GSH and UCP2 that was disclosed in the brain and lung could be confirmed in more homogeneous cell populations, we examined the GSH depletion and uptake in thioglycolate elicited peritoneal macrophages (Arsenijevic *et al.* 2000). Macrophages from WT and *UCP2*$^{-/-}$ mice displayed a punctate cytoplasmic GSH staining consistent with mitochondrial labelling (Figs 5a–f). Following LPS treatment, WT

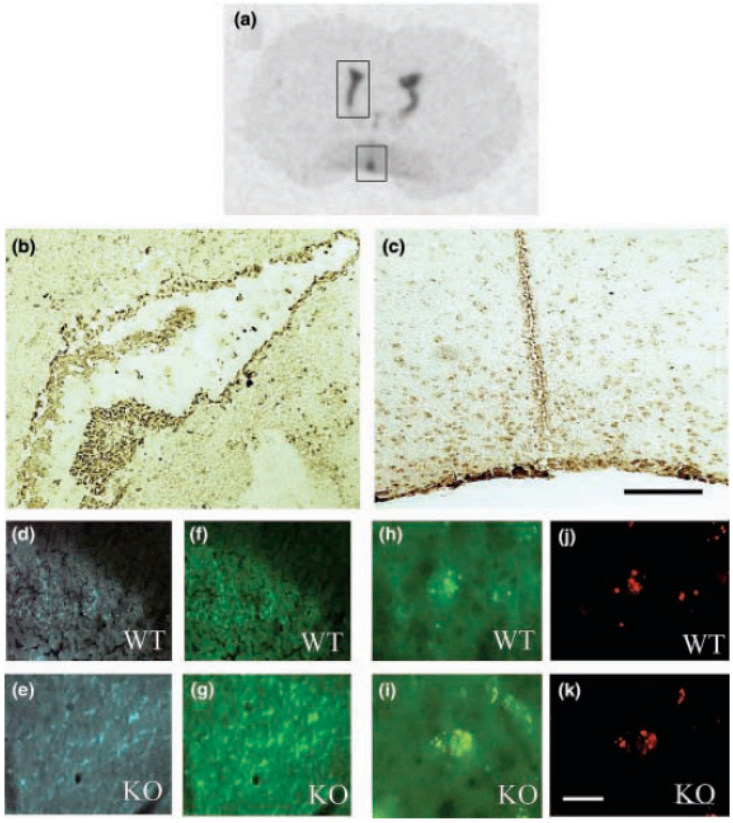

Fig. 4 GSH labelling in *UCP2* mRNA expressing cells. (a) Coronal brain sections from WT mice illustrating the distribution of *UCP2* mRNA. At these brain co-ordinates, highest levels of *UCP2* mRNA were observed in the ventricular system and the suprachiasmatic nucleus. The rectangles indicate the areas that are shown at higher magnification below for GSH labelling. (b, c) The ventricular system and the suprachiasmatic nucleus express intense immunoreactivity for GSH (scale bar, 300 μm). (d, e) Ipsilateral cortical microglial immunofluorescent labelling in WT and KO mice 3 days after ischemia (f–i) Phthaldialdehyde fluorescent labelling of GSH in WT and KO mice after ischemia. This shows that GSH levels were significantly decreased in the ischemic hemispheres of WT mice compared with $UCP2^{-/-}$ mice (j, k) Microglial mitochondria fluorolabelling with rhodamine 123 shows that GSH is located in mitochondria (scale bar, 7 μm).

macrophages showed a 42% loss of GSH, whereas $UCP2^{-/-}$ have only a 27% loss ($p < 0.05$; Figs 5g–j). After LPS treatment and addition of GSH, WT macrophages showed a markedly increased capacity for GSH uptake compared with macrophages from $UCP2^{-/-}$ mice (80 vs. 14%). (Figs 5k and l). These results indicate that mitochondrial GSH depletion and uptake occur more rapidly in WT than $UCP2^{-/-}$ macrophages, suggesting that UCP2 is involved in regulating mitochondrial GSH levels in a rapid and dynamic fashion.

Discussion

The present data show that deficiency in UCP2 results in increased resistance to cerebral ischemia. This resistance was associated with a reduced oxidative injury and an increase of the cerebral neuronal anti-oxidant state. In the light of the well-established negative regulation of ROS by UCP2 (Arsenijevic *et al*. 2000), our data may reflect a chronic adaptation to the lack of UCP2. This response involves a consistent increase in Mn SOD, which may contribute to the reduction of ischemic injury and reduced levels of lipid peroxidation in $UCP2^{-/-}$ mice (Keller *et al*. 1998; Murakami *et al*. 1998; Fujimura *et al*. 1999; Guégan *et al*. 1999). This Mn SOD anti-oxidant increase was observed in neurons and astrocytes, but not in cells that induce UCP2 after ischemic brain injury (mainly microglia and also invading macrophages and neutrophils). This specific cellular distribution suggests the presence of two biologically distinct cell populations in respect to UCP2 expression: those that produce ROS regulated by UCP2 (microglia, macrophages, neutrophils) and those that may activate the cerebral anti-oxidant system of Mn SOD (neurons and astrocytes), indicating that, in $UCP2^{-/-}$ mice, some cells may produce more ROS (Arsenijevic *et al*. 2000), while others eliminated them more efficiently. The resistance of $UCP2^{-/-}$ mice following MCAO reflects the efficient elimination of ROS by this latter cell group. In light of the known physiological role of UCP2 in the negative regulation of ROS (Arsenijevic *et al*. 2000), our observations indicating a strong link between mitochondrial GSH levels and UCP2 expression might be highly relevant. We provide evidence that *UCP2* mRNA induction was temporally associated with changes of mitochondrial GSH levels (depletion and uptake) following ischemia in WT mice.

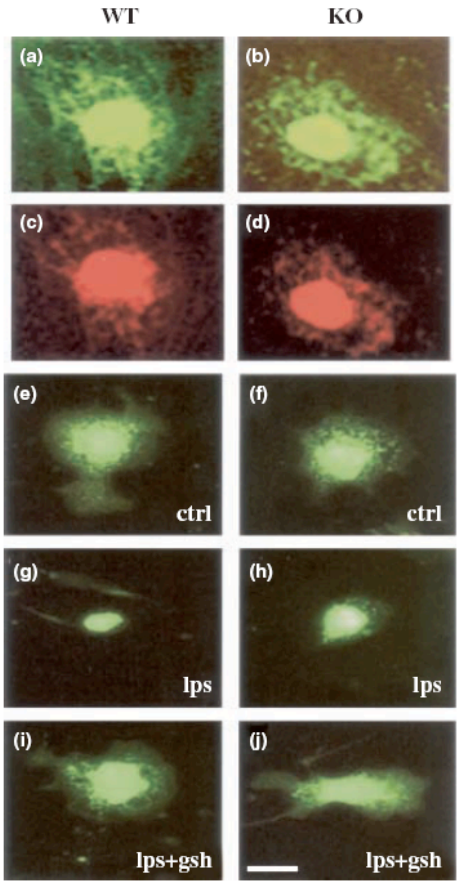

Fig. 5 Mitochondrial GSH levels in wild-type (WT) and *UCP2*$^{-/-}$ (KO) peritoneal macrophages. Peritoneal macrophages were isolated after an intraperitoneal injection of thioglycolate medium and constitute an homogenous population of UCP2 expressing cells. Phthaldialdehyde was used to visualize GSH, mitochondria by rhodamine 123. (a, b) GSH labelling in WT and KO macrophages. (c, d) Mitochondrial labelling showing that GSH is located in mitochondria (e, f). In both groups of mice, prior to LPS treatment, GSH staining was present in the nucleus and in cytoplasmic punctate structures consistent with a mitochondrial pattern. The intensity of staining was similar in WT (65 ± 4) and *UCP2*$^{-/-}$ (59 ± 3, $p > 0.05$) macrophages (30 macrophages in triplicate for each group). (g, h) Following LPS treatment, the mitochondrial GSH staining was decreased in both groups of mice. This decrease was markedly greater in WT (31 ± 3) when compared with *UCP2*$^{-/-}$ macrophages (42.6 ± 3, $p < 0.05$). (i, j) Following LPS-GSH treatment, cytoplasmic GSH levels were increased in *UCP2*$^{-/-}$ by 14% and in WT macrophages by 80% ($p < 0.05$) (scale bar, 7 μm).

This association was also observed in tissues of LPS-treated mice, indicating that it was not strictly confined to ischemic injury, but may reflect a more general phenomenon associated with UCP2 expression following stress injury. Mitochondrial GSH fluxes were also markedly altered in *UCP2*$^{-/-}$ mice compared with WT in situations involving oxidative stress. In particular, we report altered mitochondrial GSH changes in *UCP2*$^{-/-}$ brain microglia (the cells that normally produce ROS regulated by UCP2) compared with WT microglia following ischemia. Using a homogenous population of isolated peritoneal macrophages, we also observe that *UCP2*$^{-/-}$ cells showed a marked dysregulation in mitochondrial GSH depletion and uptake, UCP2-expressing cells having a more rapid and dynamic changes of mitochondrial GSH levels than *UCP2*$^{-/-}$ macrophages. We report that GSH levels were higher in LPS-treated *UCP2*$^{-/-}$ macrophages compared with WT. Although this may suggest a compensatory effect of GSH, the known increased ROS production by *UCP2*$^{-/-}$ macrophages (Arsenijevic *et al.* 2000) rather indicates that UCP2 is required for GSH to have effective anti-oxidant activity. This is in marked contrast to the efficient compensatory protective effect of Mn SOD observed in the *UCP2*$^{-/-}$ brain following ischemia. The UCP's closest structural relatives dicarboxylate and 2-oxoglutarate carriers (Ricquier and Bouillaud 2000) are thought to be involved in the mitochondrial uptake of the anti-oxidant GSH (Chen and Lash 1998). Consistent with UCP2 acting as a negative regulator of ROS in mitochondria (Arsenijevic *et al.* 2000), UCP2 would allow transport of GSH into the matrix and the consumption of GSH in the efficient elimination of ROS. Moreover, the fact that the increased expression of Mn SOD does not occur in the microglial cells of *UCP2*$^{-/-}$ mice indicates a specific association between UCP2/ROS regulatory mechanisms and mitochondrial GSH responses. In line with our results, previous data have reported that microglial cells have a prominent GSH system for the defence against the reactive compounds they generate (Hirrlinger *et al.* 2000; Ong *et al.* 2000). Mitochondrial permeability and membrane potential, which may be altered by the uncoupling activity of UCP2 (Ricquier and Bouillaud 2000), can also be influenced by GSH levels (Masini *et al.* 1992). Previously, a tight association between changes in the redox state (i.e. superoxide ion level) and compensating increases in GSH has been found in macrophages (Sato *et al.* 2001). Moreover, GSH has been shown to alter ROS formation in mitochondria and to counteract endogenous oxidative stress produced at the ubiquinone site of the electron transport chain (Garcia-Ruiz *et al.* 1995). Our results indicate that the efficiency of the anti-oxidant GSH system may be closely related to UCP2 expression.

Consistent with the recent marked progress in this field, our data support the role of UCP2 in oxidative pathophysiology (Arsenijevic *et al.* 2000; Blanc *et al.* 2003) and further contribute to the understanding of the physiological function of UCP2. It has been suggested that interaction of superoxide with UCPs may be critical for decreasing mitochondrial ROS levels *in vitro* (Echtay *et al.* 2001, 2002). We now provide evidence for a close association

between UCP2 and mitochondrial GSH levels *in vivo*. Changes in mitochondrial levels of GSH have been described in pathological states associated with oxidative stress (particularly obesity, HIV, diabetes, cancer, inflammatory and infectious diseases (Zaidan and Sims 1996; Szaleczky *et al.* 1999; Carretero *et al.* 2000; Perl and Banki 2000; Yang *et al.* 2000; Abou-Seif and Youssef 2001; Dobashi *et al.* 2001; Soltys *et al.* 2001) indicating that the regulatory role of UCP2 may be of vital importance in the progression of disease. In particular, our data draw attention to the status of UCP2 in the substantia nigra of patients with Parkinson's disease where subnormal levels of GSH have been recorded (Jenner *et al.* 1992).

Acknowledgements

The excellent technical assistance of P. Lovero and C. Schumacher is gratefully acknowledged. We thank Prof. Yoshinori Imai for providing rabbit polyclonal anti-*Iba*1 antibody; Dr S. Alberi for help with measurement of GSH in macrophages study; Drs Y. Charnay and B. Miroux for reading the manuscript and suggestions. Many thanks to Dr Ole Petter Hjelle, Myrtha Arnold, Dr A. Malafosse and Dr J. Widmer for collaboration and the Tissieres Foundation (PG).

References

Abou-Seif M. A. and Youssef A. A. (2001) Oxidative stress and male IGF-1, gonadotropin and related hormones in diabetic patients. *Clin. Chem. Lab. Med.* **39**, 618–623.

Alexander R. R. and Griffiths J. M. (1993) Cell components, in *Basic Biochemical Methods*, pp. 234–266. Wiley-Liss New York, New York.

Armstrong J. S., Steinauer K. K., French J., Killoran P. L., Walleczek J., Kochanski J. and Knox S. J. (2001) Bcl-2 inhibits apoptosis induced by mitochondrial uncoupling but does not prevent mitochondrial transmembrane depolarization. *Exp. Cell Res.* **262**, 170–179.

Arsenijevic D., Onuma H., Pecqueur C. *et al.* (2000) Disruption of the uncoupling protein-2 gene in mice reveals a role in immunity and reactive oxygen species production. *Nat. Genet.* **26**, 435–439.

Arsenijevic D., de Bilbao F., Giannakopoulos P., Girardier L., Samec S. and Richard D. (2001) A role for interferon-γ in the hypermetabolic response to murine toxoplasmosis. *Eur. Cytokine Netw.* **12**, 518–527.

Bancroft J. D. (1982) Enzyme histochemistry, in *The Theory and Practice of Histological Techniques* (Bancroft J. D. and Stevens A., eds), pp. 397–400. Churchill Livingston, London, UK.

Blanc J., Alves-Guerra M. C., Esposito B., Rousset S., Gourdy P., Ricquier D., Tedgui A., Miroux B. and Mallat Z. (2003) Protective role of uncoupling protein 2 in atherosclerosis. *Circulation* **107**, 388–390.

Boss O., Hagen T. and Lowell B. B. (2000) Uncoupling proteins 2 and 3: potential regulators of mitochondrial energy metabolism. *Diabetes* **49**, 143–156.

Candelario-Jalil E., Mhadu N. H., Al-Dalain S. M., Martinez G. and Leon O. S. (2001) The time course of oxidative damage in different brain regions following transient cerebral brain ischemia in gerbils. *Neurosci. Res.* **41**, 233–241.

Carretero J., Obrador E., Pellicer J. A., Pascual A. and Estrela J. M. (2000) Mitochondrial glutathione depletion by glutamine in growing tumour cells. *Free Radic. Biol. Med.* **29**, 913–923.

Chan P. H. (1996) Role of oxidants in ischemic brain damage. *Stroke* **27**, 1124–1129.

Chavin K. D., Yang S., Lin H. Z. *et al.* (1999) Obesity induces expression of uncoupling protein-2 in hepatocytes and promotes liver ATP depletion. *J. Biol. Chem.* **274**, 5692–5700.

Chen Z. and Lash L. H. (1998) Evidence for mitochondrial uptake of glutathione by dicarboxylate and 2-oxoglutarate carriers. *J. Pharmacol. Exp. Therapeut.* **285**, 608–618.

Cortez-Pinto H., Zhi L. H., Qi Y. S., Odwin D. C. S. and Diehl A. M. (1999) Lipids up-regulate uncoupling protein 2 expression in rat hepatocytes. *Gastroenterology* **116**, 1184–1193.

De Bilbao F., Guarin E., Nef P., Vallet P., Giannakopoulos P. and Dubois-Dauphin M. (2000) Cell death gene expression in the penumbra and thalamic fields after permanent occlusion of the middle cerebral artery in wild-type and Bcl-2 transgenic mice. *Eur. J. Neurosci.* **12**, 921–934.

Dobashi K., Aihara M., Araki T., Shimizu Y., Utsugi M., Iizuka K., Murata Y., Hamuro J., Nakazawa T. and Mori M. (2001) Regulation of LPS induced IL-12 production by IFN-γ and IL-4 through intracellular glutathione status in human alveolar macrophages. *Clin. Exp. Immunol.* **124**, 290–296.

Durmaz R., Inal M., Angin K., Atasoy M. A. and Tel Altinisik M.E. (1999) The effects of MK-801 and U-83836^{E} on post-ischemic reperfusion injury in the rat brain. *Acta Neurobiol. Exp.* **59**, 99–104.

Echtay K. S., Winkler E., Frischmuth K. and Klingenberg M. (2001) Uncoupling proteins 2 and 3 are highly active H(+) transporters and highly nucleotide sensitive when activated by coenzyme Q (ubiquinone). *Proc. Natl Acad. Sci. USA* **98**, 1416–1421.

Echtay K. S., Roussel D., St-Pierre J. *et al.* (2002) Superoxide activates mitochondrial uncoupling proteins. *Nature* **415**, 96–99.

Fleury C., Neverova M., Collins S. *et al.* (1997) Uncoupling protein-2: a novel gene linked to obesity and hyperinsulinemia. *Nat. Genet.* **15**, 269–272.

Franklin K. B. J. and Paxinos G. (1997) *The Mouse Brain in Stereotaxic Coordinates*, pp. 29–41. Academic Press Inc., San Diego, USA.

Fujimura M., Morita-Fujimura Y., Kawase M., Copin J. C., Calagui B., Epstein C. J. and Chan P. H. (1999) Manganese superoxide dismutase mediates the early release of mitochondrial cytochrome c and subsequent DNA fragmentation after permanent focal cerebral ischemia in mice. *J. Neurosci.* **19**, 3414–3422.

Garcia-Ruiz C., Colell A., Morales A., Kaplowitz N. and Fernandez-Checa J. C. (1995) Role of oxidative stress generated from the mitochondrial electron transport chain and mitochondrial glutathione status in loss of mitochondrial function and activation of transcriptional factor nuclear factor – κB: studies with isolated mitochondria and rat hepatocytes. *Mol. Pharmacol.* **48**, 825–834.

Gimeno R. E., Dembski M., Weng X., Deng N., Shyjan A. W., Gimeno C. J., Iris F., Ellis S. J., Woolf E. A. and Tartaglia L. A. (1997) Cloning and characterization of an uncoupling protein homolog: a potential molecular mediator of human thermogenesis. *Diabetes* **46**, 900–906.

Guégan C., Ceballos-Picot I., Nicole A., Kato H., Onteniente B. and Sola B. (1998) Recuitment of several neuroprotective pathways after permenant focal ischemia in mice. *Exp. Neurol.* **154**, 371–380.

Guégan C., Ceballos-Picot I., Chevalier E., Nicole A., Onteniente B. and Sola B. (1999) Reduction of ischemic damage in NGF-transgenic mice: correlation with enhancement of antioxidant enzyme activities. *Neurobiol. Dis.* **6**, 180–189.

Hirrlinger J., Gutterer J. M., Kussmaul L., Hamprecht B. and Dringen R. (2000) Microglial cells in culture express a prominent glutathione

system for the defense against reactive oxygen species. *Dev. Neurosci.* **22**, 384–392.

Jenner P., Dexter D. T., Sian J., Schapira A. H. and Marsden C. D. (1992) Oxidative stress as a cause of nigral cell death in Parkinson's disease and incidental Lewy body disease. *Ann. Neurol.* **32**, S82–S87.

Keller J. N., Kindy M. S., Holtsberg F. W., St Clair D. K., Yen H. C., Germeyer A., Steiner S. M., Bruce-Keller A. J., Hutchins J. B. and Mattson M. P. (1998) Mitochondrial manganese superoxide dismutase prevents neural apoptosis and reduces ischemic brain injury: suppression of peroxynitrite production, lipid peroxydation and mitochondrial dysfunction. *J. Neurosci.* **18**, 687–697.

Lee F. Y., Li Y., Zhu H., Yang S., Lin H. Z., Trush M. and Diehl A. M. (1999) Tumor necrosis factor increases mitochondrial oxidant production and induces expression of uncoupling protein-2 in the regenerating mice [correction of rat] liver. *Hepatology* **29**, 677–687.

Li L. X., Skorpen F., Egeberg K., Jorgensen I. H. and Grill V. (2001) Uncoupling protein-2 participates in cellular defense against oxidative stress in clonal β-cells. *Biochem. Biophys. Res. Commun.* **282**, 273–277.

Llames L., Gomez-Lucia E., Domenech A., Suarez G. and Goyache J. (2000) Analysis by sodium dodecyl sulfate polyacrylamide gel electrophoresis and western blot of non-specific and specific viral proteins frequently detected in different antigen preparations of bovine leukemia virus. *J. Vet. Diagn. Invest.* **12**, 337–344.

Love S. (1999) Oxidative stress in brain ischemia. *Brain Pathol.* **9**, 119–131.

Masini A., Ceccarelli D., Trenti T., Gallesi D. and Muscatello U. (1992) Mitochondrial membrane permeability changes induced by octadecadienoic acid hydroxide. Role of mitochondrial GSH pool. *Biochim. Biophys. Acta* **1101**, 84–89.

Mizui T., Kinouchi H. and Chan P. H. (1992) Depletion of brain glutathione by buthionine sulfoximine enhances cerebral ischemic injury in rats. *Am. J. Physiol.* **262**, H313–H317.

el Moualij B., Duyckaerts C., Lamotte-Brasseur J. and Sluse F. E. (1997) Phylogenetic classification of mitochondrial carrier family of *Saccharomyces cerevisiae*. **13**, 573–581.

Murakami K., Kondo T., Kawase M., Li Y., Sato S., Chen S. F. and Chan P. H. (1998) Mitochondrial susceptibility to oxidative stress exacerbates cerebral infarction that follows permanent focal ischemia in mutant mice with manganese superoxide dismutase deficiency. *J. Neurosci.* **18**, 205–213.

Negre-Salvayre A., Hirtz C., Carrera G., Cazenave R., Troly M., Salvayre R., Penicaud L. and Casteilla L. (1997) A role for uncoupling protein-2 as a regulator of mitochondrial hydrogen peroxide generation. *FASEB J.* **11**, 809–815.

Ohsawa K., Imai Y., Kanazawa H., Sasaki Y. and Kohsaka S. (2000) Involvement of Iba1 in membrane ruffling and phagocytosis of macrophages/microglia. *J. Cell Sci.* **113**, 3073–3084.

Ong W. Y., Hu C. Y., Hjelle O. P., Ottersen O. P. and Halliwell B. (2000) Changes in glutathione in the hippocampus of rats injected with kainate: depletion in neurons and upregulation in glia. *Exp. Brain Res.* **132**, 510–516.

Pecqueur C., Alves-Guerra M. C., Gelly C., Levi-Meyrueis C., Couplan E., Collins S., Ricquier D., Bouillaud F. and Miroux B. (2001) Uncoupling protein 2, *in vivo* distribution, induction upon oxidative stress, and evidence for translational regulation. *J. Biol. Chem.* **276**, 8705–8712.

Perl A. and Banki K. (2000) Genetic and metabolic control of the mitochondrial transmembrane potential and reactive oxygen intermediate production in HIV disease. *Antioxidants Redox Sign.* **2**, 551–573.

Pratico D., Reiss P., Tang L. X., Sung S., Rokach J. and McIntosh T. K. (2002) Local and systemic increase in lipid peroxidation after moderate experimental traumatic brain injury. *J. Neurochem.* **80**, 894–898.

Raha S. and Robinson B. H. (2000) Mitochondria, oxygen free radicals, disease and ageing. *TIBS* **25**, 502–508.

Rashid A., Wu T. C., Huang C. C., Chen C. H., Lin H. Z., Yang S. Q., Lee F. Y. and Diehl A. M. (1999) Mitochondrial proteins that regulate apoptosis and necrosis are induced in mouse fatty liver. *Hepatology* **29**, 1131–1138.

Reed D. J. (1993). *Methods in Toxicology* (Lash L. H and Jones D. P., eds), Vol. 2, pp. 219–226. Academic Press, San Diego, CA.

Richard D., Rivest R., Huang Q., Bouillaud F., Sanchis D., Champigny O. and Ricquier D. (1998) Distribution of the uncoupling protein 2 mRNA in the mouse brain. *J. Comp. Neurol.* **397**, 549–560.

Ricquier D. and Bouillaud F. (2000) The uncoupling protein homologues: UCP1, UCP2, UCP3, StUCP and AtUCP. *Biochem. J.* **345**, 161–179.

Sato H., Kuriyama-Matsumura K., Hashimoto T., Sasaki H., Wang H., Ishii T., Mann G. E. and Bannai S. (2001) Effects of oxygen on induction of the cystine transporter by bacterial lipopolysaccharide in mouse peritoneal macrophages. *J. Biol. Chem.* **276**, 10407–10412.

Shan X., Jones D. P., Hashmi M. and Anders M. W. (1993) Selective depletion of mitochondrial glutathione depletion concentrations by (R.,S)-3-hydroxy-4-pentenoate potentiates oxidative cell death. *Chem. Res. Toxicol.* **6**, 75–81.

Skulachev V. P. (1998) Uncoupling: new approaches to an old problem of bioenergetics. *Biochim. Biophys. Acta* **1363**, 100–124.

Soltys K., Dikdan G. and Koneru B. (2001) Oxidative stress in fatty livers of obese Zucker rats: rapid amelioration and improved tolerance to warm ischemia with tocopherol. *Hepatology* **34**, 13–18.

Suzuki H., Abe K., Tojo S. J., Kitagawa H., Mizugaki M. and Itoy Y. (1999) Reduction of ischemic brain injury by anti-P-selectin monoclonal antibody after permanent middle cerebral artery occlusion in rat. *Neurol. Res.* **21**, 269–276.

Szaleczky E., Prechel J., Feher J. and Somogyi A. (1999) Alteration in enzymatic antioxidant defence in diabetes mellitus – a rational approach. *Postgrad. Med. J.* **75**, 13–17.

Tietze F. (1969) Enzymatic method for quantitative determination of nanogram amounts of total and oxidized glutathione: applications to mammalian blood and other tissues. *Anal. Biochem.* **27**, 507–522.

Touzani O., Roussel S. and Mackenzie E. T. (2001) The ischaemic penumbra. *Curr. Opin. Neurol.* **14**, 83–88.

Wendel A. and Feuerstein S. (1981) Drug-induced lipid peroxidation in mice – I. Modulation by monooxygenase activity, glutathione and selenium status. *Biochem. Pharmacol.* **30**, 2513–2520.

Yang S., Zhu H., Li Y., Lin H., Gabrielson K., Trush M. A. and Diehl A. M. (2000) Mitochondrial adaptations to obesity-related oxidant stress. *Arch. Biochem. Biophys.* **378**, 259–268.

Zaidan E. and Sims N. R. (1996) Alteration in glutathione content of mitochondria following short term forebrain ischemia in rats. *Neurosci. Lett.* **218**, 75–78.

Zhang C.-Y., Baffy G., Perret P. *et al.* (2001) Uncoupling protein-2 negatively regulates insulin secretion and is a major link between obesity, β cell dysfunction, and type 2 diabetes. *Cell* **105**, 745–755.

5.4. Article II: Results and discussion

5.4.1. *UCP2 mRNA is expressed after focal cerebral ischemia*

The data presented in this report clearly demonstrate that an ischemic injury may enhance *in vivo* the expression of UCP2 mRNA in the mouse brain. Indeed, *in situ* hybridization revealed that UCP2 mRNA was strongly induced 3 and 4 days post-MCAO (Figure 1a). Given the role of UCP2 in reducing ROS production, it is noteworthy that its expression was seen in the peri-infarct area where free radical production appears largely restricted (Lipton, 1999). Importantly, expression occurs mainly in microglial cells (Figure 1b). Expression of UCP2 mRNA in microglial cells surrounding neuronal injury was also reported in a recent study describing the effect of exposure to kainic acid (Clavel *et al.*, 2003). One might assume that this occurs *in vivo* to limit the production of ROS by microglial cells. However, in contrast to the Clavel *et al.* findings (2003), we did not observed any apparent expression of UCP2 labelling in neuronal cells. This suggests that UCP2 can be induced in that type of cells in certain conditions only.

5.4.2. *UCP2 KO mice are less sensitive to permanent MCAO and this resistance may be explained by changes in anti-oxidant functions*

Infarct volume was significantly reduced in UCP2 KO mice when compared with WT mice ($p < 0.001$) (Figure 1c), indicating that the *in vivo* deletion of UCP2 may protect neocortical areas from ischemic damage. This was strengthened by our results showing that translocation of cytochrome c from the mitochondria to the cytosol was prevented in KO mice (Figure 2a) suggesting that activation of mitochondrial permeability transition and apoptotic cell death were prevented. Accordingly, the number of TUNEL cells was decreased in UCP2 KO mice compared with WT mice ($p < 0.05$).

Thus our study showing that UCP2 KO showed resistance to cerebral ischemic injury may at first glance be discrepant with what might have been expected and with respect to a report concomitant with our work showing an increase resistance

to ischemic injury in UCP2 transgenic animals (Mattiasson *et al.*, 2003). Concerning this point, our finding has been inappropriately discussed in a recent review of Mehta and Li (2009). The authors strengthened the argument that "the negative effect of UCP2" was probably ascribed to the permanent MCAO model being used. Actually, in contrast to transient MCAO, the ROS production after permanent MCAO does not seem to be a major contributor in ischemic damage progressions (Peters *et al*., 1998). However, it is noteworthy to mention that we did not observe a "negative effect" of UCP2, but rather a positive effect of its deletion. Indeed, the fact that a neuroprotective effect was evidenced when UCP2 is deleted does not mean that its biological function is a "negative" one. If the present result could be explain by the kind of ischemic model used (i.e. ROS are not the major cause of death following permanent focal ischemia), one could expect a lack of effect of the UCP2 deletion rather than a positive one. Hence, we documented in our study results that may explain this apparent contradiction.

5.4.3. *A consistent increase in MnSOD may contribute to the reduction of ischemic injury in KO mice*

UCP2 KO animals have higher brain basal levels of the anti-oxidant enzyme MnSOD compared to WT as assessed by western blot analysis (Figure 2b) and immunohistochemistry (Figures 3a and b). This basal up-regulation was mainly located in neuronal and astrocytic cells in most brain structures, including the neocortex (Figures 3c–f). Following ischemia, MnSOD levels were further induced in both WT and UCP2 KO mice (Figure 2b). Given the role of UCP2 in the regulation of ROS production, it can be argued that increased basal MnSOD levels occurs as a compensatory neuroprotective mechanism in response to UCP2 deletion and could account for the limited amount of oxidative and tissue damages following the ischemic insult. Indeed, levels of lipid peroxidation (MDA levels) were decreased by 30% in UCP2 KO mice after ischemia (Table 1), indicating a lower oxidative injury in UCP2 KO mice.

We hypothesized that a constantly increased production of ROS (such as in UCP2 KO mice) may have lead to an endogenous up-regulation of anti-oxidant defenses, which became protective following ischemic injury. In other words, the deletion of UCP2 could have lead to chronic increased levels of $O_2^{-\bullet}$ in the

mitochondria of microglial cells. Overexpression of MnSOD in neurons could have constitute an adaptative mechanism to regulate $O_2^{-\bullet}$ levels as MnSOD may detoxify $O_2^{-\bullet}$ to H_2O_2 in the mitochondria (see section 3.5.). In support of the hypothesis that increased production of ROS in UCP2 KO mice may lead to activation of mitochondrial anti-oxidant/neuroprotective genes, subsequent data show that under basal conditions, there is a source of superoxide within macrophages of UCP2 KO mice that constitutively activates the transcription factor NF-κB (Bai *et al*., 2005), which may lead to expression of neuroprotective genes such as MnSOD (Sullivan *et al.*, 1999).

Besides the fact that MnSOD up-regulation could account for the reduced injury in UCP2 KO mice, and because UCP2 dissociate oxidation from ATP production, it cannot be excluded that its deletion could have contributed to increase mitochondrial ATP production, thereby reducing the drop in ATP levels, a consequence of cerebral ischemia. Accordingly, observations on UCP2 KO animals revealed increased pancreatic ATP and ADP ratios, which were temporarily associated with increased insulin secretion by pancreatic β-cells (Zhang *et al.*, 2001). Although further investigations are needed to confirm this, an increase in ATP levels could have participated to the preservation of brain tissue.

5.4.4. *UCP2 and GSH*

In light of the known physiological role of UCP2 in the negative regulation of ROS (Arsenijevic *et al*., 2000), our observations indicating a strong link between mitochondrial GSH levels and UCP2 expression might be highly relevant. Indeed, we observed a specific association between UCP2 and mitochondrial GSH levels regulation. Following permanent MCAO, western blot analysis revealed a decrease in total GSH levels. This decrease did not differ in the ischemic hemisphere of both groups of mice ($p < 0.05$ for WT and UCP2 KO mice) (Table 1). However, we found a significant difference between the two strains of mice, when GSH levels were measured in the mitochondria. Actually, whereas mitochondrial GSH levels were significantly decreased in the ischemic hemispheres of WT mice three days after MCAO, when UCP2 mRNA is induced ($p < 0.05$), levels were unchanged in ischemic UCP2 KO mice ($p > 0.05$) (Table 1). Because depletion of mitochondrial rather than cytosolic GSH is crucial to elicit

cell damage (Armstrong *et al*., 2001), unchanged levels of mitochondrial GSH in KO animals could have also contributed to the reduction of ischemic injury. Immunohistochemical analysis revealed that strong mitochondrial GSH immunolabelling was specific to microglial cells (Figures 4d–k), the cells that normally produce ROS regulated by UCP2. Therefore, it appears that UCP2 KO mice have a dysregulated mitochondrial GSH flux response compared with WT mice following cerebral ischemia and that UCP2 and GSH function in tight association. Given the fact that efficient anti-oxidative defense mechanisms are especially required in mitochondria of microglial cells in order to prevent them from oxidative damage and because the mitochondrial GSH system strongly contribute to the anti-oxidative potential of microglia (Dringen, 2005), it can be postulated that preserved mitochondrial GSH levels in microglial cells may have also occurred in response to UCP2 deletion in order to protect these cells from high levels of ROS. In other words, microglial cells may have adapted to UCP2 deletion, a stress condition that have required an improved anti-oxidant defense. This hypothesis is in accordance with the fact that after ischemia in WT mice, UCP2 mRNA was especially induced in microglial cells. However, this compensatory effect of GSH may be rather insufficient given the known increased ROS production by UCP2 KO macrophages (Arsenijevic *et al.*, 2000). Alternatively, it can not be excluded that GSH mitochondrial content was preserved in KO animals due to an increase of GSH synthesis. However, although we cannot totally exclude this possibility, we did not evidence any difference in total GSH levels (Table 1) between the two strains of mice.

This specific association between UCP2 and mitochondrial GSH levels regulation was further confirmed *in vitro* using lipopolysaccharide (LPS) models of peripheral inflammation in purified peritoneal macrophages. Following LPS treatment, GSH depletion and uptake were decreased in the mitochondria of peritoneal macrophages of UCP2 KO mice compared to WT ($p < 0.05$; Figures 5a–j). In addition, after LPS treatment and addition of GSH, WT macrophages showed a markedly increased capacity for GSH uptake compared with macrophages from UCP2 KO mice (Figures 5k and l). These results indicate that mitochondrial GSH depletion and uptake occur more rapidly in WT than UCP2 KO macrophages, suggesting that, in WT animals, UCP2 may downregulate ROS levels by

promoting a rapid and dynamic flux of GSH in mitochondria. Consistent with UCP2 acting as a negative regulator of ROS in mitochondria (Arsenijevic *et al.,* 2000), UCP2 would allow transport of GSH into the matrix and the consumption of GSH in the efficient elimination of ROS. Evidence mainly from kidney and liver mitochondria indicated that the dicarboxylate and the 2-oxoglutarate carriers, the UCP's closest structural relatives (Ricquier and Bouillaud 2000), contribute to the transport of GSH across the mitochondrial inner membrane. However, evidences suggest the existence of additional carriers, the identity of which remains to be established (Fernandez-Checa and Kaplowitz, 2005). Although additional findings are required to confirm this hypothesis, the present results suggest that UCP2 could directly promote the transport of GSH in mitochondria.

5.5. Conclusion

All in all, our findings support the well-established idea that UCP2 expression may be an endogenous neuroprotective response to protect neurons in the CNS from increased ROS production and subsequent cell death. Our data showing consistent increase in MnSOD may reflect a chronic adaptation to the lack of UCP2 and may contribute to the reduction of ischemic injury in UCP2 KO mice. This indicates that other members of the UCP family of proteins cannot have compensated for the loss of UCP2 suggesting a specific role for this molecule in brain mitochondrial ROS detoxification. In addition, our results suggest that the anti-oxidant GSH system may be closely related to UCP2 expression, as UCP2 may favor the movement of GSH. However, whether high GSH mitochondrial levels in KO mice are part of an adaptive response to the UCP2 deletion aimed at restoring oxidative damage or are part of UCP2 deletion consequences leading to increased ROS levels by macrophages remain to be more clearly established. Finally, in support with the idea that all these results are more or less a direct consequence of UCP2 deletion, we would like to underscore the fact that, in line with the mitochondrial localization of UCP2, changes in anti-oxidant functions in KO mice were specific to those effective in mitochondria. Actually, through control of the oxidative stress, GSH and MnSOD are essential in the maintenance of mitochondrial function. In addition, we did not find any changes in catalase activity, a cytoplasmic enzyme which is absent in mitochondria. The specific

cellular distribution in anti-oxidative mechanisms (neuronal MnSOD versus microglial GSH) also suggests the presence of two biologically distinct cell populations in respect to UCP2 expression: those that produce ROS regulated by UCP2 and GSH (microglia, macrophages, neutrophils) and those that may activate the cerebral anti-oxidant system of MnSOD (neurons and astrocytes) .

Our results are in accordance with findings not yet published when our experiments were performed (Bai *et al*., 2005; Nakase *et al*., 2007) and showing that UCP2 could play a key role in neuroprotective mechanisms after ischemia. Indeed, UCP2 may reduce detrimental inflammatory response by limiting acute microglial response (Bai *et al*., 2005), or stimulating the expression of neuroprotective genes (Mattiasson *et al*., 2003) after ischemia. In addition, human cases indicate elevated expression of UCP2 in the ischemic periphery of embolic stroke cases, suggesting that UCP2 may play an important role in protecting neurons against ischemic insult (Nakase *et al*., 2007). Altogether, it is reasonable to propose that UCP2 induction will have a potential therapeutic role in the treatment of stroke. Because resistance to cerebral ischemia in UCP2 KO mice may rather reflect a chronic adaptation to the lack of UCP2, future research will be nonetheless required to further resolve our findings on neuronal UCP2 function. The next significant step could be to identify the tissue specific effects of UCP2 (as the physiological role of UCP2 may depend of the tissue specificity) (Mattiasson and Sullivan, 2006) with the development of tissue specific UCP2 KO as well as the ability to temporally regulate neuronal UCP2 suppression, through inducible KO. This should reveal new insights about the molecular events associated with mitochondrial uncoupling. Given the growing interest within the field, the potential use of pharmacological agents with uncoupling properties or regulating uncoupling expression may also provide an important avenue to combat stroke injuries. Accordingly, studies have demonstrated that the pharmacologic induction of mitochondrial uncoupling by 2,4-dinitrophenol 1 h after reperfusion reduced infarct volume by 40% following transient focal cerebral ischemia in rats (Maragos and Korde, 2004). Control of UCP2 expression could also constitute a therapeutic issue. Research in the past ten years has identified peroxisome proliferator-activated receptors (PPARs) as pivotal actors in the control of transcription of the UCP genes. An understanding of the precise

mechanisms and the PPAR subtypes involved in this regulation would provide the possibility of the development of pharmacological approaches to modulate the levels of UCPs. With regard to UCP2 expression, it has been shown to be under the control of peroxisome proliferator-activated receptor β (PPARβ) (Aubert *et al*., 1997; Wang *et al*., 2003).

6. Cerebral ischemia and peroxisome proliferator-activated receptor β

Article III: D. Arsenijevic, F. de Bilbao, J. Plamondon, E. Paradis, P. Vallet, D. Richard, W. Langhans and P. Giannakopoulos (2006) Increased infarct size and lack of hyperphagic response after focal cerebral ischemia in peroxisome proliferator-activated receptor β-deficient mice. *J Cereb Blood Flow Metab* 26:433–445.

6.1. PPARs: function and distribution

PPARs are ligand-activated transcriptional factor receptors belonging to the so-called nuclear receptor family. PPARs are activated by natural ligands such as fatty acids, eicosanoids and oxidized fatty acids and pharmacological agents (for review see Delerive *et al.*, 2001). Mechanistically, ligand binding induces PPARs to heterodimerize with the retinoid X receptor (RXR). The activated PPAR-RXR heterodimers induce the transcription of candidate genes by binding to so-called peroxisome proliferator response elements (PPREs) consisting of DNA-specific sequences (Figure 10).

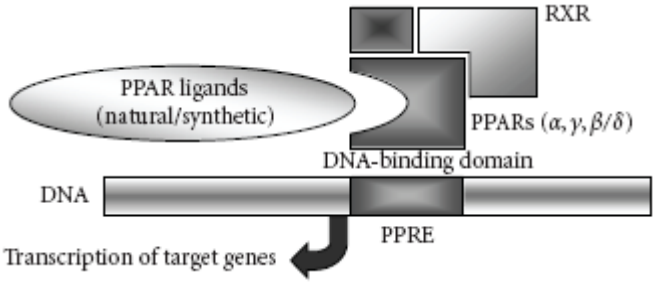

Figure 10: Mechanism of gene transcription through ligand binding on peroxisome proliferator-activated receptors (PPARs). In presence of coactivating stimuli, PPARs heterodimerize with retinoid X receptors (RXR) to form active transcription factors. The DNA binding domain on PPAR-RXR heterodimers induces the transcription of target genes by binding to peroxisome proliferator-response elements (PPREs) which consist of DNA-specific sequences (from Stahel *et al.*, 2008).

The three isoforms of PPAR (α, β, γ) share a high homology, but differ for tissue distribution and ligand specificity (Escher and Wahli, 2000) (Table). PPARs regulate the expression of genes involved in regulation of lipid or glucose metabolism (*Kersten et al*., 2000). Beyond metabolic effects, PPARs are also able to regulate inflammatory pathway by trans-repression of transcription factors (nuclear factor *κ*B) (Stahel *et al.*, 2008) or to regulate the oxidative pathway in different organs (Bordet *et al.*, 2006). PPAR*α* is mainly expressed in tissues with high catabolic rates of fatty acids, such as the liver, muscle, and heart, whereas PPAR*γ* is highly expressed in adipose tissue and in cells of the immune system, including lymphocytes and macrophages. In the brain, PPARγ is expressed in several cell types including microglia, astrocytes, oligodendrocytes, and neurons. PPARβ (also known as δ), the least known PPAR, has a ubiquitous expression compared to PPAR*α* and PPAR*γ*. In contrast with the other PPAR subtypes, PPARβ has the highest expression in the brain *(*Moreno *et al.*, 2004), and is the only one widely expressed in neurons and oligodendrocytes (Cullingford *et al*., 1998; Vanden Heuvel, 2007) suggesting a role in both myelination and neuronal function. However, the precise physiological roles of this receptor remain to be elucidated. Its importance in regulating macrophage activity and acting on various aspects of metabolic syndrome has been recently emphasized (Barish *et al.,* 2008). Recent results have also shown that PPARβ plays also a key role in lipid metabolism, as it regulates serum lipid profiles and fatty acid *β*-oxidation in muscle and adipose tissue.

Subtype	Tissue or cell type	Function
PPARα	Liver, skeletal muscle, brown adipose tissue, heart, vascular, and immune cell types: monocytes/macrophages, endothelial cells, smooth muscle cells, lymphocytes	Mediator of lipid metabolism; anti-inflammatory and cardioprotective effects; macrophage lipid homeostasis
PPARβ/δ	Ubiquitously expressed	Regulates lipid metabolism; cellular proliferation; inflammatory response
PPARγ	Brown and white adipose tissues, colon, spleen, retina vascular, and immune cell types (monocytes/macrophages, endothelial cells, smooth muscle cells, lymphocytes, dendritic cells; platelets; megakaryocytes)	Differentiation of pre-adipocytes to adipocytes; lipid metabolism; modulator of insulin action; macrophage lipid homeostasis; thrombosis and anti-inflammatory activities

Table: Tissue expression and functions of peroxisome proliferator-activated receptors (PPARs) (from Moraes *et al.*, 2006).

6.2. PPARs and cerebral ischemia

Based on their functions in inflammation, the potential for PPARs to modulate ischemic outcome has been explored (Bordet *et al.*, 2006; Stahel *et al.*, 2008). A 14-day preventive treatment with the PPARα activator fenofibrate, decreases cerebral infarct volume in WT mice following transient MCAO by anti-oxidant and anti-inflammatory mechanisms (Deplanque *et al.*, 2003) suggesting that PPARα activation is involved as a mechanism of the protection against cerebral injury. Activities of the major anti-oxidant enzymes in the brain, in particular Cu/ZnSOD and enzymes involved in GSH metabolism, were induced. In another study, it was confirmed that PPAR*α* agonists provided similar brain protection when administered respectively 3 or 7 days before induction of cerebral ischemia (Inoue *et al.*, 2003). More recently, it has been demonstrated that PPAR*α* agonists could also induce an acute neuroprotection when administered just before or after the onset of transient cerebral ischemia (Ouk *et al.*, 2005; Collino *et al.*, 2006) leading to decrease ROS production and lipid peroxidation (Collino *et al.*, 2006). PPAR*α* activation induces also a vascular protection as demonstrated by prevention of post-ischemic endothelial dysfunction. These vascular effects result from a decrease in oxidative stress and prevention of adhesion proteins (Deplanque *et al.*, 2003). Treatment with PPARγ-agonists improved survival outcome following transient focal cerebral ischemia in rats (Shimazu *et al.*, 2005; Sundararajan *et al.*, 2005; Tureyen *et al.*, 2007). It is suggested that the protective effect was related to the anti-inflammatory effects of the drug (as evidenced by decreased immunoreactivity for microglial/macrophage markers and decrease post-ischemic expression of pro-inflammatory genes) or mediated through up-regulation of anti-oxidant enzymes (CuZnSOD and catalase).

Until recently, the function of PPARβ remained elusive and unexplored despite interest in the target (Bordet *et al.*, 2006), as it is the most abundant subtype in cortical cells (Cullingford *et al.*, 1998). Despite increasing insights into beneficial effects of PPARs in the ischemic brain, the pathophysiological mechanisms are far from being completely elucidated. In contrast to other PPARs, no studies have yet been performed to analyze the effect of PPARβ in experimental models of

stroke. The purpose of Article III was therefore to determine whether PPARβ might be neuroprotective in a model of permanent focal ischemia. To this end, we used mice lacking the PPARβ receptors (PPARβ KO). We first explored the effects of *PPARβ* deletion on brain infarct size. Second, because PPARs are implicated in the regulation of inflammatory and oxidative pathways, we evaluated the response of PPARβ KO animals on these processes following permanent MCAO.

Journal of Cerebral Blood Flow & Metabolism (2006) 26, 433–445

www.jcbfm.com

Increased infarct size and lack of hyperphagic response after focal cerebral ischemia in peroxisome proliferator-activated receptor β-deficient mice

Denis Arsenijevic[1,5], Fabienne de Bilbao[2,3,5], Julie Plamondon[4], Eric Paradis[4], Philippe Vallet[2,3], Denis Richard[4], Wolfgang Langhans[1] and Panteleimon Giannakopoulos[2,3]

[1]*Institute of Animal Sciences, ETHZ, Zurich, Switzerland;* [2]*Department of Psychiatry, Geneva University Hospitals, Geneva, Switzerland;* [3]*Service of Old Age Psychiatry, University of Lausanne, Prilly, Switzerland;* [4]*Département d'Anatomie et Physiologie, Faculté de Médecine, Université Laval, Québec, Canada*

Peroxisome proliferator-activated receptors (PPARs) are involved in energy expenditure, regulation of inflammatory processes, and cellular protection in peripheral tissues. Among the different types of PPARs, PPARβ is the only one to be widely expressed in cortical neurons. Using PPARβ knockout (KO) mice, we report here a detailed investigation of the role of PPARβ in cerebral ischemic damage, associated inflammatory and antioxidant processes as well as food intake regulation after middle cerebral artery occlusion (MCAO). The PPARβ KO mice had a two-fold increase in infarct size compared with wild-type (WT) mice. Brain oxidative stress was dramatically enhanced in these KO mice, as documented by an increased content of malondialdehyde, decreased levels of glutathione and manganese superoxide dismutase, and no induction of uncoupling protein 2 (UCP2) mRNA. Unlike WT mice, PPARβ KO mice showed a marked increase of prooxidant interferon-gamma but no induction of nerve growth factor and tumor necrosis factor alpha after MCAO. In WT mice, MCAO resulted in inflammation-specific transient hyperphagia from day 3 to day 5 after ischemia, which was associated with an increase in neuropeptide Y (NPY) mRNA. This hyperphagic phase and NPY mRNA induction were not observed in PPARβ KO mice. Furthermore, our study also suggests for the first time that UCP2 is involved in MCAO food intake response. These data indicate that PPARβ plays an important role in integrating and regulating central inflammation, antioxidant mechanisms, and food intake after MCAO, and suggest that the use of PPARβ agonists may be of interest for the prevention of central ischemic damage.
Journal of Cerebral Blood Flow & Metabolism (2006) **26,** 433–445. doi:10.1038/sj.jcbfm.9600200; published online 10 August 2005

Keywords: food intake; inflammation; mice; middle cerebral artery occlusion; oxidative stress; peroxisome proliferator-activated receptor β

Introduction

Peroxisome proliferator-activated receptors (PPARs) are ligand-activated transcription factors belonging to the nuclear receptor superfamily (Kersten *et al*, 2000). Several classes of PPARs have been identified, namely PPARα, PPARβ, and PPARγ, and the latter consists of two isoforms, PPARγ1 and PPARγ2 (Kersten *et al*, 2000). Previous studies have shown that PPARs are expressed differentially in tissues, PPARα being most abundant in the liver and PPARγ in adipose tissue, the pancreas, and phagocytes (Lee *et al*, 2003). These two PPARs show a less wide tissue distribution than PPARβ, also called PPARδ, which is expressed in the lung, liver, kidney, spleen adipocytes, neurons, and oligodendrocytes (Cullingford *et al*, 1998). Prior work has documented the central role of PPARs in glucose and lipid metabolism (Kersten *et al*, 2000). Peroxisome proliferator-activated receptors have been associated with energy expenditure by regulating the expression of mitochondrial uncoupling proteins (UCPs) (Evans *et al*, 2004; Sell *et al*, 2004). In particular, PPARα and PPARγ have been shown to modulate UCP1, which participates in the control of thermogenesis in brown adipose tissue (Lee *et al*, 2003). Besides these

Correspondence: Dr D Arsenijevic, Institute of Animal Sciences, ETHZ, Schorenstrasse 16, 8604 Schwerzenbach, Switzerland.
E-mail: denis.arsenijevic@inw.agrl.ethz.ch
[5]These authors contributed equally to this work.
Received 17 May 2005; revised and accepted 28 June 2005; published online 10 August 2005

main effects, both *in vitro* and animal studies indicate that PPARs may control the expression of genes implicated in inflammatory responses and consequently alter cytokine production and cell recruitment to the inflammatory site (Hornung *et al*, 2001). For instance, PPARα knockout (KO) mice displayed a long-lasting inflammatory response to lipopolysaccharide stimulation (Delerive *et al*, 1999), and PPARα activation results in the repression of inflammatory cytokine production in different cell types (Delerive *et al*, 2001). In macrophages, PPARγ activation is thought to inhibit cytokine production (Ricote *et al*, 1998; Greene *et al*, 2000), whereas PPARβ negatively regulates specific subsets of genes that are activated by T helper 1 cytokines (Welch *et al*, 2003). In addition, PPARβ induction by inflammatory stimuli may suppress keratinocyte apoptosis during epidermal injury (Tan *et al*, 2004).

Despite this progress in the understanding of the function of PPARs, their role in central nervous system pathologies remains unclear. Recent evidence suggests that activation of PPARα receptor with selective agonists may confer neuroprotection after focal cerebral ischemia (Deplanque *et al*, 2003). In contrast, the role of PPARβ, which is abundantly expressed throughout the murine brain (Woods *et al*, 2003), remains obscure. Among the main biologic phenomena thought to be influenced by PPAR activation, cytokine-mediated inflammatory processes and activation of antioxidant mechanisms are of key importance for cell damage after acute cerebral ischemia. In this context, tumor necrosis factor alpha (TNFα) and interferon-gamma (IFNγ) are known to favor inflammatory processes (Blasko *et al*, 2001; Li *et al*, 2001), whereas nerve growth factor (NGF) may protect against inflammatory damage (Guegan *et al*, 1998) by inducing the activation of antioxidant mechanisms, such as an increase in manganese superoxide dismutase (MnSOD) (Guegan *et al*, 1999), glutathione (GSH) (Guegan *et al*, 1998), and/or UCP2 (de Bilbao *et al*, 2004). Using middle cerebral artery occlusion (MCAO) in mice, the present study explores the effects of a genetic PPARβ deficiency on brain infarct size, activation of the associated inflammatory and antioxidant processes as well as postischemic regulation of food intake.

Materials and methods

Animals, Food Intake, and Treatments

Adult male mice (3 to 6 months) were used in these experiments. The PPARα and PPARβ KO mice (weight 22 to 25 g) were established on a C57BL/6J genetic background. For each mouse strain, appropriate colittermate controls (weight 22 to 24 g) were used. These mice were kindly supplied by Professor W Wahli, University of Lausanne (Tan *et al*, 2001). The TNFα KO mice (strain *Tnftm1Gkl*, weight 21 to 23 g) (Pasparakis *et al*, 1996), IFNγ KO mice (strain B6.129S7-*Ifng*^{tm1Ts}/J, weight 20 to 23 g) (Dalton *et al*, 1993), and their wild-type (WT) counterparts (weight 21 to 24 g), all with a C57BL/6J background, were obtained from the Jackson Laboratory (Jackson-Bar Harbor, Maine, USA). The UCP2 KO mice (C57BL/6J, weight 19 to 21 g) and their WT colittermates (weight 19 to 22 g) were also used as described previously (de Bilbao *et al*, 2004). All mice strains were backcrossed for at least 10 generations to ascertain the similarity of genetic background with WT mice. Mice were housed in individual cages for food intake and body weight studies, and had *ad libitum* access to standard laboratory diet and water. Food intake was calculated using the weight of food pellets from the previous day and subtracting the weight of the remaining pellets on the following day (measured at 0900). For all feeding experiments, a minimum of eight ischemic animals (eight WT and eight PPARβ KO) and eight nonischemic animals (eight WT and eight PPARβ KO) were used. Food intake baseline levels were recorded for 3 days before MCAO, and then food intake was quantified daily for 2 weeks. To evaluate the role of central NGF in food intake regulation, 200 ng of NGF 2.5S (Chemicon, Temecula, CA, USA) was injected on the lesion site in PPARβ KO mice ($n=8$) 1 day after MCAO, as well as in sham-operated PPARβ KO mice ($n=8$). This timing was determined by the maximal NGF effect on food intake observed in WT mice. Nerve growth factor was injected with a microsyringe (5 μl vehicle containing 200 ng of NGF per mouse) after the animals had been anesthetized with isoflurane. The food intake response was studied for 4 consecutive days. Additional experiments were performed in IFNγ KO, TNFα KO, and UCP2 KO mice to explore the role of these proteins on food intake responses after MCAO (eight mice per group, as mentioned above). Because PPARβ KO and UCP2 KO mice showed no hyperphagic phase response after MCAO, we also evaluated food intake in nonoperated PPARβ KO and UCP2 KO mice after 24 h of fasting to examine whether a reduction in food intake induces a compensatory hyperphagia ($n=8$ for WT and KO groups).

Induction of Permanent Focal Cerebral Ischemia and Volume of the Infarct

We performed permanent MCAO in PPARα KO ($n_{KO}=6$ and $n_{WT}=6$) and PPARβ KO ($n_{KO}=18$ and $n_{WT}=16$) mice. Animals were anesthetized intraperitoneally with xylazine (20 mg/kg)/ketamine (100 mg/kg) in 0.9% NaCl (100 μl/10 g body weight), the right temporoparietal region of the head was shaved and a 2-mm incision was made vertically between the orbit and the ear and the skull was exposed. Under an operating microscope, a small burr hole 1 mm^2 was made with a high-speed microdrill through the outer surface of the semitranslucent skull over the visibly identified medial cerebral artery at the level of the parietal cerebral artery. Saline was applied to the area throughout the procedure, to prevent heat injury. The inner layer of the skull was removed with fine forceps, the dura and the arachnoid were opened and right permanent MCAO was performed by electrocoagulation (by means of a small-vessel cauterizer), without damaging the brain surface. Permanent inhibition of cerebral blood

flow after the lesion was assessed by visual inspection. If the brain surface was visibly damaged or if the middle cerebral artery bled owing to incomplete artery occlusion/coagulation, the animal was not used for the study. The duration of the surgery did not exceed 15 mins in any case (de Bilbao *et al*, 2000). After 4 days, the animals were perfused through the ascending aorta with a solution of 4% paraformaldehyde in phosphate-buffered saline (PBS, pH 7.35). Brains were removed and processed for paraffin embedding. Sections (7 μm) of the whole infarct area were cut with a microtome and collected on slides pretreated with 3-aminopropyltriethoxy-silane (Sigma, MO, USA). Sections were counterstained with cresyl violet for the histologic identification of the nuclear boundaries and periinfarct areas, and mounted in Eukitt. For each animal, quantification of the infarcted area was performed on the cresyl-violet-stained sections at five representative levels throughout the rostro-caudal extent of the lesion (A 0.26, −0.22, −0.40, −0.70, and −1.2 −4 mm relative to Bregma) (Franklin and Paxinos, 1997). The rostro-caudal extent of the infarct was the same in both groups of mice. The infarcted area of each section was calculated by subtraction of healthy tissue areas of the contralateral from the ipsilateral side of the section to compensate for the effect of brain edema (Guegan *et al*, 1998) using a computer-assisted image analyzing system (Software «Morphometry», Samba 2005 TITN, Alcatel, Alcatel Grenoble, France). Volumes of infarct (mm^3) were calculated for each animal after integration of areas with the distance between each level (de Bilbao *et al*, 2004).

To evaluate whether local alterations in cerebral vascular anatomy contribute to different susceptibility to injury in PPARβ KO mice, an additional series of five WT and five KO mice were killed on day 4 (D4) after ischemia. Cerebral vasculature was studied in WT and PPARβ KO mice (nonoperated and on D4 after ischemia) after intracardial perfusion with 0.9% NaCl solution followed by perfusion of a mixture of an equal proportion of gelatinous water (5%) and China ink (Sennelier, France) warmed at 40°C (1 ml). Brains were removed and immersed for 24 h in 4% paraformaldehyde at 4°C (Chen *et al*, 2005). Cerebral vasculature was observed with a Zeiss stero zoom microscope. The absence of cerebral blood flow in the infarct area was assessed by transcranial measurements of CBF that were made using laser Doppler flowmetry Oxford Optronix Ltd (UK) just before and after MCAO. Animals were placed under a sterotactic head frame and then a fine needle probe (MNP110XP, 0.48 mm diameter) was lowered onto the temporal bone surface 0.5 to 1 mm dorsal to the opening giving access to the MCA and wetted with a small amount of physiologic saline. No preoperative or postoperative strain-related differences in CBF were observed and similar reductions in CBF were observed after MCAO in both strains.

Physiologic Parameters: Physiologic parameters including arterial blood pressure (Kent mouse tail blood pressure system RTBP2000, Kent Scientific Corporation, Torrington, USA), plasma glucose (using Roche Glucotrend Active, Rotkreuz, Switzerland), and hematocrit were measured daily in KO and WT mice ($n=4$ to 5) before MCAO and on D1 and D4 after injury. Body temperature was measured before, during, and after MCAO by a rectal thermometer probe (Ellab DM 852, Roeovre, Denmark). During surgery, mice were placed on a warm mat and rectal temperature was measured. In the preoperation period, rectal temperature was similar in WT (38.0°C± 0.1°C) and PPARβ KO (38.0°C±0.1°C) mice and remained stable after the operation. Daily body temperature was measured at 1030.

In situ Hybridization for PPARβ mRNA Expression in PPARβ KO and WT Mice after MCAO

On D4 after injury, the expression of PPARβ mRNA was determined by *in situ* hybridization in WT ($n=4$) and PPARβ KO ($n=4$) mice and compared with their nonoperated counterparts. Mice were anesthetized with 0.3 ml of a mixture containing 40 mg/ml ketamine and 2 mg/ml xylazine and were immediately perfused intracardially with 20 ml of ice-cold isotonic saline followed by 100 ml of a 4% paraformaldehyde solution. At the end of the perfusion, brains were removed and kept in 4% paraformaldehyde for 3 to 4 days and then transferred to a solution containing paraformaldehyde and sucrose (10%) for 12 h. Sections (25 μm thick) were cut with a sliding microtome (Microtome HM 440E, Microm) and mounted onto slides. *In situ* hybridization histochemistry was performed using a biotin-labelled oligonucleotide PPARβ probe for mRNA (mouse 61 to 111, 5′-atgggtgacg gagccccgga gctcaatggg ggaccagaac acacgcttcc-3′, and its complementary sequence as a negative control) to detect PPARβ (Catalys, Wallisellen, Switzerland). Briefly, 9 pmol/μl of biotin-labelled oligonucleotide was incubated for 2 h at 37°C in a hybridization solution (5 mol/L NaCl, 10 × PE (0.5 M Tris, 1% sodium pyrophosphate, 2% polyvinyl pyrrolidone, 2% Ficoll, SOmMEDTA) buffer, 50% dextran sulfate, 30% formamide) in an OmniSlide Thermal Cycler. After incubation, the slices were washed and biotin labelling was detected using avidin peroxidase complex with diaminobenzidine enhanced by nickel. The specificity of the antisense riboprobe was determined by the absence of a positive signal in sections hybridized with the sense probe.

PCR Determination of mRNAs in PPARβ KO and WT Mice after MCAO

For PPARβ and UCP2 mRNA determinations, ischemic hemispheres were dissected and total RNA was isolated as described previously (Arsenijevic *et al*, 2000*a*). Brain tissues were collected ($n=4$ per group) at 1, 4, and 7 days after MCAO from WT and PPARβ KO mice, as well as from nonoperated control counterparts. In addition, we assessed mRNA expression for neuropeptide Y (NPY), melanin concentrating hormone (MCH), and orexin, three hormones involved in food intake. For this purpose, the whole hypothalamus was dissected out and the RNA was isolated. The RNA was treated with DNase and then reverse transcribed (Promega, Catalys, Wallisellen, Switzerland). Thereafter, a semiquantitative PCR (Invitrogen,

Basel, Switzerland) was performed and the product separated by gel electrophoresis containing ethidium bromide. The bands were then quantified using the Scion Image program (Scion Corporation, MD, USA). Each sample was normalized with its glyceraldehyde 3-phosphate dehydrogenase content. The primers used were as follows: UCP2 (sense 5′-TAC CAG AGC ACT GTC GAA GCC-3′, antisense 5′-AGT CCC TTT CCA GAG GCC C-3′; Yu *et al*, 2000), PPARβ (sense 5′-AGTTCTTGCGCAG TATCCG-3′, antisense 5′-AGTGTTGTGAGTGGCTCTAG -3′; Yang *et al*, 1999), NPY (sense 5′-GGG GCT GTG TGG ACT GAC CCT GG-3′, antisense 5′-GAT GTA GTG TCG CAG AGC GGA G-3′; Gallmann *et al*, 2005), MCH (sense 5′-AAA ATG ATG AGA GCG GCT TCA-3′, antisense 5′-CGA GAT TCT GCT TGG AGC CT-3′; Gallmann *et al*, 2005), orexin (sense 5′-TGG GTA TTT GGA CCA CTG CA-3′, antisense 5′-TGG TGT CTG GAG CTC AGG G- 3′; Gallmann *et al*, 2005), and glyceraldehyde 3-phosphate dehydrogenase, as reference control (sense 5′-TGA AGG TCG GTG TCA ACG GAT TTG GC-3′, antisense 5′-CAT GTA GGC CAT GAG GTC CCA CCA C-3′; Subang *et al*, 1997). All values for the semiquantitative RT-PCR expression of a gene were obtained after normalizing for glyceraldehyde 3-phosphate dehydrogenase. The level of PPARβ and UCP2 was also quantified using real-time PCR (Berthiaume *et al*, 2004). Lesioned and nonlesioned brain hemispheres ($n=4$ for each group of mice) were removed on D4 after MCAO and stored in RNA later (Ambion, TX, USA) at 4°C. Brain mRNA was extracted using the Trizol RNA extraction method. RNA concentration was estimated from absorbance at 260 nm and RNA was transcribed using Expand reverse transcriptase (Roche Diagnostics, Laval, QC, Canada). The mRNA expression level was quantified using quantitative fluorescent real-time PCR (Corbett Research, New South Wales, Australia). Amplification and detection of target mRNA were performed with Platinum *Taq* polymerase and the intercalating dye SybrGreen I (Berthiaume *et al*, 2004). The mRNA levels of PPARβ and UCP2 were normalized with beta-actin. The primers used were as follows: PPARβ, sense 5′-AGTTCTTGCGCAGTATCCG-3′, antisense 5′-AGTGTTGT GAGTGGCTCTAG-3′; UCP2, sense 5′-TTC TCC TGC GGT CCG GAC ACA ATA-3′, antisense 5′- TTGA CTC TCC CCT TGG ATC TGC AG-3′; and beta-actin, sense 5′-CTC TAG ACT TCG AGC AGG AG-3′, antisense 5′-AGA GTA CTT GCG CTC AGG AG-3′. The primers were designed using the Vector NTI program. For both experiments, gene expression represented the percentage obtained by comparing operated hemispheres to control hemispheres of nonoperated mice.

Brain Cytokine Levels after MCAO in PPARβ KO and WT Mice

The levels of TNFα, IFNγ, and NGF were measured by immunoassay in the brains of operated and nonoperated PPARβ KO and WT mice ($n_{KO}=8$ and $n_{WT}=8$, each group consisting of four ischemic and four nonoperated animals) on D1 and D4 after MCAO. Brains were aseptically removed and immediately placed on dry ice. The ischemic hemispheres of operated mice and hemispheres of nonoperated mice were put in CHAPS solution and homogenized. The supernatant was collected and frozen at −20°C (Arsenijevic *et al*, 2000*a*). Cytokines TNFα and IFNγ, as well as NGF, were measured using immunoassay kits from Amersham and Catalys (Wallisellen, Switzerland). To study possible interactions between these three cytokines, NGF levels were also assessed in IFNγ KO and TNFα KO mice, and in the corresponding WT mice 1 day after ischemia ($n_{KO}=8$ and $n_{WT}=8$, each group consisting of four ischemic and four nonoperated animals).

Lipid Peroxidation

The levels of malondialdehydes (MDA), indicators of endogenous peroxidation, were measured in PPARβ KO and WT mice on D1 and D4 after MCAO. Mice were anesthetized and perfused intracardially with saline solution. After perfusion, the brain was removed and the ipsilateral and contralateral whole hemispheres of operated and nonoperated mice were washed three times in ice-cold Tris-HCl 20 mmol/L buffer (pH 7.4). They were then gently homogenized for 1 min in a glass tissue grinder (Wheaton, Millville, NJ, USA) in 4 ml of the same buffer. Homogenates were centrifuged at 3,200*g* for 10 mins at 4°C and the supernatant was processed for MDA levels using a lipid peroxidation assay (de Bilbao *et al*, 2004). To prevent sample oxidation, 0.5 mmol/L butylated hydroxytoluene (Sigma Chemicals, St Louis, MO, USA) was added to the tissue homogenate. Optical density was measured at 586 nm using a spectrophotometer (Dynatech, Chantilly, VA, USA). Changes in oxidative stress were assessed in brain homogenates in nonoperated ($n_{KO}=8$ and $n_{WT}=8$) and operated ($n_{KO}=8$ and $n_{WT}=8$) PPARβ KO and WT mice. For each group of mice, MDA levels of the operated brain hemisphere were compared with those of the hemisphere of nonoperated animals (de Bilbao *et al*, 2004).

Glutathione Levels

Brain homogenates from WT and PPARβ KO mice, subjected or not to ischemia (1 and 4 days after ischemia) ($n=8$ per group), were processed as described previously for reduced GSH (de Bilbao *et al*, 2004). Reduced GSH levels were measured using a method based on the formation of a chromophoric product resulting from the reaction of 5,5′-dithiobis-(2-nitrobenzoic acid) (Sigma Chemicals, St Louis, MO, USA) and GSH (Sigma, Buchs, Switzerland). For each group of mice, we compared the operated brain hemisphere with the nonoperated hemisphere of control animals. To evaluate whether IFNγ administration influences oxidative stress regulation in ischemic PPARβ KO mice, these animals and their WT counterparts ($n=8$ for each group) were pretreated with IFNγ antibody 18 h before MCAO and were killed 4 days later. Interferon-gamma antibody (ATCC HB170 from American Type Culture Collection, MD, USA, provided by C Yesin, CMU, Geneva, Switzerland) was injected at 50 μg per mouse intraperitoneally (Arsenijevic *et al*,

2000*a*). Levels of MDA and GSH were also assessed in these mice as described above.

Immunohistochemistry and Double Staining Experiments

Frozen coronal sections (25 μm) from operated (1 and 4 days after ischemia) and nonoperated WT and PPARβ KO mice ($n=4$ for each group) were processed for MnSOD immunostaining using sheep anti-human MnSOD (1/100; Calbiochem, San Diego, CA, USA) and rabbit anti-sheep immunoglobulins (Dako, CA, USA) as the secondary antibody. Immunohistochemistry of MnSOD was performed on nonoperated and operated (1 and 4 days after MCAO) WT and PPARβ KO mice. We also tested MnSOD immunostaining 4 days after MCAO in WT and PPARβ KO mice treated with 200 ng NGF 2.5S on the lesion site 1 day after MCAO. Immunohistochemistry of PPARβ was performed using an anti-PPARδ rabbit polyclonal antibody (PA1-832) from Affinity Bioreagents (Golden, CO, USA) and visualized by a secondary goat anti-rabbit fluorescein isothiocyanate (Nordic Immunology, Tiburg, The Netherlands). To label astrocytes, microglia, macrophages, oligodendrocytes, and neuronal cells, mouse polyclonal anti-glial fibrillary acidic protein clone GA5 (1/400; Sigma, MO, USA), rabbit polyclonal anti-Iba1 (1 μg/ml; kindly provided by Professor Y Imai, National Center of Neurology and Psychiatry, Japan), rat anti-mouse F4/80 for macrophage (1/200; Serotec, Oxford, UK), anti-CNPase (2′3′ cyclic nucleotide 3′ phosphodiesterase) (1/200; Sigma, MO, USA), and the mouse anti-neuronal nuclei monoclonal antibody (NeuN) (1/1,000; Chemicon, Temecula, CA, USA) were used. The glial fibrillary acidic protein, anti-Iba1, anti-macrophages, and NeuN antibodies were detected using Alexa Fluor 546 rabbit anti-mouse (Molecular Probes, Eugene, OR, USA), goat anti-rabbit immunoglobulins Alexa Fluor 568 (Molecular Probes), goat anti-rabbit fluorescein isothiocyanate, goat anti-rat fluorescein isothiocyanate (Nordic Immunology), and goat anti-mouse immunoglobulins linked to AMCA (9-amino-6-chloro-2-methoxyacridine) (Dako). Negative controls included deletion of the primary or secondary antibody. Photomicrographs of immunofluorescent staining were constructed using the Axioskop 2 and the software Axiovision.

Statistical Analysis

Results are expressed as means±standard error of the mean (s.e.m.). Differences between groups were assessed using a two-way ANOVA followed by the Bonferroni *post hoc* test. $P<0.05$ was considered significant.

Results

Physiologic Parameters before and after MCAO

Arterial pressure, plasma glucose, hematocrit levels, and body temperature before and after MCAO on D1 and D4 were not significantly different between WT and PPARβ KO mice at a given time point, as shown in Table 1. There were no significant differences between WT and KO mice between the different days (Table 1). After MCAO, both WT and PPARβ KO mice showed an absence of cerebral blood flow in the infarct area.

PPARβ and UCP2 mRNA Expression in WT and PPARβ KO Mice after MCAO

The expressions of PPARβ and UCP2 mRNAs in response to ischemic brain injury were determined by semiquantitative RT-PCR. Peroxisome prolifera-

Table 1 Physiologic parameters before and after MCAO in PPARβ KO and WT mice

Group and treatment	*1 day before MCAO*	*D1 after MCAO*	*D4 after MCAO*
Hematocrit (%)			
WT	43±4	45±6	±4
PPARβ KO	45±2	46±3	48±7
Plasma glucose (mmol/L)			
WT	7.1±0.3	7.0±0.3	7.1±0.3
PPARβ KO	6.9±0.4	6.7±0.2	7.0±0.4
Body temperature (°C)			
WT	37.3±0.3	37.5±0.3	37.6±0.2
PPARβ KO	37.5±0.2	37.5±0.3	37.7±0.1
Arterial pressure (mm Hg)			
WT	136±16	123±23	136±17
PPARβ KO	134±25	128±19	132±20

Hematocrit, plasma glucose, body temperature, and arterial pressure were measured in wild-type (WT) and PPARβ knockout (KO) mice before ischemia, and then on days 1 (D1) and 4 (D4) after MCAO. No significant differences were observed between WT and KO mice on any given day, and there were no significant differences between days in WT and KO. Data are means±s.e.m. of four to five animals per group. MCAO: middle cerebral artery occlusion; PPARβ: peroxisome proliferator-activated receptor β.

tor-activated receptor β mRNA was significantly upregulated (45% to 58%, $P<0.001$) in the ischemic hemispheres of WT mice compared with nonoperated animals on D1, D4, and D7 after MCAO (Figure 1A). As expected, PPARβ mRNA was not detected in PPARβ KO mice (Figure 1A). Uncoupling protein 2 mRNA was also significantly increased (30% to 70%, $P<0.001$) in the ischemic hemispheres of WT mice on D1, D4, and D7 after MCAO (Figure 1B). Interestingly, no significant induction of UCP2 mRNA was observed in the ischemic hemispheres of PPARβ KO mice (10% to 14%, $P>0.05$) compared with nonoperated animals after MCAO (Figure 1B). Quantitative fluorescent real-time PCR also indicated that PPARβ and UCP2 were induced in WT mice on D4 after MCAO (112%±12% and 91%±10%, respectively) but not in PPARβ KO mice. *In situ* hybridization experiments also revealed induction of PPARβ mRNA in the periinfarct area on D4 after MCAO in WT mice (Figure 1C) but not in PPARβ KO mice (not shown). No labelling was observed in the contralateral hemisphere of WT mice. Induced PPARβ mRNA labelling occurred in oligodendrocytes and neurons in the border of the necrotic zone (data not shown) (Woods *et al*, 2003). Immunofluorescent staining of PPARβ showed that PPARβ protein was induced in the periinfarct area of WT mice but not in PPARβ KO mice 4 days after MCAO (Figures 1D and 1E).

Infarct Size after MCAO is Increased in PPARβ KO Mice

The infarct volume was quantified on D4 after permanent MCAO in WT and PPARβ KO mice, a time at which PPARβ mRNA was markedly increased in the periinfarct area of WT mice (Figure 1A). Infarct volume was increased two-fold in PPARβ KO mice ($10.9\pm0.2\,mm^3$, $n=18$) when compared with WT mice ($5.3\pm1.3\,mm^3$, $n=16$) ($P<0.001$) (Figure 2). No difference was observed in the vascular system (organization of the circle of Willis, position and diameters of the main cerebral arteries) between WT and KO mice. At 4 days after MCAO, no revascularization was observed on the surface of the injured hemisphere in both mice strains (data not shown).

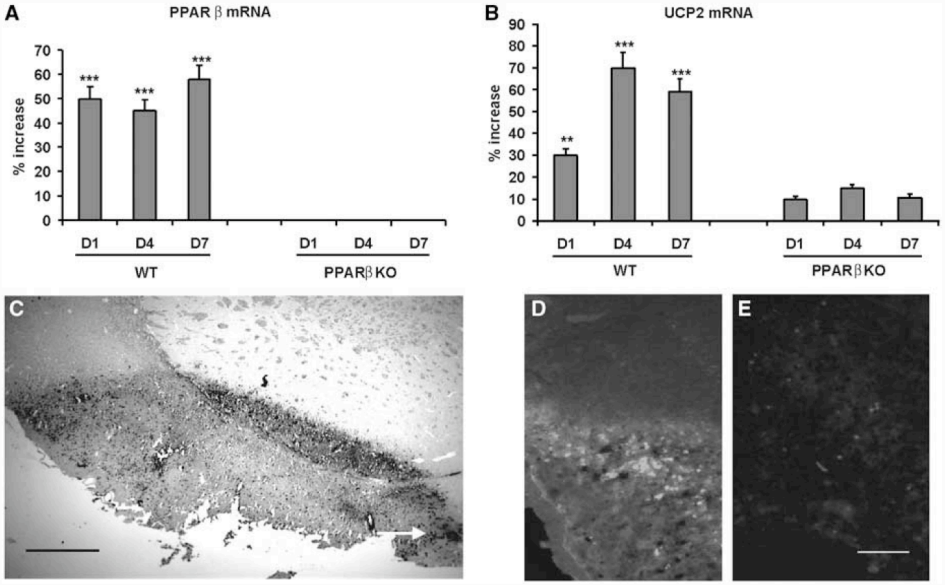

Figure 1 Expression of PPARβ and UCP2 in WT and PPARβ KO mice after MCAO. RT-PCR determination of (**A**) PPARβ and (**B**) UCP2 mRNA induction on D1, D4, and D7 after MCAO in WT and PPARβ KO mice ($n=4$ for all groups). Gene expression is reported as the percentage of increase observed in operated hemispheres compared with control hemispheres of nonoperated mice. In WT mice, PPARβ and UCP2 mRNAs were significantly induced after ischemia ($P<0.001$). The increases in PPARβ and UCP2 mRNAs in the operated hemispheres were significantly higher in WT than in KO mice at all time points ($P<0.001$). In PPARβ KO mice, PPARβ mRNA was not detected. Each value is expressed as mean±s.e.m. (***$P<0.001$, **$P<0.01$). (**C**) *In situ* hybridization localization of PPARβ mRNA. Note that PPARβ is found at the periphery of the lesion site, as indicated by the arrow; PPARβ mRNA was found in neurons and oligodendrocytes. (**D**) Immunofluorescent staining for PPARβ on D4 after MCAO in WT mice and (**E**) PPARβ KO mice. In WT mice, labelled cells were found in the cortical periinfarct area. No labelling was observed in PPARβ KO mice (scale bar: 40 μm (**C**), 15 μm (**D, E**)).

Importantly, this effect was specific for PPARβ because there was no significant difference in lesion volume between PPARα KO mice and their WT counterparts (5.6 ± 1.6 and $5.8 \pm 1.1\,mm^3$, respectively, $n = 6$ per group) ($P > 0.05$).

Altered Lipid Peroxidation and Glutathione Levels in PPARβ KO Mice after MCAO and their Regulation by IFNγ

In both groups of mice, a significant increase in MDA levels was observed in the ischemic brains when compared with the nonoperated mice (Table 2). Moreover, PPARβ KO mice had significantly higher levels of MDA than WT mice (Table 2). Reduced GSH levels were significantly decreased in the brains of WT and PPARβ KO mice on D1 and D4 after MCAO (Table 2). On D4 after ischemia, PPARβ KO mice had significantly lower levels of GSH than WT mice (Table 2).

Administration of IFNγ antibody 18 h before MCAO led to a significant reduction of MDA increase and GSH loss on D4 after ischemia in both WT and PPARβ KO mice when compared with nontreated ischemic mice, suggesting that oxidative stress is mediated by IFNγ in both types of mice. When the antibody was administered to mice that did not undergo MCAO, it did not have any effect on MDA or reduced GSH brain levels compared with nontreated mice.

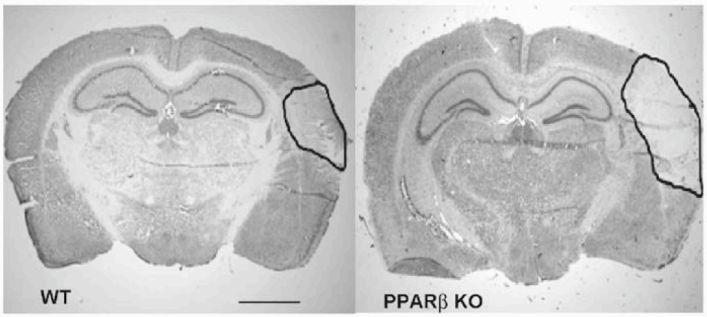

Figure 2 Effect of PPARβ deletion on infarct size. Representative coronal brain sections showing the ischemic infarct 4 days after MCAO in WT and PPARβ KO mice. Brain sections were stained with cresyl violet. The surrounded areas denote the size of the ischemic area. The infarct size was found significantly increased in PPARβ KO mice ($P < 0.001$) ($n_{KO} = 18$ and $n_{WT} = 16$) (scale bar: 120 μm).

Table 2 Brain MDA and GSH levels

Treatment	*MDA (nmol/g tissue)*	*Reduced GSH (nmol/mg tissue)*	*Bonferroni test*	
			MDA	*GSH*
WT, control	31 ± 2	1.43 ± 0.11		
WT, MCAO, D1	$89 \pm 4^{***}$	$0.94 \pm 0.12^{***}$		
WT, MCAO, D4	$67 \pm 3^{***}$	$0.91 \pm 0.09^{***}$		
WT, control, anti-IFN	29 ± 2	1.47 ± 0.12		
WT, MCAO, D4, anti-IFN	$41 \pm 3^{\dagger}$	$1.21 \pm 0.13^{\dagger}$		
KO, control	35 ± 2	1.38 ± 0.11	NS	NS
KO, MCAO, D1	$143 \pm 11^{***}$	$0.74 \pm 0.07^{***}$	***	NS
KO, MCAO, D4	$96 \pm 9^{***}$	$0.67 \pm 0.07^{***}$	****	*
KO, control, anti-IFN	38 ± 3	1.43 ± 0.10	NS	NS
KO, MCAO, D4, anti-IFN	$48 \pm 4^{\dagger}$	$1.09 \pm .014^{**,\dagger}$	NS	NS

MDA and reduced GSH levels were measured in ischemic and nonoperated wild-type (WT) and peroxisome proliferator-activated receptor β (PPARβ) knockout (KO) mice on days 1 (D1) and 4 (D4) after MCAO. Additional PPARβ KO and WT mice were also pretreated with interferon-gamma antibody (anti-IFN) 18 h before MCAO. Asterisks in the first two columns indicate comparisons between nonoperated (control) and operated animals of the same genotype. Daggers correspond to comparisons between anti-IFN-treated and nontreated mice on D4 after ischemia. In the last column, Bonferroni test after ANOVA indicates a statistical difference between WT and PPARβ KO mice with the same treatment (*$P < 0.05$, **$P < 0.01$, ***$P < 0.001$, and $^{\dagger}P < 0.001$). Data are means ± s.e.m. It should be noted that the comparison of results between operated and nonoperated mice may require sham-operated controls. However, several previous reports have demonstrated that most biochemical and morphologic markers used in the present study are only marginally affected in sham-operated animals compared to animals with cerebral ischemia (Mizui *et al*, 1992; Suzuki *et al*, 1999; Candelario-Jalil *et al*, 2001; Pratico *et al*, 2002). MDA: malondialdehydes; GSH: glutathione; MCAO: middle cerebral artery occlusion; NS: nonsignificant.

TNFα and NGF Induction is Blunted and that of IFNγ Potentiated in PPARβ KO Mice after MCAO

Tumor necrosis factor alpha was significantly induced in the brain of WT mice on D1 after MCAO (90 ± 8 pg/ml, $P<0.001$), and returned to basal levels on D4 (16 ± 3 pg/ml) compared with nonoperated WT mice (19 ± 4 pg/ml) (Figure 3A). In contrast, PPARβ KO mice showed no induction of TNFα on either day after MCAO (15 ± 3 and 18 ± 3 pg/ml for D1 and D4, respectively) when compared with nonoperated animals (17 ± 4 pg/ml, $P>0.05$ (Figure 3A).

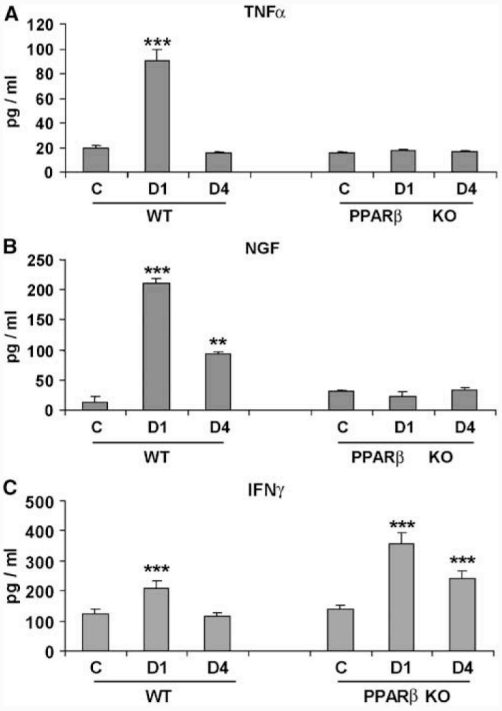

Figure 3 Levels of (**A**) TNFα, (**B**) NGF, and (**C**) IFNγ as determined by immunoassay in the hemispheres of nonoperated WT (WTc) and PPARβ KO (KOc) mice and in the ischemic hemispheres of WT and PPARβ KO mice on D1 and D4 after MCAO. (**A**) The levels of TNFα were significantly increased on D1 after ischemia in WT mice ($P<0.001$) but not in PPARβ KO mice ($P>0.05$) (WTc and KOc, respectively). (**B**) The levels of NGF were significantly increased on D1 and D4 after ischemia in WT mice ($P<0.001$ and $P<0.01$, respectively) but not in PPARβ KO mice ($P>0.05$). (**C**) The levels of IFNγ were increased on D1 after ischemia in WT mice compared with nonoperated WT animals ($P<0.001$). In PPARβ KO mice, IFNγ was also significantly increased on D1 and D4 after ischemia compared with both nonoperated PPARβ KO mice ($P<0.001$) and WT animals ($P<0.001$). Each value is expressed as mean ±s.e.m. ($n=4$ mice per group) ($^{**}P<0.01$, $^{***}P<0.001$).

Similarly, NGF levels were markedly increased on D1 (221 ± 7 pg/ml) ($P<0.001$) and D4 (93 ± 4 pg/ml) ($P<0.01$) after MCAO in the brain of WT mice when compared with nonoperated animals (21 ± 10 pg/ml) (Figure 3B). Again, the upregulation of NGF levels was completely ablated in PPARβ KO mice (24 ± 7 pg/ml on D1 and 32 ± 5 pg/ml on D4) when compared with nonoperated mice (30 ± 2 pg/ml) (Figure 3B).

Interferon-gamma was significantly increased in the brains of both WT and PPARβ KO mice on D1 after ischemia (211 ± 8 and 357 ± 15 pg/ml, respectively) when compared with nonoperated animals (125 ± 3 and 139 ± 4 pg/ml, respectively) (all comparisons $P<0.001$) (Figure 3C). At 4 days after ischemia, IFNγ was still significantly increased in PPARβ KO mice compared with nonoperated animals (242 ± 6 and 139 ± 4 pg/ml, respectively) ($P<0.001$) but returned to basal levels in WT mice (Figure 3C). Interestingly, and although IFNγ basal levels did not differ between nonoperated WT and PPARβ KO mice, IFNγ levels at D1 and D4 were significantly higher in KO (D1: 69%, $P<0.01$; D4: 74%, $P<0.01$) than in WT mice (Figure 3C).

MnSOD is Reduced in PPARβ KO mice after MCAO: Reversal by NGF Treatment

Because MnSOD is thought to be the first line of defense against oxygen toxicity, we also examined its presence in WT and PPARβ KO mice before and after MCAO. No immunostaining was detected in WT and PPARβ KO mice before MCAO. Double

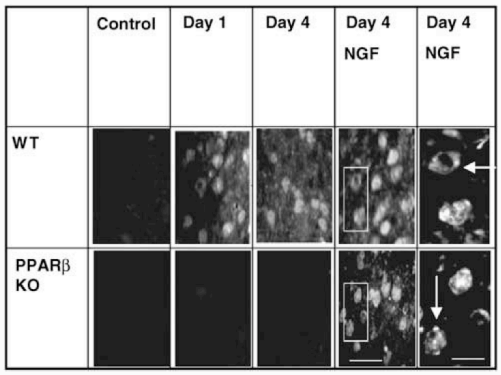

Figure 4 Wild-type but not PPARβ KO mice expressed MnSOD immunostaining in neurons on D1 and D4 after MCAO. Treatment with 200 ng NGF 2.5S on the lesion site 1 day after MCAO resulted in MnSOD induction in PPARβ KO mice (scale bar: 20 μm). The right columns show a higher magnification of the selected areas in which a punctated distribution (arrows) of the protein in mitochondria (scale bar: 7 μm) is observed. No labelling was seen in nonoperated control animals.

staining experiments revealed MnSOD-positive neurons and astrocytes in WT mice at D1 and D4 after MCAO. Positive immunostaining was observed in the striatal border and the neocortical border zones of the periinfarct area. In contrast, PPARβ KO mice did not show any staining at the same time period (Figure 4). Importantly, treatment of PPARβ KO mice with NGF 1 day after ischemia resulted in detection of MnSOD labelling at D4 after lesion (Figure 4). In Figure 4, the punctate immunostaining indicates the mitochondrial distribution of the protein in both groups of mice. Treatment with NGF was also

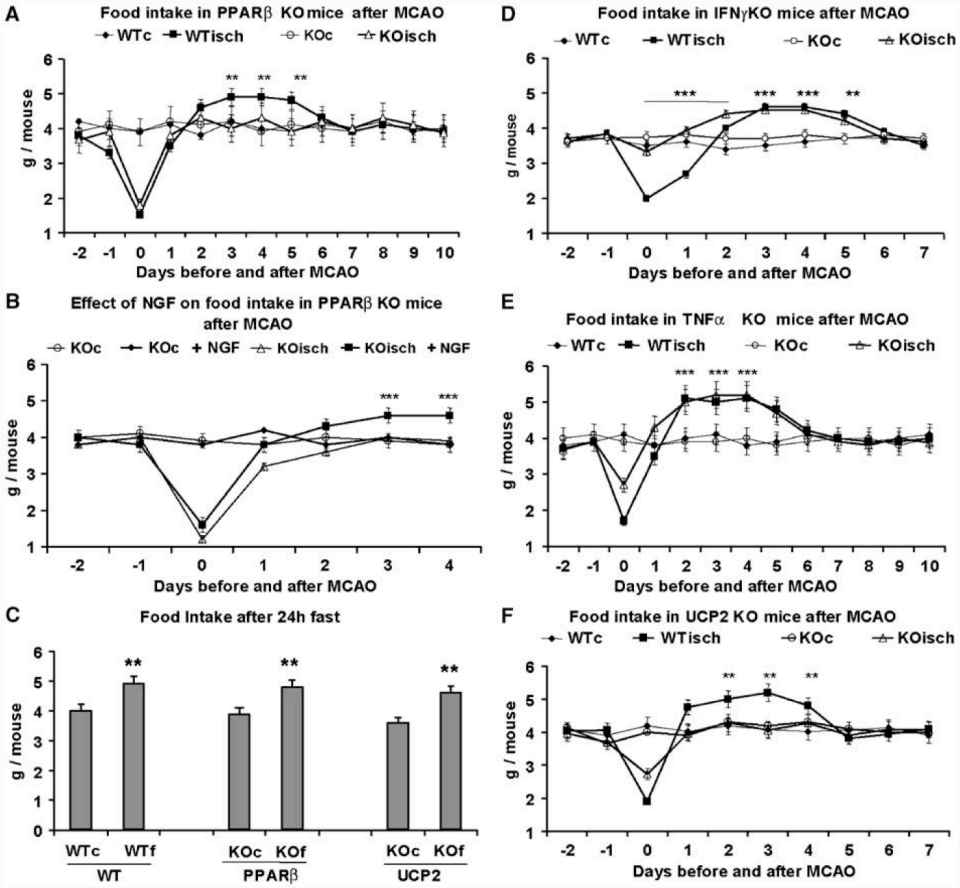

Figure 5 Food intake responses in PPARβ KO, IFNγ KO, TNF KO, and UCP2 KO mice after MCAO. (**A**) Food intake responses to MCAO in WT and PPARβ KO mice. Nonoperated PPARβ KO mice (KOc) did not differ in food intake compared with their WT counterparts (WTc) ($P>0.05$). On D3 to D5 after MCAO, WT (WTisch) but not PPARβ KO mice (KOisch) showed significant hyperphagia compared with nonoperated mice (WTc) ($^{**}P<0.01$). (**B**) Effect of NGF treatment on food intake of PPARβ KO mice after MCAO. Administration of NGF (200 ng on the lesion site 1 day after MCAO) induced a hyperphagic response on D3 to D4 after ischemia in PPARβ KO mice (KOisch + NGF) ($^{***}P<0.001$). (**C**) Food intake after 24 h fasting in WT, PPARβ KO, and UCP2 KO mice. As observed for WT mice, PPARβ KO and UCP2 KO mice were able to respond with a hyperphagic state 1 day after fasting (KOf) compared with their controls (KOc) ($^{**}P<0.01$ for each group). (**D**) Food intake responses to MCAO in IFNγ KO mice. The IFNγ KO mice (KOisch) did not show significant post-MCAO hypophagia compared with WT operated mice (WTisch). On D0 to D2, IFNγ KO mice (KOisch) ate significantly more than WT mice (WTisch) ($^{***}P<0.001$). The IFNγ KO mice showed significant hyperphagia after MCAO (KOisch) when compared with nonoperated mice (KOc) ($^{***}P<0.001$). (**E**) Food intake responses to MCAO in TNFα KO mice. The TNFα KO mice (KOisch) showed significant hyperphagia after MCAO (KOisch) when compared with nonoperated mice (KOc) ($^{***}P<0.001$). (**F**) Food intake responses to MCAO in UCP2 KO mice. The significant hyperphagia observed in WT mice after MCAO (WTisch) ($^{**}P<0.01$) did not occur in UCP2 KO mice (KOisch) ($P>0.05$). Each value is expressed as mean ± s.e.m.

associated with decreased infarct size in PPARβ KO mice (from 9.3 ± 0.6 to $6.8 \pm 0.4\,mm^3$) ($P<0.05$, $n=8$).

Lack of Hyperphagic Response to MCAO in PPARβ KO Mice: Involvement of NGF, IFNγ, and UCP2, but not TNFα

The PPARβ KO and WT mice show acute hypophagia on the day of MCAO intervention and then regain appetite. The compensatory hyperphagic phase, lasting from D3 to D5, in WT mice ($n=8$, $P<0.01$) did not occur in PPARβ KO mice (Figure 5A). Injection of NGF on the lesion site of PPARβ KO mice 1 day after MCAO resulted in significant hyperphagia from D3 to D4 after ischemia ($P<0.001$) (Figure 5B). In contrast to the patterns of food intake observed after MCAO, both WT and PPARβ KO mice displayed a significant hyperphagic response 1 day after a 24-h period of fasting ($n=8$, $P<0.01$) (Figure 5C).

Because altered levels of TNFα, IFNγ, and UCP2 were observed in PPARβ KO mice after ischemia, food intake was also measured in TNFα KO, IFNγ KO, and UCP2 KO mice. Interferon-gamma KO mice did not show hypophagia from D0 to D3 after MCAO when compared with WT ischemic mice ($P>0.05$), but rapidly entered a hyperphagic state compared with WT (Figure 5D). During the period D0 to D2 after MCAO, IFNγ KO mice ate significantly more than WT mice ($P<0.001$) (Figure 5D). Like their WT counterparts, TNFα KO and IFNγ KO mice showed significant hyperphagia after MCAO compared with their nonoperated controls (from D3 to D5, and D2 to D4, respectively) ($P<0.001$) (Figures 5D and 5E). In contrast, UCP2 KO mice did not show significant hyperphagia after MCAO when compared with WT ($P>0.05$) (Figure 5F), but were able to show a significant hyperphagic response 1 day after 24 h fasting ($n=8$, $P<0.01$) (Figure 5C). In all animals, the body weight followed a parallel time course to that of food intake (data not shown).

NPY Expression is Decreased in PPARβ KO Mice after MCAO

Basal levels of neuropeptide mRNAs (NPY, orexin, and MCH) did not differ between PPARβ KO and WT mice (data not shown). The expression of the three neuropeptides showed significant increases 4 days after MCAO in WT mice when compared with nonoperated animals (NPY: $110\% \pm 5\%$; orexin: $60\% \pm 2\%$; MCH: $69\% \pm 4\%$; $n=4$ and $P<0.001$ for the three groups) (Figure 6). However, NPY mRNA induction in PPARβ KO mice was markedly attenuated ($22\% \pm 2\%$, $P<0.001$) compared with WT mice (Figure 6). This was not the case for orexin ($51\% \pm 4\%$, $n=4$) and MCH ($57\% \pm 4\%$, $n=4$) mRNAs, which showed a similar post-MCAO increase in both PPARβ KO and WT mice (Figure 6).

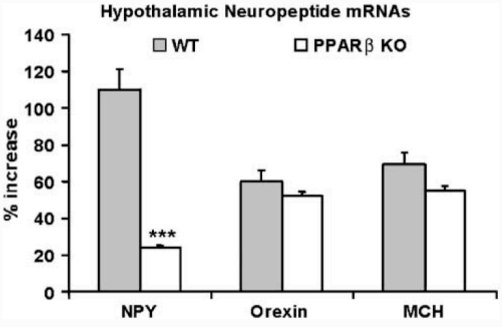

Figure 6 Induction of NPY, orexin, and MCH mRNAs on D4 after MCAO in WT (WT) and PPARβ KO (KO) mice. The induction of NPY was significantly attenuated in PPARβ KO when compared with WT mice ($n=8$ for all groups). Each value is expressed as mean ± s.e.m. ($^{***}P<0.001$).

Discussion

The major finding of this study is that the deletion of PPARβ gene in mice dramatically exacerbated the deleterious consequences of focal cerebral ischemia. The enhanced susceptibility to MCAO was revealed by a 50% increase in lesion volume in the PPARβ KO mice compared with their WT counterparts. The greater sensitivity observed after MCAO was specifically related to PPARβ absence because the infarct size was similar in PPARα WT and KO mice. This latter finding is in agreement with a recent study that clearly showed that PPARα receptor deficiency is not associated with an increased susceptibility to focal cerebral ischemia in mice (Deplanque *et al*, 2003). Although all three PPAR types are present in the brain, PPARβ receptor is the most abundant in cortical cells (Cullingford *et al*, 1998), further supporting an involvement of PPARβ activation in neuroprotective mechanisms against focal cerebral ischemia. However, and as is the case for all studies comparing WT with KO mice (Durum and Muegge, 1998; Samson and Taylor, 2005), our study does not eliminate the possibility that PPARβ regulation of MCAO lesion size could be indirect. Yet, our model showed that PPARβ deficiency results in increased lesion size, indicating that lack of PPARβ could not be compensated.

This increased susceptibility to MCAO in PPARβ KO mice was accompanied by massive changes in both antioxidant mechanisms and cytokine activation. The increase of oxidative injury in these mice was indicated by the upregulation of MDA content and reduction of MnSOD and reduced GSH levels, two classical brain antioxidants. Importantly, our results also show that, in contrast to WT mice, the transcript of UCP2, a regulator of reactive oxygen species (Arsenijevic *et al*, 2000*b*), is not upregulated in PPARβ KO mice after ischemia. In conjunction with previous studies showing that activation of

PPARs may induce UCP2 mRNA expression in various tissues (Aubert *et al*, 1997; Wang *et al*, 2003), this observation implies that UCP2 may require PPARβ to be induced in brain tissue after ischemic injury. Altered cytokine levels may also contribute to the deleterious consequences of cerebral ischemia in PPARβ KO mice. In particular, TNFα and NGF, two macrophage cytokines known to be involved in the acute phase of brain ischemic tolerance (Guegan *et al*, 1998; Scherbel *et al*, 1999), are not induced after MCAO in the brain of PPARβ KO mice. In contrast, the levels of the proinflammatory lymphocyte cytokine IFNγ were abnormally elevated in the brain of PPARβ KO mice after MCAO, suggesting that PPARβ may inhibit the induction of this inflammatory cytokine. Altogether, these results imply that PPARβ may participate in the regulation of both macrophage and lymphocyte cytokines. The lack of NGF induction after MCAO in PPARβ KO mice cannot be explained by the absence of TNFα because TNFα KO mice were still able to induce NGF (data not shown). It remains to be determined whether the higher amounts of IFNγ found in the PPARβ KO mice could partially explain the ablated NGF because IFNγ has been shown to block NGF secretion in neonatal astrocyte culture but not quiescent astrocytes (Awatsuji *et al*, 1995). Interestingly, our data also provide further evidence indicating that the oxidative status of PPARβ KO mice after MCAO may be mediated by altered cytokine levels. In fact, IFNγ antibody administered before MCAO to PPARβ KO mice reduced MDA increase and GSH loss in the mice. Consistent with previous observations in this field, acute NGF administration after ischemia led to a substantial decrease of infarct volume in WT mice (Semkova and Krieglstein, 1999). Moreover, the decreased infarct volume and upregulation of MnSOD expression observed in the brain of NGF-treated PPARβ KO mice after ischemia suggest that the reduced availability of NGF may be partly at the origin of the higher vulnerability to cerebral ischemia in PPARβ KO mice (Guegan *et al*, 1999).

Besides the importance of PPARβ in the regulation of central ischemic damage, another important finding of the present study is that PPARβ is also involved in the regulation of food intake after MCAO. The rapid hyperphagic phase induced in WT mice after MCAO was not present in PPARβ KO mice, suggesting that the cellular signalling involved in MCAO-induced hyperphagia is not functional in PPARβ KO mice. Because NGF treatment can restore hyperphagia in these mice, a role for NGF in mediating the hyperphagic response after ischemia is strongly suggested. This finding is consistent with a previous study showing that NGF induces hyperphagia when administered after hypothalamic damage (Berger *et al*, 1973). The specific role of PPARβ in MCAO-induced hyperphagia may also involve NPY, as indicated by the blunted NPY induction in PPARβ KO mice after ischemia. Whether NGF is necessary for NPY expression, as suggested by other studies (Verge *et al*, 1995), remains to be determined. In agreement with previous observations on TNFα and IFNγ anorexic effects (Arsenijevic *et al*, 2000*b*; Langhans, 2000), the fact that ischemic TNFα KO and IFNγ KO mice entered in a hyperphagic state suggests that these cytokines are not required for hyperphagia after MCAO. In addition, the hyperphagic phase observed in these two genotypes after MCAO is consistent with their associated increased NGF levels. Thus, the absence of TNFα observed in PPARβ KO mice should not play a major role in the lack of hyperphagic response observed in these mice. In contrast, because IFNγ KO mice ate significantly more than WT mice the first 2 days after MCAO, it is possible that the elevated levels of this anorexic cytokine in PPARβ KO mice could partly explain the lack of hyperphagia after MCAO (Arsenijevic *et al*, 2000*b*). Because UCP2 KO mice did not display hyperphagia after cerebral ischemia, the absence of UCP2 induction after MCAO could also contribute to the lack of hyperphagia in PPARβ KO mice. Taken together, these new data indicate that induction of PPARβ and UCP2 expression may be critical in the molecular mechanisms regulating food intake after MCAO. This regulation of food intake is MCAO specific because PPARβ KO and UCP2 KO mice are still able to display a hyperphagic response after a period of fasting. The close relationship between PPARβ and UCP2 is further highlighted in that they are expressed in the same hypothalamic nuclei known to regulate food intake (Richard *et al*, 1998; Woods *et al*, 2003).

Although our data indicate that PPARβ is involved in infarct size and regulates hyperphagic response after MCAO, the present data do not support a causal relationship between these two phenomena. Middle cerebral artery occlusion induces hypophagia followed by hyperphagia and then a return to basal food intake levels in balb/c, C57bl/J6, sv129, b6, and CFW mice strains (Arsenijevic *et al*, 2003). Several lines of evidence indicate that the size of the infarct is not necessarily related to hyperphagia. First, an increased infarct volume in the PPARβ KO mice was associated with lack of hyperphagia. Second, IFNγ KO mice have a smaller infarct size than their WT counterparts (data not shown), yet they showed a more rapid onset of hyperphagia. In contrast, our previous work revealed a smaller infarct size in UCP2 KO mice than their WT counterparts in the absence of hyperphagia (de Bilbao *et al*, 2004).

Permanent distal MCAO model affects the cerebral cortex, whereas food intake response is traditionally thought to be related to the hypothalamus. However, numerous earlier contributions showed that food intake is a complex process involving several cortical areas (Hinton *et al*, 2004; Kaye *et al*, 2005; Rolls, 2005). Similarly, lesions in the cerebral cortex may decisively influence food intake (Modo

et al, 2000). Furthermore, a recent contribution showed that altered eating behaviors are mostly related to the neural circuits between the cerebral cortex and appetite-regulating centers located in the hypothalamus (Rolls, 2005). Alternatively, appetite regulation may also be influenced by acute inflammatory phenomena related to the activation of cytokines/eicosanoids (Langhans, 2000). Although our data do not provide a definite conclusion about the etiology of feeding disorders in PPARβ KO mice, they strongly support a predominant role of cytokine and humoral immunity mechanisms in this context.

To our knowledge, this is the first study addressing the role of PPARβ in three main biologic events associated with cerebral ischemia, namely morphologic changes, activation of antioxidant and inflammatory mechanisms, as well as food intake. The above-discussed findings clearly suggest a central role of PPARβ in neuroprotection against focal cerebral ischemic damage, as well as in the molecular mechanisms involved in the associated antioxidant, inflammatory, and food intake responses. It may orchestrate energy balance and inflammation during MCAO. Based on these observations, a pharmacological modulation of PPARβ, such as that induced with the use of specific PPARβ agonists (Li *et al*, 2004), could represent a relevant therapeutic possibility in the field of cellular protection after stroke.

References

Arsenijevic D, de Bilbao F, Vallet P, Giannakopoulos P, Langhans W (2003) Cerebral ischemic injury induced hyperphagia—involvement of PPARβ and consequence of previous chronic infection. *Appetite* 40:315

Arsenijevic D, Garcia I, Vesin C, Vesin D, Arsenijevic Y, Seydoux J *et al* (2000*a*) Differential roles of tumor necrosis factor alpha and interferon gamma in mouse hypermetabolic and anorectic response induced by LPS. *Eur Cytokine Netw* 11:662–8

Arsenijevic D, Onuma H, Pecqueur C, Raimbault S, Manning BS, Miroux B *et al* (2000*b*) Disruption of the uncoupling protein-2 gene in mice reveals a role in immunity and reactive oxygen species production. *Nat Genet* 26:435–9

Aubert J, Champigny O, Saint-Marc P, Negrel R, Collins S, Ricquier D *et al* (1997) Up-regulation of UCP-2 gene expression by PPAR agonists in preadipose and adipose cells. *Biochem Biophys Res Com* 238:606–11

Awatsuji H, Furukawa Y, Hirota M, Furukawa S, Hayashi K (1995) Interferons suppress nerve growth factor synthesis as a result of interference with cell growth in astrocytes culture from neonatal mouse brain. *J Neurochem* 64:1476–82

Berger BD, Wise CD, Stein L (1973) Nerve growth factor: enhanced recovery of feeding after hypothalamic damage. *Science* 180:506–8

Berthiaume M, Sell H, Lalande J, Gelinas Y, Tchernof A, Richard D *et al* (2004) Actions of PPARγ agonism on adipose tissue remodeling, insulin sensitivity and lipemia in absence of glucocorticoids. *Am J Physiol* 287:R1116–23

Blasko I, Ranemayr G, Veerhuis R, Eikelenboom P, Grubeck-Loebenstein B (2001) Does IFNγ play a role in neurodegeneration? *J Neuroimmunol* 116:1–4

Candelario-Jalil E, Mhadu NH, Al-Dalain SM, Martinez G, Leon OS (2001) The time course of oxidative damage in different brain regions following transient cerebral brain ischemia in gerbils. *Neurosci Res* 41:233–41

Chen H, Luo J, Kintner DB, Shull GE, Sun D (2005) Na^+-dependent chloride transporter (NKCC1)-null mice exhibit less gray and white matter damage after focal cerebral ischemia. *J Cereb Blood Flow Metab* 25: 54–66

Cullingford TE, Bhakoo K, Peuchen S, Dolphin CT, Patel R, Clark JB (1998) Distribution of mRNAs encoding the peroxisome proliferators activated receptor α, β and γ and the retinoid X receptor α,β and γ in the rat central nervous system. *J Neurochem* 70:1366–75

Dalton DK, Pitts-Meek S, Keshav S, Figari IS, Bradely A, Stewart TA (1993) Multiple defects of immune cell function in mice with disrupted interferon-gamma genes. *Science* 259:1739–45

de Bilbao F, Arsenijevic D, Vallet P, Hjelle OP, Ottersen OP, Bouras C *et al* (2004) Resistance to cerebral ischemic injury in UCP2 knockout mice: evidence for a role of UCP2 as a regulator of mitochondrial glutathione levels. *J Neurochem* 89:1283–92

de Bilbao F, Guarin E, Nef P, Vallet P, Giannakopoulos P, Dubois-Dauphin M (2000) Cell death gene expression in the penumbra and thalamic fields after permanent occlusion of the middle cerebral artery in wild-type and Bcl-2 transgenic mice. *Eur J Neurosci* 12:921–34

Delerive P, De Bosscher K, Besnard S, Vanden Berghe W, Peters JM, Gonzalez FJ *et al* (1999) PPARα negatively regulates the vascular inflammatory gene response by negative cross-talk with transcription factors NF-κB and AP-1. *J Biol Chem* 274:32048–54

Delerive P, Fruchart JC, Staels B (2001) Peroxisome proliferator-activated receptors in inflammation control. *J Endocrinol* 169:453–9

Deplanque D, Gele P, Petrault O, Six I, Furman C, Bouly M *et al* (2003) Peroxisome proliferators activated receptor-α activation as a mechanism for preventive neuroprotection induced by fenofibrate treatment. *J Neurosci* 23:6264–71

Durum SK, Muegge K (1998) Preface pages vii–xvi. In: *Cytokine Knockouts* (Durum SK, Muegge K, eds), Totowa, NJ, USA: Humana Press

Evans RM, Barish GD, Wang YX (2004) PPARs and the complex journey to obesity. *Nat Med* 10:355–61

Franklin KBJ, Paxinos G (1997) *The Mouse Brain in Stereotaxic Coordinates*. San Diego, CA, USA: Academic Press Inc., 29–41

Gallmann E, Arsenijevic D, Spengler M, Williams G, Langhans W (2005) Effect of CCK-8 on insulin-induced hyperphagia and hypothalamic orexigenic neuropeptide expression in the rat. *Peptides* 26:437–45

Greene ME, Pitts J, McCarville MA, Wang XS, Newport JA, Edelstein C *et al* (2000) PPARgamma: observations in the hematopoietic system. *Prostaglandins Other Lipid Mediat* 62:45–73

Guegan C, Ceballos-Picot I, Chevallier E, Nicole A, Onteniente B, Sola B (1999) Reduction of ischemic damage in NGF-transgenic mice: correlation with enhancement of antioxidant enzyme activities. *Neurobiol Dis* 6:180–9

Guegan C, Ceballos-Picot I, Nicole A, Kato H, Onteniente B, Sola B (1998) Recruitment of several neuroprotective

pathways after permanent focal ischemia in mice. *Exp Neurol* 154:371–80
Hinton EC, Parkinson JA, Holland AJ, Arana FS, Roberts AC, Owen AM (2004) Neural contribution to motivational control of appetite in humans. *Eur J Neurosci* 20: 1411–8
Hornung D, Waite LL, Ricke EA, Bentzien F, Wallwiener D, Taylor RN (2004) Nuclear peroxisome proliferator-activated receptors alpha and gamma have opposing effects on monocyte chemotaxis in endometriosis. *J Clin Endocrinol Metab* 86:3108–14
Kaye WH, Frank GK, Bailer UF, Henry SE, Meltzer CC, Price JC, Mathis CA, Wagner A (2005) Seretonin alterations in anorexia and bulimia nervosa: new insights from imaging studies. *Physiol Behav* 85:73–81
Kersten S, Desverge B, Wahli W (2000) Role of PPARs in health and disease. *Nature* 405:421–4
Langhans W (2000) Anorexia of infection: current prospects. *Nutrition* 16:996–1005
Lee CH, Olson P, Evans RM (2003) Minireview: lipid metabolism, metabolic diseases and peroxisome proliferator activated receptors. *Endocrinology* 144:2201–7
Li AC, Binder CJ, Gutierrez A, Brown KK, Plotkin CR, Pattison JW *et al* (2004) Differential inhibition of macrophage foam-cell formation and artherosclerosis in mice by PPARα, β/δ and γ. *J Clin Invest* 114:1564–76
Li HL, Kostulas N, Huang YM, Xiao BG, van der Meide P, Kostulas V *et al* (2001) IL-17 and IFNγ mRNA expression is increased in the brain and systematically after permanent middle cerebral artery occlusion in the rat. *J Neuroimmunol* 116:5–14
Mizui T, Kinouchi H, Chan PH (1992) Depletion of brain glutathione by buthionine sulfoximine enhances cerebral ischemic injury in rats. *Am J Physiol* 262:H313–7
Modo M, Stroemer RP, Tang E, Veizovic T, Sowniski P, Hodges H (2000) Neurological sequelae and long-term behavioural assessment of rats with transient middle cerebral artery occlusion. *J Neurosci Methods* 194:99–109
Pasparakis M, Alexopoulou L, Epishopou V, Kollias G (1996) Immune and inflammatory responses in TNF alpha-deficient mice: a critical requirement for TNF alpha in the formation of primary B cell follicules, follicular dendritic cell networks and germinal centers and the maturation of the humoral immune response. *J Exp Med* 184:1397–411
Pratico D, Reiss P, Tang LX, Sung S, Rokach J, McIntosh TK (2002) Local and systemic increase in lipid peroxidation after moderate experimental traumatic brain injury. *J Neurochem* 80:894–8
Richard D, Rivest R, Huang Q, Bouillaud F, Sanchis D, Chanpigny O *et al* (1998) Distribution of the uncoupling protein 2 mRNA in the mouse brain. *J Comp Neurobiol* 397:549–60
Ricote M, Li AC, Willson T, Kelly CJ, Glass CK (1998) The peroxisome proliferators activated receptor γ is a negative regulator of macrophage activation. *Nature* 391:79–82
Rolls ET (2005) Taste, olfactory and food texture processing in the brain and the control of food intake. *Physiol Behav* 85:45–56
Samson WK, Taylor MM (2005) Knockout knockouts. *Trends Endocrinol Metab* 16:1–2
Scherbel U, Raghupathi R, Nakamura M, Saatman KE, Trojanowski JQ, Neugebauer E *et al* (1999) Differential acute and chronic responses of tumor necrosis factor deficient mice to experimental brain injury. *Proc Natl Acad Sci USA* 96:8721–6
Sell H, Berger JP, Samson P, Castriota G, Lalonde J, Deshaies Y *et al* (2004) Peroxisome proliferators activated receptor γ agonism increases the capacity for sympathetically mediated thermogenesis in lean and ob/ob mice. *Endocrinology* 145:3925–34
Semkova I, Krieglstein J (1999) Neuroprotection mediated via neurotrophic factors and induction of neurotrophic factors. *Brain Res Brain Res Rev* 30:176–88
Subang MC, Bisby MA, Richardson PM (1997) Delay of CNTF decrease following peripheral nerve injury in C57BL/Wld mice. *J Neurosci Res* 49:563–8
Suzuki H, Abe K, Tojo SJ, Kitagawa H, Mizugaki M, Itoy Y (1999) Reduction of ischemic brain injury by anti-P-selectin monoclonal antibody after permanent middle cerebral artery occlusion in rat. *Neurol Res* 21:269–76
Tan NS, Michalik L, Di-Poi N, Desvergne B, Wahli W (2004) Critical roles of the nuclear receptor PPARβ peroxisome proliferators activated receptor β in skin wound healing. *Biochem Soc Trans* 32:97–102
Tan NS, Michalik L, Noy N, Yasmin R, Pacot C, Helm M *et al* (2001) Critical roles for PPARβ/δ in keratinocyte response to inflammation. *Genes Dev* 15:3263–77
Verge VMK, Richardson PM, Wiesenfeld-Hallin Z, Hokfelt T (1995) Differential influence of nerve growth factor on neuropeptide expression *in vivo*: a novel role in peptide suppression in adult sensory neurons. *J Neurosci* 15:2081–96
Wang YX, Lee CH, Tiep S, Yu RT, Ham J, Kang H *et al* (2003) Peroxisome-proliferator-activated receptor γ activates fat metabolism to prevent obesity. *Cell* 113: 159–70
Welch JS, Ricote M, Akiyama TE, Gonzalez FJ, Glass CK (2003) PPARγ and PPARδ negatively regulate specific subsets of lipopolysaccharide and IFN-γ target genes in macrophages. *Proc Natl Acad Sci USA* 100:6712–7
Woods JW, Tanene M, Figueroa DJ, Biswas C, Zycband E, Moller DE *et al* (2003) Localisation of PPARδ in murine central nervous system: expression in oligodendrocytes and neurons. *Brain Res* 975:10–21
Yang T, Michele DE, Park J, Smart AM, Lin Z, Brosius III FC *et al* (1999) Expression of peroxisomal proliferator-activated receptors and retinoid X receptors in the kidney. *Am J Physiol* 277:F966–73
Yu XX, Barger JL, Boyer BB, Brand MD, Pan G, Adams SH (2000) Impact of endotoxin on UCP homolog mRNA abundance, thermoregulation and mitochondrial proton leak kinetics. *Am J Physiol* 279:E433–46

6.3. Article III: Results and discussion

6.3.1. *PPARβ mRNA is expressed after focal cerebral ischemia*

The data presented in this report clearly demonstrate that PPARβ mRNA was significantly enhanced in the ischemic hemispheres of WT mice compared with non-operated animals. Indeed, as assessed by semiquantitative RT-PCR, quantitative fluorescent real-time PCR determination and *in situ* hybridization, PPARβ mRNA was strongly induced as soon as one day post-ischemia and was still detected one week post-MCAO (Figures 1A and 1C). *PPARβ* transcript and protein were found in the cortical peri-infarct area (Figures 1C and 1D) suggesting a role of this protein in stroke-induced pathophysiological mechanisms. No labelling was observed in KO mice (Figure 1E). As previously reported (Cullingford *et al*., 1998), expression occurs mainly in neurons and oligodendrocytes.

6.3.2. *PPARβ KO mice have increased infarct size following permanent MCAO*

The major finding of this study is that *PPARβ* deletion exacerbates the deleterious consequences of focal cerebral ischemia as PPARβ KO mice had a two-fold increase in infarct size compared with WT mice four days post-ischemia ($P<0.001$) (Figure 2). This appears to be specific to PPARβ since, according to previous results (Deplanque *et al.*, 2003), PPARα deficiency did not induce any increase in susceptibility to cerebral ischemia when compared to their WT counterparts ($P>0.05$). Altogether, these findings suggest that, in normal conditions, the basal activity of PPARβ may be involved in endogenous neuroprotection against cerebral ischemia and that, consistent with the idea that PPARβ is the major isotype normally found in brain, PPARβ function could be central as its deletion could not be compensated. This hypothesis is in agreement with a recent study that suggests that PPARβ could be more central to suppress the progression of neurodegeneration in cerebral infarction than others PPAR subtypes (Iwashita *et al.*, 2007).

We provide some arguments about the molecular mechanisms that could account for the increase susceptibility to cerebral ischemia in KO mice. PPARβ deletion increases susceptibility to stroke in KO mice partly by increasing oxidative stress levels in the brains of these animals, because the MDA levels were higher in the brains of KO mice compared to WT (Table 2).

6.3.3. *Increased ischemic damage in PPARβ KO mice may be explained by changes in anti-oxidant functions*

As might be expected, no induction of UCP2 mRNA was observed in the ischemic hemispheres of KO mice (10% to 14%, $P>0.05$) (Figure 1B), indicating that a PPARβ-mediated increase in UCP2 may be an important physiological reaction to limit ischemic damage. In contrast, and in line with our previous results (see section 5.4.1.), UCP2 mRNA was increased ($P<0.001$) in the ischemic hemispheres of WT mice from day one to day 7 after MCAO (Figure 1B).
Considering the negative role of UCP2 in ROS production (see section 5.3.), the present lack of UCP2 mRNA induction in KO mice may at least partly explain the increased oxidative stress observed and could therefore participate in the increased infarct size. In addition, we provide here further evidence that *in vivo* 1) UCP2 expression may be under the control of the transcriptional factor PPARβ and 2) as discussed in section 5.4.5. (Article II), UCP2 expression in WT animals may be an endogenous neuroprotective response to protect neurons from oxidative stress induced by ischemia. However, beside UCP2, PPARβ may also induce expression of a number of other genes involved in oxidative stress, which could contribute to its potential therapeutic roles following stroke.

Accordingly, we provide here evidence that MnSOD induction was reduced in PPARβ KO mice after MCAO. One and four day post-MCAO, double staining experiments revealed that MnSOD was induced in neurons and astrocytes in the peri-infarct area of WT mice. Interestingly, PPARβ KO mice did not show any staining at the same time period (Figure 4). Importantly, treatment of KO mice with NGF one day after ischemia resulted in detection of MnSOD labelling four days after lesion (Figure 4) and was also associated with decreased infarct size in

PPARβ KO mice (P<0.05). Therefore, decreases in MnSOD anti-oxidant enzyme expression in the brains of KO mice might contribute to the increased deleterious consequences of ischemic stroke in these mice. The effect of PPARβ on MnSOD anti-oxidant enzyme expression could be related to a direct effect, because PPREs have been found in the gene of MnSOD (Doonan *et al.*, 2009).

Finally, although GSH levels were significantly decreased in the brains of both genotypes one and four days post-ischemia, this decrease was exacerbated in PPARβ KO mice compared to WT mice on D4 after ischemia (Table 2). Reduced GSH levels may therefore partly explain the increased oxidative injury and susceptibility to MCAO of PPARβ KO mice.

Our observations are consistent with reports indicating that PPARs may confer neuroprotection by enhancing anti-oxidative functions. In a recent study, Madrigal *et al.* (2007) showed that the neuroprotective effects of noradrenaline in primary cultures of rat cortical neurons exposed to inflammatory stimuli may involve activation of PPARβ and increases in GSH; this was partially blocked by co-treatment with an antagonist of PPARα/β. In addition, data on PPARα and PPARγ also showed that their activation could increase anti-oxidant systems. For example, PPARα and PPARγ induce expression of SOD (Inoue *et al*., 2001). A neuroprotective effect on oxidative stress-mediated neuronal damage has been recently evidenced with the use of a PPARγ agonist in epileptic rats (Yu *et al.*, 2008). The authors demonstrate that rosiglitazone, a PPARγ agonist, may offer protection *in vivo* by reducing GSH depletion and enhancing SOD activity.

6.3.4. *Increased ischemic damage in PPARβ KO mice may be also explained by altered cytokine levels*

TNFα was significantly induced in the brain of WT mice on day one after MCAO (P<0.001), and returned to basal levels on day four compared with non-operated WT mice (Figure 3A). In contrast, no induction of TNFα was observed in PPARβ KO mice on either day after MCAO when compared with non-operated animals (P>0.05) (Figure 3A). Similarly, whereas NGF levels were markedly increased

one and four days post-ischemia in WT mice (P<0.001) (Figure 3B), this up-regulation was completely ablated in PPARβ KO mice (Figure 3B). These results suggest that, in normal conditions, PPARβ expression may be needed for TNFα and NGF induction after ischemia. Although specific interactions between PPARβ, TNFα and NGF need further investigations, similar results have been obtained with other PPAR subtypes; PPAR*γ* natural ligands may increase the synthesis and release of NGF in mouse primary astrocytes, which have been proposed to contribute to neuroprotection (Toyomata *et al.*, 2004). Activation of PPARγ may inhibit inflammatory activation of cultured brain astrocytes and microglia induced by lipopolysaccharide through inhibition of the production of TNF*α* (Luna–Medina *et al.*, 2005). In addition, activation of PPARγ decreases the production of TNF*α* and IL1*β* in microglial cells while increasing the intracellular levels of GSH (Koppal *et al.*, 2000).

In contrast, the levels of the pro-inflammatory lymphocyte cytokine IFNγ were abnormaly elevated in the brain of PPARβ KO mice after MCAO. Indeed, beside the fact that IFNγ levels were significantly increased in the brains of both genotypes one day after ischemia (all comparisonsP<0.001) (Figure 3C), these return to basal levels four days after ischemia in WT only; at his time-point, IFNγ was still significantly increased in PPARβ KO mice compared with nonoperated animals (P<0.001) (Figure 3C). Interestingly, at each time-point studied IFNγ levels were significantly higher in KO than in WT mice (P<0.01) (Figure 3C). Altogether, these results suggest that PPARβ may inhibit the induction of this inflammatory cytokine and imply that PPARβ may participate in the regulation of lymphocyte cytokines as well as migration of inflammatory cells across the BBB to sites of inflammation (see section 3.7.3.). The exact interplay between these cytokines remains to be determined. In line with our results, much recent data suggest that the anti-inflammatory aspects of the PPARβ function may have an important role in inhibiting leukocyte recruitment and thus lesion progression in a murine model of atherogenesis, by down-regulating the expression of chemokines (Barish *et al.*, 2008) which mediate the recruitment of macrophages, neutrophils, and T lymphocytes. According to our findings, this effect of PPARβ is supposed to occur by the suppression of inflammatory responses elicited by cytokines such as

IL1β and IFNγ. Whether the up-regulation of IFNγ expression in PPARβ deleted-animals lead to up-regulation of chemokines in our model of ischemia can therefore be hypothesized.

6.3.5. *The oxidative status of PPARβ KO mice after MCAO may be mediated by altered cytokine levels*

Administration of IFNγ antibody 18 h before MCAO led to a significant reduction of MDA increase and GSH loss on day four after ischemia in both group of mice, suggesting that oxidative stress is mediated by IFNγ (Table 2). In these conditions, no more differences between genotypes were observed (Table 2) indicating that IFNγ alterations could have contributed to the increased vulnerability of PPARβ KO animals following ischemia.

In addition, we show that NGF treatment could reverse MnSOD expression in PPARβ KO (Figure 4). Therefore, reduced MnSOD expression in KO mice could rather be a consequence of altered NGF levels than a direct consequence of PPARβ deletion. This is in accordance with a previous finding showing a tight association between MnSOD activity and NGF levels in mice subjected to permanent MCAO (Guegan *et al.*, 1999). Nevertheless, further investigations are required to understand the relationships between NGF, MnSOD, and PPARβ.

6.4. Conclusion

Our data showing that PPARβ KO mice exhibited significantly greater infarct sizes than WT animals indicate that PPARβ agonists could be attractive therapeutic candidates for stroke. According to this view, our results have been validated by a recent study. Indeed, the neuroprotective role PPARβ in the brain was confirmed in a high-resolution MRI study for monitoring cerebral ischemic lesions (Pialat *et al.*, 2007). In line with our results, PPARβ KO mice subjected to a permanent MCAO showed significantly larger infarct size than control animals over a period of 14 days after injury. The effect was present from the very early time point (around 30 min after the injury) and was particularly marked during the first 72 h, suggesting a lesion-initiation effect. This early effect is in line with our result

showing an effect of PPARβ on anti-oxidant mechanisms known to be involved in the first few hours after cerebral ischemia (Brouns and De Deyn, 2009).

Because our data provide molecular targets through which PPARβ may promote anti-oxidative mechanisms and suppress ischemic inflammation, we concluded that a pharmacological modulation of PPARβ by PPARβ-selective drugs could constitute potential therapeutics to treat ischemia. This hypothesis was confirmed two years ago by a report of Iwashita *et al.* (2007). The authors showed that, *in vivo,* high-affinity PPARβ agonists protect against ischemic brain injury induced by transient MCAO in rats. In accordance with its cellular distributrion (Cullingford *et al*., 1998), the neuroprotective effect of the PPARβ agonists was more prominent in the cortex than in the striatum. Finally, based on *in vitro* cell death model, they indicate that the neuroprotective effects of the selective PPARβ agonists were closely correlated with caspase-3 inhibitory activity, suggesting that the agonists may possess potent anti-apoptotic properties.

7. Ischemic Tolerance and infection

Article IV: D. Arsenijevic, F. de Bilbao, P. Vallet, A. Hemphill, B. Gottstein, D. Richard, P. Giannakopoulos and W. Langhans (2007) Decreased infarct size after focal cerebral ischemia in mice chronically infected with Toxoplasma gondii. *Neuroscience* 150:537-546.

7.1. Inducers of ischemic tolerance

It is well known that pre-exposing the brain to a subthreshold level of pathologic/preconditioning stimulus markedly diminishes neuronal vulnerability to a subsequent ischemic insult, a phenomenon known as ischemic preconditioning or ischemic tolerance (Dirnagl *et al.*, 2003). A variety of potentially harmful stimuli such as transient global/focal ischemia, hypothermia and pro-inflammatory cytokines may be used to precondition the brain and induce neuroprotection. These stimuli trigger the cytokine inflammatory pathways, leading not only to inflammation but also to simultaneous up-regulation of feedback inhibitors of inflammation which may be governed by multiple mechanisms: neuronal stress proteins synthesis, protein kinase signaling, growth factors, and anti-oxidant defense enzymes overexpression (Kirino, 2002).

Among the potential inducers of ischemic tolerance are the infectious agents. However, results from the literature are conflicting. Evidences from clinical settings indicate that acute infections, mostly respiratory and of bacterial origin, may exacerbate ischemic damage during the early pro-inflammatory phase after infection (McColl *et al*., 2009). In addition, an animal study indicates that a systemic inflammation with intraperitoneal injection of lipopolysaccharide (LPS, a cell-wall component of gram-negative bacteria used as a model for infection) occurring in conjunction with a global ischemic insult may exacerbate neuronal damage in the rat hippocampus (Spencer *et al.*, 2007). This idea that infection may be a trigger for stroke and can worsen outcome seems to be inconsistent with the concept of tolerance. Actually, evidences from experimental settings have shown that preceding, sub-injurious exposure to LPS appears to confer protection against subsequent ischemia (Bordet *et al.,* 2000). This raises the

concept that preceding infection might, in some circumstances, be protective against subsequent ischemia. In fact, neuroprotective effect appears to depend on the timing or severity of the preceding infection (Bordet *et al.,* 2000). Considering these contrasting results, findings supporting that chronic infection may confer protection against subsequent ischemia warrant further investigations.

7.2. Molecular mechanisms of ischemic tolerance

The exact molecular mechanisms underlying ischemic tolerance are not well understood, but induction of inflammatory cytokines such as TNFα and IL1β have been demonstrated in most of the experimental models (for review see Dirnagl *et al.*, 2003). These inflammatory cytokines are believed to play a critical role in establishing tolerance because their inhibition eliminates protection (Cardenas *et al.,* 2002) and because administration of TNFα or IL1β alone can directly induce tolerance to cerebral ischemia. Pre-treatment with LPS, has been shown to induce tolerance following permanent and transient focal ischemia (Dawson *et al.*, 1999; Bordet *et al*., 2000). LPS-induced protection from ischemic brain damage was abolished when anti-inflammatory agents or protein synthesis inhibitors were co-administered with LPS (Bordet *et al.*, 2000), suggesting an absolute requirement for *de novo* protein synthesis and a critical role for inflammatory pathways in ischemic tolerance induced by LPS. Cytoprotection by LPS in the brain also involves an increase in activity of SOD (Bordet *et al*., 2000). Anyway, our knowledge on the underlying mechanism of ischemic tolerance is still fragmentary. Thus, a greater understanding of interactions between the immune and nervous systems is an area of growing interest; first because it constitutes a model to study endogenous neuroprotective mechanisms and, second, if tolerance induction can be manipulated and accelerated by a drug treatment that is safe and effective enough, it could greatly improve the treatment of stroke. Finally, as preconditioning may occur naturally in human brains after transient ischemic attacks and mild strokes (Wegener *et al*., 2004) and experimental tolerance paradigms that involve clinically approved drugs exist (for ref. see Dirnagl *et al.*, 2003), research focused on ischemic tolerance mechanisms are encouraged to target therapy against the consequences of brain ischemia. Also, this could open a window of opportunity to utilize these mechanisms as a

promising clinical strategy to the pharmacological brain preparation for situations when ischemia is anticipated (i.e. prior to procedures such as invasive brain surgery and in high-risk stroke patients).

Chronic murine toxoplasmosis may be of particular interest in the study of infection-related effects on brain ischemia since it is associated with a tissue-specific regulation of the oxidative state (Arsenijevic *et al*., 2001). In addition, pro-inflammatory cytokines such as TNFα and IFNγ (Arsenijevic *et al*., 1997, 2001), but also the anti-inflammatory cytokine IL10 (Arsenijevic *et al*., 1997, 1998) are induced rapidly after infection. The major aims of Article IV were to determine 1) how the brain may develop endogeneous neuroprotective mechanisms in response to chronic infection and 2) whether these mechanisms may influence the main biological phenomena associated with acute cerebral ischemia. To this end, we explored the impact of chronic *Toxoplasma gondii* infection on biological phenomena associated with permanent MCAO. We first investigated the effect of permanent MCAO on infarct size in chronically infected mice. The second goal of our research was to explore whether alterations of inflammatory and redox states in chronically infected mice may influence brain injury. Levels of main anti-oxidative molecules, as well as pro/anti-inflammatory cytokines, were therefore measured in infected and non-infected brains before and after ischemia.

Neuroscience 150 (2007) 537–546

DECREASED INFARCT SIZE AFTER FOCAL CEREBRAL ISCHEMIA IN MICE CHRONICALLY INFECTED WITH *TOXOPLASMA GONDII*

D. ARSENIJEVIC,[a1*] F. DE BILBAO,[b1] P. VALLET,[b] A. HEMPHILL,[c] B. GOTTSTEIN,[c] D. RICHARD,[d] P. GIANNAKOPOULOS[b] AND W. LANGHANS[e]

[a]*Department of Medicine, Division of Physiology, University of Fribourg, Chemin Du Musée 5, 1700 Fribourg, Switzerland*

[b]*Division of Geriatric Psychiatry, University Hospitals of Geneva, Belle-Idée, 1225 Geneva and Division of Old Age Psychiatry, University of Lausanne, 1008 Prilly, Switzerland*

[c]*Institute of Parasitology, University of Bern, 3012, Bern, Switzerland*

[d]*Institut Universitaire de Cardiologie et de Pneumologie, Hopital Laval, Quebec, Canada*

[e]*Institute of Animal Sciences, ETH Zurich, Schorenstrasse 16, Zurich 8603 Schwerzenbach, Switzerland*

Abstract—To determine whether *Toxoplasma gondii* infection could modify biological phenomena associated with brain ischemia, we investigated the effect of permanent middle cerebral artery occlusion (MCAO) on neuronal survival, inflammation and redox state in chronically infected mice. Infected animals showed a 40% to 50% decrease of infarct size compared with non-infected littermates 1, 4 and 14 days after MCAO. The resistance of infected mice may be associated with increased basal levels of anti-inflammatory cytokines and/or a marked reduction of the MCAO-related brain induction of two pro-inflammatory cytokines, tumor necrosis factor-alpha and interferon-gamma (IFNγ). In addition, potential anti-inflammatory/neuroprotective factors such as nerve growth factor, suppressor of cytokine signaling-3, superoxide dismutase activity, uncoupling protein-2 and glutathione (GSH) were upregulated in the brain of infected mice. Consistent with a role of GSH in central cytokine regulation, GSH depletion by diethyl maleate inhibited *Toxoplasma gondii* lesion resistance by increasing the proinflammatory cytokine IFNγ brain levels. Overall, these findings indicate that chronic toxoplasmosis decisively influences both the inflammatory molecular events and outcome of cerebral ischemia.

Key words: toxoplasmosis, cerebral ischemia, cytokines, redox factors, rodent.

One of the possible biological consequences of infection is a change of the redox status in both CNS and peripheral tissues (Arsenijevic et al., 2001). Although both animal models and clinical studies showed that infections promote neuronal death following cerebral ischemic injury (Sacco, 2001; Emsley and Tyrrell, 2002), activation of the immune system can also result in neuroprotection (Bordet et al., 2000). In fact, the effect of infection on ischemic damage may largely depend on the regulation of reactive oxygen species by pro-inflammatory and anti-inflammatory cytokines as well as by the main antioxidant state regulators, namely superoxide dismutase (SOD) (Guegan et al., 1998; Murakami et al., 1998), glutathione (GSH) (Nicholls and Budd, 2000; Schulz et al., 2000; Droge, 2002), uncoupling protein-2 (UCP2) (Arsenijevic et al., 2000b; Mattiasson et al., 2003) and nerve growth factor (NGF) (Brodie, 1996; Guegan et al., 1999; Villoslada et al., 2000). In addition, the newly described suppressor of cytokine signaling (SOCS) proteins are induced in peripheral and central models of inflammation (Lebel et al., 2000; Bates et al., 2001; Larsen and Ropke, 2002; Wang and Campbell, 2002; Huang et al., 2003; Park et al., 2003; Jo et al., 2005). SOCS possibly interact with cellular redox determinants (Park et al., 2003) and transgenic SOCS expression has been shown to inhibit inflammation and apoptosis following lipopolysaccharide (LPS) injection (Jo et al., 2005).

Chronic murine toxoplasmosis may be of particular interest in the study of infection-related effects on brain ischemia since it is associated with a tissue-specific regulation of the oxidative state (Arsenijevic et al., 2001) as well as activation of pro-inflammatory cytokines such as tumor necrosis factor-alpha (TNFα), interferon-gamma (IFNγ) and interleukin-2 (IL-2), but also anti-inflammatory cytokines such as interleukin-10 (IL-10) (Arsenijevic et al., 1997, 1998). Some of these cytokines are known to enhance neurodegeneration following ischemia (Arsenijevic et al., 2006). In order to determine how chronic infection influences the main biological phenomena associated with acute cerebral ischemia, the present study explores the impact of chronic *Toxoplasma gondii* infection on brain ischemic injury and inflammatory/antioxidant processes induced by permanent middle cerebral artery occlusion (MCAO).

EXPERIMENTAL PROCEDURES

All procedures were approved by the Veterinary Office of the Canton of Zurich Health Directorate and the Veterinary Office of Geneva in accordance with the Swiss Animal Care Guidelines. All efforts were made to minimize the number of animals used in this study and every effort was taken to reduce any suffering.

[1] Equal first authors.

*Corresponding author. Tel: +41-79-501-52-83; fax: +41-26-300-97-34.
E-mail address: denis.arsenijevic@unifr.ch (D. Arsenijevic).

Abbreviations: cDNA, complementary DNA; DEM, diethyl maleate; GAPDH, glyceraldehyde 3-phosphate dehydrogenase; GSH, glutathione; IFNγ, interferon-gamma; IL-2, interleukin-2; IL-10, interleukin-10; LPS, lipopolysaccharide; MCAO, middle cerebral artery occlusion; NGF, nerve growth factor; SOCS, suppressor of cytokine signaling; SOCS-3, suppressor of cytokine signaling-3; SOD, superoxide dismutase; TNFα, tumor necrosis factor-alpha; TUNEL, terminal deoxynucleotidyl transferase biotin-dUTP nick end labeling; UCP2, uncoupling protein-2.

0306-4522/07$30.00+0.00
doi:10.1016/j.neuroscience.2007.09.080

Mice and diets

Male Swiss Webster mice of 4 months of age from Charles River Laboratories (Wilmington, MA, USA) were used. Mice were chronically infected by i.p. injection of 10 cysts of *Toxoplasma gondii* (Me49 strain obtained from Dr A. Hemphill, University of Bern, Switzerland) (Arsenijevic et al., 1997). Less than 5% of mice died due to infection during weeks 2 and 3. After this time point all infected mice survived. Acute infection with *Toxoplasma gondii* results in anorexia and body weight loss (Arsenijevic et al., 1997). We followed infected mice body weight and food intake 7 days before infection and up to 28 days (chronic phase) after infection (n=10). In the chronic phase of infection, some of these mice may show a partial weight regain (50%) or no weight regain (50%) (Arsenijevic et al., 1997). For all experiments, we used only the latter type of mice since these animals had higher basal brain cytokine levels and were expected to maximally respond to a new inflammation (Arsenijevic et al., 1998). A group of non-infected mice (n=18) was chronically underfed to mimic the food intake level of infected mice from days 1–28. This group was used to determine: 1) if the reduced food intake of the infected mice may influence basal brain GSH levels (n=6); 2) the effect of underfeeding on brain GSH levels after MCAO (n=6) and 3) the effect of underfeeding on ischemic lesion size (n=6). All mice were individually weighed and food intake was measured daily. For the MCAO study, infected and non-infected mice with and without MCAO (n=18 mice per group) were monitored daily from 7 days prior to and up until 3 days after operation. Daily food intake (g/mouse/day) and body weight changes after MCAO were measured, and food intake changes after MCAO were calculated as a percentage of pre-ischemia average food intake for each mouse group.

Histology of infected brains compared with non-infected controls

Histological analysis was performed in infected (28 days following infection) (n=4) and non-infected control brains (n=4) prior to MCAO. Brain slices (20 μm) were stained with hematoxylin and eosin for histological identification of *Toxoplasma gondii* cysts and infiltrating immune cells (Frenkel and Escajadillo, 1987; Arsenijevic et al., 2007a). Detection of apoptosis in the brain of chronically infected mice was made using terminal deoxynucleotidyl transferase biotin-dUTP nick end labeling (TUNEL) labeling as previously described (de Bilbao et al., 2000). The suppressor of cytokine signaling-3 (SOCS-3) mRNA expression was determined by *in situ* hybridization in the brains of these mice (n=6 per group). Riboprobe preparation and *in situ* hybridization histochemistry were kindly performed by Dr S. Rivest (Laval University, Canada). The rat SOCS-3 complementary DNA (cDNA) fragment that was initially inserted in a pEF-FLAG-1 vector (provided by Dr. Doug Hilton, The Walter and Eliza Hall Institute of Medical Research, Melbourne, Australia) was extracted with *Xba*I and reinserted into a pCRII (Invitrogen, Carlsbad, CA, USA). The new construct was then linearized with *Xho*I. 35S-UTP was used to label the probe (for the complete *in situ* hybridization protocol conditions see reference by Lebel et al., 2000).

Induction of permanent focal cerebral ischemia and volume of the infarct

Mice were operated 28 days after infection, when their body weight and food intake had stabilized (Arsenijevic et al., 1998). We performed permanent MCAO in infected and non-infected control mice (n=6 for each group and post-MCAO time) as described in details elsewhere (de Bilbao et al., 2000). All mice survived and showed infarction after MCAO. One day, 4 days and 14 days later, the animals were perfused through the ascending aorta with a solution of paraformaldehyde 4% in phosphate-buffered saline (PBS, pH 7.35). Brains were removed and processed for paraffin embedding. Sections (7 μm) of the whole infarct area were cut on slides pretreated with 3-aminopropyltriethoxy-silane (Sigma, MO, USA), counterstained with Cresyl Violet for the histological identification of the nuclear boundaries and peri-infarct areas and mounted in Eukitt. For each animal, quantification of the infarcted area was performed on the Cresyl Violet–stained sections at five representative levels throughout the rostro-caudal extent of the lesion (A 0.26, −0.22, −0.40, −0.70 and −1.2–4 mm relative to Bregma) (Franklin and Paxinos, 1997). The rostro-caudal extent of the infarct was the same in both groups of mice. The infarcted area of each section was calculated by the subtraction of healthy tissue areas of the contralateral to the ipsilateral side of the section in order to compensate for the effect of brain edema (Guegan et al., 1998) using a computer-assisted image analyzing system (Software Morphometry, Samba 2005 TITN, Alcatel). Volumes of infarct (mm^3) were calculated for each animal after integration of areas with the distance between each level (de Bilbao et al., 2000).

To evaluate whether local alterations in cerebral vascular anatomy contribute to different susceptibility to injury in infected mice, an additional series of five non-infected and five infected mice were killed on day 1 after ischemia. Cerebral vasculature was studied in non-infected and infected mice (non-operated and on day 1 after ischemia) after intracardial perfusion of a mixture of an equal proportion of gelatinous water (5%) and China ink (Sennelier, France) warmed at 40 °C (1 ml). Brains were removed and immersed for 24 h in 4% paraformaldehyde at 4 °C (Chen et al., 2005). Cerebral vasculature was observed with a Zeiss stereo zoom microscope. The absence of cerebral blood flow in the infarct area was assessed visually and by transcranial measurements of cerebral blood flow that were made using laser Doppler flowmetry (Oxford Optronix Ltd., UK) just before and after MCAO. Animals were placed under a stereotactic head frame and then a fine needle probe (MNP110XP, 0.48 mm diameter) was lowered onto the temporal bone surface 0.5–1 mm dorsal to the opening giving access to the MCA and wetted with a small amount of physiological saline.

Physiological parameters

Physiological parameters including arterial blood pressure (Kent mouse tail blood pressure system RTBP2000, Kent Scientific Corporation, Torrington, USA), plasma glucose (using Roche Glucotrend Active, Rotkreuz, Switzerland) and hematocrit were measured daily (n=5 for each type of mice) before MCAO and on day 1 and day 4 after injury. During surgery, mice were placed on a warm mat and rectal temperature was measured. During the operation, all mice had a body temperature of 38 °C.

Northern blot for UCP2 mRNA

Infected and non-infected mice subjected or not to ischemia (1 day post-MCAO) (n=6 mice per group) were anesthetized i.p. with xylazine (20 mg/kg)/ketamine (100 mg/kg) in 0.9% NaCl (100 μl/10 g body weight). They were intracardially perfused without delay with ice-cold isotonic saline. At the end of the perfusion the whole brains were quickly dissected out and frozen. Total RNA was prepared as described before (Arsenijevic et al., 1997). Northern blot analyses were performed using the mouse UCP2 or glyceraldehyde 3-phosphate dehydrogenase (GAPDH) cDNA labeled with ^{32}P under standard conditions. A similar amount of total RNA (20 μg) was used in every lane.

Cytokines and NGF levels in brain

We measured TNFα, IFNγ, IL-10, IL-2 and NGF in the brain of infected and non-infected mice subjected or not to ischemia (1 day post-MCAO; n=6 mice per group). Brains were analyzed 1 day

after ischemia since it is well established that cytokines return to basal levels after this time point (Guegan et al., 1998). They were aseptically removed, immediately placed in dry ice and then put in CHAPS solution and homogenized (Arsenijevic et al., 2000a). The supernatant was collected and frozen at −20 °C. TNFα, IFNγ, IL-10, and IL-2 were measured by using immunoassay kits from Amersham (Switzerland) (Arsenijevic et al., 2006). An immunoassay kit was also used to determine NGF (Catalys, Switzerland) (Arsenijevic et al., 2006).

SOD activity

We investigated SOD activity using a biochemical assay (1 day post-MCAO; n=6 mice per group) (Ewing and Janero, 1995). Brains were homogenized in phosphate-buffered saline and frozen immediately in liquid nitrogen. Aliquots of brain supernatants were processed as previously described (Ewing and Janero, 1995). Brain supernatants were added (25 μl) to a 125 μl solution containing 50 mM phosphate buffer (pH 7.4, 0.1 mM EDTA, 50 μM NBT, 78 μM NADH). To start the reaction, 25 μl of 3.3 μM PMS phenazine methosulfate (Sigma) (final concentration) was added and the absorbance at 560 nm was measured continuously using a microplate reader (DynaTech MR5000). The readings were every minute for 10 min. The first 5 min were used to determine the rate of superoxide production by the samples.

GSH levels

Tissues were collected from infected (1, 3, 7, 14 and 28 days post-infection) and non-infected control mice (n=6 mice per group). The consequences of MCAO for brain GSH levels were also determined in both types of mice 1 day post-ischemia (n=6 for each group). Tissues were homogenized in phosphate buffer (50 mM, pH 7.4). Total GSH levels were measured using a method based on the formation of a chromophoric product resulting from the reaction of 5,5′-dithiobis-(2-nitrobenzoic acid) (DTNB, Sigma) and GSH (Sigma) (de Bilbao et al., 2004). The absorbance was immediately measured at 412 nm. GSH contents were calculated by using a calibration curve established with standard samples.

To test whether elevated brain GSH levels in infected mice 1) were involved in the lack of cytokine induction 1 day after MCAO and 2) may influence lesion size response after ischemia, GSH was depleted by a s.c. injection of diethyl maleate (DEM) (24 μl/ 30 g body weight and was made up to 300 μl with saline) (Pileblad and Magnusson, 1990). To determine if DEM depleted brain GSH, non-infected (n=3) and infected mice (n=3) were treated with DEM and killed 2 h later and GSH in brain was measured as described above. To determine whether GSH depletion may alter TNFα and IFNγ levels 1 day after MCAO, infected (n=4) and non-infected mice (n=4) were treated with DEM, underwent MCAO 2 h later and were killed 1 day post-ischemia. Estimates of brain cytokine levels were obtained as described above. For all experiments, mice treated with saline were used as controls for the DEM groups.

Brains of 28-day infected mice (see Histology section) were stained for GSH with the fluorescent histochemical dye phthaldialdehyde (10 mM) and then processed for microglia immunohistochemistry using the anti-Iba-1 antibody (1 mg/ml, from Dr. Y. Imai, National Center of Neurology and Psychiatry, Japan) which was detected by the fluorescent goat-anti-rabbit immunoglobulin Alexa Fluor 568 (Molecular Probes) (de Bilbao et al., 2004). Since we have previously shown that chronic toxoplasmosis results in an increased brain expression of UCP2 mRNA which is specific for microglia associated with inflammatory loci (Arsenijevic et al., 2007), we also explored whether there was an association between GSH and UCP2 in this cell type. Mounted brain sections were immunostained for GSH using rabbit polyclonal anti-GSH (1/10 dilution provided by Prof. Ottersen, University of Oslo, Norway) which was revealed by ABC kit peroxidase and subsequently processed for *in situ* hybridization using a rat UCP2 probe (de Bilbao et al., 2004).

Table 1. Physiological parameters before and after MCAO in non-infected and infected mice

Group and treatment	1 Day before MCAO	D1 after MCAO	D4 after MCAO
Hematocrit (%)			
Non-infected	42±4	44±5	45±5
Infected	48±4	50±4	51±4
Plasma glucose (mmol/L)			
Non-infected	8.2±0.2	7.9±0.3	8.1±5
Infected	7.7±0.3	7.6±0.2	7.8±4
Arterial pressure (mm Hg)			
Non-infected	94±8	96±8	95±5
Infected	105±12	98±9	101±6

Data are means±S.E.M. of 5 animals per group. See text for details.

Data analyses

All data are presented as means±S.E. Statistical analyses were performed using Kruskal-Wallis non-parametric test. P values of less than 0.05 were considered significant.

RESULTS

Physiological parameters before and after MCAO

Arterial pressure, plasma glucose and hematocrit levels before and after MCAO on day 1 and day 4 were not significantly different between non-infected and infected mice at a given time point as shown in Table 1. After MCAO, both non-infected and infected mice showed an absence of cerebral blood flow in the infarct area.

Brain histology and SOCS-3 mRNA induction in infected mice

Unlike non-infected mice, the brains of the infected mice showed many randomly located inflammatory loci (including neutrophils, macrophages/monocytes and lymphocytes) 28 days after infection. These loci were not colocalized with intact *Toxoplasma gondii* cysts (Fig. 1A, B) and also occurred around blood vessels, but not within the vessels' walls (Fig. 1C). There was no evidence of neuronal apoptosis as determined by TUNEL labeling in these mice (data not shown). *In situ* hybridization showed SOCS-3 basal expression mainly in the hypothalamic region (Fig. 1D) (Lebel et al., 2000). Following infection, SOCS-3 mRNA labeling was randomly induced throughout the cerebral cortex as well as in areas associated with brain immune cell infiltration and blood vessels (Fig. 1D). This expression was associated with neurons, microglia and infiltrating phagocytes as previously described (data not shown) (Lebel et al., 2000).

Ischemic brain injury is reduced in *Toxoplasma gondii* infected mice

One day, 4 days and 14 days after MCAO, infarct volume was decreased by 42%, 50% and 48% respectively in

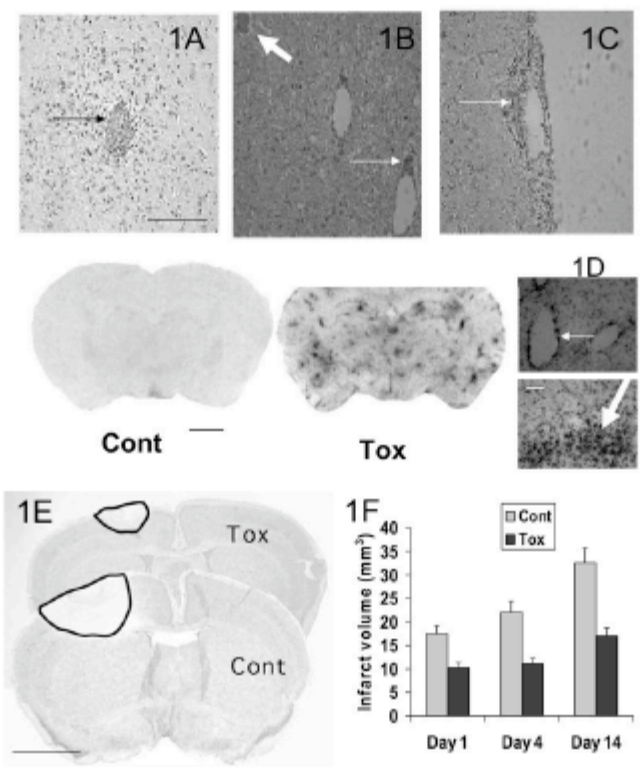

Fig. 1. Brain histology, *in situ* hybridization for SOCS-3 mRNA expression and brain infarct size in *Toxoplasma gondii* infected mice. (A–C) Coronal cross-sections of a *Toxoplasma gondii*–infected (for 28 days) mouse brain stained with hematoxylin and eosin (scale bar=15 μm). Note that infection resulted in inflammatory foci found in brain tissue (A) (thin black arrow) and in association with blood vessels (B, C) (thin black arrows). Note also that the presence of *Toxoplasma* cysts was not associated with inflammatory foci (B, thick arrow). (D) Representative *in situ* hybridization for SOCS-3 mRNA in non-infected control (Cont) and infected mice (Tox) brains (scale bar=120 μm). SOCS-3 mRNA basal expression was found in particular in hypothalamic region. Twenty-eight days following infection, SOCS-3 mRNA expression was randomly located and induced throughout the brain of infected mice in particular in the cortical area (Tox) (n=4 for each group). The right column shows a higher magnification of selected areas specific for SOCS-3 mRNA expression in infected brains. SOCS-3 mRNA was associated with microglia/infiltrated immune cells (thick arrow) and blood vessels (thin arrow). Cells are visualized with Thionin staining and SOCS-3 silver grains are black (scale bars=15 μm). (E, F) Effect of *Toxoplasma gondii* infection on infarct size. (E) Representative coronal sections showing ischemic lesion size 4 days after MCAO in control (Cont MCAO) and chronically infected mice (Tox MCAO). Sections were stained with Cresyl Violet. The surrounded areas denote the size of the ischemic area (scale bars=120 μm). (F) Infarct brain volumes were reduced in infected mice (Tox) at 1, 4 and 14 days after MCAO compared with non-infected mice (Cont).

Toxoplasma gondii infected mice when compared with non-infected control mice (P<0.01) (Fig. 1E, F), suggesting that chronic infection with *Toxoplasma gondii* may protect neocortical areas from ischemic damage.

Transient hyperphagia occurs early in *Toxoplasma gondii*–infected mice in response to MCAO

On the day of lesion, MCAO resulted in a significant reduction of food intake in both infected and non-infected control mice when compared with their pre-MCAO basal food intakes (−26±0.5% and −39±0.7% respectively, n=18, P<0.01). The day after ischemia, both non-infected and infected mice started to regain appetite. From this time point, infected mice increased food intake more rapidly than the non-infected group (−3±0.2% and −28±2%, respectively, n=18, P<0.01). Infected mice showed significantly enhanced hyperphagia on days 2 and 3 postischemia compared with their non-operated controls (28±1.2% and 1±0.2% respectively, n=18, P<0.01). Body weight loss induced by ischemia followed a similar temporal pattern to that of food intake indicating that *Toxoplasma gondii*–infected mice had attenuated negative energy balance in response to MCAO.

Brain specific alterations in GSH levels due to infection

There was a 45% decrease in brain GSH levels on day 7 postinfection when compared with non-infected control

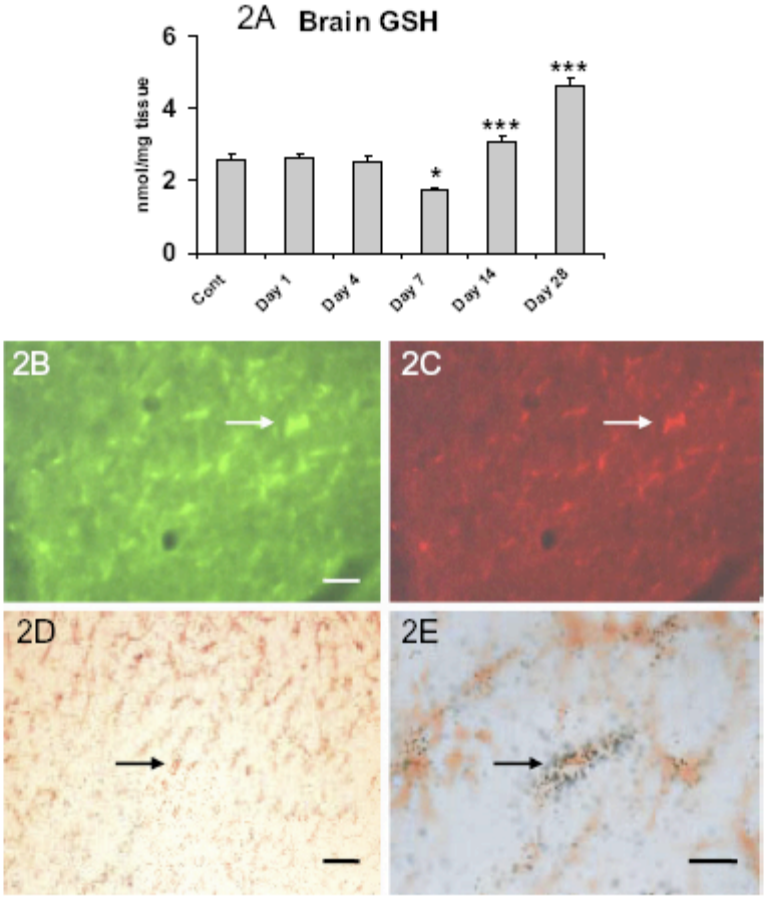

Fig. 2. Changes in brain GSH levels from day 1 to day 28 following murine *Toxoplasma gondii* infection. (A) Toxoplasmosis resulted in a slight reduction in brain GSH levels on day 7. From day 14 to day 28 after infection, GSH was significantly increased in the brain of infected mice compared with non-infected control mice (Cont). Values (nmol/mg tissue) are presented as mean±S.E. (* $P<0.05$, *** $P<0.001$, comparison to saline control). Each group represents six mice. (B) GSH (fluorescent staining, white arrow) is specifically increased in microglia in infected mice (red, white arrow) (C). Only microglia cells that have increased UCP2 mRNA (E, black arrow) show an increase in GSH (immunohistochemical detection, orange, black arrow) (D). Scale bars=15 μm (B, C, D); 7.5 μm (E). For interpretation of the references to color in this figure legend, the reader is referred to the Web version of this article.

mice ($P<0.05$). On day 14, as mice started to regain appetite, there was a progressive increase in brain GSH levels in infected mice ($P<0.001$) up to 28 days after infection ($P<0.001$) (Fig. 2A). The increase in GSH in the brains of 28-day infected mice was associated with a specific increase in microglia (Fig. 2B, C); only microglia with elevated UCP2 mRNA levels showed GSH labeling (Fig. 2D, E). In non-infected control mice, MCAO resulted in a 80% decrease of brain GSH levels (from 0.52± 0.02 nmol/mg tissue to 2.60±0.18 nmol/mg tissue) ($P<0.001$) (Fig. 3A). Interestingly, this decrease due to ischemia was only 11% in infected animals (from 4.60± 0.80–4.11±0.31 nmol/mg tissue) ($P<0.01$). In addition, GSH brain content in infected animals having undergone MCAO was significantly higher compared with non-infected MCAO animals ($P<0.001$) (Fig. 3A). Chronically underfed non-infected mice did not show altered brain GSH levels compared with non-infected controls (2.47± 0.19 versus 2.60±0.07 nmol/mg tissue) (Fig. 3A) suggesting that anorexia does not explain the increased brain GSH levels in infected mice. Although 1 day after ischemia, GSH levels were reduced in the chronically underfed non-infected mice, this decrease was significantly less pronounced compared with the non-infected control group ($P<0.01$) (Fig. 3A). This was associated with a reduced infarct size in the chronically underfed group compared with the non-infected control group (15.0±0.9 mm^3 and 19.3±1.1 mm^3, respectively, $n=6$ mice, $P<0.05$). Al-

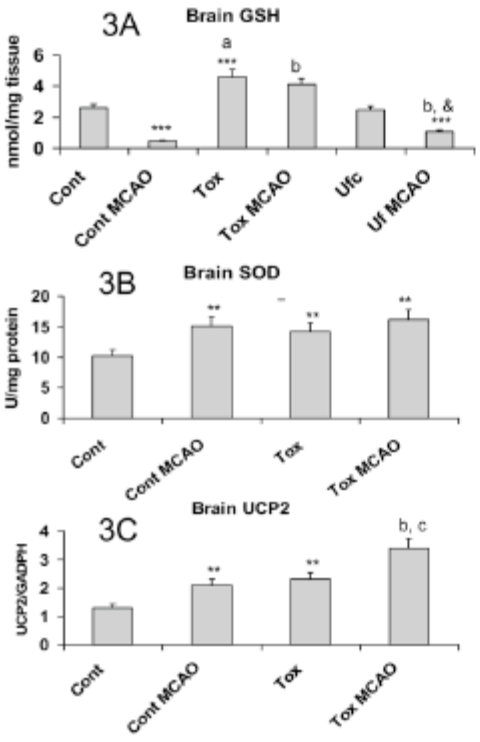

Fig. 3. Brain GSH, brain SOD activity and brain UCP2 mRNA expression. (A) One day after MCAO, we observed a reduction in brain GSH levels in non-infected mice (Cont MCAO) compared with their non-operated controls (Cont). After MCAO, brain levels of GSH in infected mice were markedly elevated compared with non-infected animals (Cont MCAO). Underfeeding (Ufc) results in no change in brain GSH levels compared with control mice (Cont). One day after MCAO, GSH level in underfed mice (Ufc MCAO) was reduced, however this reduction was less than that found in Cont MCAO mice. (B) Brain SOD activity was increased during chronic infection (Tox) when compared with non-infected animals (Cont). One day post-MCAO, SOD activities were similarly increased in both groups compared with non-infected controls (Cont). (C) Brain UCP2 mRNA expression was increased following infection (Tox) compared with non-infected controls (Cont). MCAO increased brain UCP2 mRNA levels in both infected and non-infected mice, but levels were higher in the former group. Values are presented as mean±S.E. for the various groups. Each group represents six mice. * Indicates the statistical comparison with non-infected controls (Cont), ª Indicates the statistical comparison between Tox and Ufc mice, ᵇ Indicates the statistical comparison between Tox MCAO and Cont MCAO mice, ᶜ Indicates the statistical comparison between Tox and Tox MCAO mice, & Indicates comparison between Cont MCAO and Ufc MCAO (* $P<0.05$, *** $P<0.001$, ** $P<0.01$, *** $P<0.001$, ª $P<0.001$, ᵇ $P<0.001$, ᶜ $P<0.05$, & $P<0.01$).

though a contributing effect cannot be excluded, the underfeeding effect on reduced lesion size could not totally explain the much greater reduction of infarct size observed in the infected mice (10.2±0.4 mm^3) (Fig. 1F) ($P<0.05$).

Infection increases brain SOD activity

SOD activity (Fig. 3B) was higher in the brains of infected mice (14.2±1.2 units/mg protein) compared with non-infected mice (10.2±0.8 units/mg protein) ($P<0.01$). This difference did not persist 1 day after MCAO (Fig. 3B) as SOD activities were similarly increased in both groups (17.2±1.5 and 15.1±1.1 units/mg protein respectively).

Upregulation of brain UCP2 mRNA levels in infected mice after ischemia

Toxoplasmosis resulted in a 76% increase in brain UCP2/GAPDH mRNA ratio compared with non-infected mice (2.3±0.2 versus 1.3±0.1) ($P<0.01$) (Fig. 3C). One day post-MCAO, there was a 62% increase in UCP2/GADPH mRNA ratio in infected mice compared with MCAO non-infected mice (3.4±0.2 versus 2.1±0.2) ($P<0.001$) (Fig. 3C).

Infection does not result in enhanced cytokine levels after MCAO

Basal levels of proinflammatory cytokines (TNFα, IL-2, IFNγ) were increased in *Toxoplasma gondii* infected mice on day 28 postinfection compared with non-infected controls ($P<0.001$) (Table 2). One day post-MCAO, infected mice had higher TNFα, IL-2 and IFNγ levels compared with MCAO non-infected animals ($P<0.001$). However, these higher levels did not significantly differ from those observed in infected mice not subjected to ischemia. This sharply contrasts with the results obtained in non-infected mice which showed a marked induction of cytokine levels 1 day post-MCAO compared with non-operated animals. Infected mice also had significantly higher brain levels of IL-10 and NGF compared with non-infected control mice ($P<0.001$) (Table 2). NGF and IL-10 significantly increased in non-infected mice that underwent MCAO ($P<0.001$); this induction was not observed in infected mice suggesting an attenuated immune response in the brains of infected mice (Table 2). Following MCAO, NGF levels in infected animals were doubled compared with non-infected controls ($P<0.001$). This was not the case for IL-10 suggesting that NGF may be a more important anti-inflammatory agent in infected mice.

Table 2. Basal and one day post-MCAO levels of brain TNFα, IFNγ, IL-2, IL-10 and NGF in non-infected and infected mice

	Cont	Cont MCAO	Tox	Tox MCAO
TNFα pg/ml	100±4	800±12***	993±51***	1093±50ª
IFNγ pg/ml	25±2	175±4***	330±8***	358±9ª
IL-2 pg/ml	44±2	750±23***	1622±64***	1804±61ª
IL-10 pg/ml	24±2	492±38***	504±40***	560±19
NGF pg/ml	40±3	300±12***	600±22***	624±20ª

Values (pg/ml tissue) are presented as mean±S.E.
* Indicates statistical comparison with non-infected animals (Cont) (*** $P<0.001$). Each group included six mice. See text for details.
ª Indicates statistical comparison between Tox MCAO and Cont MCAO mice (ª $P<0.001$). Each group included six mice. See text for details.

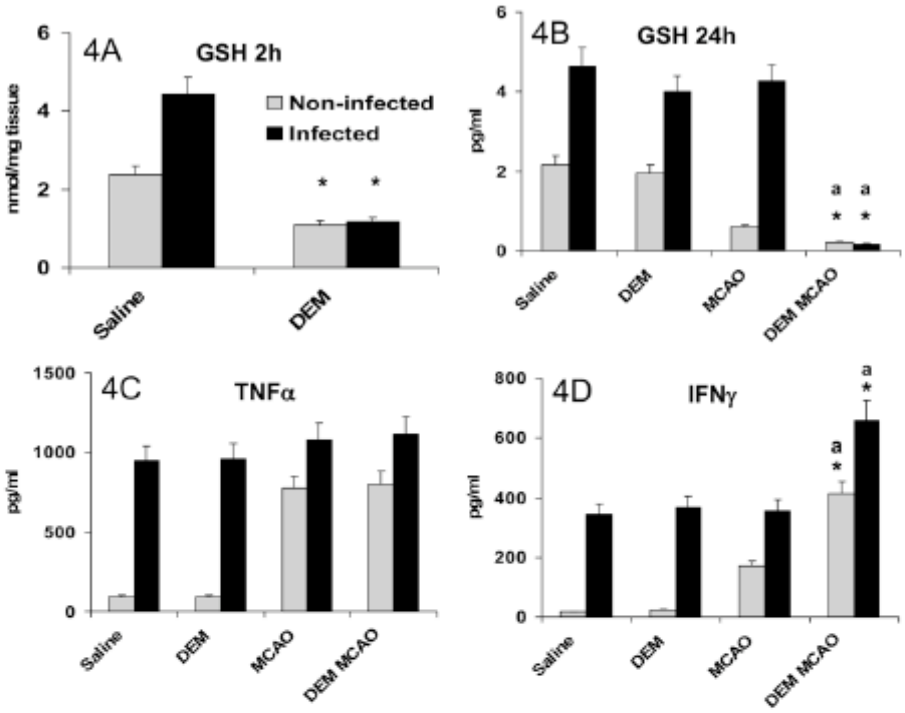

Fig. 4. GSH, TNFα and IFNγ were measured in non-infected and infected mice after ischemia; 2 h prior to MCAO, mice were treated with DEM (or saline). (A) DEM significantly reduced brain GSH in non-infected and infected mice 2 h after treatment. (B) Twenty-four hours after ischemia, DEM significantly reduced brain GSH levels in infected and non-infected mice. Note that, consistent with the known transitory effect of DEM on GSH levels (Gupta et al., 2000), GSH returned to basal levels 24 h after DEM treatment in the absence of ischemic damage in both infected and non-infected mice. (C, D) DEM did not significantly alter brain TNFα (C) but significantly increased brain IFNγ levels (D) 24 h after ischemia. Data are means±S.E. of three to five animals per group. * $P<0.001$, comparison with saline controls; ª $P<0.001$, comparison with MCAO controls.

Depletion of brain GSH by DEM reversed neuroprotection by increasing lesion size and central IFN-γ levels after MCAO in infected mice.

Brain GSH levels in both non-infected and infected mice were markedly decreased 2 h after an s.c. injection of DEM as seen in Fig. 4A. One day after ischemia (Fig. 4B), brain GSH levels were further reduced by DEM when compared with non-treated MCAO groups. This reduction was associated with an increased lesion size in infected mice when compared with infected mice not treated with DEM (22.2±1.7 mm^3 versus 12.8±0.5 mm^3, $n=6$ per group, $P<0.01$). Non-infected mice also showed an increase in lesion size when treated with DEM (15.8± 1.5 mm^3 for saline versus 20.3±1.0 mm^3 for DEM, $n=6$ per group, $P<0.05$). After ischemia, DEM treatment resulted in induction of central IFNγ levels but not TNFα in both types of mice (Fig. 4C, D). Note that, consistent with the known transitory effect of DEM on GSH levels (Gupta et al., 2000), GSH returned to basal levels 24 h after DEM treatment in the absence of ischemic damage in both infected and non-infected mice (Fig. 4C, D).

DISCUSSION

This study revealed a marked resistance of *Toxoplasma gondii*–infected mice to acute cerebral ischemia characterized by a marked decrease of infarct size one, and 4 but also 14 days post-MCAO. The reverse effect of DEM on brain infarct size implies that GSH up-regulation may play a pivotal role in the observed ischemic resistance. Our results make it also possible to propose additional biological mechanisms surrounding this phenomenon, such as marked differences in pre- and/or post-ischemic cytokine status as well as pre- and/or post-ischemic GSH, SOCS-3 mRNA and UCP2 mRNA levels in infected compared with non-infected mice.

Following the acute phase of toxoplasmosis, the initially produced pro-inflammatory cytokines will subsequently induce a counter-regulatory anti-inflammatory response (Arsenijevic et al., 1997). During the chronic phase of infection, apart from the role that the adaptive specific immune systems (CD4, CD8 T cell activation) could play, the consequence of a second inflammation caused by

cerebral ischemia may be determined by the balance between these two antagonistic systems. The basal up-regulation of antioxidant molecules such as GSH, SOD, UCP2, SOCS-3 mRNA and anti-inflammatory cytokines NGF and IL-10 may represent the two first lines of defense against ischemic damage in infected mice. One could postulate that the observed changes in redox status may be a simple epiphenomenon of the underfeeding observed in the chronically infected mice. In fact, it has been shown that underfeeding may result in protection from cerebral injury by modifying redox status (Yu and Mattson, 1999). Our findings show that both the steady increase of brain GSH levels by day 7 to day 28 post-infection as well as the brain resistance to ischemia are specific to *Toxoplasma gondii* infection and did not depend on energy intake. Actually, although we did find that post-ischemic GSH was partially dependent on energy intake, this component represented only 13% of the post-ischemic GSH levels of infected mice. We also show that energy intake does influence lesion size, but alone cannot account for the degree of resistance observed in infected animals. A possible causal relationship between redox status and cytokine production has been previously suggested in that increased basal GSH levels and SOD activity may result from high NGF levels (Guegan et al., 1998, 1999; de Bilbao et al., 2004; Arsenijevic et al., 2006). Consistent with their possible role in neuroprotection (Guegan et al., 1999; Mattlasson et al., 2003), the differences in GSH, UCP2 mRNA and NGF levels persisted between infected and non-infected mice after MCAO. In the absence of a specific antibody for brain UCP2, it was not possible to assess the impact of UCP2 mRNA changes on protein levels. However, previous data using UCP2 transgenic and UCP2 KO mice have shown that UCP2 plays a central role in brain neuroprotection following ischemia (Mattlasson et al., 2003; de Bilbao et al., 2004).

An additional molecular mechanism involved in this context may involve the absence of pro-inflammatory cytokine induction observed in infected mice after ischemia. This phenomenon could be partly due to the already elevated basal levels of these cytokines in the brains of these mice (i.e. counter-regulatory mechanisms). Although one could argue that this finding might reflect the presence of a threshold in cytokine levels reached in *Toxoplasma*-infected mice, this is an unlikely scenario since we have previously demonstrated that an i.p. injection of LPS led to a marked upregulation of pro-inflammatory cytokines in these mice (Arsenijevic et al., 1998). Importantly, infected mice showed feeding behavior concordant with the relative stunting of brain cytokine response after ischemia. In fact, transient hyperphagia started earlier in infected mice compared with non-infected mice after MCAO. This is consistent with the attenuated post-ischemic induction of anorectic cytokines (TNFα, IFNγ) in the brain.

In agreement with previous contributions, our data suggest that both SOCS-3 and GSH are plausible candidate molecules for the regulation of secondary inflammatory response and cytokine production in *Toxoplasma gondii*–infected mice (Bjorkbaek et al., 1999; Auerhammer and Melmed, 2001; Park et al., 2003). The absence of pro-inflammatory cytokine induction could be partly due to the parallel elevation of the SOCS-3 mRNA after infection. The SOCS-3 is a potent inhibitor of cytokine signaling and its transgenic over-expression may inhibit inflammation and associated apoptosis *in vivo* (Auerhammer and Melmed, 2001; Jo et al., 2005). Accordingly, although infected mice had elevated basal pro-inflammatory cytokine levels (i.e. TNFα, IFNγ and IL-2) (Elzenberg et al., 1995; Bate et al., 2006; Lee et al., 2006; Yu et al., 2006), there was no evidence of neuronal apoptosis in their brain tissue. A key role for GSH is suggested by the fact that the decreased infarct size in MCAO mice chronically infected is no longer observed when brain GSH levels have been depleted by DEM treatment. This phenomenon was specifically associated with the central up-regulation of pro-inflammatory IFNγ but not TNFα in response to MCAO. Previous studies have also shown that DEM may not have a marked effect on TNF induction in response to an inflammatory response (Kang et al., 1999; Wang et al., 1999). Further work is needed to get a better understanding of the complex interactions of molecules regulating the inflammatory response in this context. As recently proposed, the observed elevated basal SOCS-3 and GSH levels could act synergistically as GSH can interact in SOCS-3 pathways to inhibit cytokines (Ciesowski et al., 2002).

Besides its direct effect against oxidative stress, GSH may also act via the suppression of glia-mediated inflammation (Wang et al., 2006). In the same line with this idea, our contributions have shown that both UCP2 and SOCS-3 mRNA levels in brains infected with *Toxoplasma gondii* were elevated in microglia (Arsenijevic et al., 2007a). Although we cannot exclude a possible participation of infiltrated leukocytes, our evidence suggests that GSH, UCP2 and SOCS-3 may attenuate ischemic injury in infected mice by modifying microglia activity.

Despite a widely disseminated idea, only rare studies have shown that pre-existing infections can enhance brain pathology in response to a subsequent new inflammatory process (Arsenijevic et al., 1998). In contrast, several studies have shown that chronic infection can attenuate some peripheral and central pathological processes: complete Freund's adjuvant prevents the onset of experimental allergic encephalomyelitis (Bach, 2001), schistosomiasis can protect against asthma (Yang et al., 2007), coxsackievirus B3 can inhibit cardiomyopathy (Huber et al., 2006) and various infections can attenuate murine models of multiple sclerosis (Sewell et al., 2002). In some conditions, a pre-existing inflammation can induce brain neurodegeneration. This is the case for the acute peripheral and/or central injection of LPS (Nguyen et al., 2004; Cunningham et al., 2005; McColl et al., 2007; Qin et al., 2007; Spencer et al., 2007). However, it appears that the LPS dose used in these models may be a determinant in the observed degeneration. In fact, although high LPS doses may increase cytokines and oxidative stress, low doses of peripheral LPS have a neuroprotective effect (Bordet et al., 2000). This is consistent with our recent study in which we observed an increase in brain NGF and

GSH levels 3 days after peripheral LPS treatment (Arsenijevic et al., 2007b; Hernadfalvi et al., 2007). In this context, the present study provides a new model to explore the effect of a pre-existing chronic inflammatory status on the outcome of brain ischemic insult. Since each bacterium or parasite produces different cytokine and leukocyte activation profiles and, ultimately, patterns of neurodegeneration, it is crucial to investigate the molecular mechanisms surrounding the beneficial or deleterious effect of various models of chronic inflammation on cerebral ischemia.

CONCLUSION

This study revealed a marked resistance of *Toxoplasma gondii*–infected mice to acute cerebral ischemia that is characterized by a decreased lesion size 1 day, 4 days and 14 days post-MCAO. Marked differences in pre- and/or post-ischemic cytokines and antioxidant molecules could explain this phenomenon. In addition, our findings imply that GSH may play a pivotal role in these processes since pharmacological depletion of GSH resulted in increased lesion size and increased brain IFN-γ levels. Functional neurological data could be useful to confirm further the protective effect of *Toxoplasma gondii* infection on the outcome of cerebral ischemia.

REFERENCES

Arsenijevic D, Clavel S, Sanchis D, Plamondon J, Huang Q, Ricquier D, Rouger L, Richard D (2007a) Induction of Ucp2 expression in brain phagocytes and neurons following murine toxoplasmosis: An essential role of IFN-γ and an association with negative energy balance. J Neuroimmunol 186:121–132.

Arsenijevic D, Hernadfalvi N, von Meyenburg C, Ontenlente B, Richard D, Langhans W (2007b) Role of nerve growth factor in the in vivo regulation of glutathione in response to LPS in mice. Eur Cytokine Netw 18:93–101.

Arsenijevic D, de Bilbao F, Giannakopoulos P, Girardier L, Samec S, Richard D (2001) A role for interferon-γ in the hypermetabolic response to murine toxoplasmosis. Eur Cytokine Netw 12: 518–527.

Arsenijevic D, de Bilbao F, Plamondon J, Paradis E, Vallet P, Richard D, Langhans W, Giannakopoulos P (2006) Increased infarct size and lack of hyperphagic response after focal cerebral ischemia in peroxisome proliferator-activated receptor β-deficient mice. J Cereb Blood Flow Metab 26:433–445.

Arsenijevic D, Garcia I, Vesin C, Vesin D, Arsenijevic Y, Seydoux J, Girardier L, Ryffel B, Dulloo AG, Richard D (2000a) Differential roles of tumor necrosis factor-α and interferon-γ in mouse hypermetabolic and anorectic responses induced by LPS. Eur Cytokine Netw 11:662–668.

Arsenijevic D, Onuma H, Pecqueur C, Raimbault C, Manning BS, Miroux B, Couplan E, Alves-Guerra MC, Goubern M, Surwitt R, Bouillaud F, Richard D, Collins S, Ricquier D (2000b) Disruption of the uncoupling protein-2 gene in mice reveals a role in immunity and reactive oxygen species production. Nat Genet 26:435–439.

Arsenijevic D, Girardier L, Seydoux J, Chang HR, Dulloo AG (1997) Altered energy balance and cytokine gene expression in a murine model of chronic infection with Toxoplasma gondii. Am J Physiol 272:E908–E917.

Arsenijevic D, Girardier L, Seydoux J, Pechere JC, Garcia I, Lucas R, Chang HR, Dulloo AG (1998) Metabolic cytokine responses to a secondary immunological challenge with LPS in mice with T. gondii infection. Am J Physiol 274:E439–E445.

Auerhammer CJ, Melmed S (2001) The central role of SOCS-3 in integrating the neuro-immunoendocrine interface. J Clin Invest 108:1735–1740.

Bach JF (2001) Protective role of infections and vaccinations on autoimmune diseases. J Autoimmun 16:347–353.

Bate C, Kempster S, Last V, Williams A (2006) Interferon-gamma increases neuronal death in response to amyloid-beta1–42. J Neuroinflammation 3:1–7.

Bates S, Read SJ, Harrison DC, Topp S, Morrow R, Gale D, Murdock P, Barone FC, Parsons AA, Gloger IS (2001) Characterisation of gene expression changes following permanent MCAO in the rat using subtractive hybridisation. Brain Res Mol Brain Res 93: 70–80.

Bjorkbaek C, Elmquist JK, El-Haschimi K, Kelly J, Ahima RS, Hileman S, Flier JS (1999) Activation of SOCS-3 messenger ribonucleic acid in the hypothalamus by ciliary neurotrophic factor. Endocrinology 140:2035–2043.

Bordet R, Deplanque D, Maboudou P, Puisieux F, Pu Q, Martin A, Bastide D, Leys D, Lhermitte M, Dupuis B (2000) Increase in endogenous brain superoxide dismutase as a potential mechanism of lipopolysaccharide induced brain ischemic tolerance. J Cereb Blood Flow Metab 20:1190–1196.

Brodie C (1996) Differential effects of Th1 and Th2 derived cytokines on NGF synthesis by mouse astrocytes. FEBS Lett 394:117–120.

Chen H, Luo J, Kintner DB, Shull GE, Sun D (2005) Na^+-dependent chloride transporter (NKCC1)-null mice exhibit less gray and white matter damage after focal cerebral ischemia. J Cereb Blood Flow Metab 25:54–66.

Cisowski J, Zarebski A, Koj A (2002) IL-1 mediated inhibition of IL-6-induced STAT3 activation is modulated by IL-4, MAP kinase inhibitors and redox state of HepG2 cells. Folia Histochem Cytobiol 40:341–345.

Cunningham C, Wilcockson DC, Campion S, Lunnon K, Perry VH (2005) Central and systemic endotoxin challenges exacerbate the local inflammatory response and increase neuronal death during chronic neurodegeneration. J Neurosci 25:9275–9284.

de Bilbao F, Arsenijevic D, Vallet P, Hjelle OP, Ottersen OP, Bouras C, Raffin Y, Abou K, Langhans W, Collins S, Plamondon J, Alves-Guerra MC, Haguenauer A, Garcia I, Richard D, Ricquier D, Giannakopoulos P (2004) Resistance to cerebral ischemic injury in UCP2 knockout mice: evidence for a role of UCP2 as a regulator of mitochondrial glutathione levels. J Neurochem 89:1283–1292.

de Bilbao F, Guarin E, Nef S, Vallet P, Giannakopoulos P, Dubois-Dauphin M (2000) Cell death is prevented in thalamic fields by but not in injured neocortical areas after permanent focal ischemia in mice overexpressing the anti-apoptotic protein Bcl-2. Eur J Neurosci 12:921–934.

Droge W (2002) Free radicals in physiological control of cell function. Physiol Rev 82:47–95.

Elzenberg O, Faber-Elman A, Gottlieb E, Oren M, Rotter V, Schwarz M (1995) Direct involvement of p53 in programmed cell death of oligodentrocytes. EMBO J 14:1136–1144.

Emsley HC, Tyrrell PJ (2002) Inflammation and infection in clinical stroke. J Cereb Blood Flow Metab 22:1399–1419.

Ewing JF, Janero DR (1995) Microplate superoxide dismutase assay employing a nonenzymatic superoxide generator. Anal Biochem 232:243–248.

Franklin KBJ, Paxinos G (1997) The mouse brain in stereotaxic coordinates, pp 29–41. San Diego: Academic Press Inc.

Frenkel JK, Escajadillo A (1987) Cyst rupture as a pathogenic mechanism of toxoplasmic encephalitis. Am J Trop Med Hyg 36: 517–522.

Guegan C, Ceballos-Picot I, Chevallier E, Nicole A, Ontenlente B, Sola B (1999) Reduction of ischemic damage in NGF-transgenic mice: Correlation with enhancement of antioxidant enzyme activities. Neurobiol Dis 6:180–189.

Guegan C, Ceballos-Picot I, Nicole A, Kato H, Onteniente B, Sola B (1998) Recruitment of several neuroprotective pathways after permanent focal ischemia in mice. Exp Neurol 154:371–380.

Gupta A, Gupta M, Datta M, Shkla GS (2000) Cerebral antioxidant status and free radical generation following glutathione depletion and subsequent recovery. Mol Cell Biochem 209:55–61.

Hemadfahi N, Langhans W, von Meyenburg C, Onteniente B, Richard D, Arsenijevic D (2007) Role of glutathione in the hyposensitivity of LPS-pretreated mice to LPS anorexia. Eur Cytokine Netw 18:86–92.

Huang KC, Chen CW, Chen JC, Lin WW (2003) Statins induce suppressor of cytokine signaling-3 in macrophages. FEBS Lett 555:385–389.

Huber SA, Feldman AM, Sartini D (2006) Coxsackievirus B3 induces T regulatory cells, which inhibit cardiomyopathy in tumor necrosis factor-alpha transgenic mice. Clr Res 99:1109–1116.

Jo D, Liu D, Yao S, Collins RD, Hawiger J (2005) Intracellular protein therapy with SOCS3 inhibits inflammation and apoptosis. Nat Med 11:892–898.

Kang KE, Pak YMK, Kim ND (1999) Diethylmaleate and buthionine sulfoximine, glutathione-depleting agents, differentially inhibit expression of inducible nitric oxide synthase in endotoxemic mice. Nitric Oxide Biol Chem 3:265–271.

Larsen L, Ropke C (2002) Suppressors of cytokine signalling. APMIS 110:833–844.

Lebel E, Valliéres L, Rivest S (2000) Selective involvement of interleukin-6 in the transcriptional activation of the suppressor of cytokine signaling-3 in the brain during systemic immune challenges. Endocrinology 141:3749–3763.

Lee J, Shin JS, Choi IH (2006) Human brain astrocytes mediate TRAIL-mediated apoptosis after treatment with IFN-g. Yonsei Med J 47:354–358.

Mattiasson G, Shamloo M, Gido G, Gido G, Mathi K, Tomasevic G, Yi S, Warden CH, Castilho RF, Melcher T, Gonzalez-Zulueta K, Nikolich K, Wieloch T (2003) Uncoupling protein-2 prevents neuronal death and diminishes brain dysfunction after stroke and brain trauma. Nat Med 9:1062–1068.

McColl BW, Rothwell NJ, Allan SM (2007) Systemic inflammatory stimulus potentiates the acute phase and CXC chemokine responses to experimental stroke and exacerbates brain damage via interleukin-1 and neutrophil-dependent mechanisms. J Neurosci 27:4403–4412.

Murakami K, Kondo T, Kawase M, Li Y, Sato S, Chen SF, Chan PH (1998) Mitochondrial susceptibility to oxidative stress exacerbates cerebral infarction that follows permanent focal cerebral ischemia in mutant mice with manganese superoxide dismutase deficiency. J Neurosci 18:205–213.

Nguyen MD, D'Aigle T, Gowing G, Julien JP, Rivest S (2004) Exacerbation of motor neuron disease by chronic stimulation of innate immunity in a mouse model of amyotrophic lateral sclerosis. J Neurosci 24:1340–1349.

Nicholls DG, Budd SL (2000) Mitochondria and neural survival. Physiol Rev 80:315–360.

Park SH, Kim KE, Hwang HY, Kim TY (2003) Regulatory effects of SOCS on NF-KB activity in murine monocytes/macrophages. DNA Cell Biol 22:131–139.

Pileblad E, Magnusson T (1990) Effective depletion of glutathione in rat striatum and substantia nigra by L-buthionine sulfoximine in combination with 2-cyclohexene-1-one. Life Sci 47:2333–2342.

Qin L, Wu X, Block ML, Liu Y, Breese GR, Hong JS, Knapp DJ, Crews FT (2007) Systemic LPS causes chronic neuroinflammation and progressive neurodegeneration. Glia 55:453–462.

Sacco RL (2001) New risk factors for stroke. Neurology 57(5 Suppl 2): S31–S34.

Schulz JB, Lindenau J, Seyfried J, Dichgans J (2000) Glutathione, oxidative stress and neurodegeneration. Eur J Biochem 267: 4904–4911.

Sewell DL, Reinke EK, Hogan LH, Sandor M, Farby Z (2002) Immunoregulation of CNS autoimmunity by helminth and mycobacterial infections. Immunol Lett 82:101–110.

Spencer SJ, Mouihate A, Pittman QJ (2007) Peripheral inflammation exacerbates damage after global ischemia independently of temperature and acute brain inflammation. Stroke 38:1570–1577.

Villoslada P, Hauser SL, Bartke I, Unger J, Heald N, Rosenberg D, Cheung SW, Mobley WC, Fisher S, Genain CP (2000) Human nerve growth factor protects common marmosets against autoimmune encephalomyelitis by switching the balance of T helper cell type 1 and 2 cytokines within the central nervous system. J Exp Med 191:1799–1806.

Wang JY, Wen LL, Huang YN, Chen YT, Ku MC (2006) Dual effects of antioxidants in neurodegeneration: direct neuroprotection against oxidative stress and indirect protection via suppression of glia-mediated inflammation. Curr Pharm Des 12:3521–3533.

Wang J, Campbell IL (2002) Cytokine signalling in the brain: Putting a SOCS in it? J Neurosci Res 67:423–427.

Wang F, Wang LY, Wright D, Parmely MJ (1999) Redox imbalance differentially inhibits lipopolysaccharide-induced macrophage activation in the liver. Infect Immun 67:5409–5416.

Yang J, Zhao J, Zhang L, Yang X, Zhu X, Ji M, Sun N, Su C (2007) Schistosoma japonicum egg antigens stimulate CD4 CD25 T cells and modulate airway inflammation in a murine model of asthma. Immunology 120:8–18.

Yu L, Miao H, Hou Y, Zhang B, Guo L (2006) Neuroprotective effect of A20 on TNF-induced postischemic apoptosis. Neurochem Res 31:21–32.

Yu ZF, Mattson MP (1999) Dietary restriction and 2-deoxyglucose administration reduce focal ischemic brain damage and improve behavioural outcome: evidence for a preconditioning mechanism. J Neurosci Res 57:830–839.

(Accepted 3 October 2007)
(Available online 11 October 2007)

7.3. Article IV: Results and discussion

7.3.1. *Ischemic brain injury is reduced in Toxoplasma gondii infected mice*

We provide evidence here that *Toxoplasma gondii* infection induces neuroprotection against ischemic brain injury induced by permanent MCAO. Infected animals showed a 40% to 50% decrease of infarct size compared with non-infected littermates 1, 4 and 14 days (Figures 1E and 1F). Diminished activation of cellular inflammatory responses that ordinarily exacerbate ischemic injury may contribute to neuroprotection induced by toxoplasmosis. This neuroprotective effect of infection may be associated with a marked reduction of the MCAO-related brain induction of pro-inflammatory cytokines and/or increased basal levels of anti-inflammatory cytokines.

7.3.2. *Absence of pro-inflammatory cytokine induction observed in infected mice after ischemia*

Although infected mice had elevated basal levels of the pro-inflammatory cytokine TNFα, IFNγ and IL2 when compared to non-infected animals ($P<0.001$) (Table 2), we observed a marked reduction of the MCAO-related brain induction of the two pro-inflammatory cytokines, TNFα and IFNγ (Table 2). Although one could argue that this finding might reflect the presence of a threshold in cytokine levels reached in *Toxoplasma*-infected mice, this is an unlikely scenario since we have previously demonstrated that an injection of LPS led to a marked up-regulation of pro-inflammatory cytokines in these mice (Arsenijevic *et al*., 1998). Therefore, this phenomenon could be partly due to the already elevated basal levels of these cytokines in the brains of these mice (i.e. counter-regulatory mechanisms).

7.3.3. *Up-regulation of anti-inflammatory/neuroprotective factors in infected mice*

In addition, potential anti-inflammatory/neuroprotective factors were up-regulated in the brain of infected mice.

Suppressor of cytokine signaling proteins (SOCS): In accordance with previous findings showing that SOCS proteins may be induced in peripheral and central models of inflammation including permanent MCAO (Bates *et al.,* 2001), we observed an up-regulation of *SOCS-3* mRNA throughout the brain of infected mice (Figure 1D). SOCS-3 is therefore a plausible candidate molecule for the regulation of secondary inflammatory response and cytokine production in *Toxoplasma gondii*–infected mice. Actually, SOCS-3 has been shown to attenuate pro-inflammatory signaling and its transgenic over-expression may inhibit inflammation and associated apoptosis *in vivo* following LPS injection (Jo *et al.,* 2005). Therefore, the absence of MCAO pro-inflammatory cytokine induction could be partly due to the induction of the *SOCS-3* mRNA after infection.

Glutathione: We also provide various evidences that GSH could play a significant role in neuroprotection. Brain GSH basal levels are up-regulated in the chronic phase of infection (Figure 2A). This increase was specific to microglial cells (Figures 2B and 2C). In addition, the specific decrease of GSH levels following MCAO (Guégan *et al.*, 1998) was reduced in infected mice when compared to non-infected animals ($p<0.001$) (Figure 3A). Finally, decreased infarct size in MCAO mice chronically infected was no longer observed when brain GSH levels have been depleted by diethyl maleate (DEM) treatment (Figure 4B) suggesting that GSH up-regulation may play a pivotal role in the observed ischemic resistance. Consistent with a role of GSH in central cytokine regulation (Cisowski *et al.,* 2002; Haddad and Harb, 2005), this phenomenon was specifically associated with the central up-regulation of pro-inflammatory IFNγ in response to MCAO (Figure 4D).

Superoxide dismutase and UCP2: The basal up-regulation of other anti-oxidant molecules such as SOD and UCP2 mRNA may constitute the other lines of defense against ischemic damage in infected mice. SOD activity and *UCP2/GAPDH* mRNA ratio (Figures 3B and 3C) were higher in the brains of

infected mice compared with non-infected mice ($P<0.01$). Such an involvement of enhanced SOD in neuroprotection has been previously demonstrated in LPS brain preconditioning (Bordet *et al.*, 2000). In addition, our results on UCP2 are in line with previous data showing UCP2 induction by ischemic preconditioning (Mattiasson *et al.*, 2003). Whereas SOD activities were similarly increased in both groups of mice one day post-MCAO (Figure 3B), there was a significant increase in *UCP2/GADPH* mRNA ratio in infected mice compared with MCAO non-infected mice ($P<0.001$) (Figure 3C). Consistent with its role in neuroprotection (Mattiasson *et al*., 2003; de Bilbao *et al.,* 2004), the differences in *UCP2* mRNA levels persisted between infected and non-infected mice after MCAO. The overexpression of SOD activity and *UCP2* mRNA could contribute to decrease the deleterious effect of the free radicals on neurons during ischemia. This further confirms our previous finding that UCP2 could constitute a new candidate for endogenous brain neuroprotective mechanisms.

Anti-inflammatory cytokines NGF and IL10: The up-regulation of anti-inflammatory cytokines could be one of the mechanisms mediating the neuroprotection. Infected mice had significantly higher brain levels of NGF and IL10 compared with non-infected control mice ($P<0.001$) (Table 2). Interleukin-10 up-regulation could constitute one of the possible mechanisms that lead to SOCS-3 overexpression as already evidenced in neutrophils and monocytes/macrophages (Ito *et al*., 1999). In addition, because IL10 may act by suppressing the production of the pro-inflammatory molecule TNFα (Sawada *et al.,* 1999), this may partly explain the marked reduction of the MCAO-related brain induction of TNFα (Table 2). Finally, as the differences in NGF levels persisted between infected and non-infected mice after MCAO ($P<0.001$) (which was not the case for IL10), NGF may constitute a key anti-inflammatory agent in infected mice. According to previous results (Guegan et al., 1998, 1999), the high NGF levels could account for the increased basal GSH levels and SOD activity of infected mice.

7.4. Conclusion

Overall, these findings indicate that chronic toxoplasmosis decisively influences both the inflammatory molecular events and outcome of cerebral ischemia. They also support the hypothesis that the brain can be rendered preventively resistant to cerebral ischemia. Toxoplasmosis may trigger the cytokine inflammatory pathways, leading to inflammation and, consequently, to up-regulation of feedback inhibitors of inflammation such as growth factors, anti-oxidant defense enzymes overexpression and anti-inflammatoy cytokines. These phenomena could explain the marked resistance of *Toxoplasma gondii*–infected mice to acute cerebral ischemia. Therefore, the present study not only provides direct evidence that chronic infection may confer protection against subsequent ischemia, but also provides a new model to explore the effect of a pre-existing chronic inflammatory status on the outcome of brain ischemic insult. More generally, this new paradigm strongly suggests that endogenous neuroprotective mechanisms are not already maximally stimulated by cerebral ischemia and that they can be boosted (*i.e.* IL10 and GSH levels are higher in MCAO infected mice versus MCAO non-infected animals). These pathways are potential pharmacologic targets in the prevention of deleterious effects of brain ischemia. Indeed, understanding these mechanisms may allow to develop in the future a novel strategy (boosting endogenous protection in patients) to safeguard the brain against ischemic damage.

8. General conclusion

To date, the treatment of ischemic stroke is limited to the prevention of cerebrovascular risk factors and modulation of the coagulation cascade during the acute phase. Although many drugs have been developed to induce neuroprotection during stroke in the last two decades, none of them has been successful at the clinical step of their development (Bayes *et al.*, 2008). Consequently, and because ischemic stroke is the second leading cause of death and the first determinant of chronic disability in adults in industrialized countries, there is an urgent need for new therapeutics (Donnan *et al.*, 2008). The ischemic damage is characterized by two distinct cell death events: 1) a necrotic neuronal death which occurs within minutes of stroke onset in the area of no blood flow, the so-called core of the infarct; and 2) an apoptotic cell death which occurs around the area of necrosis with a delayed onset. This injured area is defined as the ischemic penumbra (Astrup *et al*., 1981). The concept of the ischemic penumbra has become increasingly important as this is a potentially salvageable tissue. Two major pathways regulate the process of apoptosis in mammalian cells, the extrinsic (receptor-mediated) and the intrinsic (mitochondrial) pathways (Galluzzi *et al.*, 2009b; Valmiki and Ramos, 2009). These pathways constitute attractive targets for the development of new neuroprotective interventions. In the present work, we mainly focused on the molecular mechanisms that could efficiently interact with the intrinsic pathway, characterized by the deterioration of mitochondrial functions, to prevent the cell death cascade induced by permanent MCAO in mice. Recently, it has been proposed that therapeutic interventions that act upstream the permeabilization of the mitochondrial membrane, the point of no return in the mitochondrial pathway (Galluzzi *et al.*, 2009b), should confer optimal neuroprotection. Among the possible candidates of such intervention, we report the effect of genetic modifications of the *bcl-2* and *ucp2* genes in mice, whose transducts have been shown to prevent the permeabilization of the mitochondrial membrane (see sections 4.1. and 5.3. respectively). Whereas Bcl-2 overexpression may exclusively protect areas remote from the infarcted tissue (Article I), UCP2 could constitute a more powerfull target to prevent ischemic damage in the affected neocortical area (Article II). These results further confirm that the extent of neuroprotection that may be afforded when considering a new

therapeutic agent may depend on various complex factors, such as the type of cell death (apoptosis/necrosis), the injury paradigm and the molecular cascade of events that have been activated. As concluded in Article III, one of the possibilities to successfully induce neuroprotection in stroke could be also to modulate pathophysiological pathways with one pharmacological agent with pleiotropic effect, *i.e.* that may affect more than one mechanism by acting upstream on transcription factor receptors. We report such a therapeutic perspective in Article III with mice genetically modified for the nuclear receptor PPARβ supposed to regulate inflammatory and oxidative processes (see section 6.2.). The phenomenon called ischemic tolerance also presumably involves the inhibition of the permeabilization of the mitochondrial membrane (Miyawaki *et al.*, 2008). Induction of cerebral resistance to ischemia before its occurrence (ischemic tolerance) constitutes an alternative therapeutic strategy to trigger neuroprotection. On the basis of experimental data, there is evidence that various harmful stimuli may render the brain resistant to the deleterious effects of ischemia by the induction of cytoprotective proteins as well as by the inhibition of deleterious inflammatory, oxidative, and apoptotic pathways (Dirnagl *et al.*, 2003). In Article IV, we provide evidence that chronic *Toxoplasma gondii* infection may confer protection against subsequent focal ischemia in mice by up-regulating and boosting the endogenous cellular mechanisms of protection. Therefore, it can be speculated that pharmacological agents able to mimic the biological effects observed in brain ischemic tolerance might increase the resistance to ischemia of patients with high risk for stroke.

One of the explanations for the failure of clinical trials is that the developed drugs are able to modulate only one molecular pathway among those involved in the pathophysiology of stroke. One of the possibilities to successfully induce neuroprotection in stroke could be to modulate simultaneously many pathophysiological pathways with a combination of several drugs that act at several steps of the ischemic cascade (De Keyser *et al*., 1999). In animal models, various neuroprotective combinations have been used successfully (for review see Lo *et al.*, 2003). As an example, a recent study demonstrates that a combined therapy with a PPARγ agonist (rosiglitazone) and anti-excitotoxic glutamate receptor antagonist (dizocilpine/MK-801) led to an improved neurological recovery

in rats undergoing MCAO (Allahtavakoli *et al.*, 2007). These considerations argue for a future possibility of a multidrug therapeutic approach. Within this theorical framework, the evaluation of a potential synergistic protective effect of molecules acting on Bcl-2, UCP2 and PPARβ effects may be of particular interest. For instance, it can be hypothesized that overexpression of Bcl-2, when combined with therapies acting on the extrinsic pathway of cell death, could enhance neuroprotection (Taoufik *et al.*, 2007; Bi *et al.*, 2008). It is undeniable that there is a long way before translating these observations to efficient and safe clinical trials. However, the perspective of a molecular therapy for stroke remains one of the most challenging and promising issue in modern neurosciences. The experimental evidences included in this work aim to support this new perspective that needs a long term investment combining the competence of basic scientists and clinicians.

Annexe

Journal of Neurochemistry

JOURNAL OF NEUROCHEMISTRY | 2009 | 110 | 12–22 doi: 10.1111/j.1471-4159.2009.06098.x

In vivo over-expression of interleukin-10 increases resistance to focal brain ischemia in mice

Fabienne de Bilbao,*[,1] Denis Arsenijevic,†[,‡,1] Thomas Moll,§ Irene Garcia-Gabay,§ Philippe Vallet,* Wolfgang Langhans‡ and Panteleimon Giannakopoulos*[,¶]

*Department of Psychiatry, University Hospitals of Geneva, Belle-Idée, Geneva, Switzerland

†Department of Medicine, Division of Physiology, University of Fribourg, Rue du Musee, Fribourg, Switzerland

‡Institute of Animal Sciences, ETHZ, Schorenstrasse, Zurich, Switzerland

§Department of Pathology, Geneva University Medical Centre, Geneva, Switzerland

¶Division of Old Age Psychiatry, University of Lausanne, Prilly, Switzerland

Abstract

Early studies showed that *the administration* of the anti-inflammatory cytokine interleukin-10 (IL10) protects against permanent middle cerebral artery occlusion (MCAO) in mice. In this study, transgenic mice expressing murine IL10 (IL10T) directed by the major histocompatibility complex Ea promoter were produced and used to explore the effect of chronically increased IL10 levels on MCAO-related molecular mechanisms. IL10 was over-expressed in astrocytes, microglia, and endothelial brain cells in IL10T compared with wild type mice. Four days following MCAO, IL10T mice showed a 40% reduction in infarct size which was associated to significantly reduced levels of active caspase 3 compared with wild type mice. Under basal conditions, anti-inflammatory factors such as nerve growth factor and GSH were up-regulated and the pro-inflammatory cytokine IL1β was down-regulated in the brain of IL10T animals. In addition, these mice displayed increased basal GSH levels in microglial and endothelial cells as well as a marked increase in manganese superoxide dismutase in endothelial lining blood vessels. Following ischemia, IL10T mice showed a marked reduction in pro-inflammatory cytokines, including tumor necrosis factor-α, interferon-γ, and IL1β. Our data indicate that constitutive IL10 over-expression is associated with a striking resistance to cerebral ischemia that may be attributed to changes in the basal redox properties of glial/endothelial cells.

Keywords: cytokines, glia, glutathione, interleukin-10, middle cerebral artery occlusion, nerve growth factor.

J. Neurochem. (2009) **110**, 12–22.

From a molecular viewpoint, the outcome of post-ischemic inflammatory processes mainly depends on the imbalance between the activation of pro-inflammatory cytokine cascade and the induction of anti-inflammatory cytokines and antioxidant mechanisms (Wang *et al.* 2007). In particular, it has been shown that the production of pro-inflammatory cytokines such as tumor necrosis factor-α (TNFα) and interferon-γ (IFNγ) leads to tissue damage because of the accumulation of secondary mediators such as reactive oxygen species (ROS) (Sawada *et al.* 1999). This effect can be counterbalanced by the activation of anti-inflammatory cytokines such as interleukin-10 (IL10) and antioxidant molecules such as GSH and manganese superoxide dismutase (MnSOD) (de Bilbao *et al.* 2004; Arsenijevic *et al.* 2006).

Received March 2, 2009; accepted March 24, 2009.

Address correspondence and reprint requests to Dr Denis Arsenijevic, Department of Medicine, Division of Physiology, University of Fribourg, Rue du Musee 5, Fribourg 1700, Switzerland.
E-mail: denis.arsenijevic@unifr.ch

[1]These authors contributed equally to this study and are equal first authors.

Abbreviations used: G6PDH, glucose-6-phosphate dehydrogenase; GCS, γ-glutamylcysteine synthase; GFAP, glial fibrillary acidic protein; Glut1 and 4, glucose transporter 1 and 4; IFN, interferon-γ; IL10, interleukin-10; IL10T, transgenic mice expressing murine IL10; MCAO, middle cerebral artery occlusion; MCH, melanin-concentrating hormone; MDA, malondialdehyde; MHC, major histocompatibility complex; MnSOD, manganese superoxide dismutase; NeuN, neuronal nuclei; NGF, nerve growth factor; NPY, neuropeptide Y; ROS, reactive oxygen species; SOD, superoxide dismutase; Tg mice, transgenic mice; TNF, tumour necrosis factor-α; WT, wild type.

Cerebral ischemia triggers complex cellular processes involving not only the activation of resident glial cells but also the recruitment of inflammatory blood cells (Wang *et al.* 2007). The triad of endothelial cells, astrocytes, and microglia is thought to play an essential role in post-ischemic immune cell trafficking, yet the exact interactions between these cell types remain poorly understood. Under basal conditions, endothelial cells are known to interact directly with astrocytes and modifications of microvascular structure induced by ischemia are likely to affect their relationships. Microglia and astrocytes may in turn interact to regulate the endothelium transmigration (Fiala *et al.* 1998). During the acute post-ischemic period, neutrophils are the first inflammatory cells to be recruited within the lesioned area followed by monocytes/macrophages and lymphocytes (Wang *et al.* 2007). Endothelial cells may participate in this event by favoring leukocyte transmigration (Fiala *et al.* 1998). Microglial cells may promote post-ischemic brain damage directly via their transformation into phagocytes (Stoll *et al.* 1998) or indirectly through the release of ROS and cytotoxic cytokines like TNFα and IL1β (Saud *et al.* 2005). Importantly, they may also exert their function by participating in the recruitment of immune cells. However, glial cells are also the source of cytokines with anti-inflammatory properties. One of these, IL10, is a potent inhibitor of inflammation. It has been proposed that IL10 mediates neuroprotection by blocking caspase 3 activity (Bachis *et al.* 2001) and reducing pro-inflammatory cytokine production (Frenkel *et al.* 2003). Previous contributions have shown that both exogenous administration (Spera *et al.* 1998; Frenkel *et al.* 2003) and gene transfer (Ooboshi *et al.* 2005) of IL10 mediate neuroprotection after an ischemic insult. However, most of these studies were undertaken on *in vitro* models of inflammation (lipopolysaccharide, cytokine-stimulated cells) and those investigating the effect of IL10 on *in vivo* models of brain ischemia were based on post-ischemic exogenous administration of this cytokine (Spera *et al.* 1998; Ooboshi *et al.* 2005). To investigate the impact of chronic IL10 up-regulation on the morphological, biochemical, and behavioral post-ischemic changes following permanent middle cerebral artery occlusion (MCAO), we produced transgenic (Tg) mice over-expressing murine IL10 (IL10T) under the control of the major histocompatibility complex (MHC) Ea promoter. The MHC class I and II molecules have also shown to be up-regulated in the periinfarct area (Stoll *et al.* 1998) and may be regulated by MCAO-induced cytokines such as TNFα or IFNγ (O'Keefe *et al.* 1999). In particular, this promoter is induced in both glial and endothelial brain cells (Stoll *et al.* 1998; Girvin *et al.* 2002; Wang *et al.* 2007) but also professional antigen-presenting cells. Our data indicate a marked resistance of IL10-over-expressing Tg mice after MCAO that was mainly because of changes in cytokine production and oxidative stress regulation.

Material and methods

All procedures were approved by the Veterinary Office of the Canton of Zurich Health Directorate and the Veterinary Office of Geneva.

Mice and diets

Adult male mice (3–4 months) were used in these experiments. The IL10T and wild type (WT) co-littermates were established on a C57BL/6J genetic background. Mice were kept at room temperature (25°C) with a 12 : 12 h light/dark cycle. They were housed in individual cages for food intake and body weight studies and had *ad libitum* access to standard laboratory diet and water. Food intake was calculated using the weight of food pellets from the previous day and subtracting the weight of the remaining pellets (and spillage) of the following day (measured at 9.00 AM). For all feeding experiments, a minimum of 24 animals (12 WT and 12 IL10T) were used in each MCAO-treated group and their respective controls. Food intake and body weight were recorded for 3 days prior to MCAO, and then were assessed daily for 1 week. Preliminary tests have shown that there was no significant difference in body weight (22–25 g) and food intake between IL10T and WT mice.

Generation of interleukin-10 transgenic mice

Murine IL10 cDNA from position +63 (14 nucleotides upstream of ATG start codon) to +665 (55 nucleotides downstream from TAA stop codon) was placed under the control of the class II MHC Ea promoter sequence in a pDOI-5 plasmid (Kouskoff *et al.* 1993). The construct was microinjected into eggs from (C57BL/6 × DBA/2)F2 females and Tg founders were backcrossed to C57BL/6 mice, yielding C57BL/6.IL10 Tg positive or negative males and females. WT and homozygote IL10T mice used in this study were generated from hemizygously transgene-positive male and female mice which were from backcross-generation N_7 and N_8. The presence of the IL10 transgene in the offspring was detected by PCR on tail DNA using the primers 5′-TCAAACAAAGGACCAGCTGGACAACA-TACTG-3′ and 5′-CTGTCTAGGTCCTGGAGTCCAGCAGACT-CAA-3′, yielding one specific fragment of 420 bp, as confirmed by using molecular weight markers from Roche (Basel, Switzerland). Basal over-expression of IL10 protein was assessed by ELISA IL10 (GE Healthcare Europe, Otelfingen, Zurich, Switzerland) in brain, liver, lung, pancreas, and plasma in WT and IL10T mice (see Determination of brain cytokine levels section for methods).

Immunohistochemistry

Frozen brain coronal sections (12 μm) from non-operated WT and IL10T mice were processed for immunostaining using the following antibodies: rat anti-mouse IL10 (1/1000; Amersham), sheep anti-human MnSOD (1/100; Calbiochem, San Diego, CA, USA). To label astrocytes, microglia, endothelial cells, and neuronal cells, mouse polyclonal anti-glial fibrillary acidic protein (GFAP; 1/1200 – Chemicon International Inc., Temecula, CA, USA), rabbit polyclonal anti-Iba1 (1 μg/mL; kindly provided by Prof. Y. Imai, National Center of Neurology and Psychiatry, Tokyo, Japan), rat anti-mouse Cd54 (Von Willebrand factor, 1/5000; ebiosource, Vienna, Austria), and the mouse anti-neuronal nuclei monoclonal antibody (NeuN) (1/1000; Chemicon International Inc.) have been used, respectively. For double staining of cell types expressing IL10, the GFAP, anti-Iba1, anti-Cd54, and NeuN antibodies were detected

by using Nova Red kit (Vector kit; Vector laboratories, Burlingham, CA, USA) and IL10 antibody was revealed by Ni–diaminobenzidine staining. For double staining of cell types expressing GSH or MnSOD, the GFAP, anti-Iba1, anti-Cd54, and NeuN antibodies were detected using species specific secondary antibodies labeled with rhodamin (Vector Laboratories). MnSOD was detected using anti-sheep IgG FITC-labeled antibodies (Vector Laboratories) and GSH was detected by phthaldialdehyde (10 mM) (de Bilbao *et al.* 2004). Negative controls included deletion of the primary or secondary antibody. Photomicrographs of double immunofluorescent staining were constructed using the MetaMorph Imaging System (Visitron Systems, West Chester, PA, USA).

Induction of permanent focal cerebral ischemia and volume of the infarct

We performed permanent MCAO in IL10T ($n = 6$) and WT ($n = 6$) mice. After 4 days, quantification of the infarct area was performed for each animal as previously described (de Bilbao *et al.* 2004). In addition, cerebral vasculature anatomy was compared between the two genotypes in non-operated and operated mice. These methods are elaborated in Supporting information – Materials and methods.

Physiological parameters for MCAO study

Physiological parameters including arterial blood pressure, plasma glucose, and hematocrit were measured daily in IL10T and WT mice ($n = 5$) before MCAO and on days 1 and 4 post-injury (de Bilbao *et al.* 2004). Body temperature was measured prior to MCAO, during and following MCAO. All these procedures are further detailed in Supporting information – Materials and methods.

Western blot procedure for glucose transporters Glut1, Glut4, caspase 3, and G6PDH enzyme activity

Western blots on protein extracts from hemispheres of non-operated WT and IL10T mice were used ($n = 4$ for each groups). Membranes were incubated overnight with primary antibody [goat anti-glucose transporter 1 (Glut1) (sc1605 – 1/200) or goat anti-Glut4 (sc1608 – 1/200; Santa Cruz Biotechnology, Santa Cruz, CA, USA) and mouse anti-tubulin (1/25 000; Sigma, Buchs, Saint Gallen, Switzerland)]. Secondary antibodies LI-COR anti-mouse for tubulin (1/1000) and LI-COR anti-goat (1/1000) were used to detect bands. The signals were visualized with the use of the Odyssey Infrared Imaging System (Li-Cor Biosciences, Bad Homburg, Germany). Protein levels were expressed as the ratio against tubulin (Viswambharan *et al.* 2007). For caspase 3, ischemic hemispheres from lesioned WT and IL10T mice were used ($n = 6$ for each group). Membranes were incubated overnight with primary antibody [rabbit anti-caspase 3 (sc1605 – 1/1000; Santa Cruz Biotechnology) and mouse anti-tubulin (1/25 000; Sigma)]. Secondary antibodies LI-COR anti-mouse for tubulin (1/1000) and Alexa Fluor anti-rabbit for caspase 3 (1/1000) were used to detect bands. For complete methods, see Supporting information – Materials and methods.

The enzyme glucose-6-phosphate dehydrogenase (G6PDH) was also studied as it plays a key role in glucose metabolism and redox regulation via the pentose phosphate pathway (Spolarics 1998). Hemispheres from non-operated WT and IL10T mice were used ($n = 4$ for each groups). They were homogenized with polytron homogenizer in 0.2 M Tris buffer, pH 7.0, kept on ice. After centrifugation at 8500 *g*, the supernatant was collected and kept at −20°C prior to assay for G6PDH activity. Fifteen microliter of extract containing 1 mg/mL of protein as determined by Bradford (Bio-RAD, Reinbach, Basel, Switzerland) was added to 100 µL buffer containing 0.2 M Tris, pH 7.0, and $NADP^+$ (10 mg/mL). To start the reaction, 50 µL of glucose-6-phosphate (0.3 g in 1 mL) was added. The activity was determined by measuring the change in optical density at 340 nm during 15 min.

Lipid peroxidation in brain homogenates

Malondialdehyde (MDA) was assayed, as an indicator of endogenous lipid peroxidation, on days 1 and 4 after MCAO in WT and IL10T mice ($n = 5$ for each group). Non-operated mice were used as controls ($n = 5$ for each group). Biotech LPO-586 colorimetric assay kit and its protocol (Oxis, Portland, OR, USA) was used to determine MDA as described previously (de Bilbao *et al.* 2004; for further details, see Supporting information – Materials and methods).

Brain superoxide dismutase activity 1 day after MCAO

Superoxide dismutase activities in the ischemic hemispheres of IL10T and WT mice subjected to ischemia (1 day post-MCAO) and in the equivalent hemisphere in control non-operated animals ($n = 6$ mice per group) were determined using a biochemical assay (Ewing and Janero 1995; see Supporting information – Materials and methods for more details).

Brain GSH levels

Total reduced GSH was measured in ischemic hemispheres of operated animals 1 and 4 days after lesion ($n = 4$) and the equivalent hemisphere for control non-operated animals ($n = 4$), using a previously described method (de Bilbao *et al.* 2004; for complete description, see Supporting information – Materials and methods).

Determination of brain cytokine levels

We measured TNFα, IFNγ, IL1β, IL10, and nerve growth factor (NGF) in the brain ischemic hemispheres of WT and IL10T mice ($n = 4$ for each group). Non-operated mice were used as controls ($n = 4$ for each group). Cytokines were measured using immunoassay kits [for the four former (Amersham) and for NGF (Catalys, Wallisellen, Switzerland)] as described previously (Arsenijevic *et al.* 2006). See Supporting information – Materials and methods for more details.

RT-PCR for γ-glutamylcysteine synthase

Brain hemispheres (1 and 4 days post-MCAO, $n = 4$) were dissected from IL10T and WT mice and total RNA was isolated as described previously (Arsenijevic *et al.* 2006). Non-operated mice were used as controls ($n = 4$). The RNA was treated with Dnase and then reverse transcribed (Promega, Catalys, Wallisellen, Switzerland). Subsequently, a semiquantitative PCR (Invitrogen, Basel, Switzerland) was performed and the product was separated by gel electrophoresis containing ethidium bromide. The bands were then quantified using the Scion Image program (Scion Corporation, Frederick, MD, USA). The primers used were as follows: GCS (gamma-glutymlcysteine synthase) (sense 5′-ATCCTCCAGTT-CCTGCACAT-3′ and antisense 5′-TGTGAATCCAGGGCAGCC-TA-3′) (Li *et al.* 1996) and glyceraldehyde 3-phosphate dehydro-

genase, as reference control (sense 5′-TGAAGGTCGGTGTCA-ACGGATTTGGC-3′ and antisense 5′-CATGTAGGCCATGAGGT-CCCACCAC-3′) (Arsenijevic *et al.* 2006). All values for the semiquantitative RT-PCR expression of a gene were obtained after normalizing for glyceraldehyde 3-phosphate dehydrogenase.

Enzyme immunoassay for neuropeptide Y, orexin-A, and melanin-concentrating hormone

Hypothalami were dissected out in WT and IL10T mice 1 day after MCAO ($n = 5$), non-operated mice were used as controls ($n = 5$). Orexin-A, melanin-concentrating hormone (MCH), and neuropeptide Y (NPY) were quantified by enzyme immunoassay (Phoenix-Peptide, Belmont, CA, USA) (Gallmann *et al.* 2006). A more complete description of this method is given in Supporting information – Materials and methods.

Data analyses

All data are presented as mean ± SD. Statistical analyses were performed using Kruskal–Wallis one-way non-parametrical ANOVA. A value of $p < 0.05$ was considered as significant.

Results

PCR genotyping of IL10T mice and their WT co-littermates

For all mice, PCR was used to detect Tg gene from tail biopsy (Fig. 1a).

Basal levels of IL10 protein are increased in peripheral and central tissues of IL10T mice

Compared with WT mice, IL10T animals displayed significant increases of IL10 in brain (56%, $p < 0.001$), liver (64%, $p < 0.001$), lung (12%, $p < 0.05$), pancreas (18%, $p < 0.01$), and plasma (200%, $p < 0.001$) tissues (Fig. 1b).

Basal immunohistochemical detection for IL10, MnSOD, and GSH in various brain cell types of IL10T and WT mice

In WT mice, IL10 immunostaining was only observed in cells surrounding the brain and lining ventricles (Fig. 2a, b, and c). In contrast, in IL10T mice immunostaining was also observed in brain astrocytes, microglia, and endothelial cells in all brain regions (including the cerebral cortex) (Fig. 2a, b, and c). Immunostaining was not observed in neuronal cells (Fig. 2b) or oligodendrocytes in both genotypes. MnSOD and GSH were detected in neurons and astrocytes of both IL10T and WT mice (data not shown). In addition, IL10T mice showed a specific labeling for GSH in microglia and endothelial cells and MnSOD in endothelial cells of blood vessels (Fig. 2d).

Physiological parameters before and after MCAO

WT and IL10T mice showed no pre- or post-operative differences in CBF (cerebral blood flow). Similar reductions were observed in both groups of mice after MCAO. Arterial pressure, plasma glucose, and hematocrit levels 1 day prior

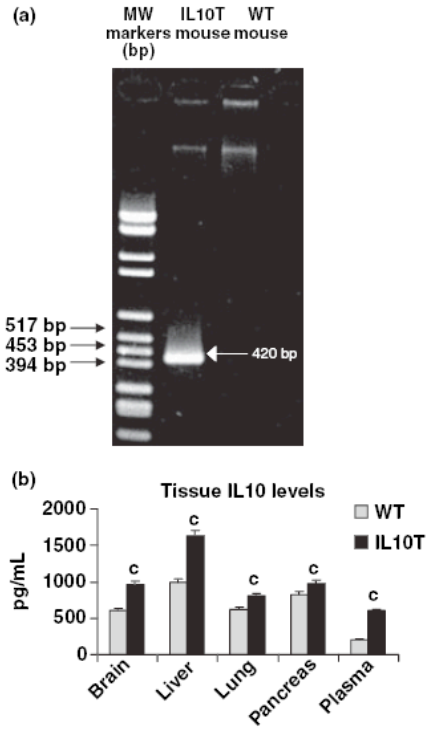

Fig. 1 (a) The presence of the IL10 transgene in the offspring was detected by PCR on tail DNA yielding one specific fragment of 420 bp after separation by gel electrophoresis (molecular weight; MW) (see text, for further details on method). (b) Basal IL10 protein levels in IL10T mice were significantly elevated in the four tissues analyzed compared with WT counterparts. Data are expressed in pg/mL. See text for details. For all groups, $n = 4$ animals; $^{c}p < 0.001$.

as well as on days 1 and 4 after MCAO were not significantly different between IL10T and WT mice (Table 1). After MCAO, both mice showed an absence of cerebral blood flow in the infarct area. Body temperature did not differ between mice 1 day prior as well as on days 1 and 4 after MCAO (Table 1). However, cytokines can modify body temperature following immunoactivation (Leon 2004) and despite the fact that we maintained body temperature by using a heating lamp post-surgery, it cannot be formally excluded that IL10 may affect body temperature once the lamp was removed. Therefore, body temperature changes may have a marginal impact on the outcome of ischemia.

Although no difference was observed in basal circulating glucose levels between IL10T and WT mice, we did observe that basal protein levels of the Glut1 and Glut4 were increased by 26% ($p < 0.001$) and 24% ($p < 0.01$), respectively, in the IL10T compared with WT brains (Table 1). Furthermore, we observed that basal G6PDH activity was increased by 2.8 times in the brain of IL10T mice compared with WT littermates ($p < 0.01$) (Table 1).

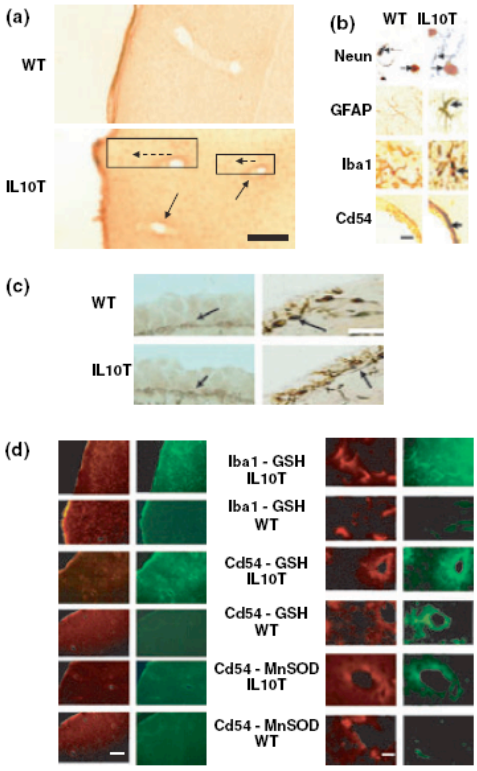

Fig. 2 (a) IL10 immunostaining in coronal sections of WT and IL10T mice. Distribution of IL10 stained cells was only observed in cells lining the brain in WT mice, whereas IL10T mice showed vast staining in endothelial cells (arrows) and non-vascular cells (dashed arrows) (see below); a selected area (thin lined rectangle) is shown magnified 1.5× in a thick line rectangle (scale bar, 30 μm) (b) NeuN positive neurons, GFAP positive astrocytes, Iba1 positive microglia, and Von Willenbrand factor/Cd54 positive endothelial cells double immunostaining for IL10 in WT and IL10T brains. Stained cells are found in the cortex and throughout the brain. Cell types were stained with Nova Red (orange-red) and IL10 with Ni–diaminobenzidine (black). Astrocytes, microglia, and endothelial cells were labeled for IL10 in IL10T brains only (thick arrow). In contrast, neurons were not positive for IL10 in both genotypes (thin arrow) (scale bar, 7 μm). (c) IL10 is detected in the epithelial cells that line ventricles (left) and the cells lining the brain (right) in both WT mice and IL10T mice (arrows) (scale bar, 7 μm). (d) Iba positive microglial cells (red) were double labeled for GSH (green) in IL10T mice. Von Willenbrand/Cd54 positive endothelial cells (red) were double labeled for GSH (green) or MnSOD (green) in IL10T brain blood vessels. Double labeling was not observed in WT mice. Left (scale bar, 30 μm) and right (scale bar, 7 μm for Iba1-GSH, 20 μm for Cd54-GSH and Cd54-MnSOD) panels correspond to low and high magnification, respectively.

Ischemic brain injury is reduced in IL10T mice

Brain weight and nuclei cytoarchitecture (cresyl violet staining) were comparable in IL10T and WT mice. Moreover, no difference was observed in vascular system (organization of the circle of Willis, position and diameters of the main cerebral arteries) between these mice. Four days after MCAO, infarct volume was decreased by 40% in IL10T mice (4.5 ± 0.5 mm^3) when compared with WT mice (7.5 ± 0.5 mm^3) ($p < 0.001$) (Fig. 3a and b), suggesting that IL10 over-expression may protect neocortical areas from ischemic damage. It is unlikely that this protective effect is because of enhanced neo-angiogenesis as the degree of revascularization assessed by endothelial cell distribution on 1 and 4 days post-MCAO was comparable in both mice strains (Fig. 3d).

Active caspase 3 protein levels in IL10T and WT mice

Ischemia resulted in the induction of active caspase 3 in both genotypes. However, active caspase 3 levels were reduced by 18% in IL10T mice compared with WT mice ($p < 0.001$; Fig. 3c). No significant differences in tubulin were detected between WT and IL10T mice that were lesioned or not.

Brain cytokine levels 1 day after MCAO

Basal brain levels of IL10 and NGF were higher in IL10T when compared with WT mice ($p < 0.001$ and $p < 0.01$, respectively) (Fig. 4a and b). One day post-MCAO, IL10 and NGF were induced in both genotypes ($p < 0.001$). However, post-MCAO levels of both cytokines were still higher in the IL10T compared with WT mice ($p < 0.001$ and $p < 0.05$, respectively) (Fig. 4a and b). Pro-inflammatory cytokines (IFNγ, TNFα, and IL1β) were induced 1 day after ischemia in the brain of WT and, to a lesser extent, IL10T mice ($p < 0.001$) (Fig. 4c, d, and e). Importantly, basal levels of IL1β were reduced in IL10T compared with WT mice ($p < 0.001$) (Fig. 4e).

Brain oxidant/antioxidant status in mice after MCAO

One and four days after MCAO, brain MDA levels were significantly increased in WT and IL10T mice ($p < 0.001$); however, this increase was significantly more pronounced in WT mice ($p < 0.01$) (Fig. 5a). To explore possible differences in oxidative stress regulation between the two strains, we studied pre- and post-ischemic brain SOD activity and GSH antioxidant levels. Following MCAO, there was increased SOD activity in both WT and IL10T mice ($p < 0.001$) without significant differences between the two genotypes (Fig. 5b). Basal GSH levels were higher in IL10T compared with WT mice ($p < 0.001$). Following MCAO, GSH levels were significantly reduced in both groups ($p < 0.001$) (Fig. 5c), yet they were still higher 1 day post-MCAO in IL10T mice ($p < 0.001$). We also determined whether the increased GSH level in IL10T mice was associated with an elevated mRNA level of γ-glutamylcysteine synthase (GCS), which is the rate-limiting enzyme in GSH synthesis. Basal brain levels of GCS mRNA were higher in IL10T mice compared with WT mice (26% increase, $p < 0.01$) (Fig. 5d). Following

Table 1 Physiological parameters prior and after MCAO in IL10T and WT mice

Group and treatment	One day prior to MCAO	D1 post-MCAO	D4 post-MCAO
Hematocrit (%)			
WT	43 ± 4	45 ± 3	46 ± 4
IL10T	45 ± 2	43 ± 4	47 ± 4
Plasma glucose (mM)			
WT	7.1 ± 0.5	7.2 ± 0.4	7.4 ± 0.4
IL10T	7.4 ± 0.6	7.3 ± 0.4	7.5 ± 0.3
Brain G6PDH activity (mU/mg)			
WT	12.1 ± 0.3		
IL10T	34.3 ± 0.4**		
Brain glucose transporters			
Glut1 WT	0.573 ± 0.012		
Glut1 IL10T	0.706 ± 0.014***		
Glut4 WT	0.170 ± 0.003		
Glut4 IL10T	0217 ± 0.009**		
Body temperature (°C)			
WT	37.6 ± 0.4	37.6 ± 0.4	37.6 ± 0.4
IL10	37.1 ± 0.3	37.1 ± 0.3	37.1 ± 0.3
Arterial pressure (mmHg)			
WT	98 ± 4	101 ± 4	105 ± 4
IL10T	102 ± 4	104 ± 4	102 ± 4

MCAO, middle cerebral artery occlusion; IL10T, transgenic mice expressing murine IL10; IL10, interleukin-10; WT, wild type; G6PDH, glucose-6-phosphate dehydrogenase; Glut1 and 4, glucose transporter 1 and 4. Hematocrit, plasma glucose, body temperature, and arterial pressure were measured in WT and IL10T mice prior to ischemia, and then on days 1 (D1) and 4 (D4) after MCAO. No significant differences were observed between WT and IL10T mice. Basal brain G6PDH activity was significantly increased in IL10T mice compared with WT (**$p < 0.01$). Basal brain glucose transporters protein levels normalized to tubulin were elevated in IL10T mice compared with WT mice, Glut1 (**$p < 0.01$) and Glut4 (***$p < 0.001$). Data are mean ± SEM of five animals per group.

MCAO, WT and IL10T mice displayed a comparable increase in GCS mRNAs (63% and 44% increases, respectively, $p < 0.001$). On day 4 after ischemia, GCS mRNAs were further increased compared with day 1 levels.

Food intake responses of IL10T mice following MCAO

Interleukin-10T and WT mice showed no significant difference in basal food intake (Fig. 6a). WT mice showed acute hypophagia on the day of MCAO intervention. The hypophagic response on this day was blunted in IL10T mice (3.4 ± 0.08 vs. 2.4 ± 0.09 g/mouse in WT mice) ($p < 0.001$). IL10T mice rapidly entered in a hyperphagic state compared with WT (Fig. 6a). During the period of days 0–2 after MCAO, IL10T mice ate significantly more than WT mice ($p < 0.001$) (Fig. 6a). From days 3–5 post-MCAO, both IL10T and WT mice displayed a similar pattern of hyperphagia. After this time point, food intake returned to basal levels. In all animals, the body weight followed a parallel time course to that of food intake (data not shown). These results suggest that IL10 attenuates negative energy balance in response to central inflammation.

Implication of orexin-A, NPY, and MCH protein levels in resistance to anorexia in IL10T mice after MCAO

To explain the reduced anorexic effect of MCAO in IL10T compared with WT mice, we studied the hypothalamic protein levels of three orexigenic peptides in the brain, orexin-A, NPY, and MCH both under basal conditions and following MCAO (Fig. 6b, c, and d). Basal protein levels of orexin-A and NPY did not differ between IL10T and WT mice (Fig. 6b and c); however, MCH basal levels were increased by 31% in the IL10T compared with WT mice ($p < 0.001$). After MCAO, we observed that the three neuropeptide levels were increased in both groups of mice compared with non-operated controls (Fig. 6b, c, and d). There was a significant increase in orexin-A and NPY levels in IL10T ischemic mice compared with WT ischemic animals (32%, $p < 0.001$ and 23%, $p < 0.01$ for orexin-A and NPY) (Fig. 6b and c).

Discussion

The main finding of the present study is that the *in vivo* endogenous over-expression of IL10 markedly protected

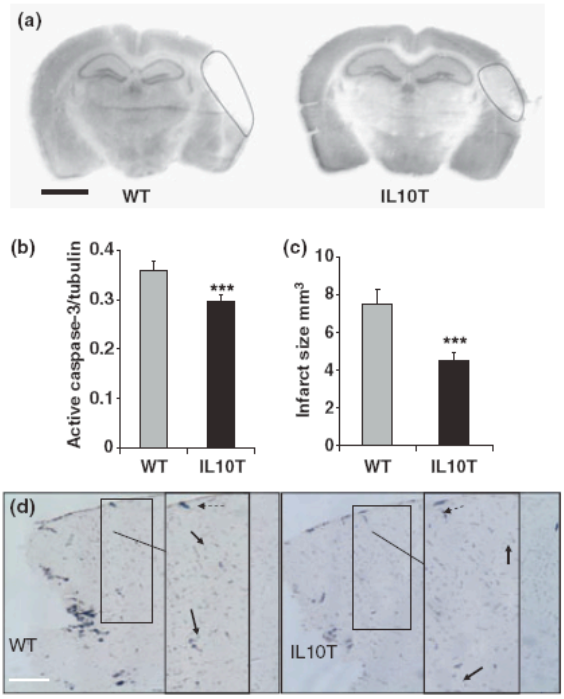

Fig. 3 Effect of IL10 over-expression on brain infarct size. (a) Representative coronal brain sections showing the ischemic infarct 4 days after MCAO in WT and IL10T mice. Brain sections were stained with cresyl violet. The surrounded areas denote the size of the ischemic area. The infarct size was found significantly decreased in IL10T mice ($p < 0.001$, $n_{IL10T} = 6$ and $n_{WT} = 6$; scale bar, 120 μm). Brain lesion size in mm^3 (b, ***$p < 0.001$) (each group included six mice). (c) On day 4 post-ischemia, induction of active caspase 3 protein levels is reduced in IL10T mice compared with WT mice (***$p < 0.01$, each group included six mice). (d) Endothelial cell immunostaining with Ni–diaminobenzidine on coronal brain sections 4 days after ischemia in WT and IL10T mice. Results indicate that no marked difference in revascularization occurred in the lesion area between the two genotypes (scale bar, 30 μm). We show by using a selected 1.5× magnification of an area (thin line rectangle) that the labeled cells are large blood vessels (dashed arrows) and capillaries (black arrow) (thick line rectangle).

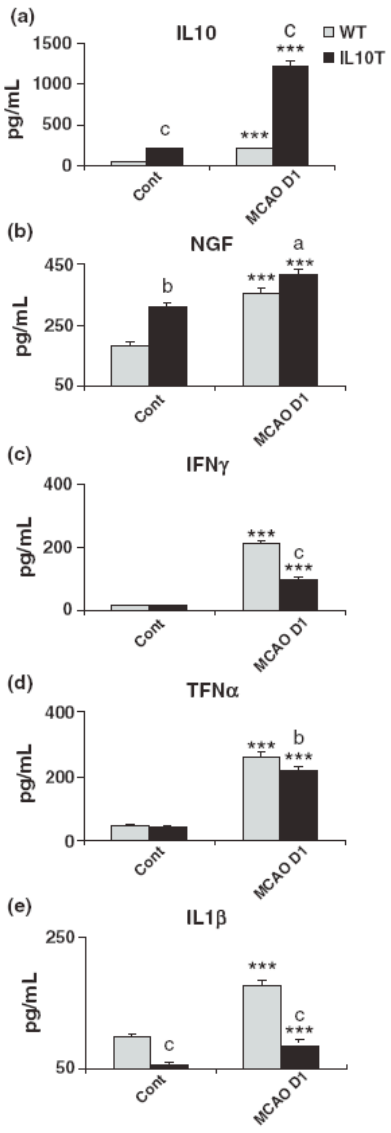

Fig. 4 Brain levels of IL10, NGF, IFNγ, and TNFα 1 day after MCAO in WT and IL10T mice. (a) IL10, (b) NGF, (c) IFNγ, and (d) TNFα were determined by immunoassay. Basal brain levels of IL10 (a) and NGF (b) were significantly higher in IL10T mice compared with WT animals. After their MCAO induction, both (a) IL10 and (b) NGF levels were significantly increased in IL10T compared with WT mice. (c) IFNγ levels were increased after MCAO in WT mice and to a significantly lesser extent in IL10T mice. (d) TNFα levels were increased to the same level after MCAO in WT and IL10T mice. (e) Basal IL1β levels were significantly higher in WT compared with IL10T mice. After their post-MCAO induction, IL1β levels remained significantly higher in WT mice. Each value is expressed as mean ± SEM ($n = 4$ mice per group) (***$p < 0.001$ indicate comparisons of mice groups with their respective controls; $^{a}p < 0.05$, $^{b}p < 0.01$, $^{c}p < 0.001$ indicate comparison between the genotypes with the same treatment). Data are expressed in pg/mL.

cortical tissue against cerebral ischemia. In line with a previous finding (Bachis *et al.* 2001), this neuroprotective effect was associated to the reduced activity of the pro-apoptotic protein caspase 3. A few previous contributions suggested that exogenous pre/post-ischemic administration of IL10 can provide neuroprotection following focal stroke (Spera *et al.* 1998; Frenkel *et al.* 2003; Ooboshi *et al.* 2005). However, these studies were based on the acute effect of IL10 administration and did not explore the cellular mechanisms involved in this neuroprotection. By using the Tg mice approach, we have been able to investigate the effect of basal IL10 Tg expression confined to brain glial cells (i.e.

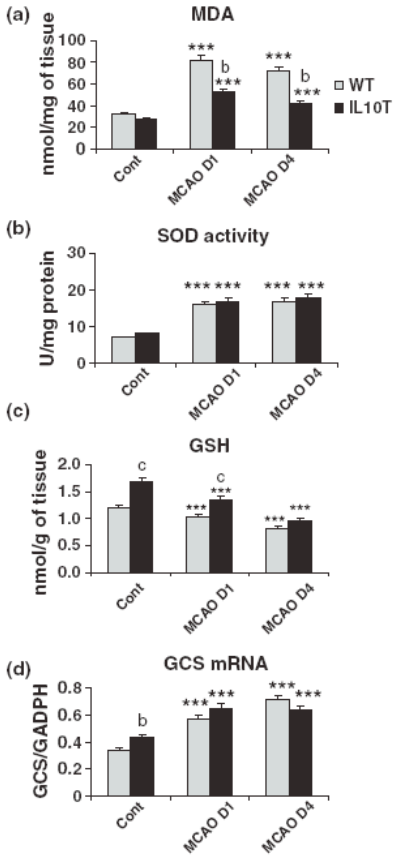

Fig. 5 Brain malondialdahyde (MDA) levels, superoxide dismutase (SOD) activity, and GSH levels on day 1 (D1) and day 4 (D4) after MCAO in WT and IL10T mice. (a) In both WT and IL10T mice, MCAO resulted in an increase in MDA; however, the increase in IL10T mice was less marked in IL10T compared with WT mice. (b) Basal SOD activity did not differ between WT and IL10T mice. MCAO increased SOD activity to similar levels in both genotypes. (c) Basal GSH was higher in IL10T than in WT mice. Although GSH levels were significantly decreased in both WT and IL10T mice 1 day after MCAO, they remained significantly higher in IL10T mice. (d) RT-PCR determination of brain γ-glutamylcysteine synthase (GCS) mRNA induction on day 1 after MCAO in WT and IL10T mice. Gene expression is reported as the ratio of the gene of interest to GADPH mRNA. Basal GCS was higher in IL10T than in WT mice. GCS mRNA was markedly induced following MCAO in both genotypes. Each value is expressed as mean ± SEM ($n = 5$ per group). ***Indicate statistical comparison of WT and IL10T mice with their respective non-treated controls (Cont), [b,c]indicate statistical comparison between WT and IL10T mice subjected to the same treatment (***$p < 0.001$, [b]$p < 0.01$, and [c]$p < 0.001$). Data are expressed in nmol/g of tissue and nmol/mg of tissue for MDA and GSH levels, respectively.

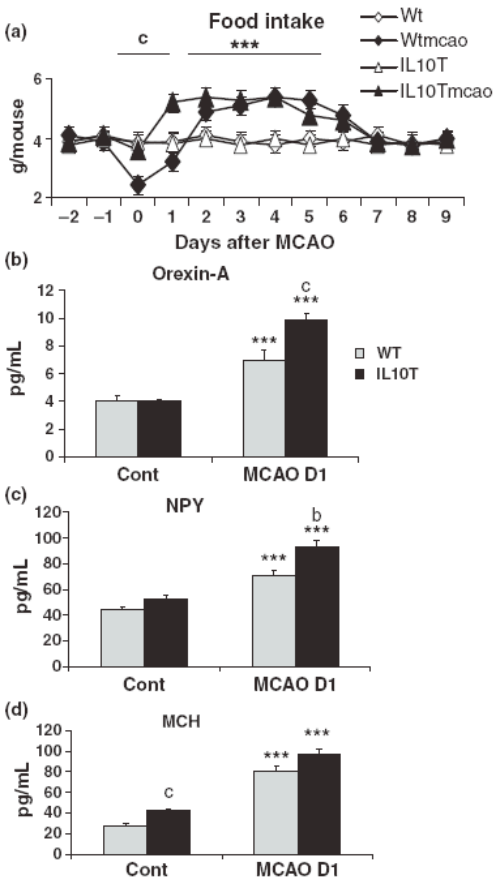

Fig. 6 Food intake responses (a) and hypothalamic protein levels of three orexigenic peptides (b, c, and d) in WT and IL10T mice following MCAO. (a) Over days 0–2, IL10T mice that had undergone ischemia (IL10Tmcao) ate significantly more than WT mice (Wtmcao). WT and IL10T mice showed similar hyperphagia on days 3–5 after MCAO when compared with non-operated mice (Wt and IL10T). Brain orexin-A (b), neuropeptide Y (NPY) (c), and melanin-concentrating hormone (MCH) (d) protein levels on day 1 after MCAO in wild type (WT) and IL10T mice. Basal MCH levels were significantly higher in IL10T compared with WT mice. MCAO resulted in significant increases in orexin-A (b) and NPY (c) in both genotypes. However, the levels of both hormones were significantly higher in IL10T compared with WT mice. (d) MCH levels were similarly increased after MCAO in WT and IL10T mice. Each value is expressed as mean ± SEM; ***$p < 0.001$ indicate comparisons of mice groups with their respective controls; [b]$p < 0.01$, [c]$p < 0.001$ indicate comparison WT and IL10T mice within a treatment group. Each group included 12 (a) and 5 (b, c, and d) mice. Data are expressed in g/mouse (a) and pg/mL for orexin-A, NPY, and MCH protein levels.

microglia, astrocytes, and endothelial cells) and analyze the chronic IL10 induced changes in inflammatory and redox regulation.

Our results provide possible molecular and cellular explanations for this IL10 mediated resistance to MCAO. Although, we cannot exclude that peripheral IL10 effects

may also participate in this phenomenon, the present study focuses on possible central mechanisms. Reduced brain lesion size in IL10 Tg mice was associated with a significant inhibition of the post-ischemic induction of central TNFα, IFNγ, and IL1β, three pro-inflammatory cytokines known to play a crucial role in the pathogenesis of ischemia (Arsenijevic *et al.* 2006). Consistent with these *in vivo* data, previous *in vitro* investigations also indicated that IL10 has the ability to inhibit the glial/lymphocyte production of these cytokines (Moore *et al.* 2001). Moreover, the inhibitory effects of IL10 on pro-inflammatory cytokine production have already been documented in various peripheral inflammatory models including endotoxemia, pancreatitis, or hepatitis (Moore *et al.* 2001). The fact that the protective effect of IL10 may be partly mediated by the relative inhibition of TNFα overproduction parallels previous *in vivo* findings showing that TNFα reduction can protect against ischemic insult (Yang *et al.* 1998). However and in contrast to these observations, neuronal injury after transient ischemia in mice genetically deficient in TNF receptors is known to be exacerbated (Bruce *et al.* 1996). Moreover, the attenuated brain infarction observed following post-ischemic IL10 gene transfer treatment in rats is associated with elevated levels of TNFα (Ooboshi *et al.* 2005). Methodological differences such as the model of cerebral ischemia used (global/focal and transient/permanent) or the post-ischemic interval may explain these discrepancies. In particular, a deleterious effect of TNFα on brain edema has been suggested (Bertorelli *et al.* 1998) and it has been proposed that the presence of TNFα may be neurotoxic or neuroprotective depending on the time points after brain injury (Scherbel *et al.* 1999). Alternatively, the beneficial/detrimental effect of TNFα may depend on threshold levels (Tracey 1995). Unlike TNFα, it is widely admitted that the cytokine IL1β exerts a potent pro-inflammatory effect. For instance, the intracerebroventricular administration of IL1β exacerbates brain damage caused by permanent focal ischemia in the rat (Loddick and Rothwell 1996). In the present experimental setting, the basal decrease in IL1β levels may participate to the increased post-MCAO resistance of IL10T mice. In contrast to pro-inflammatory cytokines, basal NGF levels were markedly elevated in brains of IL10T mice, indicating that IL10 neuroprotection after MCAO may be partly mediated by this anti-inflammatory cytokine (Guegan *et al.* 1999). To our knowledge, the present study is the first to suggest that IL10 can regulate NGF levels *in vivo*.

Another main finding of the present study concerns the effect of IL10 on antioxidant mechanisms associated with MCAO. The decrease in oxidative injury in IL10T mice is documented by the post-ischemic down-regulation of MDA contents. In addition, our data support the view that the anti-inflammatory effects of IL10 are mediated, at least in part, by the ability of IL10 to increase basal GSH levels. The basal increase in GSH could be explained by increased synthesis, decreased degradation or increase uptake of GSH from circulation. The increase in basal GCS mRNA expression in IL10T mice implies that an up-regulation in GSH synthesis may take place. In line with this possibility, a recent *in vitro* study evidenced that GCS gene expression could be up-regulated by IL10 in brain cells (Tu *et al.* 2007). Furthermore, IL10 treatment may prevent decreases in tissue GSH levels as has been shown in a model of renal ischemia-reperfusion injury (Köken *et al.* 2004). At the cellular level, the present work indicates that basal GSH is specifically detected in microglia and endothelial cells of IL10T but not WT brains. As microglia is a major source of ROS, the enhanced basal GSH levels may reduce ROS production following ischemia. Consistent with this protective effect during ischemia in IL10T animals, GSH has also been shown to modulate specific steps of the inflammatory process, including decreases in endothelial permeability and neutrophil–endothelial monolayer binding in response to ischemia–reperfusion (Kokura *et al.* 1999). Interestingly, brain SOD activity did not differ between WT and IL10T mice. However, our immunohistochemical study revealed that WT and IL10T genotypes displayed different MnSOD distribution. For instance, the mitochondrial MnSOD was only detected in IL10T brain endothelial cells. It has been previously suggested that this local MnSOD expression in endothelial cells could prevent the production of ROS. For instance, a protective role for MnSOD has been proposed in endothelial cells and blood–brain barrier following oxidative stress (Schroeter *et al.* 1999). The main objective of the present study was to analyze the molecular determinants of neuroprotection in IL10 Tg mice following brain ischemia so that we focused on antioxidant molecule expression in various types of brain cells as well as cytokines levels known to be produced by microglia, astrocytes, and macrophages. In this respect, morphological analyses including quantification of glial and infiltrating immune cells are warranted to complete our biochemical observations.

Among its plausible mechanisms of action, IL10 overexpression could improve the ischemic outcome by up-regulating glucose metabolism. Glucose is the primary energy source for the brain and, in stroke conditions, there is increased need for glucose because of rapid oxygen depletion. Therefore, brain regulators of intracellular glucose metabolism are important factors to consider in this context (Vannucci *et al.* 1997). We provide here evidence that the two main glucose transporters in the brain (i.e. Glut1 in the blood–brain barrier and Glut4 in neuronal cells) are up-regulated in IL10T mice suggesting that brain glucose uptake might be favored compared with WT mice. We also demonstrate that the G6PDH enzyme activity is up-regulated under basal condition in IL10T mice. As G6PDH is a key regulatory enzyme for the synthesis of NADPH which is involved in GSH production (Spolarics 1998; Wilmanski *et al.* 2005), one could postulate that the increased activity of

glucose transporters and G6PDH may contribute to the observed increase in brain GSH levels.

In the absence of major neurological symptoms in this ischemia model, we focused our analysis of post-ischemic behavioral changes on feeding behavior and showed that ischemic IL10T mice displayed transient hyperphagia that started earlier compared with WT. This finding is consistent with the attenuated post-ischemic induction of anorectic cytokines in the brain (TNFα and IFNγ) (Arsenijevic *et al.* 2006). In agreement with our previous observations in this field, the increased food intake in IL10T mice is associated with basal up-regulation of MCH levels and significant post-MCAO increases in NPY and orexin levels compared with WT mice (Arsenijevic *et al.* 2006). Additional studies are required to determine the role of these neuropeptides and neurotransmitters in altered food intake regulation following MCAO as they are known to influence both immune responses and neurodegeneration (Giuliani *et al.* 2006).

In conclusion, this study shows that IL10T mice were markedly resistant to permanent MCAO as assessed by reduced infarct size. This phenomenon was associated with significant changes in the pre- and post-ischemic regulation of pro- and anti-inflammatory cytokine levels as well as GSH metabolism changes. Importantly, we also documented that IL10 over-expression is associated with cell-specific antioxidant processes involving microglial GSH and endothelial MnSOD/GSH basal levels. Whether IL10 over-expression regulates the above-mentioned molecules directly or indirectly remains to be determined. Similarly, the exact functions of IL10 in the development of cellular/molecular inflammatory processes associated with cerebral ischemia require further clarification. However, these first data in a mouse model constitutively over-expressing IL10 imply that drugs targeting IL10 signaling pathways may prove beneficial in treating stroke by modulating microglia and endothelial cell GSH/MnSOD levels. Further studies including the conditioned expression paradigm are warranted to explore the relevance of IL10 over-expression as a possible molecular target for the treatment of stroke.

Supporting information

Additional Supporting information may be found in the online version of this article:

Materials and methods

Please note: Wiley-Blackwell are not responsible for the content or functionality of any supporting materials supplied by the authors. Any queries (other than missing material) should be directed to the corresponding author for the article.

References

Arsenijevic D., de Bilbao F., Plamondon J., Paradis E., Vallet P., Richard D., Langhans W. and Giannakopoulos P. (2006) Increased infarct size and lack of hyperphagic response after focal cerebral ischemia in peroxisome proliferator-activated receptor β-deficient mice. *J. Cereb. Blood Flow Metab.* **26**, 433–445.

Bachis A., Colangelo A. M., Vicini S., Doe P. P., De Bernardi M. A., Brooker G. and Mocchetti I. (2001) Interleukin-10 prevents glutamate-mediated cerebellar granule cell death by blocking caspase-3-like activity. *J. Neurosci.* **21**, 3104–3112.

Bertorelli R., Adami M., Di Santo E. and Ghezzi P. (1998) MK 801 and dexamethasone reduce both tumor necrosis factor levels and infarct volume after focal cerebral ischemia in the rat brain. *Neurosci. Lett.* **246**, 41–44.

de Bilbao F., Arsenijevic D., Vallet P. *et al.* (2004) Resistance to cerebral ischemic injury in UCP2 knockout mice: evidence for a role of UCP2 as a regulator of mitochondrial glutathione levels. *J. Neurochem.* **89**, 1283–1292.

Bruce A. J., Boling W., Kindy M. S., Peschon J., Kraemer P. J., Carpenter M. K., Holtsberg F. W. and Mattson M. P. (1996) Altered neuronal and microglial responses to excitotoxic and ischemic brain injury in mice lacking TNF receptors. *Nat. Med.* **2**, 788–794.

Ewing J. F. and Janero D. R. (1995) Microplate superoxide dismutase assay employing a nonenzymatic superoxide generator. *Anal. Biochem.* **232**, 243–248.

Fiala M., Zhang L., Gan X. *et al.* (1998) Amyloid-beta induces chemokine secretion and monocyte migration across a human blood–brain barrier model. *Mol. Med.* **4**, 480–489.

Frenkel D., Huang Z., Maron R., Koldzic D. N., Hancock W. W., Moscowitz M. A. and Weiner H. L. (2003) Nasal vaccination with myelin oligodendrocyte glycoprotein reduces stroke size by inducing IL10 producing CD4+ T cells. *J. Immunol.* **171**, 6549–6555.

Gallmann E., Arsenijevic D., Williams G., Langhans W. and Spengler M. (2006) Effect of intraperitoneal CCK-8 on food intake and brain orexin-A after 48 h fasting in the rat. *Regul. Pept.* **133**, 139–146.

Girvin A. M., Gordon K. B., Welsh C. J., Clipstone N. A. and Miller S. D. (2002) Differential abilities of central nervous system resident endothelial cells and astrocytes to serve as inducible antigen-presenting cells. *Blood* **99**, 3692–3701.

Giuliani D., Mioni C., Altavilla D. *et al.* (2006) Both early and delayed treatment with melanocortin 4 receptor stimulating melanocortins produces neuroprotection in cerebral ischemia. *Endocrinology* **147**, 1126–1135.

Guegan C., Ceballos-Picot I., Chevalier E., Nicole A., Onteniente B. and Sola B. (1999) Reduction of ischemic damage in NGF-transgenic mice: correlation with enhancement of antioxidant enzyme activities. *Neurobiol. Dis.* **6**, 180–189.

Köken T., Serteser M., Kahraman A., Akbulut G. and Dilek O. N. (2004) Which is more effective in the prevention of renal ischemia-reperfusion-induced oxidative injury in the early period in mice: interleukin (IL)-10 or anti-IL-12? *Clin. Biochem.* **37**, 50–55.

Kokura S., Wolf R. E., Yoshikawa T., Granger D. N. and Aw T. Y. (1999) Molecular mechanisms of neutrophil–endothelial cell adhesion induced by redox imbalance. *Circ. Res.* **84**, 516–524.

Kouskoff V., Fehling H. J., Lemeur M., Benoist C. and Mathis D. (1993) Q vector driving the expression of foreign cDNAs in the MHC class II positive cells of transgenic mice. *J. Immunol. Methods* **166**, 287–291.

Leon L. R. (2004) Hypothermia in systemic inflammation: role of cytokines. *Front. Biosci.* **9**, 1877–1888.

Li S., Thompson S. A. and Woods J. S. (1996) Localization of gamma-glutamylcysteine synthase mRNA expression in mouse brain following methylmercury treatment using reverse transcription in situ PCR amplification. *Toxicol. Appl. Pharmacol.* **140**, 180–187.

Loddick S. A. and Rothwell N. J. (1996) Neuroprotective effects of human recombinant interleukin-1 receptor antagonist in focal

cerebral ischemia in the rat. *J. Cereb. Blood Flow Metab.* **16**, 932–940.

Moore K. W., de Waal Malefyt R., Coffman R. L. and O'Garra A. (2001) Interleukin-10 and the interleukin-10 receptor. *Annu. Rev. Immunol.* **19**, 683–765.

O'Keefe G. M., Nguyen V. T. and Benveniste E. N. (1999) Class II transactivator and class II MHC gene expression in microglia: modulation by cytokines TGF-β, IL4, IL13 and IL10. *Eur. J. Immunol.* **29**, 1275–1285.

Ooboshi H., Ibayashi S., Shichita T. Y. *et al.* (2005) Postischemic gene transfer of interleukin-10 protects against both focal and global brain ischemia. *Circulation* **111**, 913–919.

Saud K., Herrera-Molina R. and von Bernhardi R. (2005) Pro- and anti-inflammatory cytokines regulate the ERK pathway: implications of the timing for activation of microglial cells. *Neurotox. Res.* **8**, 277–287.

Sawada M., Suzumura A., Hosoya H., Marunouchi T. and Nagatsu T. (1999) Interleukin-10 inhibits both production of cytokines and expression of cytokine receptors in microglia. *J. Neurochem.* **72**, 1466–1471.

Scherbel U., Raghupathi R., Nakamura M., Saatman K. E., Trojanowski J. Q., Neugebauer E., Marino M. W. and McIntosh T. K. (1999) Differential acute and chronic responses of tumor necrosis factor-deficient mice to experimental brain injury. *Proc. Natl Acad. Sci. USA* **96**, 8721–8726.

Schroeter M. L., Mertsch K., Giese H., Muller S., Sporbert A., Hickel B. and Blasig I. E. (1999) Astrocytes enhance radical defence in capillary endothelial cells constituting the blood–brain barrier. *FEBS Lett.* **449**, 241–244.

Spera A., Ellison J. A., Feuerstein G. Z. and Barone F. C. (1998) IL10 reduces brain injury following focal stroke. *Neurosci. Lett.* **251**, 189–192.

Spolarics Z. (1998) Endotoxemia, pentose cycle, and the oxidant/antioxidant balance in hepatic sinusoid. *J. Leukoc. Biol.* **63**, 534–541.

Stoll G., Jander S. and Schroeter M. (1998) Inflammation and glia responses in ischemic brain lesions. *Prog. Neurobiol.* **56**, 149–171.

Tracey K. J. (1995) TNF and Mae West or: death from too much of a good thing. *Lancet* **345**, 75–76.

Tu H., Rady P. L., Juelich T., Tyring S. K., Koldzic-Zinanovic N., Smith E. M. and Hughes T. K. (2007) Interleukin-10 regulated gene expression of hypothalamic – pituitary – adrenal axis origin. *Cell. Mol. Neurobiol.* **27**, 161–170.

Vannucci S. J., Maher F. and Simpson I. A. (1997) Glucose transporter proteins in brain: delivery of glucose to neurons and glia. *Glia* **21**, 2–21.

Viswambharan H., Carvas J. M., Antic V. *et al.* (2007) Mutation of the circadian clock gene Per2 alters vascular endothelial function. *Circulation* **115**, 2188–2195.

Wang Q., Tang X. N. and Yenari M. A. (2007) The inflammatory response in stroke. *J. Neuroimmunol.* **184**, 53–68.

Wilmanski J., Siddiqi M., Deitch E. A. and Spolarics Z. (2005) Augmented IL-10 production and redox dependent signalling pathways in glucose-6-phospahte dehydrogenase deficient mouse peritoneal macrophages. *J. Leukoc. Biol.* **78**, 85–94.

Yang G. Y., Gong C., Qin Z., Ye W., Mao Y. and Bertz A. L. (1998) Inhibition of TNFalpha attenuates infarct volume and ICAM-1 expression in ischemic mouse brain. *Neuroreport* **9**, 2131–2134.

References

Allahtavakoli M, Shabanzadeh A, Roohbakhsh A, Pourshanazari A (2007) Combination therapy of rosiglitazone, a peroxisome proliferator-activated receptor-γ ligand, and NMDA receptor antagonist (MK-801) on experimental embolic stroke in rats. *Basic Clinical Pharmacol Toxicol* 101:309–14.

Anderson MF, Sims NR (2002) The effects of focal ischemia and reperfusion on the glutathione content of mitochondria from rat brain subregions. *J Neurochem* 81:541–549.

Andrews ZB, Diano S, Horvath TL (2005a) Mitochondrial uncoupling proteins in the CNS: in support of function and survival. *Nat Rev Neurosci* 6:829–40.

Andrews ZB, Horvath TL (2009) Uncoupling protein-2 regulates lifespan in mice. *Am J Physiol Endocrinol Metab* 296(4):E621-7.

Andrews ZB, Horvath B, Barnstable CJ, Elseworth J, Yang L, Beal MF, Roth RH, Matthews RT, Horvath TL (2005b) Uncoupling protein-2 is critical for nigral dopamine cell survival in a mouse model of Parkinson's disease. *J Neurosci* 25:184–91.

Andreyev AY, Yu. E. Kushnareva YE, Starkov AA (2005) Mitochondrial Metabolism of Reactive Oxygen Species. *Biochemistry* 70:200-14.

Antonawich FJ, Krajewski S, J. C. Reed JC, Davis JN (1998) Bcl-x(l) Bax interactions after transient global ischemia. *J Cereb Blood Flow Metab* 18:882–6.

Armstrong JS, Steinauer KK, French J, Killoran PL, Walleczek J, Kochanski J, Knox SJ (2001) Bcl-2 inhibits apoptosis induced by mitochondrial uncoupling but does not prevent mitochondrial transmembrane depolarization. *Exp Cell Res* 262:170–9.

Arsenijevic D, Clavel S, Sanchis D, Plamondon J, Huang Q, Ricquier D, Rouger L, Richard D (2007) Induction of UCP2 expression in brain phagocytes and neurons following murine toxoplasmosis: an essential role of IFN-gamma and an association with negative energy balance. *J Neuroimmunol* 186:121–32.

Arsenijevic D, de Bilbao F, Giannakopoulos P, Girardier L, Samec S, Richard D (2001) A role for interferon-γ in the hypermetabolic response to murine toxoplasmosis. *Eur Cytokine Netw* 12:518–27.

Arsenijevic D, Girardier L, Seydoux J, Chang HR, Dulloo AG (1997) Altered energy balance and cytokine gene expression in a murine model of chronic infection with Toxoplasma gondii. *Am J Physiol* 272:E908–E917.

Arsenijevic D, Girardier L, Seydoux J, Pechere JC, Garcia I, Lucas R, Chang HR, Dulloo AG (1998) Metabolic cytokine responses to a secondary immunological challenge with LPS in mice with T. gondii infection. *Am J Physiol* 274:E439–E445.

Arsenijevic D, Onuma H, Pecqueur C, Raimbault S, Manning BS, Miroux B, Couplan E, Alves-Guerra MC, Goubern M, Surwit R *et al.* (2000) Disruption of the uncoupling protein-2 gene in mice reveals a role in immunity and reactive oxygen species production. *Nat Genet* 26:435–9.

Ashkenazi A (2002) Targeting death and decoy receptors of the tumour-necrosis factor superfamily. *Nat Rev Cancer* 2(6):420-30.

Astrup J, Symon L, Siesjö BK (1981) Thresholds in cerebral ischemia—The ischemic penumbra. *Stroke* 12:723–25.

Aubert J, Champigny O, Saint-Marc P, Negrel R, Collins S, Ricquier D, Ailhaud G (1997) Upregulation of UCP-2 gene expression by PPAR agonists in preadipose and adipose cells. *Biochem Biophys Res Commun* 238:606–11.

Bai Y, Onuma H, Bai X, Medvedev AV, Misukonis M, Weinberg JB, Cao W, Robidoux J, Floering LM, Daniel KW, Collins S (2005) Persistent nuclear factor-kappa B activation in Ucp2-/- mice leads to enhanced nitric oxide and inflammatory cytokine production. *J Biol Chem* 280:19062–9.

Baird AE (2006) The forgotten lymphocyte: immunity and stroke. *Circulation* 113: 2035–6.

Bakhshi A, Jensen JP, Goldman P, Wright JJ, McBride OW, Epstein AL, Korsmeyer SJ (1985) Cloning the chromosomal breakpoint of t(14;18) human lymphomas: clustering around JH onchromosome 14 and near a transcriptional unit on 18. *Cell* 41:899–906.

Bano D, Nicotera P (2007) Ca2+ signals and neuronal death in brain ischemia. *Stroke* 38:674–6.

Barish GD, Atkins AR, Downes M, Olson P, Chong LW, Nelson M, Zou Y, Hwang H, Kang H, Curtiss L, *et al.* (2008) *Proc Natl Acad Sci USA* 105:4271–6.

Barone FC, Arvin B, White RF, Miller A, Webb CL, Willette RN, Lysko PG, Feuerstein GZ (1997) Tumor necrosis factor-alpha. A mediator of focal ischemic brain injury. *Stroke* 28 :1233–44.

Bates S, Read SJ, Harrison DC, Topp S, Morrow R, Gale D, Murdock P, Barone FC, Parsons AA, Gloger IS (2001) Characterisation of gene expression changes following permanent MCAO in the rat using subtractive hybridisation. Brain Res Mol Brain Res 93:70–80.

Bayes M, Rabasseda X (2008) Gateways to clinical trials. *Methods Find Exp Clin Pharmacol* 30:67–99.

Bechmann I, Diano S, Warden CH, Bartfai T, Nitsch R Horvath TL (2002) Brain mitochondrial uncoupling protein 2 (UCP2): a protective stress signal in neuronal injury. *Biochem Pharmacol* 64: 363–7.

Behl C, Hovey L, Krajewski S, Schubert D, Reed JC (1993) Bcl-2 prevents killing of neuronal cells by glutamate but not by amyloid p protein. *Biochem Biophys Res Commun* 197:949-56.

Behringer W, Kentner R, Wu X, Tisherman SA, Radovsky A, Stezoski WS, Henchir J, Prueckner S, Safar P (2001) Thiopental and phenytoin by aortic arch flush for cerebral preservation during exsanguination cardiac arrest of 20 minutes in dogs. An exploratory study. *Resuscitation* 49:83–97.

Benchoua, A, Guegan C, Couriaud C, Hosseini H, Sampaio N, Morin D, Onteniente B (2001) Specific caspase pathways are activated in the two stages of cerebral infarction. *J Neurosci* 21:7127–34.

Bharath S, Hsu M, Kaur D, Rajagopalan S, Andersen JK (2002) Glutathione, iron and Parkinson's disease. *Biochem Pharmacol* 64:1037-48.

Bi FF, Xiao B, Hu YQ, Tian FF, Wu ZG, Ding L, Zhou XF (2008) Expression and localization of Fas-associated proteins following focal cerebral ischemia in rats. *Brain Res* 1191:30-8.

Bogousslavsky J, Regli F, Uske A (1988) Thalamic infarcts: clinical syndromes, etiology, and prognosis. *Neurology* 38:837-48.

Bonita R (1992) Epidemiology of stroke. *Lancet* 339:342–344.

Bordet R, Deplanque D, Maboudou P, Puisieux F, Pu Q, Robin E, Martin A, Bastide M, Leys D, Lhermitte M, Dupuis B (2000) Increase in endogenous brain superoxide dismutase as a potential mechanism of lipopolysaccharide-induced brain ischemic tolerance. *J Cereb Blood Flow Metab* 20:1190–6.

Bordet R, Gele P, Duriez P, Fruchart JC (2006) PPARs: a new target for neuroprotection. *J Neurol Neurosurg and Psychiatry* 77:285–6.

Borner C (2003) The Bcl-2 protein family: sensors and checkpoints for life-or-death decisions. *Mol Immunol* 39(11):615-47.

Brouns R, De Deyn PP (2009) The complexity of neurobiological processes in acute ischemic stroke. *Clin Neurol Neurosurgery* 111:483–95.

Bruce AJ, Boling W, Kindy MS, Peschon J, Kraemer PJ, Carpenter MK, Holtsberg FW, Mattson MP (1996) Altered neuronal and microglial responses to excitotoxic and ischemic brain injury in mice lacking TNF receptors. Nat Med 2:788–794.

Cai JY, Jones DP (1998) Superoxide in apoptosis. Mitochondrial generation triggered by cytochrome c loss. *J Biol Chem* 273:11401–4.

Cardenas A, Moro MA, Leza JC, O'Shea E, Davalos A, Castillo J, Lorenzo P, Lizasoain I (2002) Upregulation of TACE/ADAM17 after ischemic preconditioning is involved in brain tolerance. *J Cereb Blood Flow Metab* 22:1297–302.

Chan PH (2001) Reactive Oxygen Radicals in Signaling and Damage in the Ischemic Brain. *J Cereb Blood Flow Metab* 21:2-14.

Cisowski J, Zarebski A, Koj A (2002) IL-1 mediated inhibition of IL-6-induced STAT3 activation is modulated by IL-4, MAP kinase inhibitors and redox state of HepG2 cells. *Folia Histochem Cytobiol* 40:341–5.

Clavel S, Paradis E, Ricquier D, Richard D (2003) Kainic acid upregulates uncoupling protein-2 mRNA expression in the mouse brain. *Neuroreport* 14:2015–7.

Cohen G M (1997) Caspases: the executioners of apoptosis. *Biochem J* 326:1–16.

Collino M, Aragno M, Mastrocola R, Benetti E, Gallicchio M, Dianzani C, Danni O, Thiemermann C, Fantozzi R (2006) Oxidative stress and inflammatory response evoked by transient cerebral ischemia/reperfusion: Effects of the PPAR-α agonist WY14643. *Free Radical Biol Metab* 41:579–89.

Conroy BP, Lin CY, Jenkins LW, DeWitt DS, Zornow MH, Uchida T, Johnston WE (1998) Hypothermic modulation of cerebral ischemic injury during cardiopulmonary bypass in pigs. *Anesthesiology* 88:390–402.

Cory S, Adams JM (2002) The Bcl2 family: regulators of the cellular life-or-death switch. *Nat Rev Cancer* 2:647–56.

Cullingford TE, Bhakoo K, Peuchen S, Dolphin CT, Patel R, Clark JB (1998) Distribution of mRNAs encoding the peroxisome proliferator-activated receptor alpha, beta, and gamma and the retinoid X receptor alpha, beta, and gamma in rat central nervous system. *J Neurochem* 70:1366–75.

Danial NN, Korsmeyer SJ (2004) Cell death: critical control points. *Cell* 116:205-19.

Davies CA, Loddick SA, Toulmond S, Stroemer RP, Hunt J, Rothwell NJ (1999) The progression and topographic distribution of interleukin-1 beta expression after permanent middle cerebral artery occlusion in the rat. *J Cereb Blood Flow Metab* 19: 87–98.

Dawson DA, Furuya K, Gotoh J, Nakao Y, Hallenbeck JM (1999) Cerebrovascular hemodynamics and ischemic tolerance: lipopolysaccharide-induced resistance to focal cerebral ischemia is not due to changes in severity of the initial ischemic insult, but is associated with preservation of microvascular perfusion. *J Cereb Blood Flow Metab* 19:616–23.

de Bilbao F, Arsenijevic D, Vallet P, Hjelle OP, Ottersen OP, Bouras C, Raffin Y, Abou K, Langhans W, Collins S *et al.* (2004) Resistance to cerebral ischemic injury in UCP2 knockout mice: evidence for a role of UCP2 as a regulator of
mitochondrial glutathione levels. *J Neurochem* 89:1283–92.

Degasperi GR, Romanatto T, Denis RG, Araujo EP, Moraes JC, Inada NM, Vercesi AE, Velloso LA (2008) UCP2 protects hypothalamic cells from TNF-alpha-induced damage. *FEBS Lett* 582:3103–10.

Deierborg T, Wieloch T, Diano S, Warden CH, Horvath TL, Mattiasson G (2008) Overexpression of UCP2 protects thalamic neurons following global ischemia in the mouse. *J Cereb Blood Flow Metab* 28:1186–95.

De Keyser J, Sulter G, Luiten PG (1999) Clinical trials with neuroprotective drugs in acute ischaemic stroke: are we doing the right thing? *Trends Neurosci* 22:535–40.

Delerive P, Fruchart JC, Staels B (2001) Peroxisome proliferator-activated receptors in inflammation control. *J Endocrinol* 169:453–9.

Del Zoppo GJ, Poeck K, Pessin MS, Wolpert SM, Furlan AJ, Ferbert A, Alberts MJ, Zivin JA, Wechsler L, Busse O *et al*. (1992) Recombinant tissue plasminogen activator in acute thrombotic and embolic stroke. *Ann Neurol* 32:78–86.

Deplanque D, Gele P, Petrault O, Six I, Furman C, Bouly M, Nion S, Dupuis B, Leys D, Fruchart JC *et al*. (2003) Peroxisome proliferators activated receptora activation as a mechanism for preventive neuroprotection induced by fenofibrate treatment. *J Neurosci* 23:6264–71.

Derdak Z, Mark NM, Beldi G, Robson SC, Wands JR, Baffy G (2008) The mitochondrial uncoupling protein-2 promotes chemoresistance in cancer cells. *Cancer Res* 68:2813–9.

Diano S, Matthews RT, Patrylo P, Yang L, Beal MF, Barnstable CJ, Horvath TL (2003) Uncoupling protein 2 prevents neuronal death including that occurring during seizures: a mechanism for preconditioning. *Endocrinology* 144:5014–21.

Dijkhuizen RM, Beekwilder JP, van derWorp HB, Berkelbach van der Sprenkel JW, Tulleken KA, Nicolay K (1999) Correlation between tissue depolarizations and damage in focal ischemic rat brain. *Brain Res* 840:194–205.

Dimitrijevic OB, Stamatovic SM, Keep RF, Andjelkovic AV (2006) Effects of the chemokine CCL2 on blood–brain barrier permeability during ischemiareperfusion injury. *J Cereb Blood Flow Metab* 26:797–810.

Dirnagl U, Iadecola C, Moskowitz MA (1999) Pathobiology of ischaemic stroke: an integrated view. *Trends Neurosci* 22:391–7.

Dirnagl U, Lindauer U, Them A, Schreiber S, Pfister HW, Koedel U, Reszka R, Freyer D, Villringer A (1995) Global cerebral ischemia in the rat: online monitoring of oxygen free radical production using chemiluminescence *in vivo*. *J Cereb Blood Flow Metab* 15:929–40.

Dirnagl U, Simon RP, Hallenbeck JM (2003) Ischemic tolerance and endogenous neuroprotection. *Trends Neurosci* 26:248–54.

Dreier JP, Woitzik J, Fabricius M, Bhatia R, Major S, Drenckhahn C, Lehmann TN, Sarrafzadeh A, Willumsen L, Hartings JA *et al.* (2006) Delayed ischaemic neurological deficits after subarachnoid haemorrhage are associated with clusters of spreading depolarizations. *Brain* 129:3224–37.

Donnan GA, Fisher M, Macleod M, Davis SM (2008) Stroke. *Lancet* 371:1612–23.

Doonan F, Wallace DM, O'Driscoll C, Cotter TG (2009) Rosiglitazone acts as a neuroprotectant in retinal cells via up-regulation of sestrin-1 and SOD-2. *J Neurochem* 109:631-43.

Dringen R (2005) Oxidative and antioxidative potential of brain microglial cells. *Antioxid Redox Signal* 7:1223-33.

Duval C, Negre-Salvayre A, Dogilo A, Salvayre R, Penicaud L, Casteilla L (2002) Increased reactive oxygen species production with antisense oligonucleotides directed against uncoupling protein 2 in murine endothelial cells. *Biochem Cell Biol* 80:757–64.

Ellerby LM, Ellerby HM, Park SM, Holleran AL, Murphy AN, Kane DJ, Testa MP, Kayalar C, Bredesen DE (1996) Shift of the cellular oxidation–reduction potential in neural cells expressing bcl-2. *J Neurochem* 67:1259–67.

Escher P and Wahli W (2000) Peroxisome proliferator-activated receptors: insight into multiple cellular functions. *Mutation Research* 448:121–38.

Fernandez-Checa JC, Kaplowitz N (2005) Hepatic mitochondrial glutathione: transport and rolein disease and toxicity. *Toxicol Appl Pharmacol* 204 :263–73.

Ferrer I, Friguls B, Dalfo E, Justicia C, Planas AM (2003) Caspase-dependent and caspase-independent signalling of apoptosis in the penumbra following middle cerebral artery occlusion in the adult rat. *Neuropathol Appl Neurobiol* 29:472–81.

Fink BD, Reszka KJ, Herlein JA, Mathahs MM, Sivitz WI (2005) Respiratory uncoupling by UCP1 and UCP2 and superoxide generation in endothelial cell mitochondria. *Am J Physiol Endocrinol Metab* 288:E71–9.

Flanders KC, Ren RF, Lippa CF (1998) Transforming growth factor betas in neurodegenerative disease. *Prog Neurobiol* 54:71–85.

Fleury C, Neverova M, Collins S, Raimbault S, Champigny O, Levi-Meyrueis C, Bouillaud F, Seldin MF, Surwit RS, Ricquier D, Warden CH (1997) Uncoupling protein-2: a novel gene linked to obesity and hyperinsulinemia. *Nat Genet* 15:269–72.

Fujie W, Kirino T, Tomukai N, Iwasawa T, Tamura A (1990) Progressive shrinkage of the thalamus following middle cerebral artery occlusion in rats. *Stroke* 21:1485-88.

Furukawa S, Furukawa Y, Satoyoshi E, Hayashi K (1986) Synthesis and secretion of nerve growth factor by mouse astroglial cells in culture. *Biochem Biophys Res Commun* 136:57–63.

Galluzzi L, Aaronson SA, Abrams J, Alnemri ES, Andrews DW, Baehrecke EH, Bazan NG, Blagosklonny MV, Blomgren K, Borner C *et al.* (2009a) Guidelines for the use and interpretation of assays for monitoring cell death in higher eukaryotes. *Cell Death Differ* 16:1093-107.

Galluzzi L, Blomgren K, Kroemer G (2009b) Mitochondrial membrane permeabilization in neuronal injury. *Nat Rev Neurosci* 10:481-94.

Gary DS, Bruce-Keller AJ, Kindy MS, Mattson MP (1998) Ischemic and excitotoxic brain injury is enhanced in mice lacking the p55 tumor necrosis factor receptor. *J Cereb Blood Flow Metab* 18:1283–7.

Gill R, Soriano M, Blomgren K, Hagberg H, Wybrecht R, Miss MT, Hoefer S, Adam G, Niederhauser O, Kemp JA, Loetscher H (2002) Role of caspase-3 activation in cerebral ischemia-induced neurodegeneration in adult and neonatal brain. *J Cereb Blood Flow Metab* 22:420–30.

Gillardon F, Lenz C, Waschke KF, Krajewski S, Reed JC, Zimmermann M, Kuschinsky W (1996) Altered expression of Bcl-2 Bcl-x, Bax, and C-Fos colocalizes with DNA fragmentation and ischemic cell damage following middle cerebral artery occlusion in rats. *Mol Brain Res* 40:254–60.

Ginsberg MD (2003) Adventures in the pathophysiology of brain ischemia: penumbra, gene expression, neuroprotection. The 2002 Thomas Willis Lecture. *Stroke* 34:214–23.

Green RA, Odergren T, Ashwood T (2003) Animal models of stroke: do they have value for discovering neuroprotective agents? *Trends Pharmacol Sci* 24:402–8.

Green DR, Reed JC (1998) Mitochondria and apoptosis. Science 281:1309–12.

Guegan C, Onteniente B, Makiura Y, Merad-Boudia M, Ceballos-Picot I, Sola B (1998) Reduction of cortical infarction and impairment of apoptosis in NGF-transgenic mice subjected to permanent focal ischemia. *Brain Res Mol Brain Res* 55:133–40.

Guegan C, Ceballos-Picot I, Chevalier E, Nicole A, Onteniente B, Sola B (1999) Reduction of ischemic damage in NGF-transgenic mice: correlation with enhancement of antioxidant enzyme activities *Neurobiol Dis* 6:180-9.

Gillardon F, Lenz C, Waschke KF, Krajewski S, Reed JC, Zimmermann M, Kuschinsky W (1996) Altered expression of Bcl-2, Bcl-x, Bax and c-Fos co-localizes with DNA fragmentation and ischemic damage following middle cerebral artery occlusion in rats. *Mol Brain Res* 40:254–60.

Haddad JJ, Harb HL (2005) L-gamma-Glutamyl-L-cysteinyl-glycine (glutathione; GSH) and GSH-related enzymes in the regulation of pro- and anti-inflammatory cytokines: a signaling transcriptional scenario for redox(y) immunologic sensor(s)? *Mol Immunol*. 42:987-1014.

Hallenbeck JM (2002) The many faces of tumor necrosis factor in stroke. *Nat Med* 8:1363–8.

Hara H, Fink K, Endres M, Friedlander RM, Gagliardini V, Yuan J, Moskowitz MA, (1997) Attenuation of transient focal cerebral ischemic injury in transgenic mice expressing a mutant ICE inhibitory protein. *J Cereb Blood Flow Metab* 17 :370–5.

Hartings JA, Rolli ML, Lu XC, Tortella FC (2003) Delayed secondary phase of periinfarct depolarizations after focal cerebral ischemia: relation to infarct growth and neuroprotection. *J Neurosci* 23:11602–10.

Hata R, Gillardon F, Michaelidis TM, Hossmann KA (1999) Targeted disruption of the bcl-2 gene in mice exacerbates focal ischemic brain injury. *Metab Brain Dis* 14:117–24.

Henry-Mowatt J, Dive C, Martinou JC, James D (2004) Role of mitochondrial membrane permeabilization in apoptosis and cancer. *Oncogene* 23:2850–60.

Hesselgesser J, Horuk R (1999) Chemokine and chemokine receptor expression in the central nervous system. J Neurovirol 5:13–26.

Hidaka S, Kakuma T, Yoshimatsu H, Yasunaga S, Kurokawa M, Sakata T (1998) Molecular cloning of rat uncoupling protein 2 cDNA and its expression in genetically obese Zucker fatty (fa/fa) rats. *Biochim Biophys Acta* 1389:178–86.

Hill M M, Adrain C, Duriez PJ, Creagh EM, Martin SJ (2004). Analysis of the composition, assembly kinetics and activity of native Apaf-1 apoptosomes. *Embo J* 23:2134–45.

Hochman A, Sternin H, Gorodin S, Korsmeyer S, Ziv I, Melamed E, Offen D (1998) Enhanced oxidative stress and altered antioxidants in brains of Bcl-2-deficient mice. *J Neurochem* 71:741–8.

Hockenbery DM, Oltvai ZN, Yin XM, Milliman CL, Korsmeyer SJ (1993) Bcl-2 functions in an antioxidant pathway to prevent apoptosis. *Cell* 75: 241-51.

Horimoto M, Fulop P, Derdak Z, Wands JR, Baffy G (2004) Uncoupling protein-2 deficiency promotes oxidant stress and delays liver regeneration in mice. *Hepatology* 39:386–92.

Horvath TL, Warden CH, Hajos M, Lombardi A, Goglia F, Diano S (1999) Brain uncoupling protein 2: uncoupled neuronal mitochondria predict thermal synapses in homeostatic centers. *J Neurosci* 19:10417–27.

Iijima T (2006) Mitochondrial membrane potential and ischemic neuronal death. *Neurosci Res* 55:234–43.

Iijima T, Mies G, Hossmann KA (1992) Repeated negative DC deflections in rat cortex following middle cerebral artery occlusion are abolished by MK-801. Effect on volume of ischemic injury. *J Cereb Blood Flow Metab* 12**:**727–33.

Iizuka H, Sakatani K, Young W (1990) Neural damage in the rat thalamus after cortical infarcts. *Stroke* 21:790–4.

Inoue I, Goto S, Matsunaga T, Nakajima T, Awata T, Hokari S, Komoda T, Katayama S (2001) The ligands/activators for peroxisome proliferator-activated receptor alpha (PPARalpha) and PPARgamma increase Cu2+, Zn2+-superoxide dismutase and decrease p22phox message expressions in primary endothelial cells. *Metabolism* 50:3–11.

Inoue H, Jiang XF, Katayama T, Osada S, Umesono K, Namura S (2003) Brain protection by resveratrol and fenofibrate against stroke requires peroxisome proliferator-activated receptor a in mice. *Neurosci Lett* 352:203–6.

Ito S, Ansari P, Sakatsume M, Dickensheets H, Vasquez N, Donelly RP, Larner AC, Finbloom DS (1999) Interleukin-10 inhibits expression of both interferon-α- and interferon-γ-induced genes by suppressing tyrosine phosphorylation of Stat1. *Blood* 93:1456–63.

Iwashita A, Muramatsu Y, Yamazaki T, Muramoto M, Kita Y, Yamazaki S, Mihara K, Moriguchi A, Matsuoka N (2007) Neuroprotective efficacy of the peroxisome proliferator-activated receptor delta-selective agonists in vitro and in vivo. *J Pharmacol Exp Ther* 320:1087-96.

Iwata-Ichikawa E, Kondo Y, Miyazaki I, Asanuma M, Ogawa N (1999) Glial cells protect neurons against oxidative stress *via* transcriptional up-regulation of the glutathione synthesis. *J Neurochem* 72:2334-44.

Jacobson S, Trojanowski JQ (1975) Corticothalamic neurons and thalamocortical terminal fields: an investigation in rat using horseradish peroxidase and autoradiography. *Brain Res* 85:385-401.

Jo D, Liu D, Yao S, Collins RD, Hawiger J (2005) Intracellular protein therapy with SOCS3 inhibits inflammation and apoptosis. *Nat Med* 11:892–8.

Kane DJ, Sarafian TA, Anton R, Hahn H, Gralla EB, Valentine JS, Ord T, Bredesen DE (1993) Bcl-2 inhibition of neural death: decreased generation of reactive oxygen species. *Science* 262:1274-7.

Kerr JF, Wyllie A., Currie AR (1972) Apoptosis: a basic biological phenomenon with wide-ranging implications in tissue kinetics. *Br J Cancer* 26:239–57.

Kersten S, Desvergne B, Wahli W (2000) Roles of PPARs in health and disease. *Nature* 405:421–4.

Kirino T (2002) Ischemic tolerance. *J Cereb Blood Flow Metab* 22:1283–96.

Koppal T, Petrova TV, Van Eldik LJ (2000) Cyclopentenone prostaglandin 15-deoxy-Δ12,14-prostaglandin J2 acts as a general inhibitor of inflammatory responses in activated BV-2 microglial cells. *Brain Research* 867:115–21.

Kostulas N., Pelidou SH, Kivisakk P, Kostulas V, Link H (1999) Increased IL-1beta, IL-8, and IL-17 mRNA expression in blood mononuclear cells observed in a prospective ischemic stroke study. *Stroke* 30:2174–9.

Krauss S, Zhang CY, Lowell BB (2005) The mitochondrial uncoupling protein homologues. *Nat Rev Mol Cell Biol* 6:248-61.

Krep H, Bottiger BW, Bock C, Kerskens CM, Radermacher B, Fischer M, Hoehn M, Hossmann KA (2003) Time course of circulatory and metabolic recovery of cat brain after cardiac arrest assessed by perfusion- and diffusion-weighted imaging and MR-spectroscopy. *Resuscitation* 58:337–48.

Kroemer G, Galluzzi L, Vandenabeele P, Abrams J, Alnemri ES, Baehrecke EH, Blagosklonny MV, El-Deiry WS, Golstein P, Green DR *et al.* (2009) Classification of cell death: recommendations of the Nomenclature Committee on Cell Death. *Cell Death Differ* 16:3–11.

Kroemer G, Reed JC (2000) Mitochondrial control of cell death. *Nature Med* 6**:**513–9.

Kudin AP, Malinska D, Kunz WS (2008) Sites of generation of reactive oxygen species in homogenates of brain tissue determined with the use of respiratory substrates and inhibitors. *Biochim Biophys Acta* 1777:689–95.

Lambertsen K L, Gregersen R, Meldgaard M, *et al*. (2004) A role for interferon-gamma in focal cerebral ischemia in mice. *J Neuropathol Exp Neurol* 63**.**942–955.

Lapchak PA, Araujo DM, Pakola S, Song D, Wei J, Zivin JA (2002) Microplasmin: a novel thrombolytic that improves behavioral outcome after embolic strokes in rabbits. *Stroke* 33:2279–84.

Lavrik IN, Golks A, Krammer PH (2005) Caspases: pharmacological manipulation of cell death. *J Clin Invest* 115:2665–72.

Lawrence MS, Ho DY, Sun GH, Steinberg GK, Sapolsky RM (1996) Overexpression of bcl-2 with herpes simplex virus vectors protects CNS neurons against neurological insults in *vitro* and *in vivo. J Neurosci* 16:486-96.

Lee TH, Kato H, Chen ST, Kogure K, Itoyama Y (1998) Expression of nerve growth factor and trkA after transient focal cerebral ischemia in rats. Stroke 29:1687–97.

Li HL, Kostulas N, Huang YM, Xiao BG, van der Meide P, Kostulas V, Giedraitas V, Link H (2001) IL-17 and IFN-gamma mRNA expression is increased in the brain and systemically after permanent middle cerebral artery occlusion in the rat. *J Neuroimmunol* 116:5–14.

Liang D, Dawson TM, Dawson VL (2004) What have genetically engineered mice taught us about ischemic injury? *Curr Mol Med* 4:207-25.

Lin TN, He YY, Wu G, Khan M, Hsu CY (1993) Effect of brain edema on infarct Volume in a focal cerebral ischemia model in rats. *Stroke* 24:117-21.

Lindvall O, Ernfors P, Bengzon J, Kokaia Z, Smith ML, Siesjö BK, Persson H (1992) Differential regulation of mRNAs for nerve growth factor, brain-derived neurotrophic factor, and neurotrophin-3 in the adult rat brain following cerebral ischemia and hypoglycaemic coma. *Proc Natl Acad Sci USA* 89:648–652.

Linnik MD, Zahos P, Geschwind MD, Federoff HJ (1995). Expression of bcl-2 from a defective herpes simplex virus- 1 vector limits neuronal death in focal cerebral ischemia. *Stroke* 26:1670-4.

Lipton P (1999) Ischemic cell death in brain neurons. *Physiol Rev* 79: 1431–568.

Lo EH, Dalkara T, Moskowitz MA (2003) Mechanisms, challenges and opportunities in stroke. *Nat Rev Neurosci* 4:399–415.

Loddick SA, Turnbull AV, Rothwell NJ (1998) Cerebral interleukin-6 is neuroprotective during permanent focal cerebral ischemia in the rat. J *Cereb Blood Flow Metab* 18:176–9.

Lu YZ, Lin CH, Cheng FC, Hsueh CM (2005) Molecular mechanisms responsible for microglia-derived protection of Sprague–Dawley rat brain cells during in vitro ischemia. *Neurosci Lett* 373:159–64.

Luna-Medina R, Cortes-Canteli M, Alonso M, Santos A, Martınez A, Perez-Castillo A (2005) Regulation of inflammatory response in neural cells in vitro by thiadiazolidinones derivatives through peroxisome proliferator-activated receptor γ activation. *Journal of Biological Chemistry* 280:21453–62.

Mabuchi T, Kitagawa K, Ohtsuki T, Kuwabara K, Yagita Y, Yanagihara T, Hori M, Matsumoto M (2000) Contribution of microglia ⁄ macrophages to expansion of infarction and response of oligodendrocytes after focal cerebral ischemia in rats. *Stroke* 31:1735–43.

MacManus JP, Buchan AM (2000) Apoptosis after experimental stroke: fact or fashion? *J Neurotrauma* 17:899–914.

Madrigal JL, Kalinin S, Richardson JC, Feinstein DL (2007) Neuroprotective actions of noradrenaline: effects on glutathione synthesis and activation of peroxisome proliferator activated receptor delta. *J Neurochem* 103:2092–101.

Maier CM, Chan PH (2002) Role of superoxide dismutases in oxidative damage and neurodegenerative disorders. *Neuroscientist* 8:323-34.

Maragos WF, Korde AS (2004) Mitochondrial uncoupling as a potential therapeutic target in acute central nervous system injury. *J Neurochem* 91:257–62.

Martin-Villalba A, Herr I, Jeremias I, Hahne M, Brandt R, Vogel J, Schenkel J, Herdegen T, Debatin KM (1999) CD95 ligand (Fas-L/APO-1L) and tumor necrosis factor-related apoptosis-inducing ligand mediate ischemia-induced apoptosis in neurons. *J. Neurosci*. 19 :3809–17.

Martinou JC, Dubois-Dauphin M, Staple JK, Rodriguez I, Frankowski H, Missoten M, Albertini P, Talabot D, Catsicas S, Pietra C, Huarte J (1994) Overexpression of BCL-2 in transgenic mice protects neurons from naturally occurring cell death and experimental ischemia. *Neuron* 13:1017-30.

Matsushita K, Matsuyama T, Kitagawa K, Matsumoto M, Yanagihara T, Sugita M (1998) Alterations of Bcl-2 family proteins precede cytoskeletal proteolysis in the penumbra, but not in the infarct cortex following focal cerebral ischemia in mice. *Neuroscience* 83:439–48.

Mattiasson G, Shamloo M, Gido G, Mathi K, Tomasevic G, Yi S, Warden CH, Castilho RF, Melcher T, Gonzalez-Zulueta K *et al.* (2003) Uncoupling protein-2 prevents neuronal death and diminishes brain dysfunction after stroke and brain trauma. *Nat Med* 9:1062–8.

Mattiasson G, Sullivan PG (2006) The emerging functions of UCP2 in health, disease, and therapeutics. *Antioxid Redox Signal* 8:1–38.

Mazzotta G, Sarchielli P, Caso V, Paciaroni M, Floridi A, Floridi A, Gallai V (2004) Different cytokine levels in thrombolysis patients as predictors for clinical outcome. *Eur J Neurol* 11:377–81.

McColl BW, Allan SM, Rothwell NJ (2009) Systemic infection, inflammation and acute ischemic stroke. *Neuroscience* 158:1049-61.

McIlvoy LH (2005) The effect of hypothermia and hyperthermia on acute brain injury. *AACN Clin Issues* 16:488–500.

Mehta SL, Li PA (2009) Neuroprotective role of mitochondrial uncoupling protein 2 in cerebral stroke. *J Cereb Blood Flow & Metab* 29:1069–78.

Mergenthaler P, Dirnagl U, Meisel A (2004) Pathophysiology of stroke: lessons from animal models. *Metab Brain Dis* 19:151–67.

Mies G, Iijima T, Hossmann KA (1993) Correlation between periinfarctDC shifts and ischemic neuronal damage in rat. *NeuroReport* 4:709–11.

Monney L, Otter I, Olivier R., Ravn U., Poirer GG, Borner C (1996) Bcl-2 overexpression blocks activation of the death protease CPP32/Yama/Apopain. *Biochem Biophys Res Commun* 221: 340–5.

Moraes L, Piqueras L, Bishop-Bailey D (2006) Peroxisome proliferator-activated receptors and inflammation. *Pharmacol Ther* 110:371–85.

Moreno S, Farioli-Vecchioli S, Ceru MP (2004) Immunolocalization of peroxisome proliferator-activated receptors and retinoid x receptors in the adult rat CNS. *Neuroscience* 123:131–45.

Morioka T, Kalehua AN, Streit WJ (1993) Characterization of microglial reaction after middle cerebral artery occlusion in rat brain. *J Comp Neurol* 327:123–32.

Murakami K, Kondo T, Kawase M, Li Y, Sato S, Chen SF, Chan PH (1998) Mitochondrial susceptibility to oxidative stress exacerbates cerebral infarction that follows permanent focal cerebral ischemia in mutant mice with manganese superoxide dismutase deficiency. *J Neurosci* 18:205–13.

Murphy AN, D. E. Bredesen DE, G. Cotopassi G, Wang E, Fiskum G (1996). Bcl-2 potentiates the maximal calcium uptake capacity of neural cell mitochondria. *Proc Natl Acad Sci USA* 93:9893–8.

Myers KM, Fiskum G, Liu Y, Simmens SJ, Bredesen DE, Murphy AN (1995) Bcl-2 protects neural cells from cyanide/aglycemia-induced lipid oxidation, mitochondrial injury and loss of viability. *J Neurochem* 65:2432–40.

Miyawaki T, Mashiko T, Ofengeim D, Flannery RJ, Noh KM, Fujisawa S, Bonanni L, Bennett MV, Zukin RS, Jonas EA (2008) Ischemic preconditioning blocks BAD translocation, Bcl-xL cleavage, and large channel activity in mitochondria of postischemic hippocampal neurons. *Proc Natl Acad Sci USA* 105:4892–7.

Nakase T, Yoshida Y, Nagata K (2007) Amplified expression of uncoupling proteins in human brain ischemic lesions. *Neuropathology* 27:442–7.

Negre-Salvayre A, Hirtz C, Carrera G, Cazenave R, Troly M, Salvayre R, Penicaud L, Casteilla L (1997) A role for uncoupling protein-2 as a regulator of mitochondrial hydrogen peroxide generation. *Faseb J* 11: 809–15.

Nicholls DG, Locke RM (1984) Thermogenic mechanisms in brown fat. *Physiol Rev* 64: 1–64.

Nicotera P (2002) Development and death of neurons: sealed by a common fate? *Cell Death Differ* 9:1277–8.

Nigam S, Schewe T (2000) Phospholipase A2s and lipid peroxidation. *Biochim. Biophys Acta* 1488:167–81.

Okada S, Zhang H, Hatano M, Tokuhisa T (1998) A physiologic role of Bcl-xl induced in activated macrophages. *J Immunol* 160:2590-6.

Omari KM, Dorovini-Zis K (2003) CD40 expressed by human brain endothelial cells regulates CD4+ T cell adhesion to endothelium. *J Neuroimmunol* 134**:**166–178.

Ooboshi H, Ibayashi S, Shichita T, Kumai Y, Takada J, Ago T, Arakawa S, Sugimori H, Kamouchi M, Kitazono T, Iida M (2005) Postischemic gene transfer of interleukin-10 protects against both focal and global brain ischemia. *Circulation* 111:913–9.

Ouk T, Petrault O, Gautier S, Gelé P, Laprais M, Duriez P, Bastide M, Bordet R (2005) Acute treatment by a PPAR-α agonist decreases cerebral infarct volume and prevents post-ischemic endothelium and Kir 2.1 impairment. *J Cereb Blood Flow Metab* 25: (Suppl. 1), S56.

Ovbiagele B, Kidwell CS, Starkman S, Saver JL (2003) Potential role of neuroprotective agents in the treatment of patients with acute ischemic stroke. *Curr Treat Options Cardiovasc Med* 5:441–9.

Pang L, Ye W, Che XM, Roessler BJ, Betz AL, Yang GY (2001) Reduction of inflammatory response in the mouse brain with adenoviralmediated transforming growth factor-ss1 expression. *Stroke* 32:544–52.

Pecqueur C, Alves-Guerra MC, Gelly C, Levi-Meyrueis C, Couplan E, Collins S, Ricquier D, Bouillaud F, Miroux B (2001) Uncoupling protein 2, *in vivo* distribution, induction upon oxidative stress, and evidence for translational regulation. *J Biol Chem* 276: 8705–12.

Pelidou SH, Kostulas N, Matusevicius D, Kivisakk P, Kostulas V, Link H (1999) High levels of IL-10 secreting cells are present in blood in cerebrovascular diseases. *Eur J Neurol* 6:437–42.

Peters O, Back T, Lindauer U, Busch C, Megow D, Dreier J, Dirnagl U (1998) Increased formation of reactive oxygen species after permanent and reversible middle cerebral artery occlusion in the rat. *J Cereb Blood Flow Metab* 18:196–205.

Phan TG, Wright PM, Markus R, Howells DW, Davis SM, Donnan GA (2002) Salvaging the ischaemic penumbra: more than just reperfusion? *Clin Exp Pharmacol Physiol* 29:1–10.

Pialat JB, Cho TH, Beuf O, Joye E, Moucharrafie S, Langlois JB, Nemoz C, Janier M, Berthezene Y, Nighoghossian N *et al.* (2007) MRI monitoring of focal cerebral ischemia in peroxisome proliferator-activated receptor (PPAR)-deficient mice. *NMR Biomed* 20:335-42.

Plautz EJ, Barbay S, Frost SB, Friel KM, Dancause N, Zoubina EV, Stowe AM, Quaney BM, Nudo RJ (2003) Post-infarct cortical plasticity and behavioural recovery using concurrent cortical stimulation and rehabilitative training: a feasibility study in primates. *Neurol Res* 25:801–10.

Pradillo JM, Romera C, Hurtado O, Cardenas A, Moro MA, Leza JC, Davalos A, Castillo J, Lorenzo P, Lizasoain I (2005) TNFR1 upregulation mediates tolerance after brain ischemic preconditioning. *J Cereb Blood Flow Metab* 25:193–203.

Rabuffetti M, Sciorati C, Tarozzo G, Clementi E, Manfredi AA, Beltramo M (2000) Inhibition of caspase- 1-like activity by Ac-Tyr-Val-Ala-Asp-chloromethyl ketone induces long-lasting neuroprotection in cerebral ischemia through apoptosis reduction and decrease of pro-inflammatory cytokines. *J Neurosci* 20:4398–404.

Rai NK, Tripathi K, Sharma D, Shukla V K (2005) Apoptosis: a basic physiologic process in wound healing. *Int J Low Extrem Wounds* 4:138–44.

Rami A, Bechmann I, Stehle JH (2008) Exploiting endogenous anti-apoptotic proteins for novel therapeutic strategies in cerebral ischemia. *Prog Neurobiol* 85:273–296.

Reed JC (1997) Double identity for proteins of the Bcl-2 family. *Nature* 387:773–6.

Reed JC (1998) Bcl-2 family proteins. *Oncogene* 17:3225–36.

Relton JK, Martin D, Thompson RC, Russell DA (1996) Peripheral administration of interleukin-1 receptorantagonist inhibits brain damage after focal cerebral ischemia in the rat. *Exp Neurol* 138:206–13.

Richard D, Huang Q, Sanchis D, Ricquier D (1999) Brain distribution of UCP2 mRNA: *in situ* hybridization histochemistry studies. *Int J Obes Relat Metab Disord* 23(Suppl 6):S53–5.

Richard D, Rivest R, Huang Q, Bouillaud F, Sanchis D, Champigny O, Ricquier D (1998) Distribution of the uncoupling protein 2 mRNA in the mouse brain. *J Comp Neurol* 397:549–60.

Ricquier D, Bouillaud F (2000) The uncoupling protein homologues: UCP1, UCP2, UCP3, StUCP and AtUCP. *Biochem J* 345:161–79.

Sakahira H, Enari M, Nagata S (1998) Cleavage of CAD inhibitor in CAD activation and DNdegradation during apoptosis. *Nature* 391:96–9.

Salazar JJ and Van Houten (1997) Preferential mitochondrial DNA injury caused by glucose oxidase as a steady generator of hydrogen peroxide in human fibroblasts. *Mutat Res* 385:139–49.

Saleh MC, Wheeler MB, Chan CB (2002) Uncoupling protein-2: evidence for its function as a metabolic regulator. *Diabetologia* 45:174-87.

Saraste A, Pulkki K (2000) Morphologic and biochemical hallmarks of apoptosis. *Cardiovasc Res* 45(3):528-37.

Sawada M, Suzumura A, Hosoya H, Marunouchi T, Nagatsu T (1999) Interleukin-10 inhibits both production of cytokines and expression of cytokine receptors in microglia. *J Neurochem* 72:1466–71.

Schilling M, Besselmann M, Leonhard C, Mueller M, Ringelstein EB, Kiefer R (2003) Microglial activation precedes and predominates over macrophage infiltration in transient focal cerebral ischemia: a study in green fluorescent protein transgenic bone marrow chimeric mice. *Exp Neurol* 183:25–33.

Schinder AF, Olson EC, Spitzer NC, Montal M (1996) Mitochondrial dysfunction is a primary event in glutamate neurotoxicity. *J Neurosci* 16: 6125–33.

Seshadri S, Beiser A, Kelly-Hayes M, Kase CS, Au R, Kannel WB *et al.* (2006) The lifetime risk of stroke: estimates from the Framingham study. Stroke 37:345–50.

Shimazu T, Inoue I, Araki N, Asano Y, Sawada M, Furuya D, Nagoya H, Greenberg JH (2005) A peroxisome proliferator-activated receptor-gamma agonist reduces infarct size in transient but not in permanent ischemia. *Stroke* 36:353–9.

Siesjö BK, Elmer E, Janelidze S, Keep M, Kristian T, Ouyang YB, Uchino H (1999) Role and mechanisms of secondary mitochondrial failure. *Curr. Prog. Understanding Sec. Brain Damage Trauma Ischemia* 73:7–13.

Silva JP, Shabalina IG, Dufour E, Petrovic N, Backlund EC, Hultenby K, Wibom R, Nedergaard J, Cannon B, Larsson NG (2005) SOD2 overexpression: enhanced mitochondrial tolerance but absence of effect on UCP activity. *EMBO J* 24:4061–70.

Slee E A, Adrain C, Martin SJ (2001) Executioner caspase-3, -6, and -7 perform distinct, non-redundant roles during the demolition phase of apoptosis. *J Biol Chem* 276:7320–6.

Slee EA, Harte MT, Kluck RM, Wolf BB, Casiano CA, Newmeyer DD, Wang HG, Reed JC, Nicholson DW, Alnemri ES *et al.* (1999) Ordering the cytochrome c-initiated caspase cascade: hierarchical activation of caspases-2, -3, -6, -7, -8, and -10 in a caspase-9-dependent manner. *J Cell Biol* 144:281-92.

Smith WS (2004) Pathophysiology of focal cerebral ischemia: a therapeutic perspective. *J Vasc Interv Radiol* 15:S3–S12.

Smith CJ, Emsley HC, Gavin CM, Georgiou RF, Vail A, Barberan EM, del Zoppo GJ, Hallenbeck JM, Rothwell NJ, Hopkins SJ *et al.* (2004) Peak plasma interleukin-6 and other peripheral markers of inflammation in the first week of ischaemic stroke correlate with brain infarct volume, stroke severity and long-term outcome. *BMC Neurol* 4:2.

Soriano MA, Ferrer I, Rodriguez-Farré E, Planas AM (1996) Apoptosis and c-Jun in the thalamus of the rat following cortical infarction. *Neuroreport* 7:425-8.

Spencer SJ, Mouihate A, Pittman QJ (2007) Peripheral inflammation exacerbates damage after global ischemia independently of temperature and acute brain inflammation. *Stroke* 38:1570-7.

Spera PA, Ellison JA, Feuerstein GZ, Barone FC (1998) IL-10 reduces rat brain injury following focal stroke. *Neurosci Lett* 251:189–92.

Stahel PF, Smith WR, Bruchis J, Rabb CH (2008) Peroxisome Proliferator-Activated Receptors: "Key" Regulators of Neuroinflammation after Traumatic Brain Injury. *PPAR Res* :538141.

Stamatovic SM, Keep RF, Kunkel SL, Andjelkovic AV (2003) Potential role of MCP-1 in endothelial cell tight junction 'opening': signaling via Rho and Rho kinase. *J Cell Sci* 116:4615–28.

Starkov AA, Chinopoulos C, Fiskum G (2004) Mitochondrial calcium and oxidative stress as mediators of ischemic brain injury. *Cell Calcium* 36:257–264.

Starkov AA, Fiskum G, Chinopoulos C, Lorenzo BJ, Browne SE, Patel MS, Beal MF (2004) Mitochondrial alpha-ketoglutarate dehydrogenase complex generates reactive oxygen species. *J Neurosci* 24:7779–7788.

Stoll G, Jander S, Schroeter M (1998) Inflammation and glial responses in ischemic brain lesions. *Prog Neurobiol* 56:149–71.

Strle K, Zhou JH, Shen WH, Broussard SR, Johnson RW, Freund GG, Dantzer R, Kelley KW (2001) Interleukin-10 in the brain. *Crit Rev Immunol* 21:427–49.

Stumm RK, Rummel J, Junker V, Culmsee C, Pfeiffer M, Krieglstein J, Hollt V, Schulz S (2002) A dual role for the SDF-1/CXCR4 chemokine receptor system in adult brain: isoform-selective regulation of SDF-1 expression modulates CXCR4-dependent neuronal plasticity and cerebral leukocyte recruitment after focal ischemia. *J Neurosci* 22:5865–78.

Sullivan PG, Bruce-Keller AJ, Rabchevsky AG, Christakos S, Clair DK, Mattson MP, Scheff SW (1999) Exacerbation of damage and altered NF-kappaB activation in mice lacking tumor necrosis factor receptors after traumatic brain injury. *J Neurosci* 19: 6248–56.

Sundararajan S, Gamboa JL, Victor NA, Wanderi EW, Lust WD, Landreth GE (2005) Peroxisome proliferator activated receptor-gamma ligands reduce inflammation and infarction size in transient focal ischemia. *Neuroscience* 130:685–96.

Takano K, Tatlisumak T, Formato JE, Carano RA, Bergmann AG, Pullan LM, Bare TM, Sotak CH, Fisher M (1997) Glycine site antagonist attenuates infarct size in experimental focal ischemia. Postmortem and diffusion mapping studies. *Stroke* 28:1255–62.

Tamura A, Graham DI, McCulloch J, Teasdale GM (1981) Focal cerebral ischemia in the rat: 1. Description of technique and early neuropathological consequences following middle cerebral artery occlusion. *J Cereb Blood Flow Metabol* 1:53-60.

Tamura A, Tahira Y, Nagashima H, Kirino T, Gotoh O, Hojo S, Sano K (1991) Thalamic atrophy following cerebral infarction in the territory of the middle cerebral artery. *Stroke* 22:615-8.

Taoufik E, Valable S, Muller GJ, Roberts ML, Divoux D, Tinel A, Voulgari-Kokota A, Tseveleki V, Altruda F, Lassmann H *et al.* (2007) FLIP(L) protects neurons against in vivo ischemia and in vitro glucose deprivation-induced cell death. *J Neurosci* 27:6633-46.

Tarkowski E, Rosengren L, Blomstrand C, Wikkelso C, Jensen C, Ekholm S, Tarkowski A (1997) Intrathecal release of pro-and anti-inflammatory cytokines during stroke. *Clin Exp Immunol* 110:492–9.

Thornberry NA, Bull HG, Calaycay JR, Chapman KT, Howard AD, Kostura MJ, Miller DK, Molineaux SM, Weidner JR, Aunins J *et al.* (1992) A novel heterodimeric cysteine protease is required for interleukin-1β processing in monocytes. Nature 356: 768–74.

Toyomoto M, Ohta M, Okumura K, Yano H, Matsumoto K, Inoue S, Hayashi K, Ikeda K (2004) Prostaglandins are powerful inducers of NGF and BDNF production in mouse astrocyte cultures. *FEBS Letters* 562:211–5.

Traystman RJ (2003) Animal models of focal and global cerebral ischemia. *ILAR J* 44:85 – 95.

Trump B F, Berezesky IK, Chang SH, Phel PC (1997) The pathways of cell death: oncosis, apoptosis, and necrosis. *Toxicol Pathol* 25:82–8.

Tureyen K, Kapadia R, Bowen KK, Satriotomo I, Liang J, Feinstein DL, Vemuganti R (2007) Peroxisome proliferator-activated receptor-*γ* agonists induce neuroprotection following transient focal ischemia in normotensive, normoglycemic as well as hypertensive and type-2 diabetic rodents. *Journal of Neurochemistry* 101:41–56.

Unal-Cevik I, Kilinc M, Can A, Gursoy-Ozdemir Y, Dalkara T (2004) Apoptotic and necrotic death mechanisms are concomitantly activated in the same cell after cerebral ischemia. *Stroke* 35:2189–94.

Valmiki MG, Ramos JW (2009) Death effector domain-containing proteins. *Cell Mol Life Sci* 66:814-30.

Van Cruchten S, Van Den Broeck W (2002). Morphological and biochemical aspects of apoptosis, oncosis and necrosis. *Anat Histol Embryol* 31(4): 214-23.

van Exel E, Gussekloo J, de Craen AJ, Bootsma-van der Wiel A, Frolich M, Westendorp RG (2002) Inflammation and stroke: the Leiden 85-Plus Study. *Stroke* 33:1135–8.

Vanden Heuvel JP (2007) The PPAR resource page. *Biochim Biophys Acta* 1771:1108–12.

Wang XK, Feuerstein GZ (1995) Induced expression of adhesion molecules following focal brain ischemia. *J Neurotrauma* 12:825–32.

Wang YX, Lee CH, Tiep S, Yu RT, Ham J, Kang H, Evans RM (2003) Peroxisome-proliferator-activated receptor delta activates fat metabolism to prevent obesity. *Cell* 113:159–70.

Wardlaw JM, Warlow CP, Counsell C (1997) Systematic review of evidence on thrombolytic therapy for acute ischaemic stroke. *Lancet* 350:607–14.

Wegener S, Gottschalk B, Jovanovic V, Knab R, Fiebach JB, Schellinger PD, Kucinski T, Jungehulsing GJ, Brunecker P, Muller B *et al.* (2004) Transient ischemic attacks before ischemic stroke: preconditioning the human brain?: a multicenter magnetic resonance imaging study. *Stroke* 35:616–21.

Wieloch T (2001) Mitochondrial Involvement in Acute Neurodegeneration. *IUBMB Life* 52:247-54.

Wiessner C, Allegrini PR, Rupalla K, Sauer D, Oltersdorf T, McGregor AL, Bischoff S, Böttiger BW, van der Putten H (1999) Neuron-specific transgene expression of Bcl-XL but not Bcl-2 genes reduced lesion size after permanent middle cerebral artery occlusion in mice. *Neurosci Lett* 268:119–22.

Yamasaki Y, Matsuura N, Shizuhara H, Onodera H, Itoyama YKK (1995) Interleukin-1 as a pathogenetic mediator of ischemic brain damage in the rats. *Stroke* 26 :676–81.

Yang J, Liu X, Bhalla K (1997) Prevention of apoptosis by Bcl-2: release of cytochrome *c* from mitochondria blocked. *Science* 275:1129–32.

Yang GY, Gong C, Qin Z, Ye W, Mao Y, Bertz AL (1998) Inhibition of TNFalpha attenuates infarct volume and ICAM-1 expression in ischemic mouse brain. *Neuroreport* 9 :2131–4.

Yin XM, Luo Y, Cao G, Bai L, Pei W, Kuharsky DK, Chen J (2002) Bid mediated mitochondrial pathway is critical to ischemic neuronal apoptosis and focal cerebral ischemia. *J Biol Chem* 277:42074–81.

Yu X, Shao XG, Sun H, Li YN, Yang J, Deng YC, Huang YG (2008) Activation of cerebral peroxisome proliferator-activated receptors gamma exerts neuroprotection by inhibiting oxidative stress following pilocarpine-induced status epilepticus. *Brain Res* 1200:146-58.

Zhang CY, Baffy G, Perret P, Krauss S, Peroni O, Grujic D, Hagen T, Vidal-Puig AJ, Boss O, Kim YB *et al.* (2001) Uncoupling protein-2 negatively regulates insulin secretion and is a major link between obesity, beta cell dysfunction, and type 2 diabetes. *Cell* 105:745–55.

Zhao H, Yenari MA, Cheng D, Sapolsky RM, Steinberg GK (2003) Bcl-2 overexpression protects against neuron loss within the ischemic margin following experimental stroke and inhibits cytochrome *c* translocation and caspase-3 activity. *J Neurochem* 85:1026–36.

Zhong LT, Sarafian T, Kane DJ, Charles AC, Mah SP, Edwards RH, Bredesen DE (1993) Bcl-2 inhibits death of central neural cells induced by multiple agents. *Proc Natl Acad Sci USA* 90:4533-7.